

# Antibody micropatterns as a tool to study MHC class I molecules

by

Cindy Dirscherl

A thesis submitted in partial fulfillment  
of the requirements for the degree of

Doctor of Philosophy in Cell Biology

Approved Dissertation Committee

**Prof. Sebastian Springer, DPhil**

Jacobs University Bremen

**Prof. Dr. Gerhard Schütz**

Vienna University of Technology

**Dr. Susanne Illenberger**

Jacobs University Bremen

Date of Defense: 01. June 2018



# Statutory Declaration



Family Name, Given/First Name	Dirscherl, Cindy
Matriculation number	20330798
What kind of thesis are you submitting:	PhD thesis
Bachelor-, Master- or PhD-Thesis	

## English: Declaration of Authorship

I hereby declare that the thesis submitted was created and written solely by myself without any external support. Any sources, direct or indirect, are marked as such. I am aware of the fact that the contents of the thesis in digital form may be revised with regard to usage of unauthorized aid as well as whether the whole or parts of it may be identified as plagiarism. I do agree my work to be entered into a database for it to be compared with existing sources, where it will remain in order to enable further comparisons with future theses. This does not grant any rights of reproduction and usage, however.

The Thesis has been written independently and has not been submitted at any other university for the conferral of a PhD degree; neither has the thesis been previously published in full.

## German: Erklärung der Autorenschaft (Urheberschaft)

Ich erkläre hiermit, dass die vorliegende Arbeit ohne fremde Hilfe ausschließlich von mir erstellt und geschrieben worden ist. Jedwede verwendeten Quellen, direkter oder indirekter Art, sind als solche kenntlich gemacht worden. Mir ist die Tatsache bewusst, dass der Inhalt der Thesis in digitaler Form geprüft werden kann im Hinblick darauf, ob es sich ganz oder in Teilen um ein Plagiat handelt. Ich bin damit einverstanden, dass meine Arbeit in einer Datenbank eingegeben werden kann, um mit bereits bestehenden Quellen verglichen zu werden und dort auch verbleibt, um mit zukünftigen Arbeiten verglichen werden zu können. Dies berechtigt jedoch nicht zur Verwendung oder Vervielfältigung.

Diese Arbeit wurde in der vorliegenden Form weder einer anderen Prüfungsbehörde vorgelegt noch wurde das Gesamtdokument bisher veröffentlicht.

.....

Date, Signature

This work was funded by the German Federal Ministry for Education and Research (BMBF)

Strategieprozess Biotechnologie 2020+: Basistechnologien

Kooperationsprojekt 031A153A-B

"Prozessüberwachung *in vivo* und *in vitro* mit Polyelektrolyt-Nanokapseln"



Parts of this thesis were or are going to be published in:

**Dirscherl, C.**, Ramnarayan V., Hein, Z., Jacob-Dolan, C., and Springer, S. A novel two-hybrid antibody micropattern assay reveals conformation-specific cell surface clustering of MHC I proteins. *Manuscript in revision at eLife*.

**Dirscherl, C.**, Palankar, R., Delcea, M. Kolesnikova, T.A., and Springer, S. Specific capture of peptide-receptive major histocompatibility complex class I molecules by antibody micropatterns allows for a novel peptide-binding assay in live cells. *Small*. 2017, 13 (15).

**Dirscherl, C.** and Springer, S. Protein micropatterns printed on glass - novel tools for protein-ligand binding assays in live cells. *Engineering in Life Sciences*. 2017.

# Acknowledgements

Taking up this PhD project was probably one of the greatest adventures and challenges I have encountered so far and I would like to thank my supervisor Sebastian Springer for giving me this great opportunity and for his constant support and help throughout the project.

Many thanks go to the thesis committee: Susanne Illenberger, Mathias Winterhalter, and Gerhard Schütz for reviewing my thesis and for their scientific advice and guidance throughout the project.

I also would like to thank my companions on this project, the members of subgroup C: Mathias Winterhalter, Gerd Klöck, Detlef Gabel, Tatiana Kolesnikova, Sujit Kumar Verma, and Anja Albrecht. Thank you for all the discussions and wild ideas that led to the realization of this project.

My deepest thanks go to the former and current members of the Springer laboratory. Thank you so much for your warm welcome, for the friendly atmosphere, for your constant scientific support and for all the fun! With you, I found kind colleagues, but also great new friends! Thank you Esam Abualrous, Raghavendra Anjappa, Britta Borchert, Susi Fritzsche, Swapnil Ghanwat, Zeynep Hein, Linda Janßen, Sunil Kumar Saini, Natalia Lis, Sebastian Montealegre, Venkat Ramnarayan, Ankur Saikia, Sujit Verma, and Ursula Wellbrock.

I also want to thank my students who worked with me on this project: Anca Apavaloaei, Natalia Lis, Nikolett Nagy, and Catherine Jacob-Dolan.

My special thanks go to my collaborators Mihaela Delcea and Raghavendra Palankar from Greifswald for their great help, experimental advice and for the opportunity to use their facilities. I enjoyed each stay. Thanks also go to Bastian Rapp and Tobias Nargang from KIT for the trial experiments with their 'Gutenberg' protein prints.

I would also like to thank the department of life sciences and chemistry at Jacobs University for their support and the friendly working atmosphere. A special thanks to all members of the Brix lab for discussions, and Wagner lab for making molds.

Thanks to the BMBF for funding this project.

Zuletzt möchte ich aus ganzem Herzen meiner Familie und meinen Freunden danken. Dieses Jahr wird endlich gefeiert- ihr habt lang genug gewartet!

## Abbreviations

2A	ribosomal skipping sequence (GSGATNPSSLKQAGDVEENPGP) (Szymczak et al., 2004)
AF	Alexa Fluor
APTES	(3-Aminopropyl)triethoxysilane
$\beta_2m$	beta-2 microglobulin
BiFC	Bimolecular fluorescence complementation
BSA	bovine serum albumin
Cha	cyclohexylalanine (non-proteinogenic amino acid)
cLSM	confocal laser scanning microscopy
D <sup>b</sup>	the murine MHC class I protein H-2D <sup>b</sup>
D <sup>d</sup>	the murine MHC class I protein H-2D <sup>d</sup>
DTT	dithiothreitol
ER	endoplasmic reticulum
F <sub>ab</sub>	the antigen-binding regions of an antibody
FBS	fetal bovine serum
F <sub>c</sub>	fragment crystallizable (the protein A-binding region of an antibody)
FCS	fetal calf serum
FL9	FAPGNYPAL peptide sequence
FRAP	fluorescence recovery after photobleaching
g $\alpha$ m	goat anti-mouse (antibody)
g $\alpha$ r	goat anti-rabbit (antibody)
GCha	glycyl-cyclohexylalanine

## Abbreviations

---

GFP	green fluorescent protein
HA	hemagglutinin (antibody tag, sequence YPYDYPDYA)
HLA	Human leukocyte antigen
K <sup>b</sup>	the murine MHC class I protein H-2K <sup>b</sup>
KIR	killer immunoglobulin-like receptor
L <sup>d</sup>	the murine MHC class I protein H-2L <sup>d</sup>
LILR	leukocyte immunoglobulin-like receptor
MALDI	matrix-assisted laser desorption/ionization (mass spectrometry)
MHC	major histocompatibility complex
MW	molecular weight
NACS	nucleic acid cell sorting
NHS	N-hydroxysuccinimide
NK	natural killer (cells)
Oligo	oligonucleotide
PBS	phosphate-buffered saline
PDMS	polydimethyl-siloxane;
PFA	paraformaldehyde
PIR	paired immunoglobulin-like receptor
PLC	peptide loading complex
pMHC	peptide-bound major histocompatibility class I complex
scFvs	single-chain variable fragments (of antibodies)
SEM	scanning electron microscopy

# Abstract

Planar surfaces with geometric protein patterns have been developed for various applications in biotechnology, such as orienting cells, arranging membrane proteins, or studying protein-ligand binding in massively parallel approaches. Geometric shapes and dimensions of protein patterns vary depending on the application. For the study of proteins in living cells, protein patterns in the micrometer range are commonly used; these are called protein micropatterns. Diverse lithography techniques have been used and were further developed to fabricate even complicated protein micropatterns on various surfaces. One of the first techniques to immobilize proteins in geometric patterns on glass surfaces was microcontact printing, which is a rather simple stamping approach that immobilizes proteins by physical absorption onto surfaces.

MHC class I are peptide receptors that present the cell's proteome at the cell surface to T cells. They thus play an essential role in the adaptive immune response against cells that are infected by viruses, bacteria, or that carry tumorigenic mutations. We have adapted the technology of protein micropatterns to the field of MHC class I and have used microcontact printing to immobilize anti-MHC class I antibodies on glass surfaces to develop an MHC class I capture assay. The development of this assay consisted of optimization and trial experiments; they finally established a robust assay that can be used to specifically capture MHC class I in living cells.

In the field of MHC class I antigen presentation, we have identified two applications for the capture assay. First, a novel peptide binding assay was developed that allows for the monitoring of specific peptide binding to captured MHC class I in living cells. Further development of the assay led to the finding that the use of conformation-specific antibodies allows for differential capture of different structural forms of MHC class I. Excitingly, this enables the investigation of conformation-specific *in cis* interactions of MHC class I at the cell surface. With this assay, I discovered and characterized the specific cluster formation of a distinct MHC class I conformation that was previously not detectable with conventional techniques. These findings contribute to a novel hypothesis of the molecular mechanism that underlies MHC class I endocytic sorting.

# Contents

<b>Acknowledgements.....</b>	<b>IV</b>
<b>Abbreviations.....</b>	<b>V</b>
<b>Abstract.....</b>	<b>VII</b>
<b>1 Introduction.....</b>	<b>1</b>
1.1 Soft lithography and generation of protein micropatterns.....	1
1.2 Applications of protein micropatterns to cell biology.....	2
1.3 Generation of micropatterns by direct printing on glass surfaces.....	3
1.3.1 About chapter 1.3 .....	3
1.3.2 Abstract.....	3
1.3.3 Introduction: The production and use of protein patterns so far.....	3
1.3.4 The uses of protein patterns at the single cell level .....	6
1.3.5 Technical implementations: Challenges and the way ahead .....	9
1.3.6 Conclusion.....	17
1.3.7 Materials and Methods.....	17
1.3.8 Acknowledgements.....	18
1.3.9 Copyright Transfer Agreement .....	19
1.4 MHC class I molecules .....	20
1.4.1 MHC class I and its role in the immune response .....	20
1.4.2 Structure and folding of MHC class I molecules .....	21
1.4.3 Peptide binding.....	23
1.4.4 Forms and stability of MHC class I molecules at the cell surface .....	24
1.4.5 STF1 cells, TAP deficiency, and class I stability .....	25
1.4.6 Interactions of MHC class I <i>in trans</i> .....	26
1.4.7 Known <i>in cis</i> interactions of MHC class I.....	29
1.4.8 MHC class I interact <i>in trans</i> and <i>in cis</i> with inhibitory receptors.....	30
1.4.9 Methods for the investigation of <i>in cis</i> interactions .....	32
1.4.10 Anticipated properties of MHC class I clusters and applicability of known interaction analysis methods .....	34
1.5 Anti-MHC class I antibodies.....	35
1.6 T cell arrays.....	36

1.7	Project motivation.....	37
<b>2</b>	<b>Materials and methods .....</b>	<b>38</b>
2.1	Preparation of antibodies.....	38
2.2	Fabrication of antibody micropatterns .....	51
2.3	Incubation of cells on antibody micropatterns .....	61
2.3.1	Cell seeding on antibody micropatterns.....	61
2.3.2	Incubation temperature and incubation times.....	61
2.3.3	Fixation of cells .....	62
2.4	Plasmids and generation of stable cell lines .....	63
2.5	Microscopy .....	64
2.5.1	Fluorescence microscopy.....	64
2.5.2	Live cell microscopy .....	64
2.6	Glass functionalization .....	65
2.6.1	Glass cleaning with RCA cleaning.....	65
2.6.2	Plasma cleaner .....	66
2.6.3	Coating of the glass coverslips .....	68
2.6.4	Oriented immobilization .....	72
2.7	Blocking antibody prints with BSA .....	80
<b>3</b>	<b>Results summary.....</b>	<b>83</b>
3.1	Summary of chapter 4: Development of anti-MHC class I antibody micropatterns and optimization .....	83
3.2	Summary chapter 5: Anti-MHC class I antibody micropatterns as a tool to study conformation-specific <i>in-cis</i> interactions .....	84
3.3	Summary chapter 6: Additional Results and Discussions on Pattern Fabrication .....	84
<b>4</b>	<b>Development of anti-MHC class I antibody micropatterns and their applications .....</b>	<b>85</b>
4.1	Specific capture of peptide-receptive Major Histocompatibility Complex class I molecules by antibody micropatterns allows for a novel peptide binding assay in live cells.....	86
4.1.1	About chapter 4.1 .....	86
4.1.2	Abstract.....	86
4.1.3	Introduction .....	87
4.1.4	Results.....	88
4.1.5	Discussion and Conclusion .....	96
4.1.6	Outlook .....	98
4.1.7	Experimental Section .....	99

4.1.8	Supporting Information .....	103
4.1.9	Copyright Transfer Agreement .....	106
4.2	Additional Data.....	107
4.2.1	Different approaches to generate anti-MHC class I micropatterns.....	107
4.2.2	The special case of the 25.D1.16 antibody .....	112
4.2.3	Peptide binding to captured D <sup>b</sup> on 27.11.13S prints .....	113
4.2.4	Cells sense antibody micropatterns: ‘feet’ formation .....	114
4.2.5	Dipeptide exchange trials .....	116
4.2.6	Release from pattern with HA peptide .....	120
4.2.7	Bifunctional patterns .....	127
<b>5</b>	<b>Anti-MHC class I antibody micropatterns as a tool to study conformation-specific <i>in cis</i> interactions.....</b>	<b>131</b>
5.1	A novel two-hybrid antibody micropattern assay reveals conformation-specific cell surface clustering of MHC I proteins.....	131
5.1.1	About chapter 5.1 .....	131
5.1.2	Abstract.....	131
5.1.3	Introduction .....	132
5.1.4	Results.....	133
5.1.5	Discussion .....	144
5.1.6	Materials and Methods.....	146
5.1.7	Acknowledgements.....	149
5.1.8	Supporting Information .....	150
5.2	Additional Data.....	153
5.2.1	Co-expression and immunostaining of marker proteins to characterize captured K <sup>b</sup> -GFP .....	153
5.2.2	Allele specificity of MHC class I <i>in cis</i> interactions.....	163
5.3	Further discussions.....	165
5.3.1	Localization of MHC class I clusters .....	165
5.3.2	General ideas and remarks on MHC class I clusters .....	165
<b>6</b>	<b>Additional results and discussion on pattern fabrication .....</b>	<b>167</b>
6.1	Patterns from the KIT .....	167
<b>7</b>	<b>Future perspectives.....</b>	<b>169</b>
7.1	Further investigations of MHC class I clusters .....	169
7.1.1	Role of cysteines in the cytoplasmic tail .....	169
7.1.2	Functional analysis of cluster formation.....	171



---

7.2	Testing the dynamics of MHC class I capture and clusters .....	171
7.2.1	Analysis of capture dynamics with FRAP .....	172
7.2.2	Class I interaction dynamics.....	173
7.2.3	Single antibody patterns.....	174
7.2.4	Electron microscopy of antibody micropatterns .....	175
7.3	Interaction partners of MHC class I proteins .....	175
7.3.1	Probing other proposed candidates for <i>in cis</i> interactions with MHC class I .....	175
7.3.2	Development of an open screen.....	176
7.4	Possible technical developments .....	176
7.4.1	Antibody micropatterns for induced capture .....	177
7.4.2	Release of captured proteins from antibody micropatterns .....	177
8	<b>References.....</b>	<b>180</b>



# 1 Introduction

The introduction is divided into six major sections. It gives an overview of the technology of micropatterned surfaces in general and their applications in cell biology in particular, as well as an overview of the cell biology of MHC class I. The first three sections of this chapter (sections 1.1-1.3) give an overview of protein micropatterns. A general overview of applications for micropatterns in cell biology is presented in section 1.2. Section 1.3 contains a published review article that describes the fabrication of micropatterns by the technique of microcontact printing.

In the following part (section 1.4), I give detailed information about those MHC class I characteristics that are relevant for this project. This section also includes background information of MHC class I interactions *in trans* and *in cis* that have been detected or are still under investigation.

A detailed list of anti-MHC class I antibodies and their specific epitopes on the MHC class I that were used in this study are described in section 1.5.

I have included one section about MHC class I patterns and their application in T cell arrays (see section 1.6).

The last section of the introduction describes the project motivation (see section 1.7).

## 1.1 Soft lithography and generation of protein micropatterns

The structuring of material is generally referred to as lithography. In biotechnology, the term applies to all printing or stamping procedures of biomolecules (proteins, DNA) or particles (nanoparticles, quantum dots). Depending on the dimension of the fabricated structures, one can distinguish microlithography (structures smaller than 10  $\mu\text{m}$ ) from nanolithography (structures smaller than 100 nm).

In this project, I used microcontact printing, which belongs to the category of soft lithographic techniques in the micrometer regime. 'Soft' lithography indicates that soft materials, such as elastomeric stamps, molds, or conformable photomasks, are used for the structuring process. Microcontact printing represents one of the oldest soft lithographic techniques and has led to a set of related soft lithography methods such as replica molding, microtransfer molding, micromolding in capillaries, and solvent-assisted micromolding (see Xia and Whitesides, 1998 for review).

The soft lithography process generally consists of two parts. First, the elastomeric elements are fabricated, and then, they are used to generate geometric features according to their relief structure.

Microcontact printing, invented by George M. Whitesides at Harvard University, uses a high-resolution stamp as elastomeric element (Wilbur et al., 1994). This stamp is made with the help of a so-called ‘master’ or ‘mold’. The mold itself can be fabricated by various techniques that are able to produce well-defined relief structures. Photolithography techniques are commonly used to pattern a layer of photoresist on a Si wafer, similar to the fabrication of microchips in the semiconductor industry. The elastomeric stamps are finally generated by casting a light- or heat-curable pre-polymer such as polydimethylsiloxane (PDMS) against this mold.

Besides the development of various lithography technologies or combinations of these, microcontact printing still represents a convenient, effective, and low-cost method for structuring biomolecules on various surfaces.

### **1.2 Applications of protein micropatterns to cell biology**

Protein micropatterns are used for various applications. They are commonly used to control shape or adhesion geometries of cultured mammalian cells, in advanced forms also for tissue engineering (see Kane et al., 1999; Falconnet et al., 2006; Khademhosseini et al., 2006 for reference). Another typical application is the investigation of protein-protein interactions with bait-prey experiments (Schwarzenbacher et al., 2008; Weghuber et al., 2010; Lanzerstorfer et al., 2014; Löchte et al., 2014). I have transferred this concept to establish our own assay for the investigation of protein-protein interactions (see section 1.3 for more details).

## 1.3 Generation of micropatterns by direct printing on glass surfaces

### 1.3.1 About chapter 1.3

Chapter 1.3 is a published review paper that contains some original data. The experiments in this manuscript were designed by me and performed by myself or by my students as indicated. The manuscript was written by Sebastian Springer and me.

The full citation of the paper is:

Cindy Dirscherl and Sebastian Springer: **Protein micropatterns printed on glass: Novel tools for protein-ligand binding assays in live cells.** *Eng. Life Sci.* **18** (2018), 124-131; DOI: 10.1002/elsc.201700010.

The paper is online at <http://onlinelibrary.wiley.com/doi/10.1002/elsc.201700010/full>.

The figure numbers were changed to match the format of this thesis.

### 1.3.2 Abstract

Micrometer-sized patterns of proteins on glass or silica surfaces are in widespread use as protein arrays for probing with ligands or recombinant proteins. More recently, they have been used to capture the surface proteins of mammalian cells seeded onto them, and to arrange these surface proteins into pattern structures. Binding of small molecule ligands or of other proteins, transmembrane or intracellular, to these captured surface proteins can then be quantified. However, reproducible production of protein micropatterns on surfaces can be technically difficult. In this review, we outline the wide potential and the current practical uses of printed protein micropatterns in a historical overview, and we detail some potential pitfalls and difficulties from our own experience, as well as ways to circumvent them.

### 1.3.3 Introduction: The production and use of protein patterns so far

Patterned protein surfaces that interact with cell surface proteins were first developed for shaping and positioning cells (or parts of cells, such as neurites) with the aim of engineering tissues and specific microenvironments, for example to study the growth of cells in response to specific patterns and microstructures (Xu et al., 2013); for reviews see (Falconnet et al., 2006; Satav et al., 2015; Thery, 2010; Barthes et al., 2014). One convenient way to achieve this is a soft lithography method called

microcontact printing (Kane et al., 1999), in which a polydimethylsiloxane (PDMS) stamp is inked with the protein solution and then stamped onto the surface (for example, a glass coverslip). Recently, researchers have decreased the sizes of individual pattern elements (*i.e.*, dots or squares) that can be printed to the lower micrometer to nanometer range. Such small pattern elements allow the redistribution of cell surface proteins, such as receptors, into the shape of the printed pattern: if the printed protein is an antibody that binds to the extracellular domain of the cell surface protein of interest, then cells can be seeded onto the glass slide that contains the pattern, and the surface protein will be captured by the printed antibody into the shape of the pattern (figure 1.3.3 A). This technique has allowed researchers to study cell adhesion and phagocytosis (Cavalcanti-Adam et al., 2006; Freeman et al., 2016), signaling (Mossman et al., 2005; Wu et al., 2004), cellular protein-protein interactions (Schwarzenbacher et al., 2008; Weghuber et al., 2010; Löchte et al., 2014; Wedeking et al., 2015), and protein-ligand interactions (Gandor et al., 2013; Dirscherl et al., 2017). The advantage of using printed protein patterns to measure protein interactions is that the cell surface protein is in its native environment and composition, and that the assay can be performed in the living cell. In this review, we focus on the use of printed protein patterns for single-cell applications, more specifically on proteins that are printed directly onto the glass surface. We take the perspective of the researcher with a background in cell biology who is entering this exciting field. There are good reviews available about protein arrays for *in vitro* studies (Wilson and Nock, 2003; Weinrich et al., 2009; Korf, 2011; You and Piehler, 2016), so we do not include these. We mention, but do not review in detail, the significant recent developments in protein micropatterns that are generated by indirect immobilization or sophisticated attachment chemistry (Löchte et al., 2014; Waldbaur et al., 2012; Matic et al., 2013).

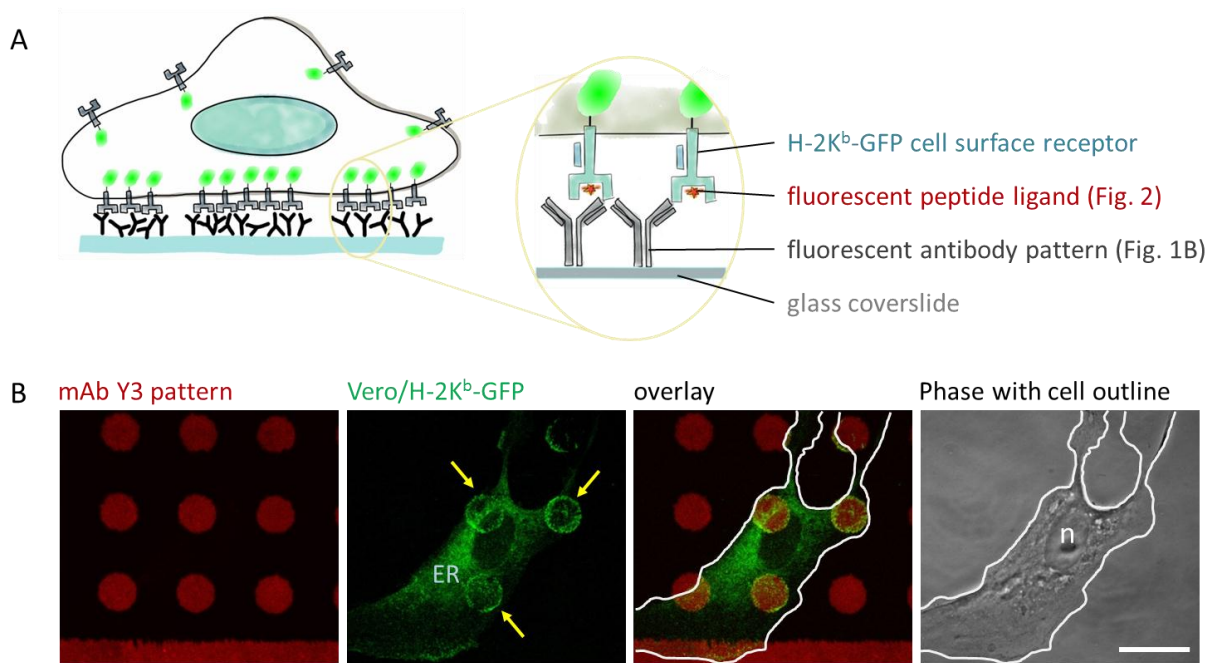


**Figure 1.3.3: A, Schematic of a cell surface GFP fusion protein binding to a printed protein micropattern in a ligand binding assay.** The peptide receptor H-2K<sup>b</sup>, a type I transmembrane major histocompatibility complex (MHC) class I protein, is produced in epithelial cells with the green fluorescent protein (GFP; green) fused to its C terminus. The cells are seeded onto a glass surface that is printed with a micropattern of the monoclonal antibody (mAb) Y3, which recognizes H-2K<sup>b</sup>. Upon binding to Y3, the H-2K<sup>b</sup>-GFP proteins on the cell surface are recruited into the printed patterns. In the insert, two H-2K<sup>b</sup>-GFP proteins are shown binding their natural peptide ligand (red), here labeled with a fluorophore. **B, A cell spreads out over several pattern elements to allow assessment of surface protein patterning.** A pattern of mAb Y3 labeled with Alexa Fluor 647 (red; pattern element diameter 10  $\mu\text{m}$ , interspace 15  $\mu\text{m}$ ) was printed onto a glass coverslide using a PDMS stamp. Vero (African green monkey kidney epithelial) cells expressing H-2K<sup>b</sup>-GFP (green) were then seeded onto this pattern and grown for 24 hours. In the phase contrast picture (right), the cell is outlined in white, and the nucleus is labeled with the letter n. Yellow arrows show the circular patterning of H-2K<sup>b</sup>-GFP by the antibody pattern, as depicted in A. The intracellular stain of H-2K<sup>b</sup>-GFP (overlaid with the blue letters ER) is in the endoplasmic reticulum. Bar, 25  $\mu\text{m}$ . The technique is described in detail in (Dirscherl et al., 2017).

### 1.3.4 The uses of protein patterns at the single cell level

When proteins that were printed in a pattern onto a glass slide interact with a surface protein of a single cell, then the isotropic distribution of that surface protein is altered, and it becomes rearranged into the printed pattern. In contrast to proteins bound to supported lipid bilayers (Mossman et al., 2005), protein patterns have a defined distribution, and they do not allow the captured cell surface protein to diffuse further. Its rearrangement can thus be conveniently read out by microscopy in the fixed or even live cell (figure 1.3.3 B). Sometimes, the distribution of the surface protein is identical to that of the pattern, but sometimes, the protein is more concentrated on the edges of the pattern elements, as one would expect if proteins on the plasma membrane are freely diffusing and becoming mechanically trapped as they encounter the edges of the pattern elements and bind to the printed proteins (figure 1.3.3 B, yellow arrows). Consequently, single-cell experiments are especially well suited to detect interactions of the patterned protein with other proteins, or with ligands, for microscopic readout.

One example for this are protein-ligand binding assays (Löchte et al., 2014), our own work being a recent example (Dirscherl et al., 2017). We print a monoclonal antibody called Y3 that binds to a cell surface peptide receptor of the adaptive immune system, a major histocompatibility complex (MHC) class I protein called H-2K<sup>b</sup>. When cells that contain a green fluorescent protein (GFP) fusion of H-2K<sup>b</sup>, H-2K<sup>b</sup>-GFP, are seeded onto the glass slides with the Y3 patterns, then the H-2K<sup>b</sup>-GFP protein is arranged on the cell surface in the shape of the pattern (figure 1.3.3). Binding of the peptide ligand can be assessed by labeling it with a fluorescent dye and adding the labeled peptide to the cells that are growing on the patterns. When the peptide ligand binds to its receptor H-2K<sup>b</sup>-GFP, then the peptide fluorescence also becomes visible in the shape of the pattern, but not in the interspaces of the pattern elements (figure 1.3.4). We have shown that by competition with a fluorescently labeled index peptide, the binding affinity of any prospective ligand to H-2K<sup>b</sup>-GFP can be measured (for details see (Dirscherl et al., 2017)). This competition assay principle might be applicable to other cell surface receptors whose ligands can be fluorescently labeled, and its special advantages are that the affinity measurement is done on the receptor in its natural condition and environment (*e.g.*, with all of its subunits, auxiliary proteins, and the native lipid environment present).



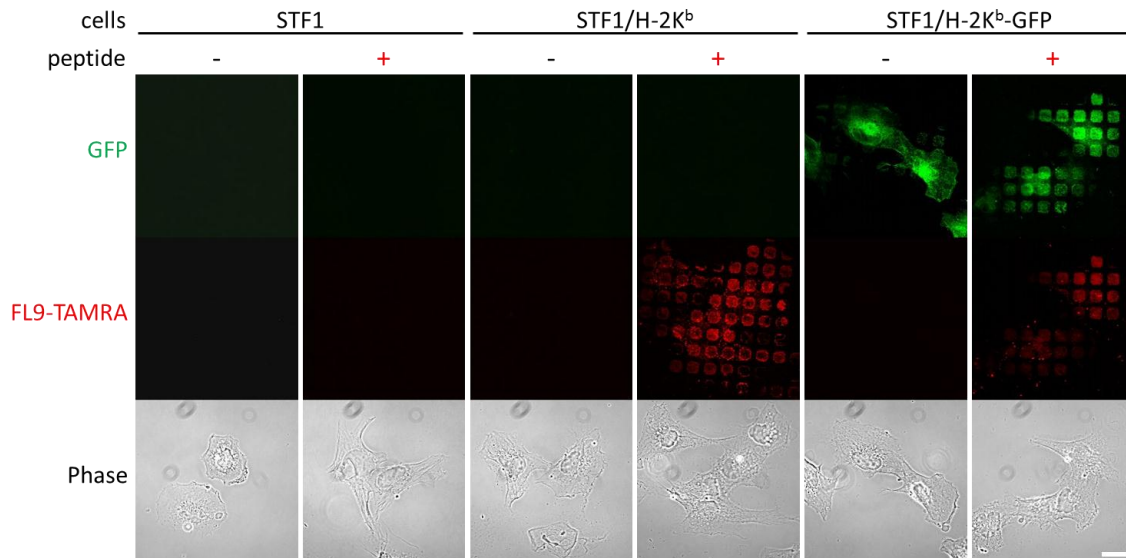


**Figure 1.3.4: Binding of the peptide ligand FL9-TAMRA to the MHC class I receptor H-2K<sup>b</sup> captured by printed antibody.** A pattern of mAb Y3 was printed onto a glass coverslide with a PDMS stamp as in figure 1.3.3, but this time, the antibody was not fluorescently labeled. STF1 (human fibroblast) cells were then seeded onto this pattern and grown for 16 hours. Then, a specific peptide ligand binding to H-2K<sup>b</sup> (the nonapeptide FAPK<sup>TAMRA</sup>NYPAL (FL9-TAMRA), labeled on the lysine side chain with the fluorescent dye TAMRA) was added (1  $\mu$ M final concentration), and cells were incubated at 37°C for four hours. The cells were then washed with phosphate-buffered saline (PBS), fixed, and imaged. STF1 cells stably expressing H-2K<sup>b</sup> without GFP (center panels) show only the red pattern of the peptide bound to the patterned H-2K<sup>b</sup>, while STF1 cells expressing H-2K<sup>b</sup>-GFP show in addition the green fluorescent patterns of the protein (right panels; this is the situation shown in the insert of the schematic in figure 1.3.3 A). As a control, STF1 cells not expressing H-2K<sup>b</sup> show no patterning of peptide or protein (left panels). Bar, 25  $\mu$ m. The peptide binding assay is described in more detail in (Dirscherl et al., 2017).

Another advantage of optical ligand binding assays with printed antibody patterns is that conformation- or assembly-specific antibodies can be used to pattern particular assembly states or conformations of the receptor, and that ligand binding measurements are therefore conducted only on this form of the receptor and not on any of its other forms that are present in the same membrane at the same time. For example, in our example of the H-2K<sup>b</sup> peptide receptor, the printed antibody Y3 only recognizes the heterodimeric form (heavy chain + light chain) of H-2K<sup>b</sup>, but not for example the single heavy chain. This ensures that in the binding assay, only the heterodimeric contributes to the observed binding of the ligand. In principle, ligand association and dissociation kinetics can also be measured in such assays (Löchte et al., 2014).

In addition to binding their ligands, cell surface proteins also interact with other proteins, which may also be membrane-bound, or else cytosolic and soluble. Several groups have used printed protein patterns to demonstrate interactions between cell surface proteins (which they call 'baits') and intracellular (cytoplasmic) non-membrane proteins ('preys') (Löchte et al., 2014; Gandor et al., 2013). In the simplest instance, which is technically a one-hybrid assay, the cell surface 'bait' protein (which is unmodified) is arranged by a printed antibody pattern to catch the intracellular 'prey' protein (which is fused to a fluorescent protein such as GFP). The arrangement of the intracellular 'prey' protein in the shape of the pattern is then observed by microscopy. Ideally, in live cells, one can even follow in real time the association and dissociation kinetics of the intracellular 'prey' protein (Weghuber et al., 2010), such as the recruitment of elements of the signal cascade to the plasma membrane in a kinetic study (Lanzerstorfer et al., 2014). Grinstein and collaborators have used this approach to investigate in an elegant study how the formation of the phagocytic cup is regulated (Freeman et al., 2016). It is also possible to lyse the cells and then follow the dissociation of the cytosolic 'prey' protein from the surface 'bait' protein that is still attached to the antibody pattern (Wedeking et al., 2015). The assay might also be converted to a two-hybrid assay by printing antibodies against an universal epitope tag such as the hemagglutinin (HA) tag and fusing that tag to the extracellular domain of the cell surface 'bait' protein.

Interactions of surface proteins with other surface proteins can be measured in the same way (Löchte et al., 2014). For example, if the question is asked whether two membrane proteins that are located in the plasma membrane of the same cell interact with each other (*'in cis'*), one protein is fused to the epitope tag (such as HA), and the other to GFP. Cells are transfected with both fusion (hybrid) proteins and seeded onto anti-HA patterns. Arrangement of the GFP-fused protein then demonstrates that it interacts, in the natural membrane environment of the live cell, with the HA tagged protein (Weghuber et al., 2010).

### **1.3.5 Technical implementations: Challenges and the way ahead**

In the following, we would like to point out some important technical issues in the implementation of assay systems based on protein patterns, focusing especially on those that we have encountered during recent work with single-cell investigations (Dirscherl et al., 2017), with the aim of perhaps making others, who wish to enter this exciting field, aware of potential problems and how to avoid them.

#### **1.3.5.1 Attaching proteins to the surface**

The simplest way of attaching proteins to a glass surface is to directly print them. A PDMS stamp is inked with the protein solution (usually in phosphate-buffered saline, PBS) and lowered gently onto the glass surface, or else the stamp is laid down with the inked side up, and the coverslip is laid onto it. After some minutes, the contact is broken (and the stamp discarded), the glass surface is washed, and the printed protein pattern is used further. The presence and patterning of the printed proteins can be assessed by scanning force microscopy (LaGraff and Chu-LaGraff, 2006), by fluorescence microscopy (after additional antibody labeling), or by gold labeling and electron microscopy (Dirscherl et al., 2017). The native character of the printed protein then needs to be shown through its functionality. Printed antibodies, for example, should be tested for binding to their antigen. Indeed, it was shown by Graber and collaborators that many antibodies can be printed directly, in this way, onto untreated glass coverslips without loss of specificity of binding (LaGraff and Chu-LaGraff, 2006; St John et al., 1998; David J. Graber et al., 2003).

It is not entirely clear what holds proteins on glass surfaces, though it is fair to speculate that the 'adsorption forces' are a mixture of ionic interactions and hydrogen bonds, depending on the surface and the protein (Messing, 1975). We have found that patterns of antibodies that are printed directly onto untreated glass with PDMS stamps are resistant to wash-off (figure 1.3.5.1)

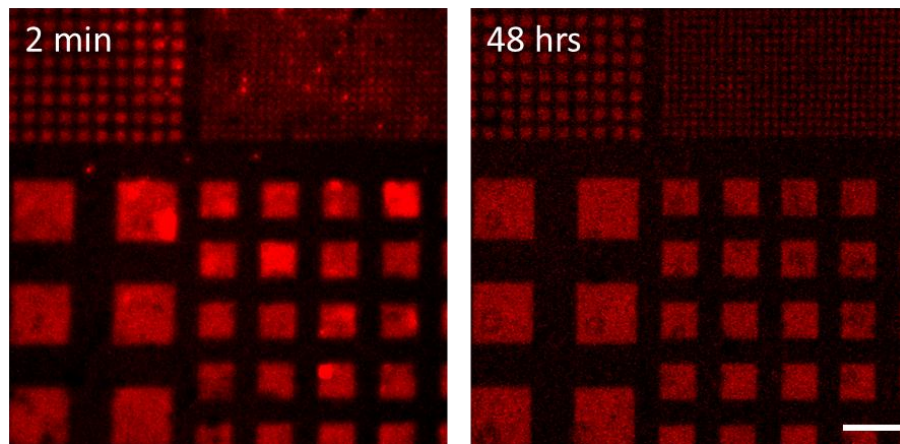


**Figure 1.3.5.1: Directly printed antibody patterns are stable over time.** PDMS stamps were inked with mAb Y3-AF647 in PBS for 15 min and printed onto untreated glass coverslips for 10 min. Patterns were washed and incubated in PBS for the times indicated, then imaged by cLSM. Bar, 50  $\mu$ m.

Unfortunately, we as well as others have encountered problems with this direct printing method, such that some printed proteins were present on the glass but nonfunctional. For example, we have reproducibly obtained patterns of the MHC class I-specific monoclonal antibody (mAb) Y3 in its functional form (Dirscherl et al., 2017) (as judged by its ability to bind MHC class I in the overlaying cell), but this was not achieved for the antibody 25.D1.16 (Dirscherl, unpublished). The most likely reason for this is that when the protein is bound directly to the glass surface, the surface-protein adsorption forces lead to the denaturation (unfolding) and subsequent loss of function of the protein. Whether this will occur with a given protein, or not, is currently impossible to predict. Another possibility is that an epitope in the protein antigen that is accessible to the soluble antibody might not be accessible to the immobilized one, for sterical reasons.

Simple treatments of the glass surface, such as cleaning with ethanol or acid (*e.g.*, 'piranha' solution of sulfuric acid and hydrogen peroxide), are sometimes used to generate a uniform and defined glass surface for printing proteins. In reports from the literature (Seu et al., 2007) and in our own experience, acid treatments alter the glass surface to decrease, or to increase, protein denaturation, depending again on the type of protein. The same may be said for plasma cleaning (Liston, 1989). Thus, even though the surface treatments presumably generate reproducible surface conditions, a given treatment may or may not work for the protein of interest. In our experience, since fabrication-fresh coverslips are usually fat- and dust-free, pre-treatments are not generally necessary.

In addition to the danger of protein denaturation, direct printing of proteins onto glass has the theoretical disadvantage that the protein is printed in a random orientation, which may obscure its binding site for the cellular interaction partner. Whether this actually poses a problem has, to our knowledge, never been systematically investigated. One possible solution to both issues, denaturation and random orientation, is the directed attachment of the proteins of interest to other proteins that are themselves adsorbed to the glass ('anchor proteins'). For example, antibodies may be printed as anchor proteins, which then hold the protein of interest. Or, secondary antibodies may be printed, which then hold the antibody of interest that should interact with the cellular surface protein. Other possible anchor proteins for antibodies are the *S. aureus* protein A or the *Streptococcus* protein G, both of which bind the Fc regions of antibodies with high affinity. It is obvious that this strategy depends on being able to print the anchor proteins themselves in a functional state; for us, direct printing of protein A or G onto glass has been fraught with difficulties. Still, this path is worth pursuing in the future, since indirectly coupled antibodies might be less randomly oriented and better positioned for binding to their ligands.

In addition to printing proteins directly onto glass, and to attaching them to anchor proteins, more elaborate systems that use the very tight biotin-streptavidin interaction have been developed. Printing of streptavidin as an anchor protein (Iversen et al., 2008) allows the attachment of proteins that are biotinylated *in vitro* (using a biotinylating enzyme) or *in vivo*. Since streptavidin has several binding sites for biotin, it can itself be used in a sandwich mode: biotin is attached to the glass surface, streptavidin is bound to the immobilized biotin, and then biotinylated proteins are bound to the free binding sites of streptavidin, resulting in a directed-attachment protein pattern. The patterned attachment of biotin to the glass is not trivial, but several ingenious ways have been developed: Rapp and collaborators have used projection lithography to create biotin patterns by light-triggered covalent coupling of biotin-fluorescein to BSA-coated glass surfaces (Waldbaur et al., 2012). Proteins can also be indirectly attached to the glass *via* nucleic acids; this allows multiplexing (Gandor et al., 2013; Kumar et al., 2016) or the creation of nanometer-sized patterns on DNA origami structures.

### 1.3.5.2 Differentiating between pattern elements and interspaces

A related issue is the differentiation between pattern elements and interspaces, that is, to make sure that the interspaces are free of protein and do not present a highly adhesive surface in the assay. In protein arrays that are subsequently incubated with other proteins (for example, for interaction studies), this is a serious problem that must be overcome by blocking the interspaces. For single-cell experiments with directly printed protein patterns, untreated interspaces may be less of a problem if the cell culture medium (as usually) contains 5-10% fetal bovine serum (FBS), which may accomplish the blocking without the need for further steps. But if the protein pattern is built up in several steps, for example by printing protein A and then binding an antibody to it (see above), then blocking of the interspaces is a necessity. Popular blocking (or 'passivation') reagents are grafted polyethylene glycol, block copolymers, and bovine serum albumin (Falconnet et al., 2006).

An interesting alternative approach that at the same time patterns the protein of interest and blocks the interspaces has been developed by Schütz, Weghuber and collaborators (Weghuber et al., 2010; Lanzerstorfer et al., 2014). In one example (Lanzerstorfer et al., 2014), they use commercially available streptavidin-coated glass slides and print the interspaces of the pattern elements with BSA-Cy5-biotin, blocking them from further interaction. The protein to be patterned, a biotinylated antibody, is then simply added to the prepared slides and binds to the pattern elements only, since the interspaces are blocked.

Another 'negative patterning' technique (*i.e.*, that first derivatizes the interspaces and then the pattern elements, (Falconnet et al., 2006) that does not use printing at all was described by Piehler and collaborators (Löchte et al., 2014). They uniformly coat the glass slide with a maleimide-functionalized polymer and then attach integrin-binding arginine-glycine-aspartate (RGD) peptides to the interspaces only by a photolithographic reaction. The remaining maleimide groups, which are only in the pattern elements, are then used to attach a HaloTag ligand (Los and Wood, 2007). The resulting patterns of HaloTag ligand are used to pattern cell surface receptors that are fused to the HaloTag sequence.

### **1.3.5.3 Binding of cells to the pattern elements**

In single-cell experiments, the printed proteins usually interact with a component of the cell membrane (usually also a protein), arranging it into a pattern of similar shape (see above) (Dirscherl et al., 2017). For this to occur, it must be ensured that the cells spread evenly over the pattern, covering the pattern elements and the interspaces (the areas between the pattern elements) alike. To a cell, however, the pattern element, rich in printed protein, and the interspace, with a glass surface or a different coating on it, may provide very different attachment opportunities. We have seen cells clinging preferentially to the pattern elements or to the interspaces (figure 1.3.5.3 A). The different cell densities achieved on different pattern scales in a competitive setting suggested to us that cells may especially preferentially adhere to substrates with alternating surface structure of a certain scale (figure 1.3.5.3 B), as observed by others (Bettinger et al., 2009; Nikkhah et al., 2012; Nguyen et al., 2016). These properties varied from one cell line to the other, and with the growth state of the cells, and it is likely that with primary cells, such preferential adhesion will be a major problem. Here again, special treatment (passivation) of the interspaces with an agent that is cell-compatible without encouraging too tight binding, for example with polylysine-polyethylene glycol (PLL-PEG), may be helpful (Liu et al., 2009).

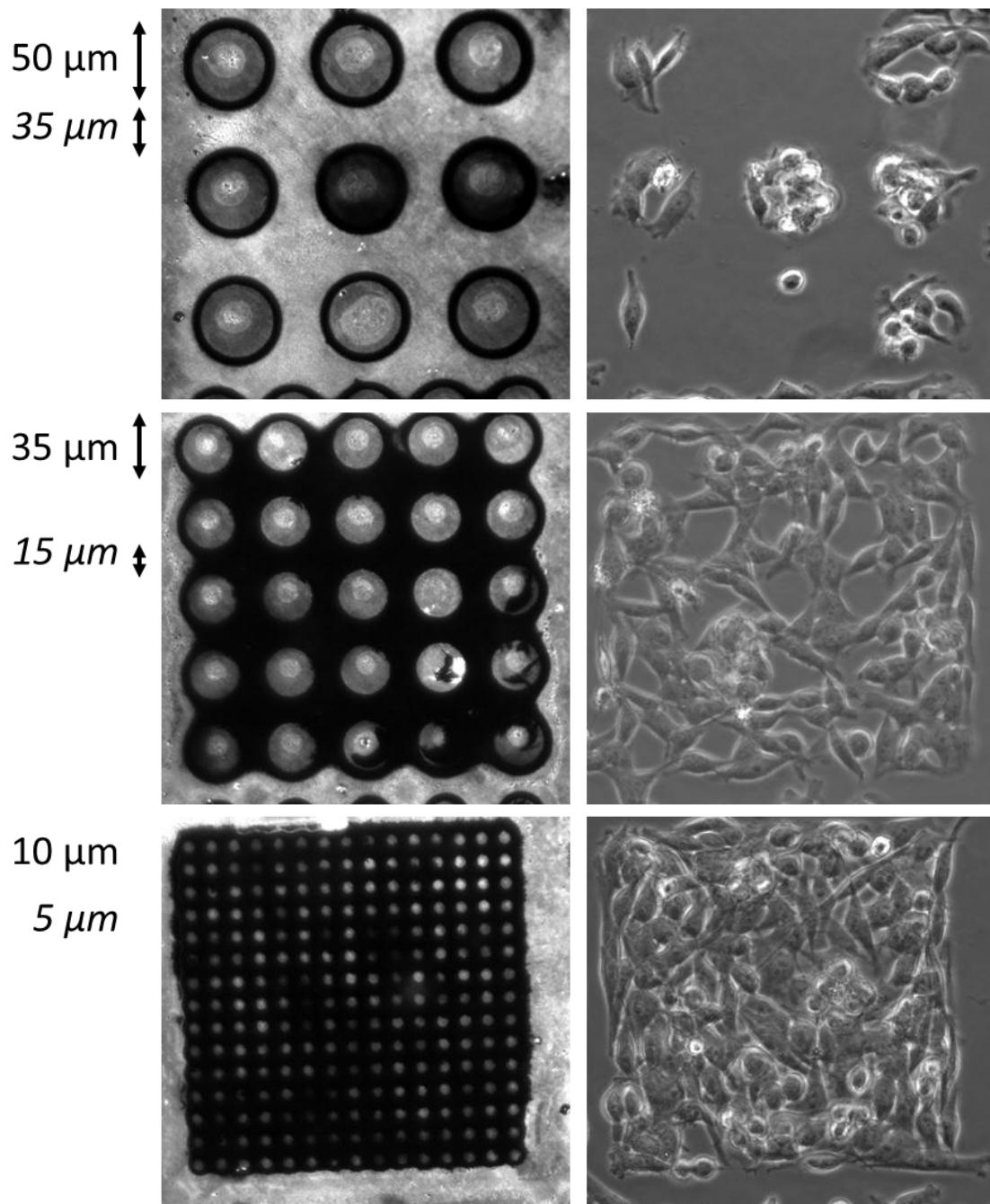


**Figure 1.3.5.3 A: Cells may prefer pattern elements or interspaces, or spread across both.** Patterns of mAb Y3 stained with fluorescent secondary antibody (left) and seeded with HeLa wt cells for 60 hours (right). Widths of pattern elements and of interspaces (in italics) are indicated.



To make sure that cells spread out evenly over the pattern, both elements and interspaces must have an appropriate size and shape, such that they are too small for cells to exclusively occupy. We have found it most convenient to use 10  $\mu\text{m}$  dots or squares as pattern elements and interspaces of 5  $\mu\text{m}$  (or wider) between the dots (figure 1.3.3). This fits with the pattern element sizes between 3 and 10  $\mu\text{m}$  given in the literature for similar approaches (Löchte et al., 2014; Gandor et al., 2013; Sunzenauer et al., 2013). For even spreading, treatment of the interspaces with a protein (*e.g.*, BSA) or other coating (see 3.2.) may also be necessary.

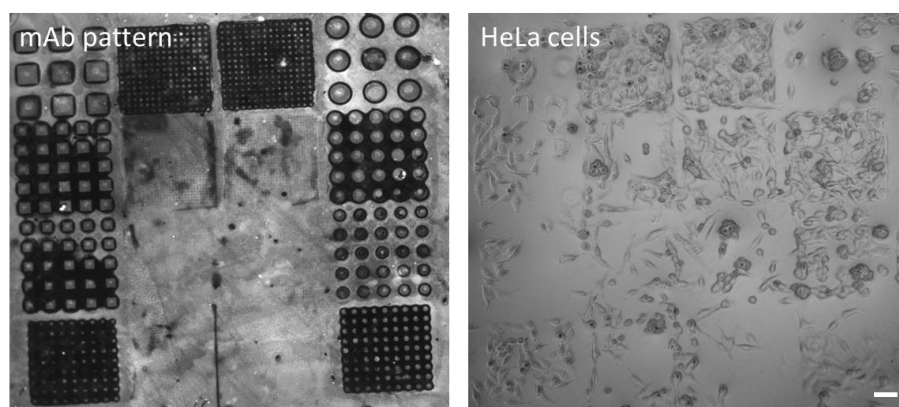


**Figure 1.3.5.3 B: Cells may prefer structured over unstructured areas, and some pattern sizes over others.** The same experiment as in Figure 5, larger area shown. Bar, 50  $\mu\text{m}$ .

The other important concern in single-cell experiments with protein patterns is that the cell membrane is not deformed above the pattern elements. For example, tight binding of non-specific cell surface adhesion proteins to the patterned protein might hold the cell membrane very close to the glass surface right over the pattern elements, whereas in between, the cell membrane might arch upwards because the repulsion between the charges on the plasma membrane and whatever is used to passivate the interspaces, or because of the natural urge of the cell to move or to undulate its plasma membrane. In such cases, the plasma membrane will acquire pattern-shaped protuberances that are closer to the glass surface than the remainder of the cell surface, and thus in a different focal plane in the confocal laser scanning microscope (cLSM), or more prominent in total internal reflection fluorescence (TIRF) microscopy. This might mislead the investigator to believe that an accumulation of the protein of interest has occurred over the pattern elements through specific interaction, when in reality, the protein is still evenly distributed on the plasma membrane. It is therefore very important to use negative controls such as test proteins that are not bound by the printed protein, and printed proteins that do not

bind to the test protein of interest. We think that it is essential to show that such plasma membrane deformations do not occur (Dirscherl et al., 2017), for example by staining with rhodamine phalloidin (which binds to the cortical actin cytoskeleton), anti-actin antibody, wheat germ agglutinin, which binds to the protein- and lipid-linked glycans of the plasma membrane, or perhaps a fluorescent lipid that is inserted into the membrane.

### 1.3.5.4 Readout of cell-based assays

In all publications known to us, readout of single-cell experiments with protein patterns is by cLSM or TIRF microscopy. The intracellular portion of the protein of interest is fused to a fluorescent domain (most frequently the green fluorescent protein, GFP), and in the experiment, the arrangement of the GFP into the printed pattern is followed. In principle, such patterning may be followed in live cells, such that changes can be observed over time; in this case, special care must be taken to avoid the bleaching of the fluorescent protein domains, which easily occurs.

An alternative detection method is the staining of the protein of interest with antibodies, and subsequent detection by immunofluorescence microscopy. In our experience, the gap between the glass surface and the cell is very narrow, and antibodies (molecular weight (MW) 155 000) do not easily penetrate into it, and cells must be permeabilized or lysed before proteins of interest can be stained. In our experiments, the glass-cell gap did admit fluorescently labeled nonapeptides (MW 1200).

Any serious use of single-cell experiments with protein patterns, such as *in cis* interaction assays or ligand screening in a high throughput format, will require quantification of the microscopic readout. This is not trivial, since intracellular background signals can occur. For example, our model protein H-2K<sup>b</sup>-GFP is present to only about 50% at the cell surface, whereas the remainder is in the endoplasmic reticulum (ER). This ER background is visible in addition to the surface-patterned protein in our experiments, which are done with cLSM (figure 1.3.3 B, label e). Thus, simply integrating over one pattern element and comparing to an interspace area of similar size (similar to what one would do when, for example, quantifying a band in a protein gel) does not yield reproducible results. Instead, the information from many pattern elements must be processed. We have found it most convenient to compare the spatial distribution of the pattern elements (*i.e.*, the fluorescence of the printed protein) and the protein of interest by means of the Pearson coefficient (Dirscherl et al., 2017) (Bolte and Cordelières, 2006). To this end, it is best if the printed antibody is directly covalently labeled with a fluorescent dye (figure 1.3.3 A); this can easily be achieved with N-hydroxysuccinimide (NHS) chemistry. Pearson coefficient analysis has

the added advantage that it can be standardized between experiments and even be automated for high-throughput analysis. Alternatively to this analysis, TIRF images may, if the cell type is right and the ER is sufficiently far above the plasma membrane, avoid the background signal altogether.

### **1.3.6 Conclusion**

Single-cell experiments with protein patterns are useful for basic research, assay, and screening applications. Their special advantage is that the cell surface proteins that are investigated are in their native protein and lipid environment, and as such, they might be a significant extension to conventional printed protein arrays that are probed not with cells but with ligands or recombinant proteins, with exciting future development opportunities.

### **1.3.7 Materials and Methods**

Patterns of antibodies on glass surfaces were produced, incubated with cells, and evaluated by microscopy as described (Dirscherl et al., 2017). The same publication also lists the cell lines, antibodies, and reagents.

For the experiment in figure 1.3.3, patterns of fluorescently labeled mAb Y3 (Y3-AF647) were PDMS-printed for 15 min on glass coverslips. Then, Vero cells stably transduced with H-2K<sup>b</sup>-GFP were seeded on the Y3 patterns, incubated at 37 °C for 24 hours, fixed, and imaged by confocal laser scanning microscopy (cLSM).

For the experiment in figure 1.3.4, patterns of mAb Y3 were PDMS-printed for 15 min on glass coverslips. STF1 wt cells, either untransduced or stably transduced with H-2K<sup>b</sup>-GFP, were seeded on the Y3 patterns and incubated at 37 °C until they adhered, then shifted to 25 °C and incubated overnight. The next day, fluorescently labeled peptide-ligand (1 μM FL9-TAMRA) was added and cells were incubated at 37 °C for 4 hours, washed with PBS, fixed, and imaged with cLSM.

For the experiment in figure 1.3.5.1, fluorescently labeled mY3 (AF647) was printed for 10 min and the protein pattern was then incubated in PBS for 2 min or 48 hrs at 4 °C, then rinsed with PBS and imaged by cLSM.

For the experiment in figures 1.3.5.3 A and 1.3.5.3 B, patterns of mAb Y3 were PDMS-printed for 60 min on plasma-cleaned glass coverslips, the interspaces were blocked with 5% milk for 30 min, and the patterns were stained for 60 min with goat anti-mouse antibody conjugated with Alexa Fluor 488 (gam-

AF488). Then, HeLa wt cells were seeded on the Y3/gam-AF488 patterns and incubated at 37 °C for 60 hours and imaged with cLSM.

### **1.3.8 Acknowledgements**

We thank Amélie Skopp, Nikolett Nagy, Natalia Lis, and Catherine Jacob-Dolan for their dedicated work on the project, Uschi Wellbrock for expert technical support and for reading the manuscript, and the Federal Ministry for Education and Research (BMBF) for financial support (Grant No. 031A153A).

### 1.3.9 Copyright Transfer Agreement

#### JOHN WILEY AND SONS LICENSE TERMS AND CONDITIONS

Feb 23, 2018

This Agreement between Mrs. Cindy Dirscherl ("You") and John Wiley and Sons ("John Wiley and Sons") consists of your license details and the terms and conditions provided by John Wiley and Sons and Copyright Clearance Center.

**License Number** 4294850670820

**License date** Feb 23, 2018

**Licensed Content Publisher** John Wiley and Sons

**Licensed Content Publication** ENGINEERING IN LIFE SCIENCES (ELECTRONIC)

**Licensed Content Title** Protein micropatterns printed on glass: Novel tools for protein ligand binding assays in live cells

**Licensed Content Author** Cindy Dirscherl, Sebastian Springer

**Licensed Content Date** Sep 15, 2017

**Licensed Content Pages** 8

**Type of use** Dissertation/Thesis

**Requestor type** Author of this Wiley article

**Format** Print and electronic

**Portion** Full article

**Will you be translating?** No

**Title of your thesis /dissertation** Antibody micropatterns as a tool to study MHC class I molecules

**Expected completion date** Mar 2018

**Expected size (number of pages)** 190

**Requestor Location** Mrs. Cindy Dirscherl

Ingelheimer Strasse 34

Bremen, 28199

Germany

Attn: Mrs . Cindy Dirscherl

**Publisher Tax ID** EU826007151

**Total** 0.00 EUR

## 1.4 MHC class I molecules

### 1.4.1 MHC class I and its role in the immune response

The gene cluster called the major histocompatibility complex (MHC) is located on chromosome 6 in humans and chromosome 17 in mice. The genes encoding the  $\alpha$  chain of the MHC class I proteins (also called MHC class I molecules) are found in this complex. In humans, there are three main gene loci called human leukocyte antigen (HLA), and the encoded proteins are thus termed HLA-A, HLA-B, and HLA-C. In mice, these loci are referred to as the Histocompatibility-2 (H-2) genes H-2K, H-2D, and H-2L. Each of these genes encodes the  $\alpha$  chain of the respective MHC class I protein; since the expression is co-dominant, human and mouse cells produce up to six different allotypes of the MHC class I heavy chain. The light chain beta-2 microglobulin ( $\beta_2m$ ) of the MHC class I protein is encoded by another gene outside the MHC on a different chromosome (chromosome 15 in humans and chromosome 2 in mice). Both chains associate non-covalently to form the MHC class I protein.

MHC class I molecules are expressed on the surface of all nucleated cells in mammalian organisms and are part of the cell-mediated adaptive immune system, where they play a central role in the immune response against intracellular parasites, viruses, and tumors. They bind peptides in the cell interior and carry them to the plasma membrane. At the cell surface, the MHC class I-peptide complex is bound by the T cell receptor (TCR) of CD8<sup>+</sup> cells, which is similar in shape and variability to the Fab region of an antibody. Since all those T cells that recognize self-peptides bound to MHC class I are eliminated in the thymus, the binding of the TCR to the peptide-MHC complex signifies the presence of a non-self protein antigen inside the cell. The antigen-presenting cells that are thus recognized are eliminated by the initiation of apoptosis.

The MHC class I genes are the genes with the highest degree of polymorphism in mammals. In humans, an individual allele (gene) or allotype (the protein derived from it) is characterized by a four-digit number, such as HLA\*02:01. In mice, alleles are labeled with superscript indices (such as H-2D<sup>b</sup> or H-2K<sup>b</sup>). MHC class I polymorphism has a major effect on antigen recognition by T cells; it lies primarily in the peptide-binding groove and determines which kinds of peptides an allele can bind. Allelic variation of MHC class I molecules thus extends the range of peptides that can be presented to T cells in a population and limits the spread of infections.

### 1.4.2 Structure and folding of MHC class I molecules

MHC class I molecules consist of the MHC  $\alpha$  chain – also termed MHC class I heavy chain or simply heavy chain – and the non-covalently bound light chain, called  $\beta_2m$ . The folded heavy chain consists of three genetically defined domains, the  $\alpha_1$ ,  $\alpha_2$ , and  $\alpha_3$  domains (see figure 1.4.2 for reference). In the folded protein, the  $\alpha_1$  and  $\alpha_2$  domains together form a single structural unit, a binding groove for peptides that consists of an eight-stranded beta sheet topped by two alpha helices. This structural unit is often called the  $\alpha_1/\alpha_2$  superdomain. The  $\alpha_3$  domain of the heavy chain, and the  $\beta_2m$  light chain that binds to it, both adopt conventional IgC folds. Newly synthesized MHC class I heavy chains are cotranslationally inserted into the ER and, after folding, bind  $\beta_2m$ . The MHC class I heterodimer thus formed then binds to the peptide-loading complex (PLC). The PLC functions as a quality control system to keep the MHC class I heterodimer in a peptide-receptive state to allow for the scanning of optimal peptides (see (Van Hateren et al., 2010) for review). The antigenic peptides are generally derived from proteins in the cytosol of the infected cell, and they are then actively transported into the lumen of the ER by the TAP (transporter associated with antigen processing). The stable binding of peptide finally releases the MHC class I-peptide complex from the PLC; it is then transported to the cell surface to fulfill its function.

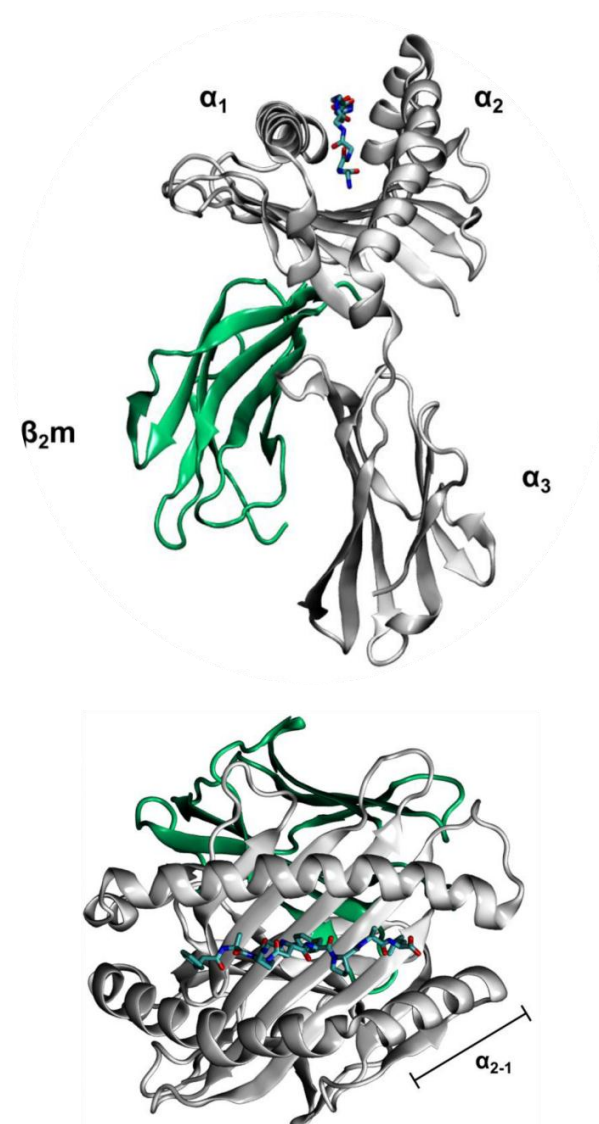


**Figure 1.4.2: Crystal structure of the luminal domain of MHC class I complex and the peptide binding groove.** H-2K<sup>b</sup> bound to the FAPGNYPAL peptide. **Upper panel**, peptide binding groove ( $\alpha_1$  and  $\alpha_2$  domains) and the  $\alpha_3$  domain of the heavy chain are shown in grey, and the light chain  $\beta_{2m}$  is shown in green. **Lower panel**, top view of the peptide binding groove ( $\alpha_1$  and  $\alpha_2$  domains) and the beta sheet. *Figures courtesy of Esam Tolba Abualrous.*



### 1.4.3 Peptide binding

Stable peptide binding is important to generate a peptide-MHC class I complex whose peptide cannot be exchanged at the cell surface to prevent binding of exogenous peptides that would falsely initiate the elimination of uninfected cells (bystander killing).

The MHC class I peptide binding groove is closed at both ends, and thus only peptides with a length of eight to ten amino acids can bind. The bound peptide is held by hydrogen bond networks at both the amino and carboxy terminus (Bouvier and Wiley, 1994). Anchor residues at specific positions in the peptide sequence bind into pockets at the bottom of the peptide binding groove and thus stabilize the complex further.

Each MHC class I allotype carries specific residues around the binding pockets of the peptide binding groove such that it binds a set of allotype-specific peptides with the corresponding anchor residues (Madden, 1995). To determine the sequence motif of peptides that bind to a particular class I allotype, peptides are eluted from purified MHC class I complexes by acid denaturation and analyzed by mass spectrometry to identify their polypeptide sequence (Bassani-Sternberg and Coukos, 2016). Synthetic peptides can then be produced and used for analysis of MHC class I molecules. Table 1.4.3.1 lists the high-affinity peptides for the murine allotypes K<sup>b</sup> and D<sup>b</sup> that were used in this project. For control experiments, peptides specific for human MHC class I allotypes were used. The indicated fluorophores were always attached to the side chains of the peptide at positions that do not interfere with peptide binding as determined from the crystal structures of the MHC class I-peptide complexes.

#### 1.4.3.1 MHC class I peptide exchange

In his PhD project, Sunil Kumar Saini of the Springer group investigated the peptide binding properties of peptides to MHC class I and discovered that one can use small molecules such as dipeptides to modulate the binding properties. It was then shown that it is possible to fold MHC class I proteins *in vitro* with small molecules to bring them into, and keep them in, a folded and peptide-receptive state (Saini, 2014).

Besides folding, dipeptides can be used to catalyze peptide exchange on recombinant proteins as well as on the surface of living cells (Saini et al., 2015, 2013b). A proposed mechanism for this dipeptide-mediated peptide exchange suggests that the dipeptides interact with the F pocket of the peptide binding groove (which usually binds the side chain of the carboxy-terminal amino acid of the full-length peptide) and thus increase the dissociation rate of the leaving peptide (Saini et al., 2015). This exchange technology has broad use in diagnostic applications, where it allows for the rapid generation of

MHC class I proteins loaded with any peptide of interest; such recombinant peptide-MHC complexes are used in MHC multimers (such as tetramers, dextramers, streptamers, etc.) for the staining of patient T cells in immunotherapy approaches (Bentzen and Hadrup, 2017).

According to the peptide binding specificities of individual MHC class I allotypes, specific dipeptides need to be tested and identified for each allotype. In the case of K<sup>b</sup>, the dipeptide glycyl-cyclohexylalanine (GCha) gave the best results for peptide exchange (see table 1.4.3.1).

**Table 1.4.3.1: MHC class I-specific peptide ligands.** Peptide sequences are in the single letter amino acid code. The fluorophores (brackets) are attached to the lysine residues of the peptides to not interfere with peptide binding. Allotype specificities and origin of peptides as indicated.

	Abbreviation	Amino acid sequence	MHC class I allotypes	Source of peptide
Full-length peptides				
1	SL8	SIINFEKL	K <sup>b</sup>	Ovalbumin (257-264)
2	SL8 <sup>TAMRA</sup>	SIINFEK(TAMRA)L	K <sup>b</sup>	
3	FL9	FAPGNYPAL	K <sup>b</sup> , D <sup>b</sup>	Sendai virus (324-332)
4	FL9 <sup>TAMRA</sup>	FAPK(TAMRA)NYPAL	K <sup>b</sup> , D <sup>b</sup>	
5	FL9 <sup>Dy633</sup>	FAPK(Dy633)NYPAL	K <sup>b</sup> , D <sup>b</sup>	
6	NV9	NLVPMVATV	HLA-A2	HCMV (protein pp65)
Dipeptides				
7	GCha	Glycyl-cyclohexylalanine	K <sup>b</sup>	-

#### 1.4.4 Forms and stability of MHC class I molecules at the cell surface

Peptide binding is an essential step in the assembly of a stable MHC class I complex. In TAP mutant cells, where the supply of peptides into the endoplasmic reticulum (ER) is disrupted, newly synthesized MHC class I proteins are held in the ER in a partly folded state with low-affinity peptides or without ligands at all (Townsend et al., 1989). This explains why TAP1/TAP2 mutant cells (such as the STF1 cells used in our studies) fail to express MHC class I at the cell surface.

As described above, different forms of MHC class I exist, namely the peptide-bound trimer, the empty dimer of heavy chain and  $\beta_2m$ , and the free heavy chain. These forms have been investigated in previous

studies, and it was shown that they have different stabilities and lifetimes at the cell surface. The trimeric complex, consisting of the heavy chain,  $\beta_2m$  and the peptide, is read out by cytotoxic T cells and represents the most stable form of MHC class I proteins. When the peptide dissociates from this complex, the 'empty' dimer of heavy chain and  $\beta_2m$  remains. Since binding of peptide and  $\beta_2m$  is cooperative, the dimer generally starts to disintegrate once the peptide has dissociated; the  $\beta_2m$  is released into the environment of the cell as a soluble protein, and the 'free' heavy chain is removed from the cell surface, trafficked to the lysosomes, and destroyed there by proteolysis (Montealegre et al., 2015). This agrees with the observation that the loss of peptide quickly leads to the unfolding of the peptide binding site (Zacharias and Springer, 2004). Other studies have claimed that free heavy chains are permanently present at the cell surface at least in some disease states (Tsai et al., 2002).

#### **1.4.5 STF1 cells, TAP deficiency, and class I stability**

After a few trial experiments with Vero and HeLa cells, I decided to use STF1 cells for my cell experiments. STF1 cells are human fibroblasts isolated from a patient that lacked the TAP2 transporter; STF1 cells are thus unable to import peptides into the ER and consequently cannot load MHC class I with cytosol-derived peptides. Since ER proteolysis is generally unable to break up proteins into peptides, this leaves very few peptides as potential class I ligands, most of them derived from signal peptides via the signal peptidase. In STF1 cells, like in other TAP-deficient cells such as RMA-S (Townsend et al., 1989), mostly unstable dimers and trimers with low-affinity peptides are therefore found at the plasma membrane (Hein and Springer, 2018). Their steady-state amounts are low because the  $\beta_2m$  dissociates from empty dimers, and the free heavy chains are efficiently endocytosed and degraded (see section 5.1).

To obtain larger amounts of class I molecules at the surface of TAP-deficient cells, one can make experimental use of the 25 °C effect. Incubation of murine TAP-deficient cells at 25 °C leads to a remarkable increase of empty MHC class I dimers at the surface at steady state (Ljunggren et al., 1990). This is because the binding affinity of  $\beta_2m$  to the heavy chain is strongly temperature-dependent; at 25 °C,  $\beta_2m$  binds more tightly. For endocytic removal from the cell surface, dissociation of  $\beta_2m$  is required, and so the empty dimers do not dissociate at 25 °C and thus do not disappear from the cell surface, resulting in an increase in their steady-state levels (Montealegre et al., 2015). If cells are afterwards shifted to 37°C, the accumulated dimers dissociate, and the resulting free heavy chains are rapidly removed from the cell surface (Montealegre et al., 2015). One can use this 25 °C effect to

accumulate empty dimers at the cell surface and to then load them with exogenously added peptides (Montealegre et al., 2015).

An alternative way to stabilize empty MHC class I proteins at the cell surface is to use MHC class I disulfide mutants, where the F-pocket is stabilized by a disulfide bond between residues 84 and 139. This mutation mimics the peptide-bound state of class I, and these disulfide-stabilized class I molecules thus have a very long half-life as empty dimers at the cell surface (Hein et al., 2014; Hein and Springer, 2018).

### 1.4.6 Interactions of MHC class I *in trans*

Direct cell-cell communication is generally achieved through the interaction of cell surface receptors with ligands on other cells. The interaction of peptide-MHC class I complexes (pMHCs) of antigen presenting cells with the TCR of T cells is one example of such an *in trans* interaction (Garcia et al., 1996). Excitingly, MHC class I does not exclusively interact with TCRs. The additional *in trans* interactions of MHC class I are often very specific and are only found in particular cells or tissues. Additionally, there are often differences between human and murine MHC class I. Due to the complexity, I will give an overview with selected examples of alternative *in trans* interactions of MHC class I that were identified with references to review articles, rather than a complete list.

#### 1.4.6.1 MHC class I-T cell receptor interaction

Cytotoxic T cells (or simply T cells) carry out the adaptive immune response. The T cell receptors (TCRs) recognize antigens (peptides) of eight to ten amino acids that are presented on MHC class I at the cell surface. The interaction between TCR and pMHC is highly specific and well-investigated (Townsend et al., 1985; Bodmer et al., 1989). Upon successful binding of the TCR (and CD8) to the pMHC, an immunological synapse is formed (which involves many pMHC-TCR complexes as well as additional adhesion proteins) that initiates a signaling event inside the T cell. Depending on the developmental stage of the T cell, this signal may lead to differentiation and/or survival of the T cell, or to the killing of the presenting cell by induced apoptosis (Huppa and Davis, 2003).

The affinity of a single TCR to a single pMHC is rather low, in the micromolar range (Matsui et al., 1991). In order to form the required tight interaction between a T cell and the antigen presenting cell, the immunological synapse relies on many protein-protein interactions (avidity effect). For diagnostic purposes, the low-affinity limitation was overcome by the development of tetrameric (or otherwise

multimeric) pMHC complexes (MHC I tetramers or multimers in short) that are used to stain T cells (see section 1.4.6.2)

Immunological synapse formation and the involved proteins have been studied intensely over the past 20 years and are reasonably well understood (Bromley et al., 2001; Huppa and Davis, 2003). The detailed mechanism of T cell activation and signaling is still being investigated. One current finding describes the requirement of a catch-bond interaction between pMHC and TCR initiate signaling (Das et al., 2015; Kim et al., 2009).

For signal transmission into the cell, simple binding of the pMHC to the TCR is not sufficient, but the top domains of the TCR must be tilted or bent by the pMHC ligand. The required bending force can be achieved by the movement of the T cell relative to the antigen presenting cell, or by the centripetal transport of TCR complexes by actin flow in the T cell (Yu et al., 2010). Interestingly, only high affinity agonist peptide can deform the TCR, whereas peptides with low affinities dissociate from the TCR when force is applied (Das et al., 2015).

#### **1.4.6.2 MHC class I tetramers**

Due to the low affinity of single pMHC-TCR interactions, multimers such as tetramers or dextramers are used for the staining of T cells. For the diagnostic screening of T cells, commercially available MHC class I tetramers are used. Although they are common, their production remains complicated, slow, and cost-intensive. To generate MHC class I tetramers, recombinant MHC class I molecules are folded *in vitro*. They are then biotinylated and loaded onto streptavidin to form a tetrameric complex (Altman et al., 1996). Recombinant MHC class I proteins only fold in the presence of peptide. In order to load the MHC class I tetramers with the peptide of interest, they are usually first folded with a UV-cleavable peptide in the folding reaction, which is then replaced by UV irradiation. During UV exposure, the folding peptide is specifically cleaved and dissociates from the folded MHC class I, such that an incoming peptide can bind (Rodenko et al., 2006). Although there are improvements in the MHC class I tetramer production such as ‘one pot reactions’ (Leisner et al., 2008), the process remains technically demanding, and for some allotypes such as HLA-B\*44:02, HLA-B\*27:05, and H-2L<sup>d</sup>, *in vitro* folding is still not possible at all, or with all peptides (S. Springer, pers. commun.).

### 1.4.6.3 Insulin receptor in neurons

Despite their prominent role in the immune system, MHC class I proteins have also non-immunological functions in specialized tissues such as the nervous system (Shatz, 2009). One example is a novel MHC class I signaling pathway detected in neurons of the hippocampus, where MHC class I inhibits insulin receptor signaling (Dixon-Salazar et al., 2014). While glucose uptake in neurons is independent of insulin receptors (Tomlinson and Gardiner, 2008), synapse density is regulated by insulin signaling. Interestingly, MHC class I was found to interact with the insulin receptors and to specifically inhibit insulin signaling. Co-immunoprecipitation experiments from hippocampal lysates suggested an interaction between MHC class I and the insulin receptor. Further experimentation then led to a model mechanism where MHC class I unmask a cytoplasmic epitope of the insulin receptor, thus changing phosphorylation patterns (Dixon-Salazar et al., 2014). This interaction correlates with the observation that changes in MHC class I expression in the aging and diseased brain regulate neuronal insulin sensitivity. However, the underlying molecular mechanism that mediates this interaction was not completely elucidated. Several models were proposed that include as well *in trans* as *in cis* interactions of both proteins.

### 1.4.7 Known *in cis* interactions of MHC class I

While some researchers have identified alternative ligands for MHC class I *in trans* (see section 1.4.6), others have discovered that MHC class I can also interact with proteins of the same cell on the plasma membrane. Several interaction partners involved in these *in cis* interactions have been identified for human and murine MHC class I, which will be briefly introduced in the following. Excitingly, homotypic *in cis* interactions (*i.e.*, interactions between one MHC class I protein and another MHC class I protein) were also suggested by the investigations of other researchers, although their hypotheses often lacked clear experimental evidence. In the following paragraph, I give a brief overview about what is known about homo- and heterotypic MHC class I *in cis* interactions.

#### 1.4.7.1 Homotypic *in cis* interactions of human MHC class I

Matko and Edidin detected homotypic *in cis* interactions by fluorescence resonance energy transfer (FRET) (Matko et al., 1994). They used fluorescent antibodies to label MHC class I to perform FRET measurements. Their experiments showed that the HLA-A cluster formation correlates with the presence of the HC-10 epitope at the cell surface. The HC-10 antibody binds specifically HLA-A and –B free heavy chains (see section 1.5 for antibody reference), indicating the involvement of free heavy chains in the cluster formation. This hypothesis was strengthened by their observation that the addition of exogenous  $\beta_2m$  reversed the cluster formation (Matko et al., 1994). Interestingly, the HC-10 signal was not influenced by the addition of  $\beta_2m$ . In agreement with these observations, the authors concluded that the HLA-A clusters consist of a mix of MHC class I trimers and free heavy chains. Later investigations of HLA-A cluster formations in B cells have also implicated free heavy chains and MHC class I trimers (Bodnár et al., 2003).

#### 1.4.7.2 Homotypic *in cis* interactions of murine MHC class I

Zuñiga and coworkers performed co-immunoprecipitation experiments with conformation-dependent antibodies and showed that dimers and trimers of the murine allotype  $L^d$  exist (Capps et al., 1993). Through the intelligent choice of anti-MHC class I and anti- $\beta_2m$  antibodies, they were able to identify free MHC class I heavy chains as the specific components of the detected dimers. For further analysis, they compared reducing and non-reducing SDS electrophoresis and demonstrated that the dimers can be reduced to monomers. This observation led them to suggest that the conserved cysteines in the cytoplasmic tail of the investigated MHC class I allotypes form disulfide bonds that lead to their

dimerization (though this does not explain the formation of trimeric complexes). Although they propose a functional role for the detected clusters, they did not formally show this in their work.

Also, they were not able to conclude where the dimers are formed in the cells. They co-immunoprecipitated from whole cell lysates, and it cannot even be excluded that the observed dimers are formed post lysis.

### **1.4.7.3 Heterotypic *in cis* interactions of murine MHC class I**

Similar to the FRET measurements of human MHC class I (see section 1.4.7.1), Liegler and coworkers performed analogous experiments for murine H-2 allotypes by staining with different anti-MHC class I antibodies. According to their results, H-2 molecules exist only as monomers on the cell surface of NIH3T3 cells. Interestingly, heterotypic *in cis* interactions were detected between H-2K and H-2D molecules and the insulin receptor (Liegler et al., 1991). The researchers used the conformation-independent anti-H-2K antibody 28.12.8 (see section 1.5 for antibody reference) for their experiments. Therefore one can only speculate about which MHC class I form (trimer or free heavy chain) is responsible for the observed interactions, since all possible conformations are labeled by this antibody.

Further examples of heterotypic *in cis* interactions are described in the next section (1.4.8).

### **1.4.8 MHC class I interact *in trans* and *in cis* with inhibitory receptors**

In some cases, MHC class I proteins were found to bind the same interaction partner *in trans* and *in cis*. Natural killer (NK) cells express MHC class I-specific inhibitory receptors on their cell surface that protect healthy cells from NK cell attacks ('missing self hypothesis', see Held and Mariuzza, 2011 for review). The general idea is that loss of MHC class I surface expression is caused by an attempt of the cell to escape cytotoxic T cell surveillance, for example because it is infected by a virus and antigen presentation is inhibited by viral immunoevasin proteins; or because it bears a tumorigenic mutation. Such diseased cells are removed by NK cells. *In cis* interactions of such immunoreceptors and MHC class I have been proposed to modulate the threshold at which cellular activation signaling leads to a biological response. In the following sections, example of such immunoreceptors will be described.



#### 1.4.8.1 Ly49 and KIR receptor families

Several NK cell receptors have been identified that interact with MHC class I *in trans*, such as the murine Ly49 receptor family. Interestingly, many of these receptors can acquire an alternative conformation ('stalk') that allows for an *in cis* interaction with MHC class I molecules on the same membrane (Doucey et al., 2004).

The murine NK receptor Ly49A, which interacts most strongly with H-2D<sup>d</sup> (D<sup>d</sup>), but also with other allotypes with lower affinities, measures MHC class I surface levels. While binding of Ly49A to D<sup>d</sup> requires peptide, it is independent of the peptide sequence. This was explained by the finding that the interaction sites of Ly49A are located underneath the peptide binding groove of MHC class I, such that Ly49A binds not to the peptide but to the peptide-induced conformation of the class I heavy chain (Deng et al., 2008). Interestingly, the binding capacity *in trans* is modulated by the D<sup>d</sup> expression level of the NK cell itself (as compared to NK cells lacking D<sup>d</sup> expression). The *in cis* interaction of D<sup>d</sup> and Ly49A on the same cell restricts the number of Ly49A molecules available for *in trans* binding and thus reduces inhibition of NK cells through Ly49A (Doucey et al., 2004).

In human NK cells, killer cell immunoglobulin-like receptor (KIRs) correspond to the Ly49 receptors in rodents, where they also monitor MHC class I expression levels by binding *in trans*. KIRs pre-dominantly bind the classical MHC class I family members while different family members recognize only specific MHC class I allotypes. In contrast to the murine Ly49 family, human KIRs bind onto the top of the peptide binding domain of MHC class I, similar to the MHC class I-TCR interaction but at distinct binding sites (Sun et al., 2000).

#### 1.4.8.2 LILR and PIR receptor family

Other inhibitory MHC class I receptors include leukocyte immunoglobulin-like receptors (LILRs) and their murine homologues, paired immunoglobulin-like receptors (PIRs). A subset of this receptor family, LILRB1/LILRB2 and PIRB, binds a wide range of classical and non-classical MHC class I. Structural knowledge of these interactions is mainly obtained from the LILRB1-HLA-A2 crystal structure (Willcox et al., 2003). While LILRB1 consists of a total of four immunoglobulin-like domains (D1-D4), the structure resolved the complex of the D1 and D2 domains with HLA-A2. According to the structure, *in trans* binding of LILRB1 to HLA-A2 on the effector cell, comprises the  $\alpha_3$  domain of the HLA-A2 free heavy chain and  $\beta_2m$  and the two N-terminal immunoglobulin-like domains (D1 and D2)(Masuda et al., 2007). For *in cis*

binding of HLA-A2 on the same cell, LILRB1 is presumably bent back at the connecting region between D2 and D3 to reach the same binding sites on HLA-A2 accordingly (see figures in Held and Mariuzza, 2008).

### 1.4.9 Methods for the investigation of *in cis* interactions

Various methods exist for the investigation of protein-protein interactions (as described in sections 1.4.7 and 1.4.8). In the following, I highlight a few other common methods and comment on their use for the investigation of MHC class I *in cis* interactions.

Common biophysical methods are surface plasmon resonance (SPR) and fluorescence polarization (also called anisotropy). SPR detects changes in the refractive index at the surface of a sensor chip (Nguyen et al., 2015). An incident light beam is reflected at a gold surface, and the reflected light is detected as resonance signal. The sensor chip is a glass slide with a thin gold coating that is functionalized with the protein of interest. The chip is then flooded with the ligand. During ligand binding, mass accumulates at the sensor surface which is detected as an increase in signal. After the binding, the sensor chamber is washed with buffer until the ligand dissociates, the mass reduces, and the resonance signal decreases accordingly. Repetitions of this cycle allow for the calculations of kinetic binding constants ( $k_a$  and  $k_d$ ) and, from them, the equilibrium affinity constant  $K_D$ , assuming simple law of mass action kinetics. SPR measurements are usually performed with purified proteins, and they have been applied to MHC class I proteins to determine class I-TCR binding constants with purified TCR (Gao et al., 2007). While protein-protein interactions with purified peptide-bound MHC class I exist, SPR does not allow for the detailed study of free heavy chains due to their instability. Although Burian et al. studied the interaction partners of free heavy chains of the non-classical MHC class I, HLA-F, which they generated by acid treatment to remove  $\beta_2m$  (Burian et al., 2016)

Fluorescence polarization (FP; also called fluorescence anisotropy, FA) is another commonly used technique to characterize protein-protein interaction and derive binding constants (Valeur and Berberan-Santos, 2013). With this technique, one interaction partner is labeled with a fluorophore, which is then excited with polarized light of the appropriate wavelength. Anisotropy refers to the average angular displacement of a polarized light beam between excitation and emission. Anisotropy measurements are thus sensitive to the rotational diffusion such as the apparent molecular size of the labeled protein. For optimal measurements the smaller interaction partner is generally labeled (e.g. the MHC class I peptide ligands). Generally, to obtain reliable measurements, the smaller binding partner should be no larger in mass than about 10-15% of the bigger one.) Upon binding of the small

fluorescently labeled peptide to the MHC class I heavy chain, the rotational diffusion of the fluorophore changes due to the high molecular weight of the newly formed complex, which is then detected as anisotropy signal (Saini et al., 2013a).

Both described methods are generally more suitable for the characterization of already detected protein-protein interactions rather than for their discovery.

An alternative biochemistry method that was tried in this project is co-immunoprecipitation (see section 5.1.8.1). Co-immunoprecipitation experiments are based on the principle that one protein is pulled down with the help of an affinity tag, and any interacting proteins that remain bound in the detergent cell lysate will precipitate together with it. One major drawback of this method is that it does not allow for distinguishing whether the co-immunoprecipitated proteins interact directly or indirectly. Also, cell lysis is required for co-immunoprecipitation protocols in order to isolate the proteins of interest. Due to cell lysis, this method does not allow for the spatial analysis of protein-protein interactions. Additionally, it is also possible that the detected protein interactions are artificially introduced during cell lysis. In contrast, an advantage of co-immunoprecipitation is that it allows for an open screen: the co-precipitates can be analysed by mass spectrometry which will allow for the screen and the identification of unknown interaction partner.

An *in vivo* approach for the investigations of protein-protein interactions is bimolecular fluorescence complementation (BiFC) (Kerppola, 2008). Here, the interaction candidates are each genetically tagged with one half of a fluorescent protein such as split-GFP, and both constructs are then co-expressed in the cell. Upon interaction of the two protein candidates, the two halves of the fluorescent protein will come into close proximity and will eventually fold into one fluorescent protein and fluoresce. Compared to co-immunoprecipitation, this method allows for a spatial resolution, e.g. the identification of the cellular compartment where the proteins interact. In contrast, BiFC requires two fusion constructs and cannot be used for an open screen. One also has to consider that the folding of the fluorophore will take time until one can read out the fluorescent signal, which may render the assay ineffective for short-lived proteins or interactions in the early secretory pathway.

### 1.4.10 Anticipated properties of MHC class I clusters and applicability of known interaction analysis methods

MHC class I clusters at the cell surface are a difficult problem for various reasons. First, they may be so weak that they only occur when binding is potentiated through dimensional reduction, *i.e.*, when the proteins are restricted to the membrane (McCloskey and Poo, 1986; Singer and Nicolson, 1972) or even to microdomains within the membrane (Nicolau et al., 2006). If this is so then lysis of the cells will result in the loss of these interactions, and if recombinant class I molecules are used for the investigation of their interactions, then such interactions might not be detected. This *a priori* excludes methods that work only with recombinant proteins, such as SPR and FP (1.4.9). Immunoprecipitation may also not work for the detection of such interactions since upon cell lysis, the membranes and/or microdomains are disrupted, leading to the loss of interaction. Additionally, the detergents used in immunoprecipitation may directly interfere with protein-protein interaction by modifying the interface of the proteins, or they may change the conformation of the class I molecules such that no interaction is possible.

Second, class I molecules exist in several forms (1.4.4), and especially for the free heavy chain and the empty dimer of heavy chain and  $\beta_2m$ , it is unknown what their structure and dynamics are (Bouvier and Wiley, 1998), and whether they are the same in cells and in recombinant proteins *in vitro*. This is why generally, such investigations ought to be carried out in live cells.

But with live cells, several new problems arise. In cells, different forms of proteins must be detected specifically, and GFP fusions (such as used in BiFC) cannot report on the form or conformation of the fusion partner. To detect specific conformations, one might use antibodies, but this restricts analysis to the plasma membrane, where the forms of interest may be non-existent or short-lived.

Anti-MHC class I antibody micropatterns solve these problems in an ideal way (1.7).

## 1.5 Anti-MHC class I antibodies

A variety of anti-MHC class I antibodies exist and are commonly used for the identification and characterization of class I molecules in research, diagnosis, and therapy. Table 1.5 lists all used antibodies with the respective epitopes used in this study.

**Table 1.5: Summary of anti-MHC class I antibodies.** Primary antibodies used for the fabrication of anti-MHC class I antibody micropatterns or for immunostaining.

Antibody	MHC class I allotype	Epitope	References
murine allotypes			
<b>20-8-4S</b>	H-2K <sup>b</sup> , H-2D <sup>b</sup>	$\alpha_1$ domain	(Ozato and Sachs, 1981)
<b>25.D1.16</b>	K <sup>b</sup> with OVA peptide SIINFELK	Reads peptide sequence like TCR	(Porgador et al., 1997) (Mareeva et al., 2008)
<b>27-11-13S</b>	H-2D <sup>b</sup> , H-2D <sup>d</sup> , H-2D <sup>q</sup>	$\alpha_3$ domain	(Ozato and Sachs, 1981)
<b>28-14-8S</b>	H-2L <sup>d</sup> , H-2L <sup>q</sup> , H-2D <sup>b</sup> , H-2D <sup>q</sup>	$\alpha_3$ domain (disulfide bond)	(Ozato and Sachs, 1981)
<b>B22.249</b>	H-2D <sup>b</sup> , H-2D <sup>q</sup> , H-2L <sup>d</sup> , H-2L <sup>q</sup>	$\alpha_1$ domain ( $\beta_2m$ -bound heavy chain)	(Solheim et al., 1995) (Hämmerling et al., 1982)
<b>Y3</b>	H-2K <sup>b</sup> , H-2K <sup>d</sup> , H-2K <sup>s</sup> , H-2K <sup>r</sup> , H-2K <sup>q</sup>	$\alpha_1$ domain ( $\beta_2m$ -bound heavy chain)	(Hämmerling et al., 1982)
Antibody	MHC class I allotype	Epitope	References
human allotypes			
<b>HC-10</b>	HLA-B, HLA-C	'open heavy chains'	(Harris et al., 1998) (Perosa et al., 2003)
<b>W6/32</b>	All folded HLA/ $\beta_2m$	residue 3 of h $\beta_2m$ and residue 121 of heavy chain	(Barnstable et al., 1978) (Stam et al., 1986)
<b>BBM.1</b>	h $\beta_2m$		(Brodsky et al., 1979)

### 1.6 T cell arrays

As an alternative to MHC class I tetramer staining, the development of pMHC class I arrays have been proposed to increase throughput and to multiplex of T cell screening and sorting. Conventional spotting methods that are commonly used to fabricate protein microarrays are limited by the intrinsic protein instability of empty MHC class I proteins and lack the required reproducibility.

To circumvent these limitations, Kwong and coworkers have established a platform that allows for nucleic acid cell sorting (NACS) (Kwong et al., 2009). In their approach, they use pMHC class I tetramers that are labeled with single-stranded DNA oligonucleotides. With conventional spotting methods, they fabricated an array of complementary oligomers on a glass surface and let the pMHC class I bind to the array through hybridization of the two oligomers. To test their system for T cell sorting, they incubated the array with T cell suspensions and also with primary T cells from cancer patients. Excitingly, they showed that T cells bind to the immobilized pMHC class I spots with antigen specificity. They even eluted captured T cells from the array by cleaving the double-stranded oligonucleotides with restriction endonucleases.

Similar approaches to generate pMHC class I arrays include MHC class I tetramers that were directly printed on coated microscope slides (Soen et al., 2003) or hydrogels (Brooks et al., 2015). In another approach, the researchers first stained T cells with dimers of MHC class I (the dimerization was achieved by fusion of the MHC class I heavy chain to immunoglobulin  $F_c$  regions), and then they captured the stained T cells on anti-IgG antibody spots that bind to the  $F_c$  portion of the MHC class I dimer (Deviren et al., 2007; Yue et al., 2010). Another approach combined pMHC class I arrays with ELISPOT to read out T cell activation (Stone et al., 2005)

Although the proof-of-concept experiments of these pMHC class I arrays were successful, the sensitivity of the developed arrays was never better than the conventional staining methods, and they often lacked the formal demonstration of the required degree of multiplexing (Bentzen and Hadrup, 2017).

## 1.7 Project motivation

The project idea was to develop a new kind of sensor for the detection of small analytes by a unique combination of existing methodologies from different scientific fields. Due to the existing expertise in the Springer laboratory, it was an intuitive decision to define MHC class I as the model analyte protein in this project. The defined major aim was to establish a new sensor assay to detect functional MHC class I molecules and to demonstrate in a proof-of-concept experiment the specificity, selectivity, and sensitivity of the newly developed assay.

After establishing and optimizing the novel assay, I decided to apply the method to a relevant biological question in the field of MHC class I. An immediate idea with respect to the model protein was the measurement of peptide binding of captured MHC class I molecules in live cells. After establishing a binding assay, another application came up. During the course of experiments I found out that I can capture specific forms of MHC class I depending on the conformation specificity of the epitope of the capture antibody. This gave me a unique opportunity to study the different forms of MHC class I at the cell surface of living cells. This finding was especially interesting, since the MHC class I dimer and the free heavy chains generally have a very short half-life at the cell surface and are extremely difficult to investigate with classical biochemistry methods (1.4.10). With these tools in hand, I used the antibody micropatterns to study protein-protein interactions, a rather typical application of micropatterns in bait-prey experiments. I had added a further perspective to this assay by the ability to study the interaction of two MHC class I molecules in a defined conformation.


## **2 Materials and methods**

The material and methods section gives a complete overview of all methods that were used in the entire project. The experimental procedures are generally rather short in published manuscripts according to the publication guidelines. Here, I give additional information, my optimization procedures and add relevant observations that I have made during my experiments. For those techniques that I have developed and optimized myself, I have written detailed SOPs that describe the final protocols that I am using today.

### **2.1 Preparation of antibodies**

This chapter explains in detail the preparation of antibodies for the fabrication of antibody micropatterns. It contains an optimized SOP for the purification of antibodies from hybridoma supernatant, which is now shorter than the original protocol. The second SOP in this chapter describes the labeling of the purified antibodies with NHS-dyes. Based on the standard manufacturer's protocol, I have made some changes for simplicity and convenience.



	<b>Springer Group Standard Operating Procedure (SOP)</b>
SOP No.:	CD 01
Title:	<b>Antibody purification from hybridoma supernatant</b>
Revision No.:	2
Revision Date:	17. August 2017

### 1. Information about this Standard Operating Procedure

SOP No., Title, Revision No., Revision Date: see page header			
Author of this Revision:	Cindy Dirscherl		
Signature of Principal Investigator:			
Revision History:	Revision No.	Author	Date
	01	Catherine Jacob-Dolan	10. 03. 2017
Other SOPs, documents, or attachments required for the procedure	Production of hybridoma supernatant		

### 2. Purpose and general description of the procedure (1-2 sentences)

To purify antibodies from prepared hybridoma using protein A beads, elution, and dialysis.
--

### 3. Terms and abbreviations used in this document

Term or Abbreviation	Explanation
SOP	Standard Operating Procedure
TRIS	TRIS-(hydroxymethyl)-aminomethane
PBS	phosphate buffered saline
SDS PAGE	sodium dodecyl sulfate polyacrylamide gel electrophoresis

**4. Cells or plasmids required**

None

**5. Chemicals required**

Chemical	Company and Catalog No.	Safety? <sup>1</sup>	Batch? <sup>2</sup>
1. TRIS base (C <sub>4</sub> H <sub>11</sub> NO <sub>3</sub> )	AppliChem, A1379,5000		
2. Glycine (H <sub>2</sub> NCH <sub>2</sub> COOH)	AppliChem, A1377,5000		
3. sodium chloride (NaCl)	AppliChem, 146994.1214		
4. potassium chloride (KCl)	AppliChem, A2939,5000		
5. disodium hydrogenphosphate (Na <sub>2</sub> HPO <sub>4</sub> * 2H <sub>2</sub> O)	AppliChem, A3905,1000		
6. monopotassium phosphate (KH <sub>2</sub> PO <sub>4</sub> )	AppliChem, A3095,0250		

**6. Safety considerations**

Chemical Reagent	or Toxic <sup>3</sup>	Carcinogenic	Allergen	Safety considerations (H/P numbers, S1/S2, Radioactivity)

<sup>1</sup> Insert the 'Signal word' (Warning, Danger, ...) of the GHS system (in the Lab chemicals database) if it applies. **And** enter detailed safety information in table 6 (Safety).

<sup>2</sup> Insert 'Yes' if necessary to record the batch number of this chemical.

<sup>3</sup> Check whatever applies.

**7. Buffers and stock solutions (= 'reagents')**

Reagent	Preparation, aliquotting, storage
1. 1 M TRIS	For 1 L, dissolve 121.14 g of TRIS in 1 L ddH <sub>2</sub> O, store at room temperature and check before use for precipitation or other contaminations
2. 100 mM TRIS	For 1 L, dissolve 12.141 g of TRIS in 1 L ddH <sub>2</sub> O, or dilute from 1 M TRIS Stock, 1:10, store at room temperature and check before use for precipitation or other contaminations
3. 10 mM TRIS	For 1 L, dissolve 1.2141 g of TRIS in 1 L ddH <sub>2</sub> O, or dilute from 1 M TRIS Stock, 1:100, store at room temperature and check before use for precipitation or other contaminations
4. 100 mM glycine	For 1 L, dissolve 7.5 g of glycine in ddH <sub>2</sub> O
5. 10x PBS	For 1 L, dissolve 80 g of sodium chloride (NaCl), 2 g of potassium chloride (KCl), 14.4 of disodium hydrogen phosphate (Na <sub>2</sub> HPO <sub>4</sub> ), and 2.4 g of monopotassium phosphate (KH <sub>2</sub> PO <sub>4</sub> ) in 1 L ddH <sub>2</sub> O, store at room temperature and check before use for precipitation or other contaminations
6. 1x PBS	Prepare from 10x PBS stock via a 1:10 dilution with ddH <sub>2</sub> O

**8. Equipment and accessories required**

Type of equipment	Special Instruction? <sup>4</sup>
1. pH strips	-
2. BIO-RAD poly-prep chromatography column	-
3. Protein A bead slurry	Yes. Follow lab protocol.
4. Centrifuge tubes (15 and 50 mL)	-
5. 5 L beaker for dialysis	-

Table continues on next page

<sup>4</sup>Insert 'Yes' if special instruction is necessary to operate this equipment.

Table continued from previous page

6. Dialysis tubing and clamps (Zellu Trans MWCO 6000-8000, flat width 25 mm, from Roth, item No: E 665.1)	Pre-soak in PBS
7. Microcentrifuge tube 1.5 mL	-
8. NanoDrop	Yes. Read manual.
9. Centrifuges	Yes. Read manual.

**9. Procedure (numbered list)**

1. Retrieve the desired hybridoma supernatant from the freezer
2. Thaw the hybridoma supernatant in a water bath at 37 °C
3. Adjust the pH of the hybridoma supernatant with 1 M TRIS to pH 8.0. Start by adding 1/20 the volume of the hybridoma. Check pH with pH strips
4. *Optional: Take a 10 µL sample for SDS PAGE for quality control later store in freezer (-20°C)*
5. Add 1-1.5 mL of protein A slurry to a 15 mL centrifuge tube.  
*Optional: Re-use protein A beads from previous purifications:*
  - I. Retrieve the specific BIO-RAD column for the desired antibody with the bead slurry inside
  - II. Using 1 mL of 100 mM TRIS, pH 8.0, (if the column does not already contain sufficient buffer) pipette up and down to resuspend the beads in the column
  - III. Pipette the suspended beads from the column into a 15 mL centrifuge tube
  - IV. Add a small amount, ~500 µL, of 100 mM TRIS, pH 8.0, to the BioRad column so that it will not dry out and return it to the refrigerator
  - V. Proceed with step 6.
6. Add 10 mL of 100 mM TRIS, pH 8.0, to the slurry in the 15 mL centrifuge tube
7. Centrifuge at 60 xg for 5 minutes at 4 °C
8. Remove supernatant
9. *Optional: Repeat washing step*
10. Re-suspend the beads in ~2 mL of the hybridoma supernatant
11. Transfer the bead suspension to the centrifuge tube containing the hybridoma supernatant
12. Pipette the hybridoma supernatant up and down with the same tip in order to ensure the complete transfer of all the beads into the hybridoma supernatant

Table continues on next page

Table continued from previous page

13. Incubate for 48 hours at 4 °C in the cold room on a turning wheel
14. Spin down the tubes containing the hybridoma and the beads at 60 xg for 2-3 minutes
15. Remove and discard the supernatant
16. Add 10 mL of 100 mM TRIS, pH 8.0 to the beads
17. Centrifuge at 60 x g for 2-3 minutes
18. Remove and discard the supernatant
19. Re-suspend the beads in 10 mL of 100 mM TRIS, pH 8.0
20. Transfer the bead suspension to the BioRad poly prep chromatography column
21. Use up to 5 mL extra 100 mM TRIS, pH 8.0, to wash the centrifuge tube and ensure the complete transfer of all the beads to the column
22. Prepare 5, 1.5 mL microcentrifuge tubes containing 50 µL 1 M TRIS, pH 8.0
23. Elute five fraction of the antibody from the column with 500 µL 100 mM glycine, pH 2.5, into these five tubes
24. Mix each fraction after elution by flipping them upside down
25. Shortly spin down the five fractions to ensure no drops are caught in the cap
26. Measure the protein concentration of each fraction at the NanoDrop.  
Blank: 500 µL 100 mM glycine, pH 2.5 + 50 µL 1 M TRIS, pH 8.0
27. Pool the fractions that contain the protein (a significant concentration of the protein is usually > 0.100 mg/mL)
28. Prepare dialysis of the samples by cutting 5 – 7 cm of tubing and soaking it in 1 x PBS
29. Close one end of the tubing with the dialysis tubing clamp
30. Add the necessary protein fractions
31. Close the remaining end of the tubing with another dialysis tubing clamp
32. Label the samples in a clear manner if there is more than one
33. Dialyze overnight against 5 L 1x PBS, pH 7.4, at 4 °C (in the cold room)
34. Change the buffer the next day and dialyze again overnight against 5 L 1x PBS, pH 7.4, at 4 °C (in the cold room)
35. Collect the antibody from the dialysis tube in a microcentrifuge tube
36. Measure the concentration of the samples at the NanoDrop. Blank: 1x PBS
37. *Optional: Run 11% SDS PAGE to check purification*

**10. Interpretation and reporting of the data:**

(no instructions)

**11. Potential pitfalls, errors, and other issues (each in one table row)**

Issue	Known resolution
Elution of antibody from column	The antibody is usually found in the first two fractions. I have sometimes observed that the antibody comes only in fraction 3, so I recommend to always collect 5 fractions for elution.
Stock of protein A bead slurry	Common stock of protein A bead slurry is prepared: Buffer of protein A beads is exchanged for PBS+0.1% triton. Slurry is stored in aliquots at 4 °C.


**12. Instructions for the use of SOPs****General Rules:**

- Use the newest version of an SOP for your experiment.
- Record the number of the SOP (found in the page header) in your experiment protocol.
- Any changes between the SOP and your experiment must be documented in your experiment protocol.
- If you believe that the SOP needs to be changed or extended, bring it up in the subgroup meeting.

**Explanations of the individual points:**

3. **Abbreviations:** Abbreviations of chemicals are explained in 5.

5. **"Chemicals"** are all powders (but not stock solutions, see 6.)

	<b>Springer Group Standard Operating Procedure (SOP)</b>
SOP No.:	CD 02
Title:	<b>Antibody labeling with NHS-dyes</b>
Revision No.:	2
Revision Date:	17. August 2017

### 1. Information about this Standard Operating Procedure

SOP No., Title, Revision No., Revision Date: see page header			
Author of this Revision:	Cindy Dirscherl		
Signature of Principal Investigator:			
Revision History:	Revision No.	Author	Date
	01	Catherine Jacob-Dolan	10. 03. 2017
Other SOPs, documents, or attachments required for the procedure	SOP: SDS PAGE		

### 2. Purpose and general description of the procedure (1-2 sentences)

Labeling antibodies with fluorescent NHS dyes. Coupling reactive NHS-dyes to the primary amines of the lysine-residues of the antibody via an NHS-coupling reaction.
--

### 3. Terms and abbreviations used in this document

Term or Abbreviation	Explanation
SOP	Standard Operating Procedure
NHS	N-hydroxysuccinimide esters (NHS esters)
AF	Alexa Fluor

Table continues on next page

Table continued from previous page

TRIS	tris-(hydroxymethyl)-aminomethane
PBS	phosphate buffered saline
SDS PAGE	sodium dodecyl sulfate polyacrylamide gel electrophoresis

**4. Cells or plasmids required**

None

**5. Chemicals required**

Chemical	Company and Catalog No.	Safety? <sup>5</sup>	Batch? <sup>6</sup>
1. NHS-AF647	Invitrogen, A37566		
2. NHS-Atto542	Atto Tec, AD 542-31		
3. sodium bicarbonate (NaHCO <sub>3</sub> )	AppliChem, 131638.1210		
4. sodium chloride (NaCl)	AppliChem, 146994.1214		
5. potassium chloride (KCl)	AppliChem, A2939,5000		
6. disodium hydrogenphosphate (Na <sub>2</sub> HPO <sub>4</sub> * 2H <sub>2</sub> O)	AppliChem, A3905,1000		
7. monopotassium phosphate (KH <sub>2</sub> PO <sub>4</sub> )	AppliChem, A3095,0250		

<sup>5</sup> Insert the 'Signal word' (Warning, Danger, ...) of the GHS system (in the Lab chemicals database) if it applies. **And** enter detailed safety information in table 6 (Safety).

<sup>6</sup> Insert 'Yes' if necessary to record the batch number of this chemical.



**6. Safety considerations**

Chemical Reagent	or Toxic <sup>7</sup>	Carcinogenic	Allergen	Safety considerations (H/P numbers, S1/S2, Radioactivity)

**7. Buffers and stock solutions (='reagents')**

Reagent	Preparation, aliquotting, storage
1. 200 mM sodium bicarbonate	For 1 L, dissolve 0.8401 g of sodium bicarbonate, NaHCO <sub>3</sub> in 1 L ddH <sub>2</sub> O, store at room temperature and check before use for precipitation or other contaminations
2. NHS-dye of choice	Store at -80°C in either stock concentration or aliquots of lesser concentration (~80 µM)
3. 1 M TRIS	For 1 L, dissolve 121.14 g of TRIS in 1 L ddH <sub>2</sub> O, store at room temperature and check before use for precipitation or other contaminations
4. 200 mM TRIS	For 1 L, dissolve 24.282 g of TRIS in 1 L ddH <sub>2</sub> O, or dilute from 1 M TRIS stock, 1:5, store at room temperature and check before use for precipitation or other contaminations
5. 10x PBS	For 1 L, dissolve 80 g of sodium chloride (NaCl), 2 g of potassium chloride (KCl), 14.4 of disodium phosphate (Na <sub>2</sub> HPO <sub>4</sub> ), and 2.4 g of monopotassium phosphate (KH <sub>2</sub> PO <sub>4</sub> ) in 1 L ddH <sub>2</sub> O, store at room temperature and check before use for precipitation or other contaminations
6. 1x PBS	Prepare from 10x PBS stock via a 1:10 dilution with ddH <sub>2</sub> O

<sup>7</sup> Check whatever applies.

8. Equipment and accessories required	
Type of equipment	Special Instruction? <sup>8</sup>
1. pH strips	-
2. Vivaspin 2 columns, 10,000 MWCO HY (Sartorius, Product No VS02H02)	Yes. Read manual
3. Centrifuge	Yes. Read manual
4. Thermo Shaker	-
5. Nano Drop	Yes. Read manual
6. 15 mL centrifuge tubes	-
7. 1.5 mL microcentrifuge tubes	-
8. 1.5 mL light protected microcentrifuge tubes	-
9. Phosphor Imager	Yes. Read manual

9. Procedure (numbered list)
<ol style="list-style-type: none"> <li>1. Dissolve NHS-dyes in anhydrous, amine-free DMSO. (Usually stock is 1mM; check manufacturer's suggestions).</li> <li>2. Calculate the molar concentrations of the antibody solution and the NHS-dye.</li> <li>3. <i>Optional: Keep and aliquot (10 µL) of unlabeled antibody for SDS-PAGE</i></li> <li>4. Adjust the pH of the antibody solution to pH 8.3 with 200 mM sodium bicarbonate solution, pH 9.0 Start by adding 1/20<sup>th</sup> of the volume of the antibody solution. Check pH by pipetting a droplet on pH strips.</li> <li>5. Calculate the equimolar concentrations of dye and antibody</li> <li>6. Take then 1/4<sup>th</sup> of the calculated amount of dye and add it to the antibody solution</li> <li>7. Incubate antibody solution and NHS-dye at room temperature, shaking (Thermo Shaker) for 1 hour at xyz rpm</li> <li>8. Transfer the solution to a 15 mL centrifuge tube and inactive the solution with 1 mL 200 mM TRIS pH 8.0 per 0.5 mL of reaction sample (antibody-dye solution)</li> <li>9. Transfer 2 mL (or entire volume if the volume is less than 2 mL) into a Vivaspin 2 (for 2 mL) column</li> <li>10. Spin down to between 1 and 0.5 mL (usually ~5 min.) and add the remainder of the solution 8,000 x g, 4 °C</li> <li>11. After each spinning-down step, empty the liquid collected in the bottom of the column into a waste container</li> <li>12. Wash by adding 2 mL 1x PBS and spinning down to 0.3 – 0.2 mL (spin for about 5 minutes)</li> </ol>

Table continues on next page

<sup>8</sup> Insert 'Yes' if special instruction is necessary to operate this equipment.

Table continued from previous page

13. Dissolve NHS-dyes in anhydrous, amine-free DMSO. (Usually stock is 1mM; check manufacturer's suggestions).
14. Calculate the molar concentrations of the antibody solution and the NHS-dye.
15. *Optional: Keep and aliquot (10  $\mu$ L) of unlabeled antibody for SDS-PAGE*
- 16.
17. Adjust the pH of the antibody solution to pH 8.3 with 200 mM sodium bicarbonate solution, pH 9.0  
Start by adding 1/20<sup>th</sup> of the volume of the antibody solution. Check pH by pipetting a droplet on pH strips.
18. Calculate the equimolar concentrations of dye and antibody
19. Take then 1/4<sup>th</sup> of the calculated amount of dye and add it to the antibody solution
20. Incubate antibody solution and NHS-dye at room temperature, shaking (Thermo Shaker) for 1 hour at xyz rpm
21. Transfer the solution to a 15 mL centrifuge tube and inactive the solution with 1 mL 200 mM TRIS pH 8.0 per 0.5 mL of reaction sample (antibody-dye solution)
22. Transfer 2 mL (or entire volume if the volume is less than 2 mL) into a Vivaspin 2 (for 2 mL) column
23. Spin down to between 1 and 0.5 mL (usually ~5 min.) and add the remainder of the solution 8,000 x g, 4 °C
24. After each spinning-down step, empty the liquid collected in the bottom of the column into a waste container
25. Wash by adding 2 mL 1x PBS and spinning down to 0.3 – 0.2 mL (spin for about 5 minutes) 8,000 x g, 4 °C
26. Repeating washing (step 11) and spin for only 3 or 4 minutes in order to ensure 0.2 mL remaining for elution
27. Carefully pipette up and down inside the column with a gel loading tip as to loosen the antibody-dye complexes stuck to the membrane during the centrifugation of the washing steps
28. Elute the antibody by reverse spinning, elution volume should be approximately 200  $\mu$ L 4,000 x g, 4 °C
29. *Optional: Run the labelled and unlabeled sample on an 11% SDS-PAGE to check if the labelling worked*  
*Before staining with Coomassie, check the fluorescence at the Phosphor Imager. Sample can be kept in ddH<sub>2</sub>O for this short period. Then stain with Coomassie as usual*
30. Measure antibody-dye complex antibody at the Nano Drop.  
Transfer antibody-dye complex into a light protected microcentrifuge tube (e.g. Eppendorf tube, amber

**10. Interpretation and reporting of the data:**

(no instructions)

**11. Potential pitfalls, errors, and other issues (each in one table row)**

Issue	Known resolution
Calculation of required dye	The used dye aliquots are from Esam Tolba Abualrous and were not labeled. We assume the concentration is 1 mM, and used it accordingly. This is also the reason, why we use only $\frac{1}{4}$ of the calculated amount of dye. The calculated amount seemed too much.
NHS-dyes	In presence of water, NHS-esters hydrolyze. It is recommended to freshly prepare the NHS-dye solution immediately before use.
Antibody solution	Antibody solution must be free of any amine containing substances such TRIS-buffer, amine containing acids etc., since these will quench the reaction.
Staining with Coomassie	So far I have observed that Coomassie quenches the fluorescent dye. Therefore the gel should be only stained with Coomassie after detection of fluorescence in the Phosphor Imager.

**12. Instructions for the use of SOPs****General Rules:**

- Use the newest version of an SOP for your experiment.
- Record the number of the SOP (found in the page header) in your experiment protocol.
- Any changes between the SOP and your experiment must be documented in your experiment protocol.
- If you believe that the SOP needs to be changed or extended, bring it up in the subgroup meeting.


**Explanations of the individual points:**

1. **Abbreviations:** Abbreviations of chemicals are explained in 5.
2. **"Chemicals"** are all powders (but not stock solutions, see 6.)

## **2.2 Fabrication of antibody micropatterns**

For the generation of anti-MHC class I antibody micropatterns I have adapted standard protocols for PDMS stamps and optimized the printing method throughout the project. The SOPs for the fabrication of PDMS stamps and printing procedure are the current used protocols, which have worked best for me.

The photolithography steps were carried out by our postdoc Dr. Tatiana Kolesnikova in the lab of Professor Veit Wagner according to the protocol in (Dirscherl et al., 2017).

	<b>Springer Group Standard Operating Procedure (SOP)</b>
SOP No.:	CD 03
Title:	<b>Fabrication of PDMS stamps</b>
Revision No.:	1
Revision Date:	05. September 2017

### 1. Information about this Standard Operating Procedure

SOP No., Title, Revision No., Revision Date: see page header

Author of this Revision:	Cindy Dirscherl		
Signature of Principal Investigator:			
Revision History:	Revision No.	Author	Date
	01	Cindy Dirscherl	05.09.2017
Other SOPs, documents, or attachments required for the procedure			

### 2. Purpose and general description of the procedure (1-2 sentences)

Casting PDMS stamps from silica molds

### 3. Terms and abbreviations used in this document

Term or Abbreviation	Explanation
SOP	Standard Operating Procedure
PDMS	Polydimethylsiloxane
w	Weight

**4. Cells or plasmids required**

None

**5. Chemicals required**

Chemical	Company and Catalog No.	Safety? <sup>9</sup>	Batch? <sup>10</sup>
Sylgard® 184 Silicone Elastomer Kit	Dow Corning		

**6. Safety considerations**

Chemical Reagent	or	Toxic <sup>11</sup>	Carcinogenic	Allergen	Safety considerations (H/P numbers, S1/S2, Radioactivity)
Sylgard® Silicone Elastomer Kit	184	x			H315, H319, H335, P261-P305, P351, P338

**7. Buffers and stock solutions (= 'reagents')**

Reagent	Preparation, aliquotting, storage
1. PDMS	Mix base and curing agent in a 10 (base): 1 (curing agent) ratio (w/w) , mix thoroughly with a glass stick and store at 4 °C

<sup>9</sup> Insert the 'Signal word' (Warning, Danger, ...) of the GHS system (in the Lab chemicals database) if it applies. **And** enter detailed safety information in table 6 (Safety).

<sup>10</sup> Insert 'Yes' if necessary to record the batch number of this chemical.

<sup>11</sup> Check whatever applies.

**8. Equipment and accessories required**

Type of equipment	Special Instruction? <sup>12</sup>
1. Centrifuge tube 50mL	-
2. Glass stick	-
3. Glass coverslips #3 22x22mm from Menzel	-
4. Plastic container or plastic petri dishes	-
5. Incubator 50°C	Yes. Read manual.
6. Scalpel	

**9. Procedure (numbered list)**

1. Cover the bottom of a plastic container with a piece of paper towel; choose a proper container so that it does not melt at 55°C.
2. Place the glass coverslips onto the paper towel.
3. Place a small droplet of prepared PDMS on the glass slide. Make sure to remove any bubbles.
4. Place the silica mold carefully with the pattern facing downwards onto the PDMS droplet, let it sink by its own weight.
5. Incubate at 50-55°C overnight.
6. Test if the PDMS has hardened. Then remove the silica mold carefully. The PDMS stamp should stick on the glass coverslip.
7. Cut the stamp with a scalpel to a size of ~ 5 mmx 5 mm. Choose an area that does not contain any bubbles.

**10. Interpretation and reporting of the data:**

(no instructions)

<sup>12</sup> Insert 'Yes' if special instruction is necessary to operate this equipment.



11. Potential pitfalls, errors, and other issues (each in one table row)	
Issue	Known resolution
Removal of the silica molds	To separate the PDMS stamp from the silica mold, the excess PDMS should be removed. Then, one uses the scalpel and inserts it carefully at one corner between PDMS stamp and the mold. Continue with the other corners. If you use too much pressure, the glass or the silica mold might break!
Sticky PDMS	Sometimes, the PDMS does not cure properly. It will be sticky and the consistency is rather soft. This can happen if the silicone elastomer and curing agent were not properly mixed and a fresh batch of PDMS should be prepared.
PDMS is too fluid	The PDMS becomes more and more viscous over time. If it is too fluid, leave it out at room temperature for 10-15 min.
Silica molds are dirty	The molds can be cleaned carefully, without pressing on the patterned surface with isopropanol.
Re-use of PDMS stamps	In general, the stamps can be re-used. I did not have good experiences with this, so I always prepared fresh ones. But in principle one can remove any access proteins by incubating the stamp in 70% EtOH (or isopropanol) and afterwards rinse with ddH <sub>2</sub> O. The stamps will swell during this treatment, so they need to dry for several days to acquire the proper shape again. Also, I advise to re-use stamps only for the same inking solution. It is impossible to clean the PDMS completely.

## 12. Instructions for the use of SOPs


### General Rules:

- Use the newest version of an SOP for your experiment.
- Record the number of the SOP (found in the page header) in your experiment protocol.
- Any changes between the SOP and your experiment must be documented in your experiment protocol.
- If you believe that the SOP needs to be changed or extended, bring it up in the subgroup meeting.

### Explanations of the individual points:

3. **Abbreviations:** Abbreviations of chemicals are explained in 5.

5. **"Chemicals"** are all powders (but not stock solutions, see 6.)

	<b>Springer Group Standard Operating Procedure (SOP)</b>
SOP No.:	CD 04
<b>Title:</b>	<b>Printing antibody micropatterns</b>
Revision No.:	1
Revision Date:	06. September 2017

### 1. Information about this Standard Operating Procedure

SOP No., Title, Revision No., Revision Date: see page header			
Author of this Revision:	Cindy Dirscherl		
Signature of Principal Investigator:			
Revision History:	Revision No.	Author	Date
	01	Cindy Dirscherl	05.09.2017
Other SOPs, documents, or attachments required for the procedure			

### 2. Purpose and general description of the procedure (1-2 sentences)

Printing antibody micropatterns with PDMS stamps (microcontact printing).
---

### 3. Terms and abbreviations used in this document

Term or Abbreviation	Explanation
SOP	Standard Operating Procedure
PDMS	Polydimethylsiloxane
PBS	phosphate buffered saline
RT	Room temperature

**4. Cells or plasmids required**

None

**5. Chemicals required**

Chemical	Company and Catalog No.	Safety? <sup>13</sup>	Batch? <sup>14</sup>
1.sodium chloride (NaCl)	AppliChem, 146994.1214		
2.potassium chloride (KCl)	AppliChem, A2939,5000		
3.disodium hydrogenphosphate (Na <sub>2</sub> HPO <sub>4</sub> * 2H <sub>2</sub> O)	AppliChem, A3905,1000		
4.monopotassium phosphate (KH <sub>2</sub> PO <sub>4</sub> )	AppliChem, A3095,0250		

**6. Safety considerations**

Chemical Reagent	or Toxic <sup>15</sup>	Carcinogenic	Allergen	Safety considerations (H/P numbers, S1/S2, Radioactivity)

<sup>13</sup> Insert the 'Signal word' (Warning, Danger, ...) of the GHS system (in the Lab chemicals database) if it applies. **And** enter detailed safety information in table 6 (Safety).

<sup>14</sup> Insert 'Yes' if necessary to record the batch number of this chemical.

<sup>15</sup> Check whatever applies.

**7. Buffers and stock solutions (= 'reagents')**

Reagent	Preparation, aliquotting, storage
1. antibody solution	Prepare PBS dilutions from stock. (Usually concentration between 0.3-0.6 $\mu\text{g}/\mu\text{L}$ )
2.	
3. 10x PBS	For 1 L, dissolve 80 g of Sodium Chloride (NaCl), 2 g of Potassium Chloride (KCl), 14.4 of Disodium Phosphate ( $\text{Na}_2\text{HPO}_4$ ), and 2.4 g of Monopotassium Phosphate ( $\text{KH}_2\text{PO}_4$ ) in 1 L ddH <sub>2</sub> O, store at room temperature and check before use for precipitation or other contaminations
4. 1x PBS	Prepare from 10x PBS stock via a 1:10 dilution with ddH <sub>2</sub> O

**8. Equipment and accessories required**

Type of equipment	Special Instruction? <sup>16</sup>
1. PDMS Stamps 2. Nitrogen gas 3. Wet chamber 4. Parafilm 5. Scissors 6. Tweezers 7. Round coverslips $\varnothing$ 22 mm, #1	

**9. Procedure (numbered list)**

1. Take a prepared PDMS stamp and rinse it thoroughly with ddH <sub>2</sub> O. 2. Dry it under the nitrogen flow 3. Place the PDMS stamp into the wet chamber with the pattern facing upwards, pipette a 5 $\mu\text{L}$ droplet of antibody solution on the pattern. 4. To spread the droplet, carefully cover it with a small (5 mmx 5mm) piece of parafilm .
---

Table continues on next page

<sup>16</sup>Insert 'Yes' if special instruction is necessary to operate this equipment.

Table continued from previous page

5. Ink the stamp for 15 min at RT in the wet chamber. If fluorescent antibodies are used, protect it from light to avoid bleaching of the fluorophore.
6. Remove the parafilm and rinse the stamp with ddH<sub>2</sub>O.
7. Dry the stamp under the nitrogen flow
8. For printing, carefully place the inked PDMS stamp on a clean surface, the pattern facing upwards. Carefully place a dust free glass coverslip on the PDMS stamp. If the microcontact is not formed immediately, press very gently with tweezers on the glass coverslip.
9. Mark the areas of the pattern on the glass coverslip carefully with a marker.
10. Transfer the sandwich into the wet chamber and incubate for 15 min at RT
11. Remove the stamp carefully and discard.
12. Until use, keep the coverslips with the printed micropatterns facing upwards in a wet chamber and protect from light.

**10. Interpretation and reporting of the data:**

(no instructions)

**11. Potential pitfalls, errors, and other issues (each in one table row)**

Issue	Known resolution
Storage of the antibody micropatterns	The printed antibody micropatterns can be stored in a wet chamber at 4 °C for several hours. I have not tried long term storage.

**12. Instructions for the use of SOPs****General Rules:**

- Use the newest version of an SOP for your experiment.
- Record the number of the SOP (found in the page header) in your experiment protocol.
- Any changes between the SOP and your experiment must be documented in your experiment protocol.
- If you believe that the SOP needs to be changed or extended, bring it up in the subgroup meeting.

**Explanations of the individual points:**

3. **Abbreviations:** Abbreviations of chemicals are explained in 5.

5. **"Chemicals"** are all powders (but not stock solutions, see 6.)

## **2.3 Incubation of cells on antibody micropatterns**

For incubation of cells on antibody micropatterns, cells are seeded onto the glass coverslips with the printed antibodies. In the early beginning, I did some cell seeding trial experiments and tried HeLa and Vero cells. But eventually, I decided to work with STF1 cells and used these generally throughout the project. The seeding procedure is rather simple and according to standard cell culture protocols, but I will outline a few critical steps in the following.

### **2.3.1 Cell seeding on antibody micropatterns**

I generally used 6-well plates for experiments with cells. Before seeding, I placed the coverslips with the printed antibody micropatterns facing upwards into the individual wells. Then, I trypsinized the cells according to standard protocols and transferred cells to the wells of the 6-well plate. One has to consider two facts when deciding on cell density: Too few cells will take much longer to adhere to the glass surface, whereas too many cells will form a coherent monolayer that is not suitable for imaging. Thus, I recommend counting cells when starting with cell experiments until one has enough experience to estimate cell numbers. The optimal number of cells per well in a 6-well plate is between 50 000 and 100 000 for STF1 cells.

### **2.3.2 Incubation temperature and incubation times**

After seeding, cells are incubated at 37 °C for 2-3 hours to adhere at optimal cell density. For temperature shift experiments, they are shifted to 25 °C for overnight incubation. During my project, I worked with the cell culture incubator with and without CO<sub>2</sub> supply (Binder, article No. 9040-0013 and Sanyo). When using the incubator without CO<sub>2</sub>, I had to exchange the cell culture medium for CO<sub>2</sub>-independent medium (Gibco CO<sub>2</sub> Independent Medium from Thermo Fisher Scientific, Germany, Catalog No. 18045-054) before shifting. This was not optimal, since I experienced that the additional step of medium exchange stressed the cells, and they did not spread nicely during overnight incubation. This step was omitted when using the 25 °C incubator with CO<sub>2</sub>, and I also believe that the temperature in was generally more constant in this incubator. Due to this experience, I would clearly recommend an incubator with CO<sub>2</sub> supply.

For typical clustering experiments (as in 5.1), cells are generally shifted back to 37 °C the next day for 4 to 6 hours.

Cells are thus generally incubated on the antibody micropatterns for 15-24 hours in total. In principle, cells can also grow longer on the antibody micropatterns, but longer incubation generally causes more “dirt” on the pattern, such as cell debris, etc. I therefore recommend incubation on patterns for the mentioned time. Also, the STF1 cells tend to crawl over the surface and thus leave traces of membrane pieces on the antibody micropatterns (see figure 4.2.4).

### 2.3.3 Fixation of cells

I followed the established fixation protocol for cells in our lab: we generally fix cells in 3% para-formaldehyde (PFA) in PBS for 10 min at RT. But the fixation of STF1 cells after incubation on the antibody micropatterns was often problematic throughout the project. And it remains a problem until now, i.e., the cells detach from the glass surface or shrink or they undergo apoptosis and start blebbing so that the samples become useless for microscopy. I have seen better results when cells were split regularly so that they do not overgrow on the plate. Also, it is a common known problem of cells that they react to changes in the supplements of cell culture medium such as FCS, Glutamine or Penicillin/Streptomycin and the DMEM itself. Although I cannot prove this, I experienced major problems after the FCS batch was changed in our lab. Due to these experiences, I strongly recommend to avoid any such changes during STF1 cultivation. Still, fixation with PFA has given best results. I usually fix cells with a 4% solution of PFA for 5 min. However, when I encountered problems, sometimes a dilution to 2% PFA and incubation for 10 min helped.

I also tried methanol fixation as alternative fixation agent. According to standard protocols, I overlaid the cells with ice-cold 100% methanol and incubated them for 15 min at -20 °C. Then I washed the cells three times with PBS. This alternative approach usually did not significantly improve the appearance of the cells after fixation and thus I usually repeated the experiments until the cells had “recovered” and were fixable under normal conditions.



## 2.4 Plasmids and generation of stable cell lines

For my experiments, I mostly used expression plasmids that were already available in the lab. All constructs are listed in the Springer lab Plasmid Data base. The generation of stable cell lines with the lentiviral system was done according to the described protocol in (Hein et al., 2014). Table 2.4 lists all used plasmids and generated stable cell lines of this research project.

**Table 2.4: List of plasmids used for transient transfections and stable transductions, and generated stable cell lines.** The respective antibiotics used for selection are indicated.

Plasmids				
	Constructs	Resistance	Generated by	SPB
1	pEGFP-N1/K <sup>b</sup> wt	Kanamycin	G. Garstka	536
2	pEGFP-N1/HAI1-K <sup>b</sup> wt	Kanamycin	Z. Hein	905
3	pEGFP-N1/human $\beta_2$ m-2A-E3-K <sup>b</sup> wt-GFP	Kanamycin	Z. Hein	1416
4	pEGFP-N1/K <sup>b</sup> wtSTOP	Kanamycin	Z. Hein	911
5	pEGFP-N1/human $\beta_2$ m-2A-E3-K <sup>b</sup> wtSTOP	Kanamycin	Z. Hein	1417
6	pEGFP-N1/human $\beta_2$ m-2A-HA-K <sup>b</sup> wt STOP	Kanamycin	Z. Hein	1183
7	pEGFP-N1/D <sup>b</sup> wt	Kanamycin	G. Garstka	566
8	pEGFP-N1/D <sup>b</sup> wtSTOP	Kanamycin	Z. Hein	907
9	pEGFP-N1/K <sup>b</sup> single chain	Kanamycin	G. Garstka	849
10	IP/K <sup>b</sup> wt-GFP	Ampicillin	Z. Hein	1354
11	IP/HA-K <sup>b</sup> wt-GFP	Ampicillin	Z. Hein	1042
12	IP/E3-HA-K <sup>b</sup> wt-GFP	Ampicillin	Z. Hein	n.a.
13	IP/HA-K <sup>b</sup> wtSTOP	Ampicillin	Z. Hein	1090
14	IP/E3-HA-K <sup>b</sup> wtSTOP	Ampicillin	Z. Hein	1339
15	IP/HA-D <sup>b</sup> wtSTOP	Ampicillin	Z. Hein	1095
16	IP/ D <sup>b</sup> wt-GFP	Ampicillin	corrected by C.Dirscherl	1477

Table continues on next page

Table continued from previous page

Stable cell lines			
	Cell line	Resistance	Generated by
1	STF1/ K <sup>b</sup> -GFP	Puromycin	Z. Hein
2	STF1/ HA-K <sup>b</sup> -GFP	Puromycin	Z. Hein
4	STF1/ E3-HA-K <sup>b</sup> STOP	Puromycin	Z. Hein
5	STF1/ E3-HA-K <sup>b</sup> STOP+K <sup>b</sup> eGFP	Puromycin	C. Dirscherl and Z. Hein (Oct 2016)
6	STF1/ HA-D <sup>b</sup>	Puromycin	C. Dirscherl (Aug 2017)
7	STF1/ HA-K <sup>b</sup> STOP+D <sup>b</sup> GFP	Puromycin	C. Dirscherl (Nov 2017)
8	STF1/ HA-K <sup>b</sup> STOP+Kb-GFP	Puromycin	C. Dirscherl (Nov 2017)
9	STF1/ HA-D <sup>b</sup> +D <sup>b</sup> GFP	Puromycin	C. Dirscherl (Nov 2017)

## 2.5 Microscopy

### 2.5.1 Fluorescence microscopy

All fluorescence images (except where stated otherwise) in this project were acquired with the Zeiss confocal laser scanning microscope LSM 510. A detailed protocol of the acquisition parameters can be found in section 5.1.6.

### 2.5.2 Live cell microscopy

I did some trials with live-cell microscopy with the laser scanning microscope of our collaborators in Greifswald and also with our Zeiss LSM 510 (see figure 4.2.6.2).

For the Zeiss LSM 510, we installed the ibidi heating system (Model: universal fit for 1 chamber from ibidi GmbH, Germany) according to the manual. For live cell experiments, I tried different incubation chambers from ibidi with glass surfaces that are suitable for microcontact printing and live cell imaging. Ibidi offers dishes with untreated glass surfaces that meet these requirements, and I especially liked the

8-well sticky slides for parallel measurements (e.g. when testing peptide binding). I also tried polystyrene dishes.

For a live cell imaging experiment, I followed the protocol in the manual of the ibidi heating system. Briefly, the heating chamber was preheated to 37 °C or 25 °C depending on the experimental setup. Before bringing the samples to the LSM, the cell culture medium was exchanged for microscopy medium (without phenol red). Our imaging system is not supplied with gas, but the cells seemed to tolerate this for the duration of the experiment of about one hour. Fluorescence images were recorded as described previously (5.1.6).

## **2.6 Glass functionalization**

According to other functionalization protocols in the literature, I tried different glass surface treatments in order to optimize the immobilization of antibodies on the glass coverslips and to generate a surface with defined properties or coatings. In contrast to published procedures of protein attachments to glass surfaces, I did not detect any major improvements of the antibody micropatterns upon glass pre-treatments. Thus, in the final standard protocol, I only included a washing step to remove any dust particles from the surfaces. For an overview, I will highlight and comment on the procedures that I have tried.

### **2.6.1 Glass cleaning with RCA cleaning**

To obtain a clean glass surface, I tried the first step of the RCA cleaning method. RCA cleaning is a standard cleaning procedure of silicon wafers in semiconductor manufacturing (Kern, 1990) and includes four steps. To remove any organic contaminants or particles from the glass surface, I cleaned the coverslips with the standard clean 1 (SC-1) of RCA cleaning. For this, the glass coverslips are cleaned in a 1:1:5 solution of  $\text{NH}_4\text{OH}$  (ammonium hydroxide) :  $\text{H}_2\text{O}_2$  (hydrogen peroxide) :  $\text{H}_2\text{O}$  (water) at 70 °C for 10 min. The SC-1 cleaned glass coverslips are then dried under nitrogen flow and used for microcontact printing. I observed very precisely printed antibody patterns on the cleaned glass surfaces, but when seeding cells onto the micropatterns, no capture was observed. After several repeats, I concluded that the cleaned glass surfaces cause this loss of functionality, perhaps by impairing the functionality of the printed antibodies. In agreement with this observation, I skipped the SC-1 cleaning step to recover antibody functionality.

### 2.6.2 Plasma cleaner

Many standard protocols for the protein functionalization of surfaces such as the fabrication of immunosensors recommend plasma cleaning to generate clean and standardized surfaces. Accordingly, I compared antibody micropatterns that were printed on untreated and on plasma cleaned glass surfaces. Low pressure air plasma cleaning is a standard procedure to remove any organic contaminants from the glass surface and to generate hydroxyl and carboxyl surface moieties. The glass surface will thus become negatively charged and become more hydrophilic. This will lead to increased wettability of the glass surface and enhance adhesion between two surfaces, e. g. the glass surface and the PDMS stamp. Also, plasma cleaning is used to enhance the biocompatibility of surface, e.g. promoting cell attachment to surfaces (de Valence et al., 2013) without changing the bulk material of the coverslides.

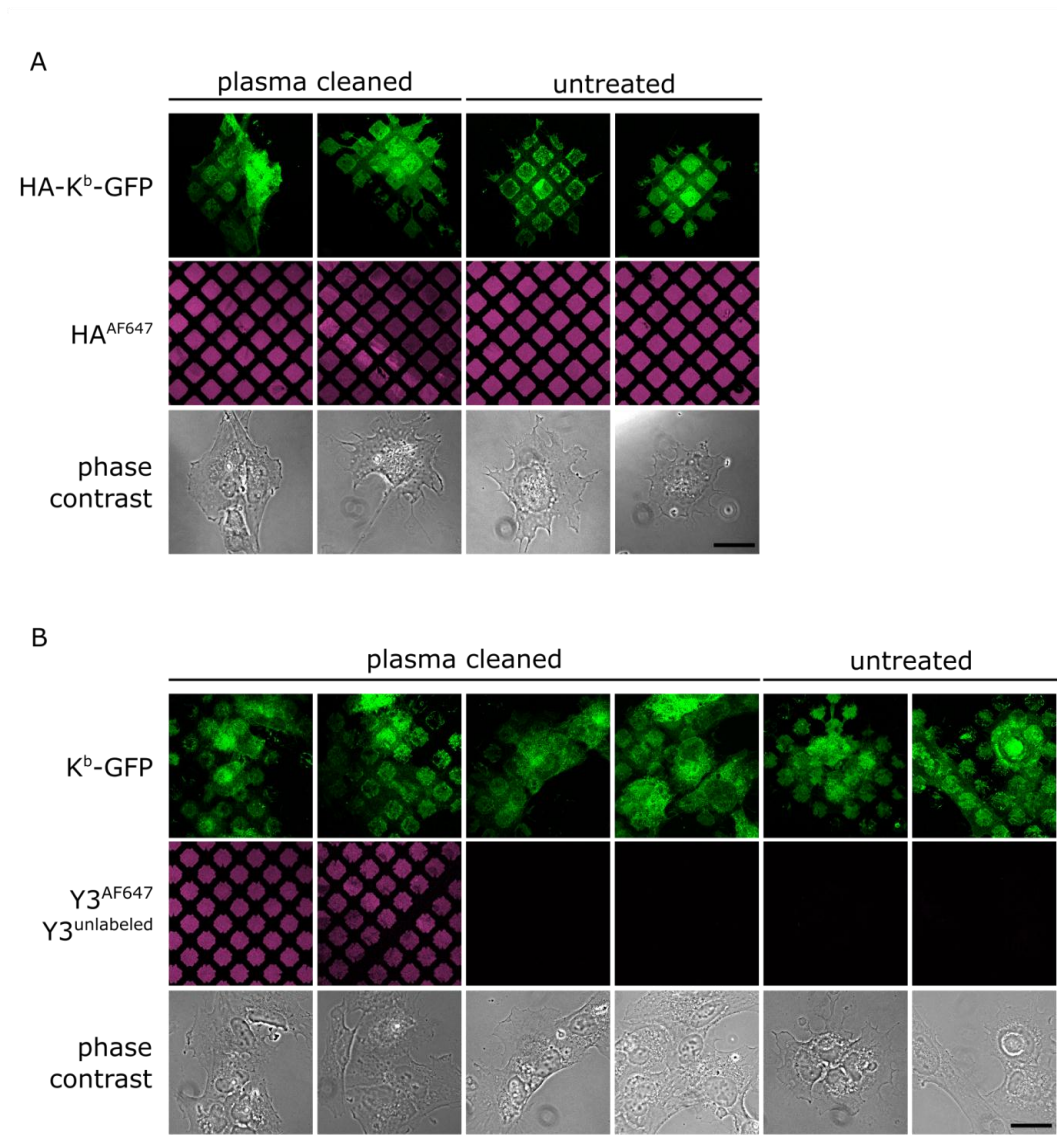


**Figure 2.6.2: Testing plasma treated glass surfaces.** STF1 cells were seeded on antibody micropatterns printed on plasma cleaned or untreated glass surfaces, and incubated according to the standard protocol. **(A)** STF1/HA-K<sup>b</sup>-GFP cells on anti-HA<sup>AF647</sup> antibody micropatterns. **(B)** STF1/K<sup>b</sup>-GFP cells on Y3<sup>AF647</sup> or Y3<sup>unlabelled</sup> antibody micropatterns. Duplicates are shown for each condition. Bar 25  $\mu$ m.

In Figure 2.6.2, I tested our most commonly used antibodies, HA and Y3, and printed them on glass coverslips that were either plasma cleaned or left untreated. I did not see a major difference between the prints on the different coverslips, but I had the overall impression that the antibody micropatterns on the plasma treated coverslips were a little better, i.e., the edges of the individual pattern elements were sharper and the surface appeared cleaner. To test the functionality of the printed antibodies, I seeded STF1/HA-K<sup>b</sup>-GFP or STF1/K<sup>b</sup>-GFP cells on the antibody micropatterns and compared the amounts of captured K<sup>b</sup>-GFP on the surface. However, there was no major improvement visible in the case of plasma cleaned surfaces. The amount of captured K<sup>b</sup>-GFP was similar (see Figure 2.6.2 A and B) and was mostly dependent on the expression levels of the individual cells. But in some samples, the treatment with plasma seemed to reduce the amount of captured K<sup>b</sup>-GFP, although the amounts of the printed antibodies were comparable as judged by fluorescence intensity (see Figure 2.6.2).

I concluded that plasma cleaning did not significantly improve either the appearance of the antibody prints or the amount of captured surface K<sup>b</sup>-GFP. Contrarily, it even seemed to reduce the functionality (capture of surface proteins) of the printed antibody in some cases. Therefore, I did not include this additional step in the antibody micropattern fabrication protocol. However, I can only judge the two tested antibodies, Y3 and HA. I also tested plasma cleaned and untreated glass coverslips for the oriented immobilization experiments, where I printed protein A and G (see figure 2.6.4.2 ). But also in these experiments, I came to the same conclusion that the plasma treatment did not have a positive effect on the printed proteins. However, for other antibodies or proteins, the observations might be different, and I would advise to test plasma cleaned coverslips for each individual setup.

### 2.6.3 Coating of the glass coverslips

Previous studies have shown that the antigen specificity of antibodies printed onto unmodified glass surfaces can be decreased compared to antibodies that were passively bath-adsorbed (David J. Graber et al., 2003). I thus tested whether any protein coatings of the glass surface will increase the antigen binding specificity of the antibodies that I used in my system. For optimization experiments we tested poly-L-lysine and sticky glass for the pre-treatments of glass coverslips.

### 2.6.3.1 Poly-L-lysine

Poly-L-lysine (PLL) is a standard coating agent that is commonly for enhanced attachment of cells to cell culture dishes. PLL is positively charged and thus enhances the electrostatic interactions between the negatively charged plasma membrane of cells and the glass surface, to increase the cell-surface contacts. Better cell attachment might positively influence the interaction between cell surface class I and the antibody micropatterns. Moreover, the pre-coating of plates with PLL was shown to increase antibody sensitivity in ELISA assays (Stearns et al., 2016).

For optimization experiments (see figure 2.6.3.1), we incubated plasma-cleaned glass coverslips with 200  $\mu$ l of PLL solution (0.01% Poly-L-Lysine solution from Sigma P4707) for 30-60 min at 37 °C, then rinsed the coverslips thoroughly with ddH<sub>2</sub>O and dried them under the nitrogen flow. We then printed Y3<sup>AF647</sup> according to the standard protocol (see 2.2). STF/K<sup>b</sup>-GFP cells were seeded according to the standard protocol on the antibody micropatterns and incubated overnight at 25 °C, fixed, and imaged. In this experiment, we were interested to see whether the antibodies printed on PLL pre-coated coverslips show a significant increase of captured K<sup>b</sup>-GFP in the pattern elements, indicating that the printed antibodies are stabilized on the PLL-surface. In our experiments, we did not detect a significant improvement, and thus continued with untreated glass coverslips.

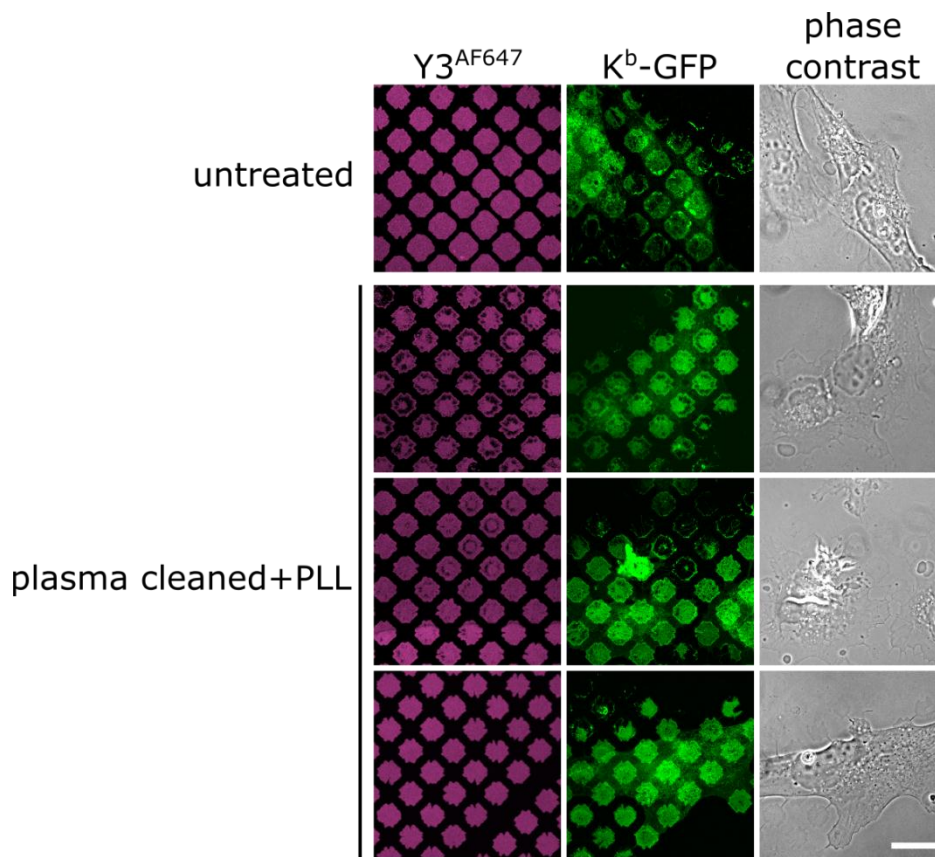


**Figure 2.6.3.1: Testing PLL-coated glass coverslips.** Y3<sup>AF647</sup> was printed on untreated glass coverslips or plasma cleaned coverslips that were pre-incubated with PLL. STF/K<sup>b</sup>-GFP (STF1/HA-K<sup>b</sup>-GFP for the bottom row) cells were seeded on the antibody micropatterns and incubated according to the standard protocol. Bar, 25  $\mu$ m. The experiment was designed by me and performed by Nikolett Nagy.



### 2.6.3.2 Sticky glass

The sticky glass method of T.E. Philipps<sup>17</sup> produces covalently bound amino groups on the glass surface. Similar to PLL coating, the positively charged sticky glass also helps the negatively charged cells to adhere to the glass surface, and thus might help to enhance the amount of captured protein due to increased contact between the surface and cells.

According to the protocol by Philipps, I used plasma cleaned glass coverslips and coated them with 2% of 3-aminopropoyl-triethoxysilane (APTES) in ddH<sub>2</sub>O for 5 min at RT. Then, the coverslips were washed twice in ddH<sub>2</sub>O and dried in the incubator at 55°C overnight. We then printed unlabeled Y3 and HA antibodies ( $c = 0.3 \mu\text{g}/\mu\text{l}$  and  $0.6 \mu\text{g}/\mu\text{l}$ ) according to the standard protocol (see 2.2). According to the standard protocol, STF1/HA-K<sup>b</sup>-GFP cells were seeded on the antibody micropatterns and incubated overnight at 25 °C, fixed, and imaged. In figure 2.6.3.2, I compared treated and untreated glass coverslips to judge whether the functionality of the printed antibodies (amount of captured protein) can be enhanced by the APTES treatment. In the micrographs, we did not observe any significant improvement over the conventional method (not shown), since the capture capacity of the printed antibodies was comparable on both surfaces. We therefore decided to continue our work with untreated glass coverslips.

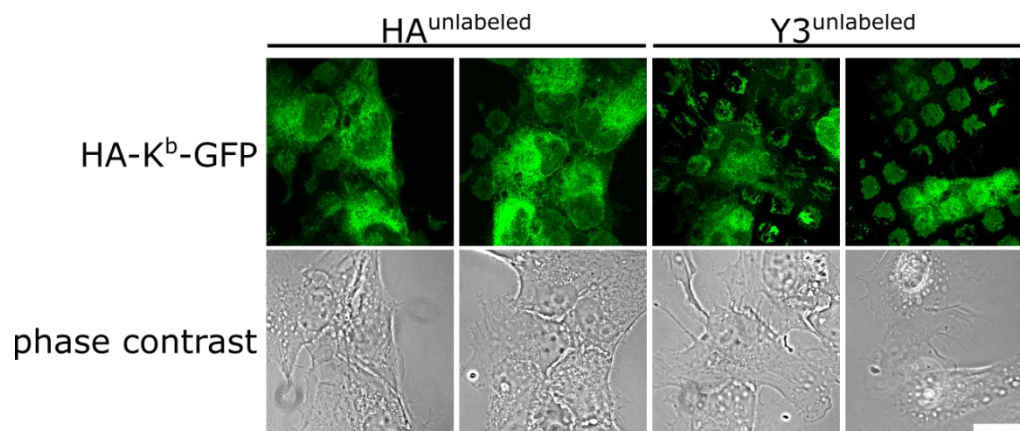


**Figure 2.6.3.2: Testing antibody micropatterns on sticky slides.** Antibody micropatterns of unlabeled HA and Y3 were printed on APTES coated glass coverslips. Then, STF1/HA-K<sup>b</sup>-GFP cells were seeded and incubated in the antibody micropatterns according to the standard protocol and MHC class I capture was analyzed. Two cells are shown for each tested antibody. Bar, 25  $\mu\text{m}$ .

<sup>17</sup> [https://www.bio.umass.edu/microscopy/APTS\\_Methods.htm](https://www.bio.umass.edu/microscopy/APTS_Methods.htm)

### 2.6.4 Oriented immobilization

The principle of antibody immobilization in general is not limited to our system but is commonly used in immunoassays or biosensors. Previous studies including our own work demonstrated that the sensitivity and stability of the immobilized antibodies directly depends on the quantity of antibodies and the remaining activity after immobilization.

Another factor is the proper orientation of the antibody. Antibodies are asymmetrical, and the definition of a properly oriented antibody is when the  $F_c$  region (which has no antigen binding affinity) is bound to the surface rather than the antigen binding sites ( $F_{ab}$  regions). With our method of microcontact printing, antibodies are most likely randomly oriented, with some antibodies therefore unable to bind their antigen. For oriented immobilization,  $F_c$ -binding proteins have been suggested and tested previously (Lee et al., 2013; Makaraviciute and Ramanaviciene, 2013). The principle of this site-directed immobilization is to use  $F_c$  binding proteins as anchor proteins that will orient the sensor or capture antibodies properly, e.g. in our system facing upwards towards the cell membrane, and thus enhance the sensitivity (amount of captured protein) of our antibody micropatterns. In our experiments, we tested a goat anti-mouse antibody and protein A and protein G, all of which bind to the  $F_c$  region of the capture antibodies. In these approaches, one has to consider that the orientation of the  $F_c$  binding proteins themselves is random. Similar to the direct printing of antibodies, only a fraction of the immobilized  $F_c$ -binding protein will probably be bound to the surface in such an orientation that the  $F_c$  binding site is available for the capture antibody. Nevertheless, in some previous studies, this method of site-directed immobilization via  $F_c$  binding proteins significantly increased antibody sensitivity (Makaraviciute and Ramanaviciene, 2013).

Protein A and G have different affinities for specific antibody isoforms, which should be considered in the experimental setup. Table 2.6.4 lists anti-MHC class I antibodies and their respective affinities for protein A and protein G. The affinities for protein A and G are also important for the antibody purification (see 2.1)

**Table 2.6.4: Antibody isoforms of used anti-MHC class I antibodies.** The affinities of antibodies for protein A and protein G depend on the antibody isoforms as indicated.

antibody isoform	protein A affinity	protein G affinity	anti-MHC class I antibody
mouse IgG1	+	++++	25.D1.16
mouse IgG2A	++++	++++	20.8.4S 28.14.8S B22.249 W6/32
mouse IgG2b	+++	+++	Y3 BBM.1

#### 2.6.4.1 Polyclonal anti-mouse antibody

To test site-directed immobilization of the antibody, we first tried to immobilize the capture antibodies via a goat anti-mouse antibody. For this, the glass coverslips were uniformly pre-coated with the polyclonal goat anti-mouse antibody, and subsequently, the capture antibody was printed onto this antibody layer. Due to the affinity of the coat antibody to the  $F_c$  region of the capture antibody, the  $F_{ab}$  fragments should be positioned in a proper orientation.

For our experiments (see figure 2.6.4.1), we used a goat anti-mouse IgG (goat polyclonal antibody to mouse IgG, Cy3-conjugated, from Abcam: ab97035; abbreviated  $\gamma\text{am}^{\text{Cy3}}$  in the following) with a final concentration of 5  $\mu\text{l}/\text{ml}$  to coat the glass surfaces of either plasma treated or untreated glass coverslips for 15 min at RT (same conditions that we use for printing). For coating, we placed a droplet of  $\gamma\text{am}^{\text{Cy3}}$  on one coverslip and covered it with parafilm. Then,  $\text{Y3}^{\text{AF647}}$  was printed according to the standard protocol (see 2.2), and STF1/ $K^b$ -GFP cells were seeded on the antibody micropatterns and incubated overnight at 25 °C. We first checked whether prior plasma cleaning of the glass coverslips improved the attachment of the  $\gamma\text{am}^{\text{Cy3}}$  coating antibody, but did not detect any major differences. Similar to our previous observations, we did not see any difference between untreated and plasma-cleaned glass coverslips. In general, the amount of immobilized coating antibodies ( $\gamma\text{am}^{\text{Cy3}}$ ) appeared low compared to the amounts of printed antibody ( $\text{Y3}^{\text{AF647}}$ ), as judged by the fluorescence intensity. In this experiment, we compared whether the amount of captured  $K^b$ -GFP on the pattern elements was increased compared to other experiments without the antibody pre-coating (such as figure 2.6.2). Overall, we did not observe any significant improvements, and thus we continued with untreated glass coverslips.

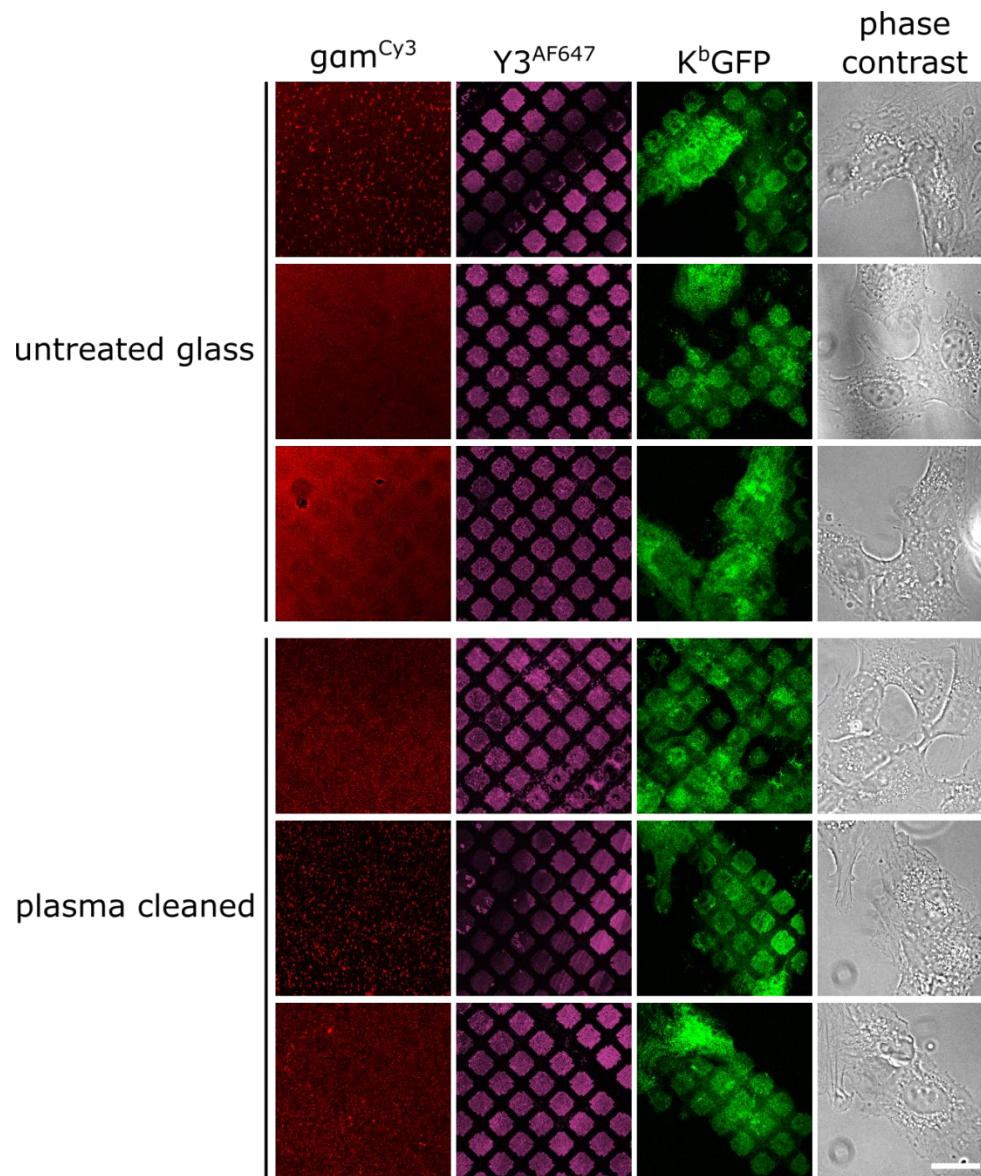


**Figure 2.6.4.1: Printing antibody micropatterns on antibody-coated glass coverslides.** Goat pAb to mouse IgG coupled to Cy3 ( $\text{gam}^{\text{Cy3}}$ ) was used to coat the glass surfaces of either plasma treated or untreated glass coverslides. Then,  $\text{Y3}^{\text{AF647}}$  was printed and STF1/ $\text{K}^{\text{b}}$ -GFP cells were seeded on the antibody micropatterns and incubated according to the standard protocol. Bar, 25 $\mu\text{m}$ . The experiment was designed by me and performed by Nikolett Nagy.

#### 2.6.4.2 Immobilization via protein A

In a second approach, we performed trial experiments with protein A and protein G to orient the capture antibodies properly. Protein A and protein G are antibody binding proteins that are mostly used in affinity chromatography, especially for the purification of antibodies and for immunoprecipitation. Protein A and protein G bind also bind to the  $F_c$  region of the antibodies, but have different affinities for different species and antibody isoforms (see table 2.6.4).

For the site-specific immobilization via protein A and protein G, we performed different experiments as described in the following.

In the first approach, we first printed labeled protein A (protein A<sup>AF647</sup>;  $c = 10 \mu\text{g/mL}$ ) according to our standard protocol. Then, we placed a droplet of unlabeled capture antibody (Y3) onto the printed protein A micropattern to allow the antibody to bind via its  $F_c$  region to the printed protein A<sup>AF647</sup>. In figure 2.6.4.2, the prints of protein A<sup>AF647</sup> are nicely visible. In this experiment, we compared plasma-cleaned and untreated glass coverslides and coated them with PLL. Similar to previous comparative studies, the untreated glass coverslides gave much better results. Based on the fluorescence intensity, more antibodies were deposited on the surface and the prints were also cleaner. Since the capture antibody is unlabeled, we cannot see where it was immobilized. But when we seeded STF1/K<sup>b</sup>-GFP cells onto the antibody micropattern, we observed that the protein was mostly captured in the pattern interspaces. Thus, we conclude that against our expectations, the antibody did not bind to protein A but to the interspaces, and we were not able to produce antibody micropatterns with proper orientation.

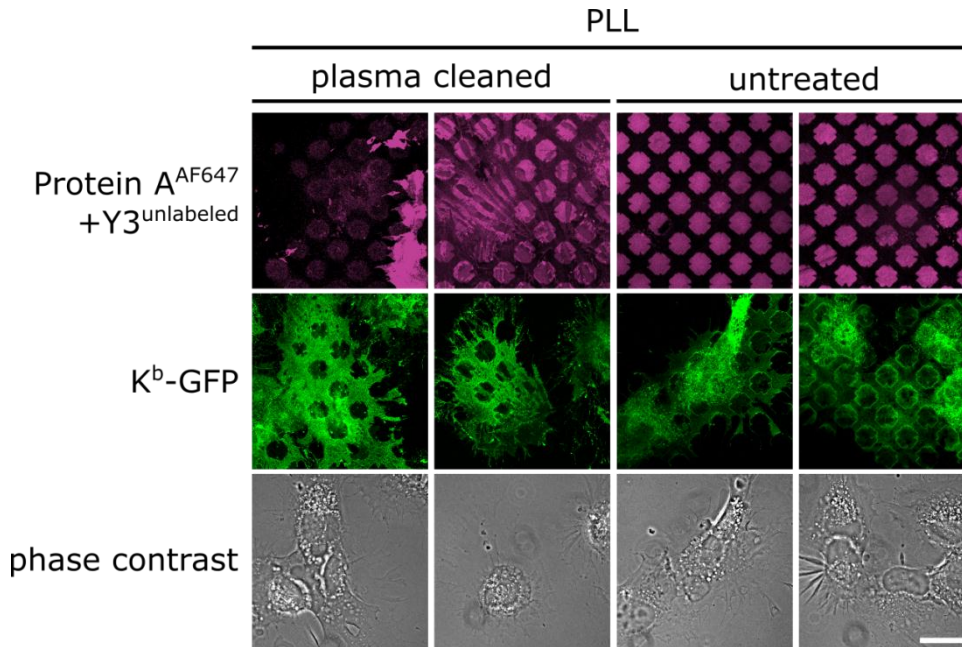


**Figure 2.6.4.2: Oriented immobilization of antibodies via protein A micropatterns.** Labeled protein A (protein A<sup>AF647</sup>) was printed according to the standard protocol onto plasma cleaned or untreated glass coverslides that were pre-coated with PLL. The fabricated protein A<sup>AF647</sup> was then incubated with unlabeled Y3 (Y3<sup>unlabeled</sup>) overnight at 4°C in a wet chamber. STF1/K<sup>b</sup>-GFP were seeded the next day and incubated on the protein A<sup>AF647</sup>-Y3 micropatterns according to the standard protocol. Bar, 25 µm.

### 2.6.4.3 Immobilization via protein G

We repeated the experiment described above with protein G. In this experiment, we also used unlabeled protein G (protein G<sup>unlabeled</sup>) and printed it on PLL-coated glass coverslides according to our standard printing protocol. These protein G micropatterns were then either incubated with labeled or unlabeled capture antibody (see figure 2.6.4.3 A for Y3<sup>AF647</sup> and 2.6.4.3 B for Y3<sup>unlabeled</sup>). Then, STF1/K<sup>b</sup>-GFP cells were seeded onto the antibody micropatterns. The results of this experiment were heterogeneous: In some areas of the pattern, the Y3<sup>AF647</sup> antibody actually bound to the printed protein G pattern elements (see figure 2.6.4.3 A, column 2, 3, and 5), but in other areas, it preferred the pattern element interspaces just as in the protein A experiments (see figure 2.6.4.3 A, column 1, 4, and 6). However, the capture of K<sup>b</sup>-GFP from the cells occurred mostly on the pattern element interspaces (except for figure 2.6.4.3 A, column 2, 5, and 6) and does not necessarily correlate with the capture antibody pattern.

In figure 2.6.4.3 B, we see the same phenomenon that the capture antibody binds randomly to the protein G pattern elements or the interspaces, according to the captured K<sup>b</sup>-GFP. Taking all observations together, the results are inconclusive. Since the capture antibody binds either to the pattern elements or to the interspaces, there seems to be an interaction between the printed protein G and Y3, which is so far not predictable. I suspect that this depends on the local concentrations of the antibodies, but this would need further investigation.



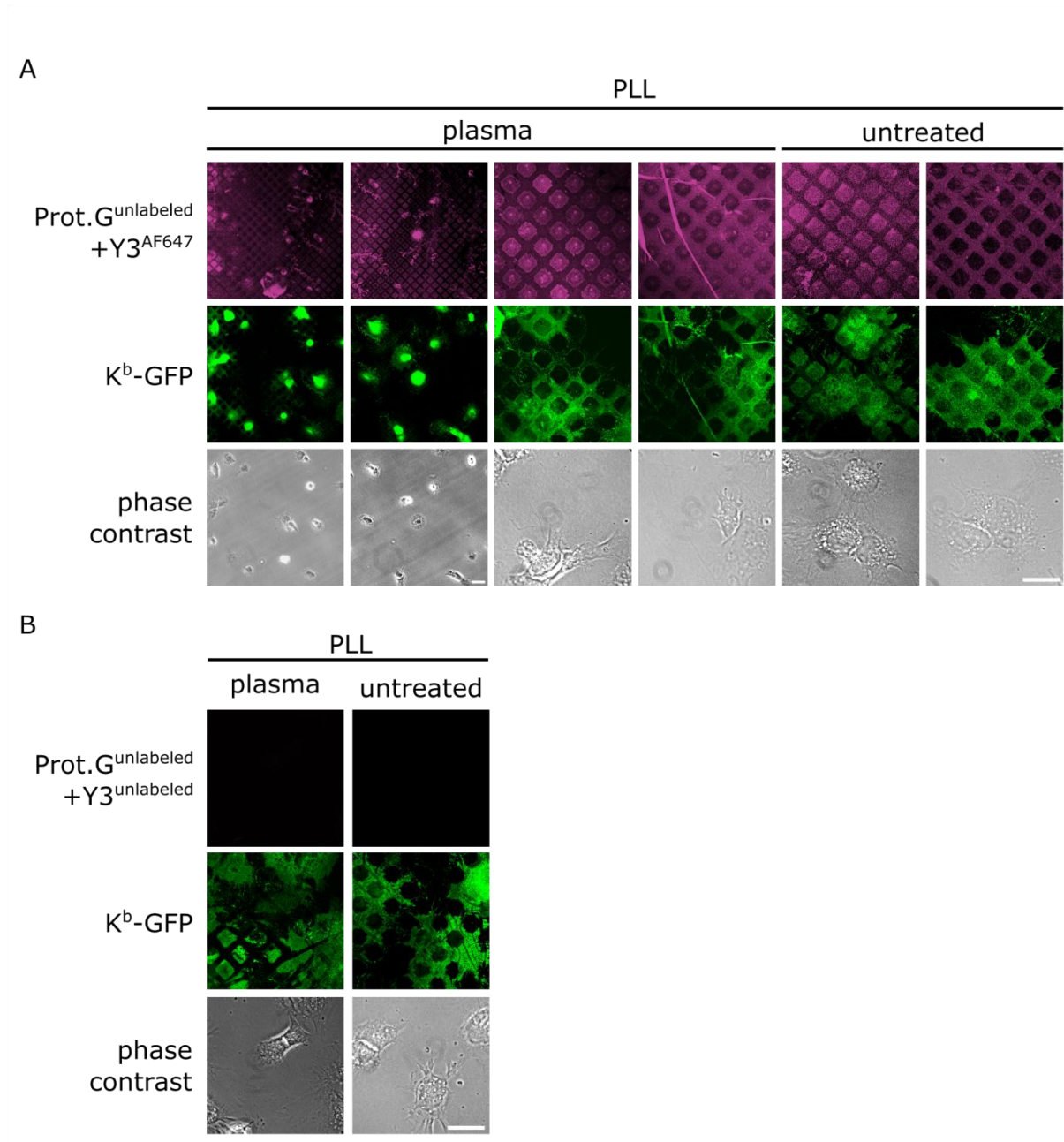


**Figure 2.6.4.3: Oriented immobilization of antibodies via protein G micropatterns.** Unlabeled protein G (Prot. G<sup>unlabeled</sup>) was printed according to the standard protocol onto plasma cleaned or untreated glass coverslides that were pre-coated with PLL. **(A)** The fabricated protein G micropatterns were then incubated with labeled Y3 (Y3<sup>AF647</sup>) or **(B)** unlabeled Y3 (Y3<sup>unlabeled</sup>) overnight at 4°C in a wet chamber. STF1/K<sup>b</sup>-GFP were seeded the next day and incubated on the protein protein G-Y3 micropatterns according to the standard protocol. Bar, 25 µm.



#### 2.6.4.4 Pre-binding the antibody to protein G

Our initial trial experiments of immobilization of antibodies via protein A and protein G prints were not successful (see 2.6.4.2 and 2.6.4.3). The main problem was that the antibody did not specifically bind to the printed protein A or protein G patterns as predicted, but was randomly distributed on the pattern elements and the interspaces. To circumvent this problem, we tried to pre-incubate the antibody with protein G and then print the protein G-antibody complex. For the experiment, we used protein G at a concentration of 5  $\mu\text{g/mL}$  and incubated them with 1 or 5  $\mu\text{g/mL}$  of labeled antibody ( $\text{Y3}^{\text{AF647}}$ ) overnight at 4 °C. The next morning, we used this solution to ink the stamp according to our standard protocol, and then seeded STF1/ $\text{K}^{\text{b}}$ -GFP cells. As control, we repeated the previous protein G trials where we printed protein G and incubated these micropatterns with  $\text{Y3}^{\text{AF647}}$ . Similar to our previous trials, the  $\text{Y3}^{\text{AF647}}$  antibody was again binding to the pattern interspaces as visualized by the grid pattern in figure 2.6.4.4. Despite this undesired localization, the antibody also lost its functionality, since it did not capture any  $\text{K}^{\text{b}}$ -GFP. In our new approach of printing the complex of protein G and  $\text{Y3}^{\text{AF647}}$ , there was no micropattern visible, but we detected some fluorescent signal ( $\text{Y3}^{\text{AF647}}$ ) inside the cells (see figure 2.6.4.4, columns 3-6). We hypothesized that the cells have internalized the protein G- $\text{Y3}^{\text{AF647}}$  complexes. Since we did not check the micropatterns prior to cell seeding, we cannot judge whether the printing was not successful or if it detached during cell incubation. Without further information, I speculate that either the protein concentration was too low or that the protein G- $\text{Y3}^{\text{AF647}}$  complexes were irreversibly adsorbed to the PDMS stamps. Our results also do not support the published finding that large molecular weight of biological inks enhance the formation of well-defined, high contrast patterns due to their limited diffusion (Kaufmann and Ravoo, 2010).

Since our method of direct antibody printing appeared quite robust and the capture of protein was sufficient, we did not invest more time in the approach.

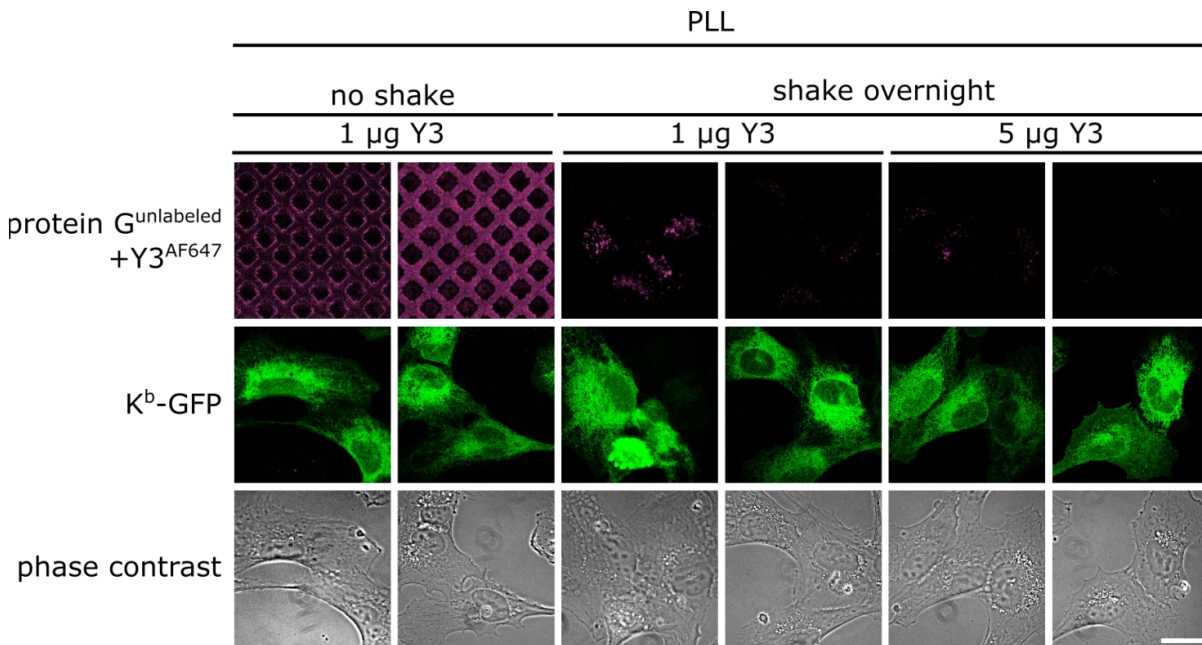


**Figure 2.6.4.4: Comparison of sequential binding and printing of a pre-mixed protein G-Y3 complex.** Unlabeled protein G (protein G<sup>unlabeled</sup>) was printed and then incubated with labeled Y3 (Y3<sup>AF647</sup>) as described previously (no shake). In an alternative approach, unlabeled protein G (protein G<sup>unlabeled</sup>) was incubated with different concentrations of labeled Y3 (Y3<sup>AF647</sup>) overnight at 4°C (shake overnight). The pre-formed protein G-Y3 complex was then printed according to the standard protocol. Then, STF1/K<sup>b</sup>-GFP cells were seeded onto both protein G-Y3 patterns according to the standard protocol. Bar, 25  $\mu$ m.

## 2.7 Blocking antibody prints with BSA

From time to time, we observed that the cells did not spread evenly over the micropatterned surfaces (see 4.2.4). This was especially prominent when the pattern elements had dimensions in the range of the cell's size (see 1.3.5.3). But also with our generally used pattern sizes of 5-10  $\mu$ m, we sometimes observe that the cells stick to the antibody pattern elements, forming little "feet". We hypothesized that the cells can sense the micropatterned surface and although cells generally adhere to the glass surface, they develop a preference for the protein coated pattern element when they have the choice between uncoated and coated glass. Since we did not want to change cell shape but only the protein distribution inside the cell's plasma membrane, we wanted to generate a surface that is homogenously coated with proteins. But at the same time, we did not want to coat the surfaces with proteins of the extracellular matrix to give them extra adhesion sites that would indeed influence cell adhesion and thus the spreading of cells. Since the interspaces appear as a grid pattern, we would probably trigger cell

rearrangement on these patterns. Similar approaches are indeed used in trial experiments for 3D tissue models where cell spreading is guided along specific scaffolds (Khademhosseini et al., 2006). The Schütz group uses BSA to fabricate antibody micropatterns in an indirect approach (Schwarzenbacher et al., 2008). Since BSA does not add specific adhesion sites, we performed a trial experiment in which we blocked the printed antibody micropattern with a 5% BSA solution. For this, we added a droplet of the BSA solution onto the  $Y3^{AF647}$  micropattern and incubated it for 15 min at RT, washed, before we seeded the cells. In Figure 2.7, the micrographs are shown.

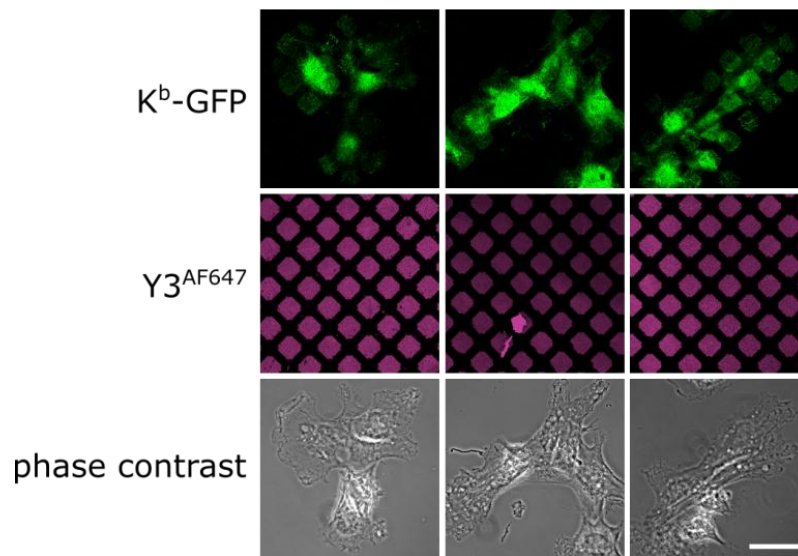


**Figure 2.7: Blocking micropattern interspaces with BSA.**  $Y3^{AF647}$  antibody micropatterns (magenta) were printed according to the standard protocol and the interspaces were then blocked with BSA and washed. Next, STF1/ $K^b$ -GFP cells were seeded on the antibody micropatterns and incubated overnight. Bar, 25 $\mu$ m.

Compared to the standard procedure, there were only minor differences detectable. My first impression was that the capture efficiency was decreased. I assumed that BSA may also stick to the pattern elements and thereby block some of the antigen binding sites of the immobilized antibody. However, the amount of captured proteins generally varies from experiment to experiment for reasons that I could never completely understand; they are probably an intrinsic problem when working with living cells and may have several causes. The decrease in the capture of  $K^b$ -GFP may therefore not necessarily correlate with the BSA blocking and needs further investigation.

Under these conditions, cell spreading was comparable to the unblocked micropatterns. The cells adhered to the glass surface in a similar fashion. In agreement with these observations, blocking with

BSA did not show great improvements over the conventional method, and thus, I skipped this additional step in the standard protocol.

### 3 Results summary

For my thesis work, I developed and optimized the fabrication of printed antibody micropatterns. After establishing the methodology, I applied my developed technique to murine MHC class I molecules, namely H-2K<sup>b</sup> and H-2D<sup>b</sup> (K<sup>b</sup> and D<sup>b</sup>) in living cells. I studied the functionality of the captured K<sup>b</sup> by the addition of peptides. This application was then used as a novel peptide binding assay to study peptide binding in living cells. This method can in principle be applied to other proteins to study ligand binding in the natural, cellular environment.

Next, I investigated the stability of captured K<sup>b</sup> on the antibody micropatterns and found that the use of different antibodies influences the conformational stability of the captured K<sup>b</sup>. In this assay, I can specifically influence the conformation of the captured cell surface proteins and thus investigate even protein conformations of K<sup>b</sup> with a short half-life at the plasma membrane such as the free heavy chain. With these tools in hand, I discovered *in cis* interactions of the free heavy chains of K<sup>b</sup>.

In this thesis, the research findings are distributed into three chapters. The two main findings of this thesis – the development of anti-K<sup>b</sup> antibody micropatterns as novel peptide binding assay, and the *in cis* interactions of K<sup>b</sup> free heavy chains – are described in chapter 4 and 5, respectively. Additional findings are added after each major section. Chapter 6 completes the results section and describes additional findings of this research project.

#### 3.1 Summary of chapter 4: Development of anti-MHC class I antibody micropatterns and optimization

In the first part of chapter 4, I present antibody micropatterns as a novel tool to capture cell surface class I proteins (see section 4.1). The second part of chapter 4 highlights additional data that was generated during the optimization of the novel tool (see section 4.2). It includes trial experiments for alternative approaches to capture MHC class I proteins such as anti-β<sub>2</sub>m or peptide micropatterns. Since I successfully showed peptide binding to captured K<sup>b</sup>-GFP in the first part of this chapter, I show trial experiments for the exchange of this bound peptide with dipeptides in the second part. Another section of the second part deals with the blocking of anti-HA micropatterns with the HA peptide. In the last section of chapter 4, I present trial experiments in which I try to multiplex the antibody micropatterns by generating patterns with two different antibodies such as Y3 and HA (see section 4.2.7).

### **3.2 Summary chapter 5: Anti-MHC class I antibody micropatterns as a tool to study conformation-specific *in-cis* interactions**

Chapter 5 is divided into three parts. The first part presents the application of antibody micropatterns as a two-hybrid assay to detect conformation-dependent *in cis* interactions at the cell surface (see section 5.1). The second part summarizes trial experiments that I performed to characterize the detected clusters further, e.g. by immunostainings of typical marker proteins. For a better cell biological understanding of cluster formation, heterotypic *in cis* interactions between different murine MHC class I alleles were also investigated (see section 5.2). The chapter ends with general remarks and thoughts on my findings concerning cluster formation and future ideas (see section 5.3).

### **3.3 Summary chapter 6: Additional Results and Discussions on Pattern Fabrication**

During my project, I tried alternative approaches for the generation of antibody micropatterns to allow for more applications of the developed micropatterns and to test other opportunities. Besides alternative methods for protein immobilization such as maskless photography (see section 6.1), I performed trial experiments in which I printed purified MHC class I proteins instead of antibodies to test for their stability and the sensitivity of other proteins. This represents an approach that might finally lead to the development of a T cell screening assay (see section **Error! Reference source not found.**).

## **4 Development of anti-MHC class I antibody micropatterns and their applications**

In this chapter, I report on the development of anti-MHC class I antibody, in particular K<sup>b</sup> micropatterns, using the technique of microcontact printing. I further studied the properties, i. e. the peptide binding capacity of the captured MHC class I molecules to develop a peptide binding assay.

The chapter is divided into two parts. Chapter 4.1 is a published manuscript, and chapter 4.2 lists additional experiments that were performed during optimization of the anti-MHC class I antibody micropatterns. All the experimental work in chapter 4.1 was carried out by me, except the generation of the plasmids, which were partly generated by our postdoc Zeynep Hein, and the generation of molds, which were produced by our postdoc Tatiana Kolesnikova. I generated all figures, and the manuscript was written by Sebastian Springer and me.

The experiments in chapter 4.2 were all designed by me and carried out by me or by my students where indicated.

## **4.1 Specific capture of peptide-receptive Major Histocompatibility Complex class I molecules by antibody micropatterns allows for a novel peptide binding assay in live cells**

### **4.1.1 About chapter 4.1**

Chapter 4.1 is a published paper that contains some original data. The experiments in this manuscript were designed by me and performed by myself or the indicated co-authors. The manuscript was written by Sebastian Springer and me.

The full citation of the paper is:

Dirscherl, C., Palankar, R., Delcea, M., Kolesnikova, T. A., and Springer, S.: **Specific Capture of Peptide-Receptive Major Histocompatibility Complex Class I Molecules by Antibody Micropatterns Allows for a Novel Peptide-Binding Assay in Live Cells.** *Small.* **13** (15) (2017), DOI: 10.1002/smll.201602974.

The paper is online at: <http://onlinelibrary.wiley.com/doi/10.1002/smll.201602974/abstract>

The figure numbers were changed to match the format of this thesis.

### **4.1.2 Abstract**

Binding assays with fluorescently labeled ligands and recombinant receptor proteins are commonly performed in 2D arrays. But many cell surface receptors only function in their native membrane environment and/or in a specific conformation, such as they appear on the surface of live cells. Thus, receptors on live cells should be used for ligand binding assays. Here, it is shown that antibodies preprinted on a glass surface can be used to specifically array a peptide receptor of the immune system, i.e., the major histocompatibility complex class I molecule H-2K<sup>b</sup>, into a defined pattern on the surface of live cells. Monoclonal antibodies make it feasible to capture a distinct subpopulation of H-2K<sup>b</sup> and hold it at the cell surface. This patterned receptor enables a novel peptide-binding assay, in which the specific binding of a fluorescently labeled index peptide is visualized by microscopy. Measurements of ligand binding to captured cell surface receptors in defined confirmations apply to many problems in cell biology and thus represent a promising tool in the field of biosensors.



### 4.1.3 Introduction

Major histocompatibility complex class I molecules are transmembrane proteins that act as peptide receptors and are central to the mammalian immune response against viruses, intracellular parasites, and tumors. Class I molecules bind peptides (which are constantly generated by protein degradation) in the cell interior, transport them to the plasma membrane, and present them to the T-cell receptors of cytotoxic T cells. If the T cells recognize the peptides as non-self, they force the presenting cell to undergo apoptosis, and the spread of the virus, parasite, or tumor is inhibited (Townsend and Bodmer, 1989). The strength of an antiviral or antitumor immune response in patients is largely determined by the binding of the available peptides to the class I molecules of the presenting cell (Yewdell, 2006). This is why assays for peptide binding to class I molecules are crucial for the design of vaccines and therapies. But such assays are difficult to realize since peptide-empty recombinant class I molecules, which are necessary for such assays, are difficult to produce and conformationally unstable (Saini et al., 2013a and references therein). Recombinant class I molecules from *E. coli* or insect cells also do not have their native glycosylation, which is known to influence peptide binding (Springer, 2015). Thus, class I molecules from mammalian cells should be used in a binding assay. Peptide-empty class I molecules do occur on the plasma membrane of many cells, but at low levels. They have a very short half-life, since they are rapidly endocytosed to avoid bystander killing (Montealegre et al., 2015). To use these peptide-empty class I molecules for a peptide-binding assay, it is necessary to accumulate them at the cell surface, in their native form and membrane environment. We therefore coupled an antibody to the glass surface that the cells were growing on, to capture class I molecules at the cell surface and prevent their endocytosis. Class I molecules are dimers of a polymorphic heavy chain and the noncovalently bound light chain, beta-2 microglobulin ( $\beta_2m$ ). Thus, we decided to use a  $\beta_2m$ -dependent monoclonal antibody (mAb), Y3, which recognizes the murine class I molecule H-2K<sup>b</sup> (K<sup>b</sup>) if and only if bound to  $\beta_2m$ , both in the presence and absence of bound peptide (Hämmerling et al., 1982). We arranged the antibody in a pattern on the glass surface in order to use the antibody-free areas as controls for nonspecific peptide binding to cells and glass. Such antibody patterns have been used to arrange whole cells or membrane proteins, and it was shown recently that at least some antibodies remain functional when printed directly onto untreated glass coverslips (St John et al., 1998; David J. Graber et al., 2003; LaGraff and Chu-LaGraff, 2006). In the work presented here, we created micropatterns of the mAb Y3 on unmodified glass surfaces by microcontact printing with polydimethylsiloxane (PDMS) stamps. When seeded with cells, the pattern elements of the Y3 antibody micropatterns specifically capture cell surface K<sup>b</sup> molecules, thus arranging them in a defined pattern in the plasma membrane. These captured K<sup>b</sup> molecules can bind

fluorescently labeled exogenous peptides, demonstrating that the Y3 antibody traps and preserves the peptide-receptive state of  $K^b$ . We then tested unlabeled peptides for competition with the fluorescent index peptide in binding to  $K^b$  and thus demonstrate a rapid and highly sensitive peptide binding assay with microscopic read-out. With this, we describe a novel method to hold cell surface receptors in a specific conformation or state, as defined by an antibody reactive to that conformation, and in their native environment at the cell surface in order to use them in binding assays. Such assays are useful to address many questions in cell biology, and they may be developed further into cellular biosensors or toward high-throughput screening approaches.

### 4.1.4 Results

#### 4.1.4.1 Characterization of Class I Antibody Micropatterns

For the generation of micropatterns of  $\beta_2m$ -dependent antibodies by microcontact printing (Figure 4.1.4.1 A), stamps with a height of two micrometers (Figure 4.1.4.1 B) were made from PDMS using master molds fabricated by standard photolithography. The stamps were inked with a solution of the monoclonal anti- $K^b$  antibody Y3 and gently pressed onto the surface of untreated glass coverslips. We assume that in this way, the antibody molecules were deposited in a random orientation on the glass surfaces. After microcontact printing, the presence of geometric micropatterns of antibody molecules was confirmed by scanning confocal fluorescence microscopy. For visualization of the antibody micropatterns, either directly fluorescently labeled antibodies were used for printing, or the unlabeled antibody prints were detected after incubation with a fluorescent secondary antibody, both yielding high-contrast images (Figure 4.1.4.1 C). These data, and the detection of the printed pattern elements with a secondary antibody conjugated to gold nanoparticles, and their detection by scanning electron microscopy (SEM), showed that the printed antibody molecules were generally evenly distributed within each pattern element (Figure 4.1.4.1 D).

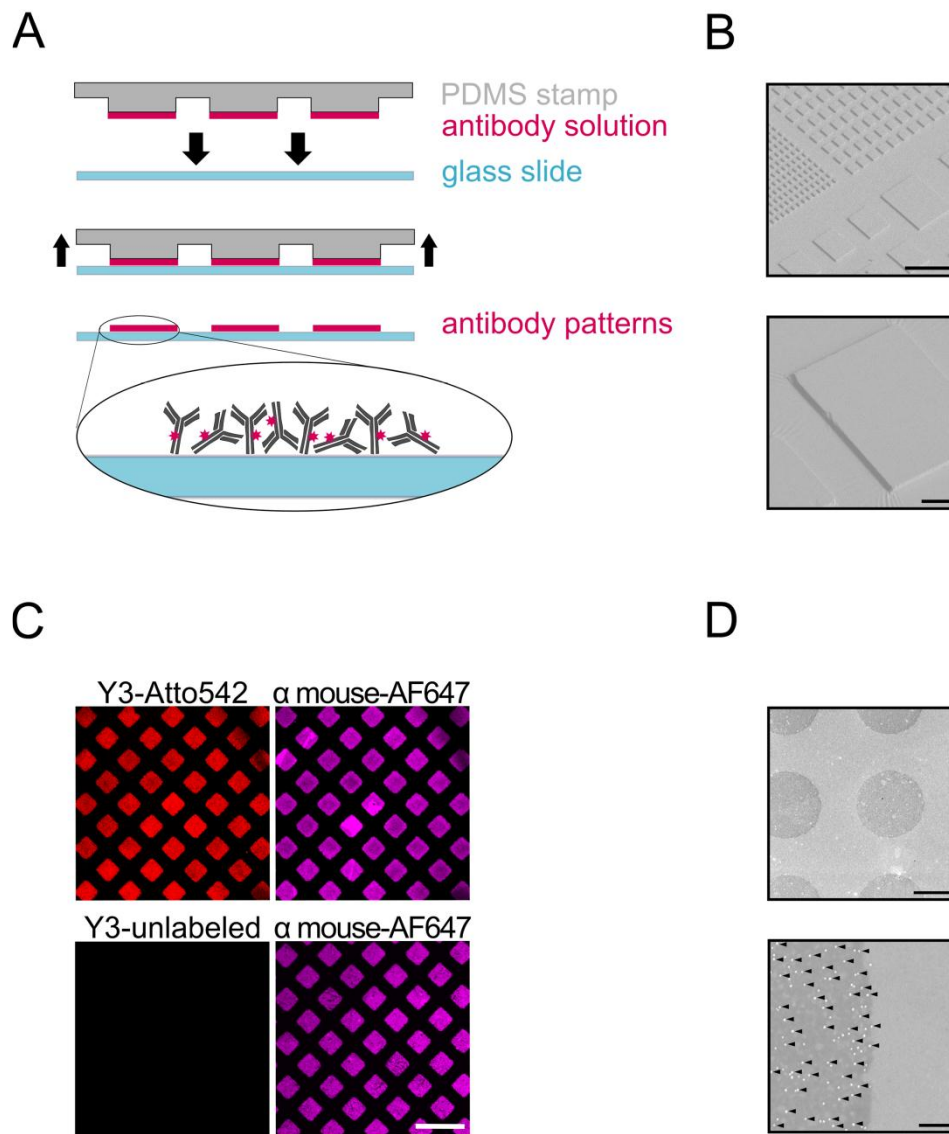


**Figure 4.1.4.1: Fabrication and characterization of antibody micropatterns.** (A) Schematic of printing an antibody pattern onto a glass slide with a PDMS stamp. (B) SEM image of a PDMS stamp. Bars, 50  $\mu\text{m}$  (top) and 10  $\mu\text{m}$  (bottom). (C) Printed patterns of unlabeled (bottom row) or fluorescently labeled (Atto 542, top row) murine monoclonal antibody Y3 on a glass coverslip detected with goat anti-mouse antibody conjugated with Alexa Fluor 647. Bar, 25  $\mu\text{m}$ . (D) SEM image of pattern elements (top) and pattern boundary (bottom) of mAb Y3 detected with goat anti-mouse secondary antibody conjugated with gold nanoparticles. The printed pattern elements are visible as dark patches in SEM imaging (top). At higher magnification, the individual gold nanoparticles appear as bright dots on this dark background. For better visualization, some gold nanoparticles are highlighted with black arrowheads (bottom). Bars, 20  $\mu\text{m}$  (top) and 500 nm (bottom).

### 4.1.4.2 Anti-Class I Antibody Micropatterns Are Functional and Target-Specific

We next tested whether the printed antibody micropattern elements were able to capture class I molecules on the plasma membrane of live cells (Figure 4.1.4.2 A). For this, we used human STF1 cells, since they lack the TAP2 peptide transporter, which transports peptides into the lumen of the endoplasmic reticulum. In these cells, class I molecules are not loaded with peptides and travel to the cell surface in a peptide-empty state. For our study, we stably introduced the murine class I molecule  $K^b$  into these STF1 cells as a green fluorescent protein (GFP) fusion. Since the empty  $K^b$ -GFP proteins have a short half-life at the cell surface before being degraded in lysosomes (Montealegre et al., 2015), their steady state cell surface population is small. We reasoned that this would result in a low background signal for our capture assay. To test the functionality of the antibody micropatterns, we printed the monoclonal anti- $K^b$  antibody Y3 as above and then seeded the STF1/ $K^b$ -GFP cells onto these antibody micropatterns. We used pattern element sizes of ten micrometers in diameter and interspaces of five micrometers to enable cells to spread across several pattern elements. We grew the cells for six hours on the antibody patterns, fixed them, and observed them by fluorescence microscopy. The arrangement of the  $K^b$ -GFP fluorescence in the patterns of the printed antibody was clearly visible, suggesting that  $K^b$ -GFP molecules were captured on the pattern elements (Figure 4.1.4.2 B). This patterning of  $K^b$ -GFP was protein-specific, since it was only visible with the  $K^b$ -specific antibody, Y3, but not when an antibody to the class I molecule H-2D<sup>b</sup>, 27-11-13S, was printed (Figure 4.1.4.2 B, right column). In a time course experiment, the patterned  $K^b$ -GFP was visible as early as the two-hour time point after seeding (Figure S1, Supporting Information). This suggests that the class I molecules are rapidly captured by the antibody. Indeed, by live-cell microscopy, we found that patterning of surface class I molecules occurs immediately after cell contact with a pattern element. In order to optimize the binding capacity of the antibody micropatterns, we tested different concentrations of the antibody solution used to ink the stamps. Fluorescence imaging of captured  $K^b$ -GFP revealed that a high contrast between the pattern elements and interspaces was achieved over a range of concentrations of the printed mAb Y3. To ensure a robust signal-to-noise ratio of the patterned  $K^b$ -GFP, we used a Y3 antibody concentration of  $0.1 \mu\text{g} \mu\text{L}^{-1}$  for all experiments (Figure S2, Supporting Information). We conclude that when cells adhere and spread on class I molecule-specific antibody micropatterns, their class I molecules are bound by the antibodies and trapped on these pattern elements (Figure 4.1.4.2 A). We next wanted to ensure that growth on antibody patterns, and patterning of membrane proteins, did not disturb the overall organization of the plasma membrane. With fluorescently labeled wheatgerm agglutinin (WGA; a lectin that binds to all glycosylated cell surface proteins and lipids), cell surfaces stained normally and without

noticeable anomalies (Figure 4.1.4.2 C, left column). To test integrity and distribution of the cytoskeleton, we also immunostained  $\beta$ -actin and  $\beta$ -tubulin (Figure 4.1.4.2 C, center and right columns). Cells growing on and off the antibody micropatterns did not exhibit any differences, which demonstrates that cells spread on antibody micropatterned surfaces with normal kinetics and morphology (Figure 4.1.4.2 C; enlargements in Figure S3, Supporting Information).

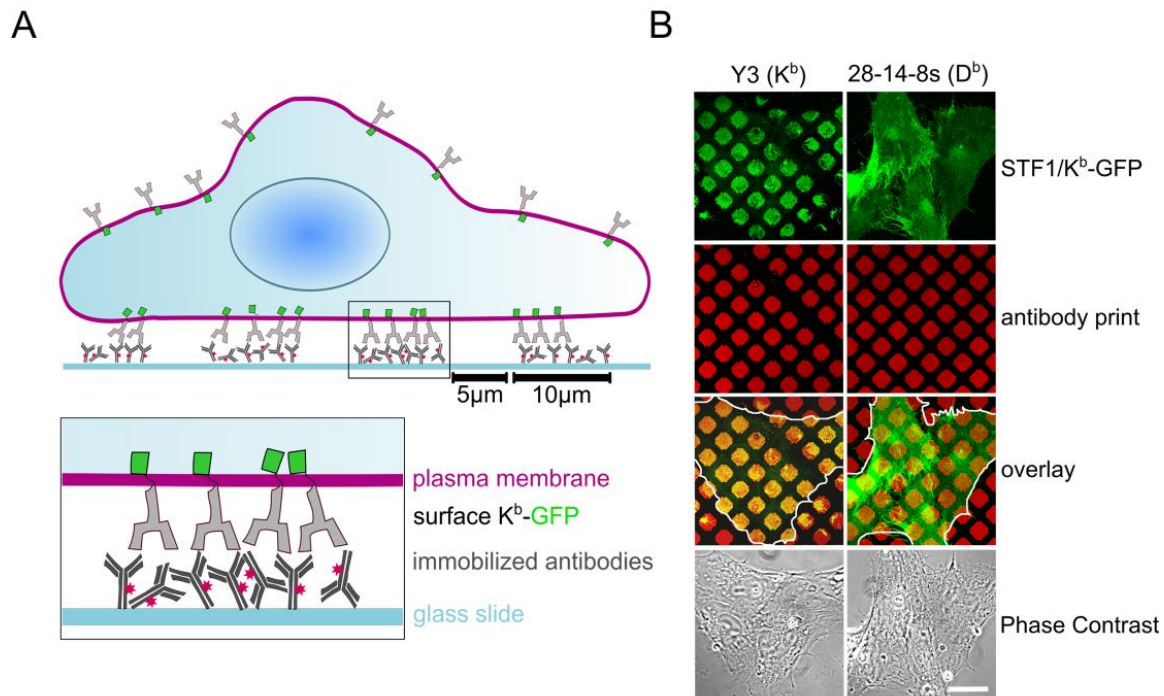


**Figure 4.1.4.2: Specific capture of class I molecules by printed antibody micropatterns.** (A) Schematic of the antibody micropattern capture assay. 10  $\mu\text{m}$  squares of the  $\text{K}^{\text{b}}$ -specific mAb Y3 were printed on glass coverslips, which were then seeded with STF1 cells expressing the target protein  $\text{K}^{\text{b}}$ -GFP. Upon binding of  $\text{K}^{\text{b}}$ -GFP to the antibody, the proteins are arranged in the plasma membrane according to the antibody micropattern. (B) Patterning of  $\text{K}^{\text{b}}$ -GFP in STF1 cells seeded on antibody micropatterns of mAb Y3 ( $\text{K}^{\text{b}}$ -specific, left column; setup exactly as in Figure 2A) but not 27-11-13s ( $\text{D}^{\text{b}}$ -specific, right column). Cells were incubated at 37°C until they adhered, and then shifted to 25°C overnight, and then fixed and imaged. Bar, 25  $\mu\text{m}$ . (C) Growth on antibody micropatterns does not generally alter cell growth and surface or cytoskeleton structure. STF1/ $\text{K}^{\text{b}}$ -GFP cells grown overnight at 37°C on Y3 antibody micropatterns were fixed and stained with wheat germ agglutinin (WGA) or permeabilized with 0.1% Triton X-100 or methanol and stained with antiserum to  $\beta$ -actin or  $\beta$ -tubulin, then labeled with fluorophores as indicated and imaged. Bar, 25  $\mu\text{m}$ .

Figure continues on next page.

C

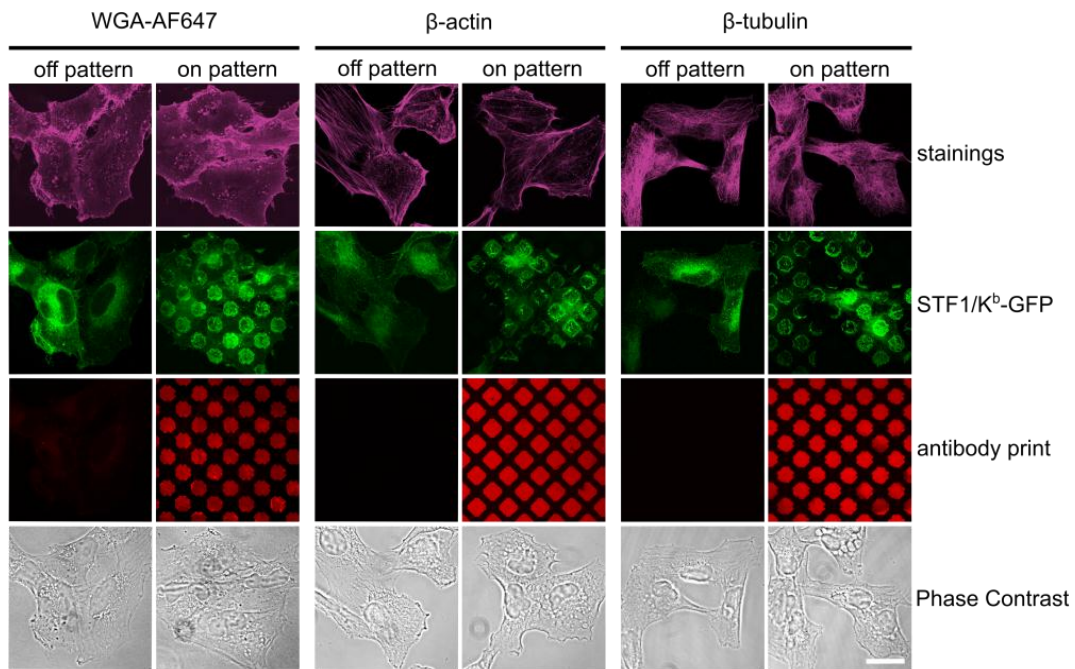


**Figure 4.1.4.2 (continued): Specific capture of class I molecules by printed antibody micropatterns. (C)** Growth on antibody micropatterns does not generally alter cell growth and surface or cytoskeleton structure. STF1/K<sup>b</sup>-GFP cells grown overnight at 37°C on Y3 antibody micropatterns were fixed and stained with wheat germ agglutinin (WGA) or permeabilized with 0.1% Triton X-100 or methanol and stained with antiserum to β-actin or β-tubulin, then labeled with fluorophores as indicated and imaged. Bar, 25μm.

#### 4.1.4.3 Capture of Class I Molecules Occurs Specifically at the Cell Surface

To compare the spatial distribution of K<sup>b</sup>-GFP at the cell–glass interface and in the internal compartments of the cell, we recorded 3D z-stack images (Figure 4.1.4.3 A). Patterning of K<sup>b</sup>-GFP was mainly visible in the bottom layers, where the cell contacted the surface. Quantification by the Pearson coefficient showed that the patterning of K<sup>b</sup>-GFP correlated in the z-direction (orthogonal to the surface) with the fluorescence of the printed antibody (Figure 4.1.4.3 B, C). Since K<sup>b</sup>-GFP and antibody micropatterns thus correlate in 3D, we conclude that K<sup>b</sup>-GFP patterning occurs only at the cell–glass interface at the bottom of the cell and does not influence the intracellular distribution of class I molecules.



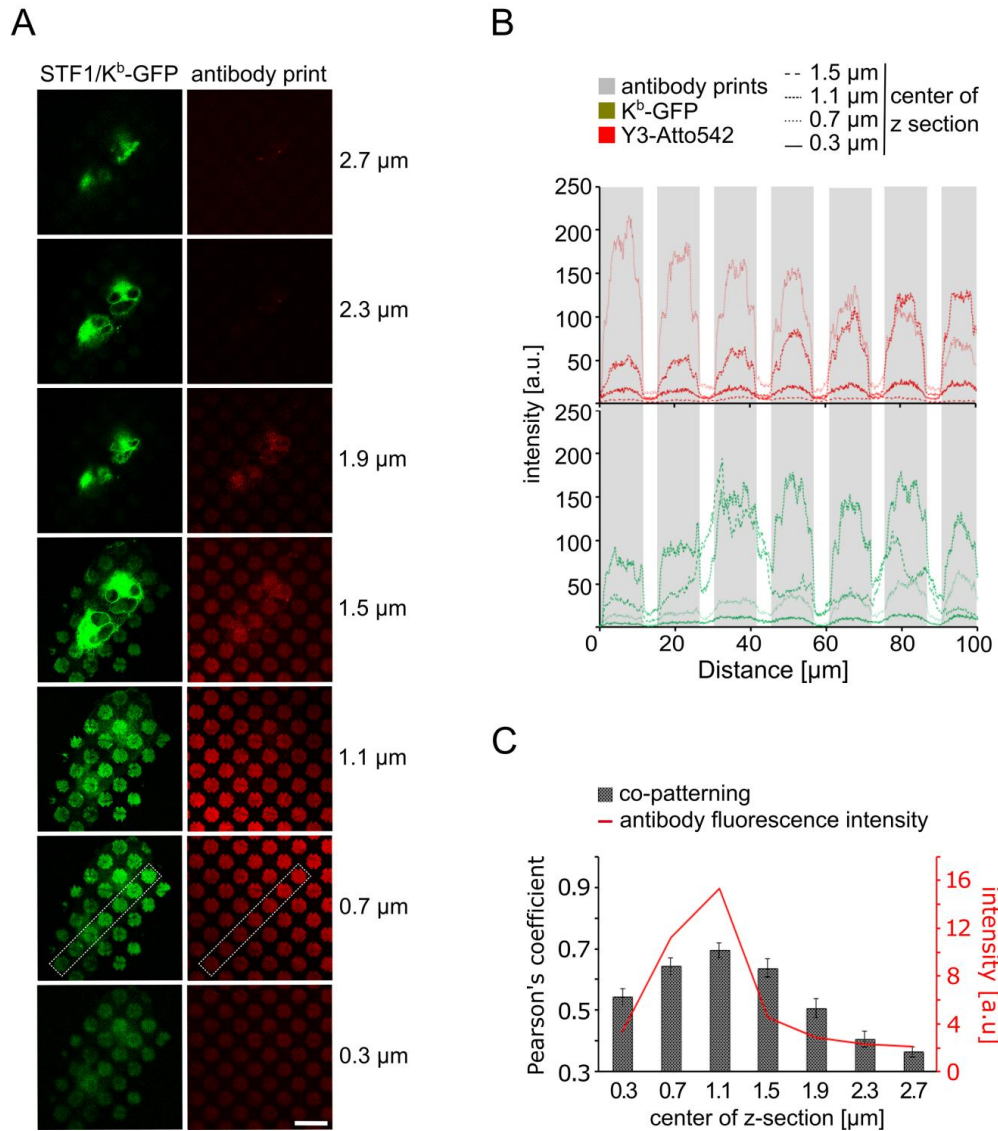


**Figure 4.1.4.3: Class I molecule capture occurs at the cell-glass interface. (A)** Z stack images of STF1/K<sup>b</sup>-GFP cells seeded on mAb Y3 antibody micropatterns. Cells were incubated at 37 °C until they adhered, then shifted to 25 °C overnight, then fixed and imaged. Images show optical sections ( $\approx 600$  nm thickness) of the same cell, demonstrating that the pattern of K<sup>b</sup>-GFP correlates with the antibody micropatterns in the z direction. Numbers indicate the center of the individual layers of the z-stack. Bar, 25  $\mu\text{m}$ . **(B)** Integrated intensity profiles of antibody (upper) and GFP (lower) fluorescence from the rectangles shown in A in the different layers of the z stack as indicated. **(C)** Quantification of the layers of the z stack. The colocalization of GFP fluorescence with the antibody fluorescence pattern was determined as the Pearson coefficient. The x axis intersection of the y axis (0.28) corresponds to random distribution. n=7, SEM shown. A representative fluorescence intensity profile of the antibody pattern corresponds to the co-patterning of GFP, indicating the level of the plasma membrane in z-direction.

#### 4.1.4.4 Captured Class I Molecules Are Functional and Can Bind Fluorescently Labeled Peptides

STF1 cells lack the TAP2 peptide transporter and hence cannot load class I molecules with peptides in the ER (de la Salle et al., 1999). Thus, class I molecules trapped at the cell surface by the Y3 antibody micropatterns should be mostly peptide-free, and so they should be able to bind an externally added peptide. We therefore next tested peptide binding to the patterned class I molecules. We grew STF1/ K<sup>b</sup>-GFP cells on the Y3 micropatterns overnight at 25 °C to inhibit the dissociation of  $\beta$ 2m (Montealegre et al., 2015 see the Experimental Section) and thus to allow large amounts of intact surface K<sup>b</sup> molecules to become captured. We then incubated cells for 30 min with the K<sup>b</sup> specific ligand peptide, FL9 (sequence: FAPKNYPAL, in the single letter amino acid code). The lysine side chain of FL9 was modified with the carboxytetramethylrhodamine (TAMRA) fluorophore, which does not interfere with peptide binding to K<sup>b</sup> (FL9-TAMRA) (Saini et al., 2015). As anticipated, we observed fast and strong binding of FL9-TAMRA onto the K<sup>b</sup>-GFP pattern (Figure 4.1.4.4 A, column 1), which demonstrates that at least some, if not many, of the class I molecules that are captured by the antibody micropatterns are folded and functional in binding peptide. Finally, we realized the competitive peptide-binding assay. For this, we used FL9-TAMRA as a readout (index) peptide. First, we treated the cells with the unlabeled test peptide SL8 (sequence: SIINFEKL), which binds tightly to K<sup>b</sup>, at different concentrations. Then, we incubated with FL9-TAMRA as above. For the SL8-treated cells, no binding of the index peptide was observed (Figure 4.1.4.4 A, columns 2 and 3, and B). Pre-incubation with different concentrations of the peptide NV9 (sequence: NLVPMVATV), which does not bind to K<sup>b</sup>, did not inhibit binding of the index peptide (Figure 4.1.4.4 A, columns 4 and 5, and B). This result demonstrates that the patterned K<sup>b</sup>-GFP molecules bind peptides with their native specificity, and that this method can be used as a simple and rapid assay for class I molecule-peptide binding.



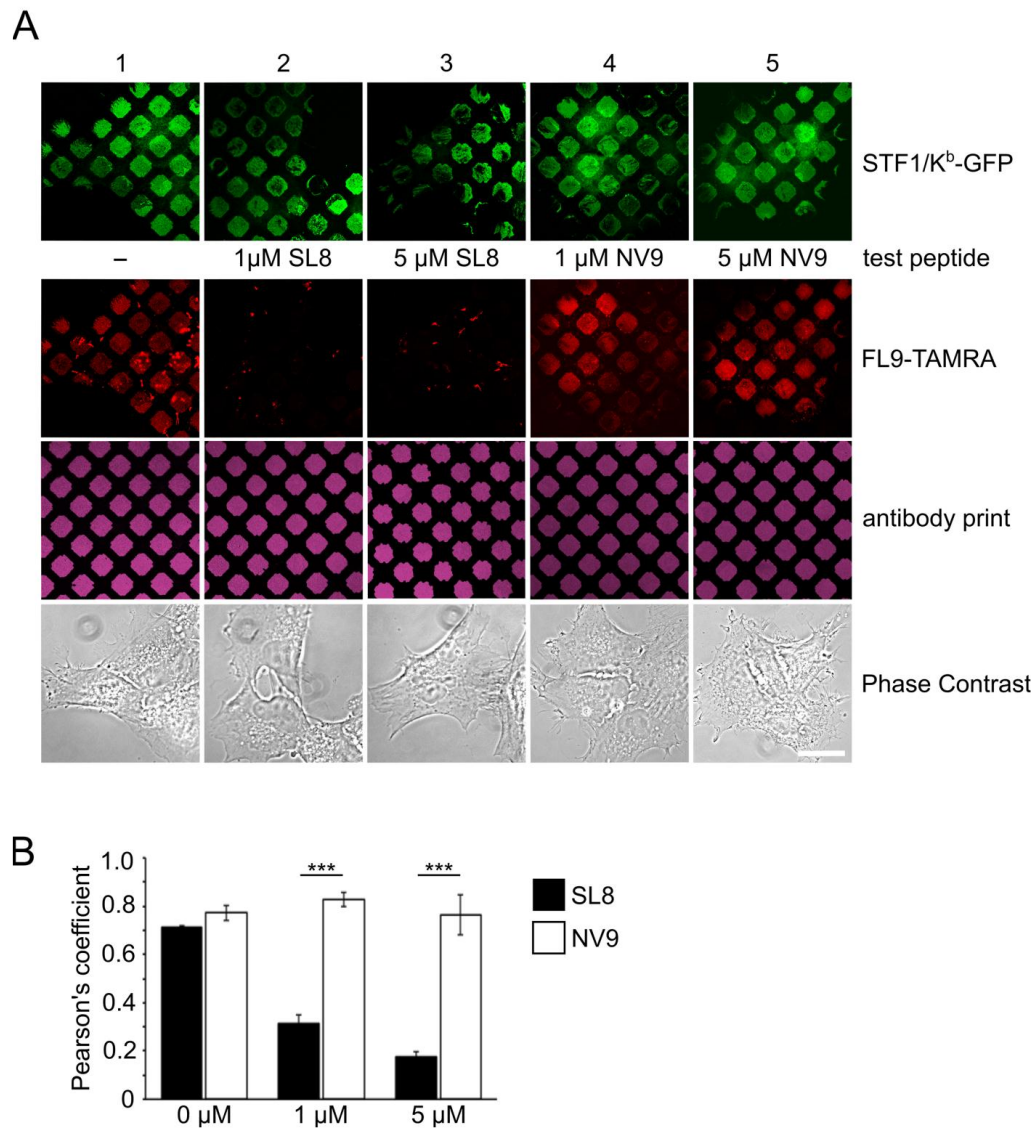


**Figure 4.1.4.4: Peptide-specific binding assay with captured class I molecules. (A)** STF1/K<sup>b</sup>-GFP cells were grown on mAb Y3 antibody micropatterns at 37 °C until they adhered, shifted to 25 °C overnight to accumulate empty K<sup>b</sup> at the cell surface, incubated first for 15 min with SL8 (K<sup>b</sup>-binding) or NV9 (non-K<sup>b</sup>-binding) test peptide at the indicated concentration, and then incubated with 1 μM FL9-TAMRA index peptide. The cells were then fixed and imaged. Bar, 25 μm. **(B)** Quantification of data in A performed as in Figure 4.1.4.3C.

### 4.1.5 Discussion and Conclusion

To study the emerging complexity of receptor–ligand interactions, researchers need new and better methods. The assessment of the effects of protein glycosylation, particular states or conformations, or the role of the cellular environment for ligand binding capacity often requires receptor analysis in, or on, live cells. For example, our work described here was prompted by the need to investigate the binding of peptide ligands to glycosylated class I molecules in their native membrane environment and in the peptide-empty  $\beta_2m$  associated state. In order to work with class I molecules embedded in the plasma membrane, we captured them on the surface of living cells with antibodies printed on the glass culture surface. With this method, we were able to prevent the internalization of the peptide-empty state, which is otherwise rapidly endocytosed and degraded. Now, by the addition of peptide ligand to the cell culture medium, we were able to measure the binding of fluorescently labeled peptide ligand to these captured class I molecules, i.e., its co-localization with the pattern of the receptor (You and Piehler, 2016; Moore et al., 2016). In principle, capture of cell surface proteins can also be achieved on glass surfaces that are homogeneously coated with antibodies. Our patterning approach has the advantage that it allows for an internal control: the unpatterned interspaces provide an optimal control for peptide background binding to cells and glass. To achieve this micrometer-spaced patterning of the antibody, we used microcontact printing with PDMS stamps (Kane et al., 1999). Similar patterning of membrane proteins has recently been used to study cell adhesion and phagocytosis, (Cavalcanti-Adam et al., 2006; Freeman et al., 2016) signaling, (Mossman et al., 2005; Wu et al., 2004) cellular protein–protein interactions, (Schwarzenbacher et al., 2008; Weghuber et al., 2010; Löchte et al., 2014; Wedeking et al., 2015) and protein–metabolite interactions (Gandor et al., 2013). Here, we address for the first time the challenge to study only one particular state of class I molecules, namely the peptide-empty (also called the peptide-receptive) state, which is rare at the cell surface (since it is rapidly internalized and degraded) and which is intermixed with other states such as the free heavy chain (which lacks the light chain  $\beta_2m$ ). Both problems were solved by printing a  $\beta_2m$ -dependent specific antibody, Y3, which only recognizes the heavy chain in complex with the light chain. This allowed us to trap exclusively the peptide-empty form, but not the free heavy chain. Our assay thus enables state specific binding studies for class I and other receptors using the many other state- or conformation-specific antibodies that have been described. The attachment of antibodies to glass surfaces, especially to surfaces treated for cell growth, has been studied intensively, and many of the currently used protocols are complex, with often several layers of compounds (Schwarzenbacher et al., 2008; Löchte et al., 2014; Gandor et al., 2013; Wilson and Nock, 2003; Iversen et al., 2008; Blackburn and Shoko, 2011; Matic et al., 2013). We decided

to follow other studies where antibodies were printed directly onto untreated glass coverslips, (St John et al., 1998; David J. Graber et al., 2003; LaGraff and Chu-LaGraff, 2006) as this direct printing is simpler and faster than indirect methods of attachment. Initially, we were concerned that the (presumably) random orientation of antibody molecules on the glass surface (Figure 4.1.4.1 A) would lead to their inactivation, but indirect attachment of the antibodies by printing protein A or secondary (anti-mouse) antibodies gave no improvement over direct printing (data not shown). Due to the random immobilization of antibodies, it is likely that the antibody molecules are positioned in all possible spatial orientations (Figure 4.1.4.4 A) and that not all antigen-binding sites face upward toward their target protein in the cell membrane. We showed that we could improve the signal-to-noise ratio of K<sup>b</sup>-GFP patterning by increasing concentrations, with saturation when the majority of surface K<sup>b</sup>-GFP was captured (Figure S2, Supporting Information). Therefore, the required antibody concentration highly depends on the protein expression level of the seeded cells, especially on the cell surface levels of the protein being captured. These can vary between different stable cell lines and/or transfection levels. We used no coating agent (such as bovine serum albumin or milk) to block the interspaces between the pattern elements before immunostaining with fluorescently labeled secondary antibody (Figure 4.1.4.4 C), and we did not observe any nonspecific binding of the secondary antibody to the untreated glass surface. However, in the cell experiments, we incubated the antibody micropatterns with the cell culture media supplemented with fetal bovine serum (FBS) once we seeded the cells. The serum proteins of the FBS are likely to adsorb to the interspaces between the pattern elements, thus coating these areas with proteins. This would be similar to the seeding of cells on plain glass coverslips for conventional fluorescence microscopy. While direct printing of antibodies might reduce their activity, (David J. Graber et al., 2003) we conclude that for the purpose of our peptide-binding assay, direct printing on untreated glass is sufficient. In our experiments, we observed that the fluorescence of the captured K<sup>b</sup>-GFP is often not uniformly distributed across the pattern elements but rather concentrated along their edges (Figure 4.1.4.2 C). It is unlikely though that the antibody is distributed unevenly in a pattern element, since the fluorescence signals of the antibody in the pattern elements look much more homogeneous than those of K<sup>b</sup>-GFP (Figure 4.1.4.4 C). The simplest explanation is that K<sup>b</sup>-GFP molecules, which can laterally diffuse in the plasma membrane, become captured into the edges of the pattern elements as they collide with them. This notion of rapid capture of diffusive membrane proteins is also supported by our observation that patterning of K<sup>b</sup>-GFP is visible as soon as the cells settle on the substrate: in live-cell recordings, we observed that when a moving cell reaches a new pattern element, K<sup>b</sup>-GFP is captured at that site within seconds to minutes (not shown). We have demonstrated that the observed patterning of K<sup>b</sup>-GFP is at the

bottom of the cell, where it sits on the glass coverslip, since K<sup>b</sup>-GFP co-localizes in the z-dimension with the glass surface antibody micropattern (Figure 4.1.4.3 B, C). We show that the patterned K<sup>b</sup>-GFP is on the cell surface, since its extracellular peptide-binding domain binds membrane-impermeable peptides that are added to the medium (Figure 4.1.4.4 A). This result also confirms that the captured K<sup>b</sup>-GFP is folded and functional. This is important, since peptide-empty class I molecules are thought to be partially unfolded and are notoriously difficult to study, be it as recombinant proteins or in the cellular environment (Springer, 2015). We show here that even such sensitive proteins can be captured, held, and subjected to investigation with antibody micropatterns. Our blocking experiments show that peptide binding to the captured class I molecules is specific, and that our assay can be used for peptide-ligand screening approaches. We demonstrate here the use of these captured K<sup>b</sup>-GFP molecules in a class I molecule-peptide binding assay that is read out with a fluorescence microscope (Figure 4.1.4.4).

### 4.1.6 Outlook

We think that patterning class I molecules, and other receptors, will in the future allow automatic readout, in which pattern recognition software, guided by the fluorescent signal of the antibody micropatterns, can distinguish autonomously between areas of the signal (the pattern elements) and background (the gap areas). In such an automated scanning system, the researcher would be able to scan multiple cells in parallel for quantitative analyses. Such a system will be useful for many receptor–ligand studies, especially those that require receptors to be glycosylated, in their native membrane environment, and/or in a defined state or conformation. Beyond this, directly printed antibody arrays have great potential for discovery. The *in cis*-interaction between two plasma membrane proteins can be detected in their native environment if one of them (the membrane protein) is captured in a pattern, and the other (a membrane or cytosolic protein) is fluorescently labeled (Schwarzenbacher et al., 2008; Löchte et al., 2014; Gandor et al., 2013). In the future, it may be possible to extend this work toward discovery of novel interacting proteins by immunostaining patterned cells for proposed interaction partners. In such a hypothetical experiment, a known membrane protein would be arranged according to the antibody micropatterns, and the cells would be subsequently stained with an antibody against a proposed interaction partner by conventional immunofluorescence methods. Co-localizing signals of patterned membrane protein and antibody stain will then indicate possible *in cis*-interactions of the two proteins. Or, in an even more advanced project, the pattern elements can be subjected, after cell lysis, to 2D matrix-assisted laser desorption ionization (MALDI) imaging to discover proteins that interact with those membrane proteins bound by the printed antibodies (Pröschel et al., 2015). For synthetic biology,

membrane proteins might be arrayed into defined signaling complexes, (Wedeking et al., 2015) or in the absence of cells, antibody arrays might be used for arranging enzymes to encourage substrate channeling and enhance turnover in micrometer-sized bioreactors (Wilson and Nock, 2003; Pröschel et al., 2015). Such options are currently being studied by us and others.

### 4.1.7 Experimental Section

#### 4.1.7.1 Photolithography

Silicon master molds were prepared by semiconductor photolithography. Briefly, silicon wafers were cleaned with acetone and isopropanol, followed by UV plasma cleaning for 5 min and spin-coating with SU-8 negative epoxy based photoresist (MicroChem Corp., USA) to produce a film of 2  $\mu\text{m}$  thickness. Samples were pre-baked on a hot plate at 65  $^{\circ}\text{C}$  for 1 min followed by soft baking at 95  $^{\circ}\text{C}$  for 3 min. To fabricate the silicon master, we used a negative transparency mask with pre-designed geometries (NB Technologies GmbH, Germany). Wafers were exposed to UV light for 3 s under the transparency mask, then post-baked at 95  $^{\circ}\text{C}$  for 1 min and developed in SU-8 developer (MicroChem Corp., USA). To further crosslink the material, wafers were hard baked at 95  $^{\circ}\text{C}$  for 5 min.

#### 4.1.7.2 PDMS stamps

PDMS stamps were generated from basic elastomer and curing agent (Sylgard 184 Silicone Elastomer Kit) mixed in a 10:1 ratio. For each stamp, a droplet of premixed PDMS was applied onto a glass coverslip (#3) and covered with a silicone master containing an array of squares (dimensions: 10  $\mu\text{m}$  diameter and 5  $\mu\text{m}$  interspace). For curing, the stamps were incubated at 55  $^{\circ}\text{C}$  for a minimum of 3 hours. Then, the mold was carefully peeled off the silicone master, and the surrounding areas of the array were cut away with a scalpel. Stamps were stored at room temperature (RT).

#### 4.1.7.3 Antibody patterns

For printing antibody patterns, the prepared PDMS stamps were rinsed with ddH<sub>2</sub>O, dried under nitrogen flow, and inked with 5  $\mu\text{l}$  of antibody solution (0.1  $\mu\text{g } \mu\text{l}^{-1}$ ). After incubation for 10 min at RT in a dark humidity chamber, the stamp was rinsed with ddH<sub>2</sub>O and dried under nitrogen flow. For transfer of the antibody, the stamp was placed under its own weight on a round microscopy glass coverslip (#1, 22 mm) and incubated for 15 min at RT in a dark humidity chamber. The stamp was then removed carefully.

### 4.1.7.4 Scanning electron microscopy (SEM)

Imaging of PDMS stamps and antibody prints was performed with a Zeiss Supra 40 VP scanning electron microscope (Zeiss GmbH, Germany) operated at an acceleration voltage of 5 kV. Prior to the measurements, samples were washed with ddH<sub>2</sub>O, dried under the nitrogen flow, and sputtered with gold.

### 4.1.7.5 Gold immunolabeling of printed antibodies.

Murine monoclonal Y3 antibody micropatterns were incubated with goat anti-mouse IgG 15 nm gold conjugate antibodies (Aurion, Wageningen, Netherlands) for 1 h at RT and then rinsed with ddH<sub>2</sub>O. Binding of the gold-conjugated antibodies was visualized by SEM.

### 4.1.7.6 Patterning cell surface proteins

Coverslips were placed into a sterile cell culture dish with the antibody micropatterns facing upwards. Cells were seeded at a concentration of ~50.000 cells per well immediately onto the antibody patterns. Following incubation as indicated (usually 24 hours), patterns were detected by the fluorescence of directly labeled printed antibodies or after reaction with fluorescently labeled goat anti-mouse secondary antibodies (15 min incubation) by confocal laser scanning microscopy (CLSM) on a Zeiss LSM 510.

### 4.1.7.7 Antibodies

Monoclonal antibodies Y3 (against the complex of K<sup>b</sup> with its light chain beta-2 microglobulin ( $\beta_2m$ ; (Ozato and Sachs, 1981)) and 27-11-13S (against D<sup>b</sup>/ $\beta_2m$ ; (Hämmerling et al., 1982)) were harvested from hybridoma supernatants and purified by affinity chromatography on protein A sepharose. Antibodies were labeled with Atto and Alexa Fluor fluorescent dye NHS esters (ATTO-TEC and Invitrogen) according to the manufacturers' instructions. Secondary polyclonal antibodies were obtained from Abcam.

### 4.1.7.8 Peptides

Peptides were synthesized by Genecust (Luxemburg) and emc microcollections (Tübingen, Germany) and purified by HPLC (90% purity). The K<sup>b</sup>-specific peptide FL9 (FAPGNYPAL in the single-letter amino acid code) was labeled with the fluorescent dye TAMRA on the lysine side chain (avoiding interference with peptide binding to class I) to give FL9-TAMRA. This fluorescent peptide was added to cells at a final concentration of 1  $\mu$ M for 30 min at 37 °C to allow binding, then cells were washed in phosphate

buffered saline (PBS, 10 mM phosphate pH 7.5, 150 mM NaCl), fixed, and observed by CLSM. Prior blocking with the SL8 (SIINFEKL) or NV9 (NLVPMVATV) peptides was for 15 min at 25 °C, where applicable. Binding of the peptides to K<sup>b</sup> was studied in (Saini et al., 2013a) and references therein.

#### **4.1.7.9 Cell lines, gene expression, and immunofluorescence stainings**

TAP-deficient human fibroblasts STF1 (kindly provided by Henri de la Salle, Etablissement de Transfusion Sanguine de Strasbourg, Strasbourg, France) were stably transduced with K<sup>b</sup>-GFP. Lentiviruses were produced and used for gene delivery as described previously (Hananberg et al., 1997). For capture experiments, cells were trypsinized, seeded on the antibody patterns, and incubated at 37 °C (in the presence of the K<sup>b</sup> ligand peptides SL8 or FL9, where indicated). To accumulate peptide-empty K<sup>b</sup>, cells seeded onto the patterns were incubated at 37 °C until they had adhered to the surface (usually 3-6 hours) and then shifted to 25 °C overnight (Montealegre et al., 2015). Cells were washed twice with PBS and fixed with 3% paraformaldehyde for 15 min at RT. Patterned proteins were observed *via* GFP fluorescence by CLSM. Stainings with wheat germ agglutinin (WGA)-Alexa Fluor (AF) 647 (Molecular Probes, Thermo Fisher Scientific, Germany), anti-β-actin-AF647 (Cell Signaling Technology), and anti-β-tubulin (Abcam) were performed according to the manufacturers' protocols. Briefly, for WGA-AF647, the staining solution was added to the fixed cells for 10 min at RT and washed twice with PBS. For β-actin and β-tubulin, cells were first fixed with 3% paraformaldehyde (PFA) and then permeabilized with methanol or 0.1% Triton-X-100. For actin stainings, a fluorescently labeled primary antibody (anti-β-actin-AF647) was used, whereas the β-tubulin stain required a secondary antibody stain with a goat-anti-mouse-Cy3 conjugated antibody (Abcam).

#### **4.1.7.10 Microscopy**

A confocal laser scanning microscope was used (LSM 510, Zeiss, Germany). Argon and He/Ne lasers were used for selective excitation of mGFP, TAMRA, Cy3, and Alexa Fluor 647 at 488 nm, 514 nm, and 633 nm. Samples were illuminated with a 63 x oil immersion objective (Plan Apochromat, Zeiss, NA 1.4). Emission fluorescence was detected with standard filter sets (GFP: band pass (BP) 505-530 nm; TAMRA/Cy3: BP 560-615 nm; AF647: long pass 650 nm). All scans were performed sequentially for the respective wavelengths. For z-scans, optical sections with a thickness of 600-700 nm (488 nm = 1 Airy unit and 633nm = 0.72 Airy units) were recorded with an overlap of 200 nm. Images were processed with ImageJ (National Institutes of Health), and figures were made with Inkscape (inkscape.org).

### **4.1.7.11 Data analysis**

For data analysis, the Pearson colocalization coefficient between pattern (antibody) fluorescence and GFP (protein) fluorescence was determined in rectangular boxes across the pattern elements (JACoP tool of ImageJ, National Institutes of Health). For statistics, the mean and standard error of the indicated number of cells was calculated.



### 4.1.8 Supporting Information

#### 4.1.8.1 Class I molecule patterning is visible after 2 hours and persists afterwards

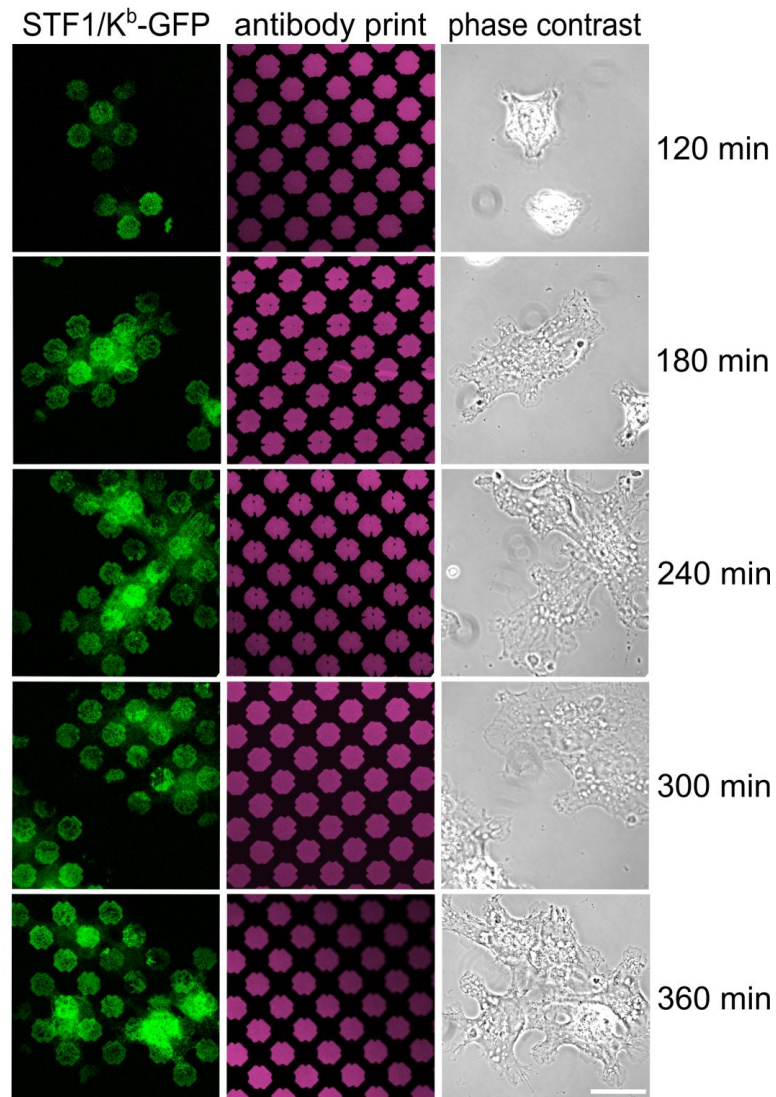


**Figure 4.1.8.1: Class I molecule patterning is visible after 2 hours and persists afterwards.** STF1/Kb-GFP cells were seeded onto mAb Y3 antibody micropatterns, grown at 37 °C in presence of the Kb ligand peptide SL8 for the indicated times, fixed, and imaged. Bar, 25  $\mu$ m.

#### 4.1.8.2 Capture efficiency of class I molecules correlates with printed antibody concentration

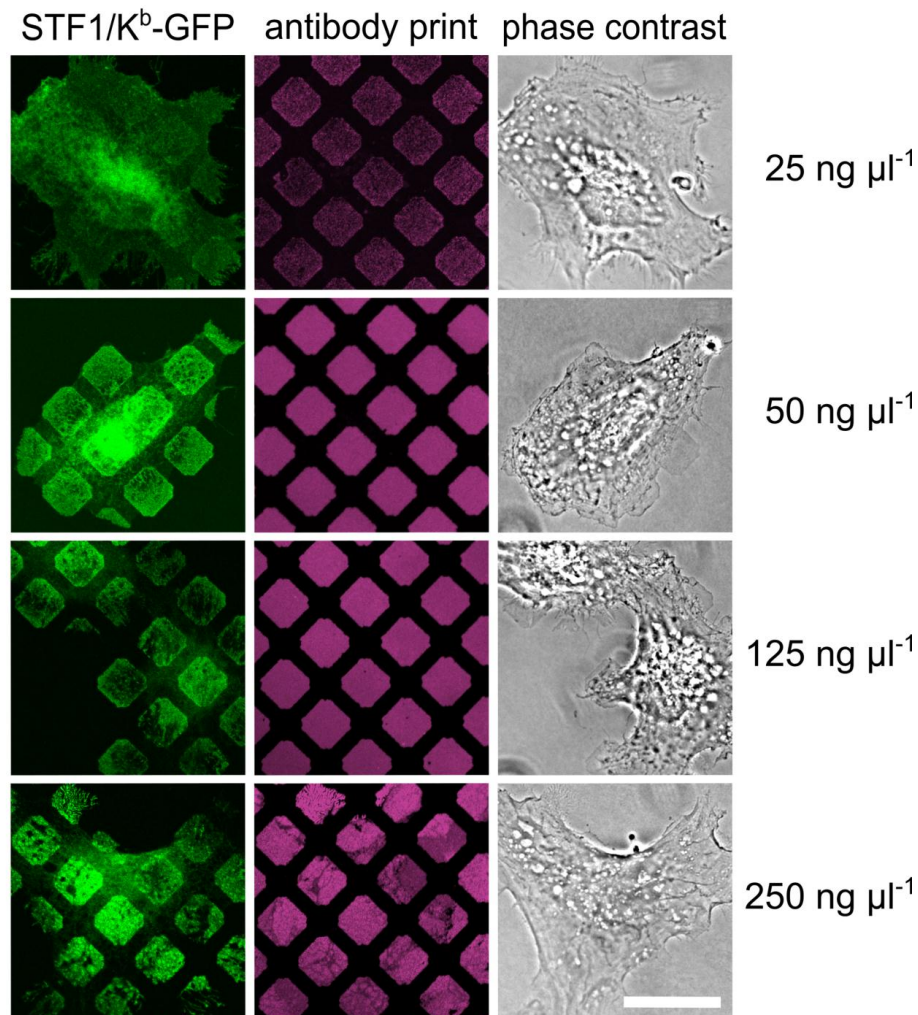


**Figure 4.1.8.2: Capture efficiency of class I molecules correlates with printed antibody concentration.** STF1/K<sup>b</sup>-GFP cells were seeded onto mAb Y3 antibody micropatterns printed at the indicated concentrations, grown for 5 hours in presence of the K<sup>b</sup> ligand peptide FL9, fixed, and imaged. The test of different concentrations suggests that a minimal antibody concentration of 50-125 ng  $\mu\text{l}^{-1}$  is required for a good signal-to-noise ratio between patterned K<sup>b</sup>-GFP and background. This is achieved if the majority of the overall surface K<sup>b</sup>-GFP binds to the antibody pattern elements, thus keeping the level of free diffusing K<sup>b</sup>-GFP in the interspaces low, resulting in low background levels. Bar, 25  $\mu\text{m}$ .

**4.1.8.3 Immunostaining of  $\beta$ -actin of STF1/K<sup>b</sup>-GFP cells reveals no difference between cells seeded on or off antibody micropatterns**

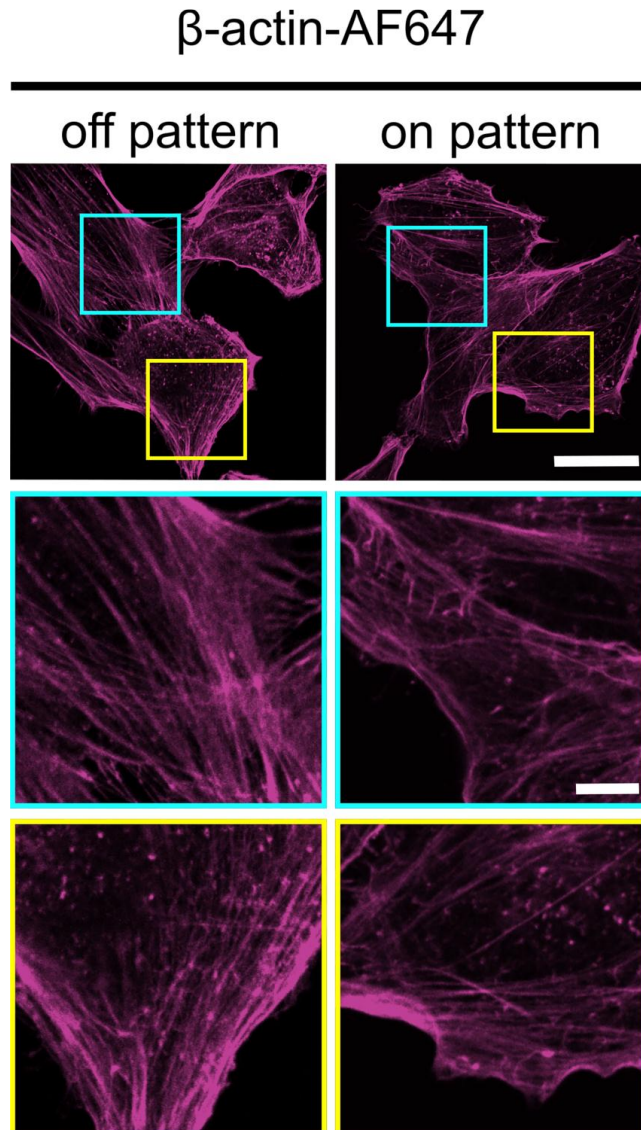


**Figure 4.1.8.3: Immunostaining of  $\beta$ -actin of STF1/K<sup>b</sup>-GFP cells reveals no difference between cells seeded on or off antibody micropatterns.** STF1/K<sup>b</sup>-GFP cells were grown overnight at 37 °C on Y3 antibody micropatterns and fixed. Cells were subsequently permeabilized with 0.1% Triton X-100 and stained with an Alexa Fluor 647-conjugated anti- $\beta$ -actin antibody. Upper row: Fluorescence images of cells off and on antibody micropatterns. Lower rows: enlarged areas of upper images as indicated by colored boxes. Bars, 25  $\mu$ m (upper) and 5  $\mu$ m (lower).

### 4.1.9 Copyright Transfer Agreement

The following email grants permission to re-use the published manuscript in *Small* in this thesis:

Dear Cindy Dirscherl,

**We hereby grant permission for the requested use expected that due credit is given to the original source.**

If material appears within our work with credit to another source, authorisation from that source must be obtained.

Credit must include the following components:

- Journals: Author(s) Name(s): Title of the Article. Name of the Journal. Publication year. Volume. Page(s). Copyright Wiley-VCH Verlag GmbH & Co. KGaA. Reproduced with permission.

If you also wish to publish your thesis in electronic format, you may use the article according to the Copyright transfer agreement:

#### 3. Final Published Version.

Wiley-VCH hereby licenses back to the Contributor the following rights with respect to the final published version of the Contribution:

a. [...]

b. Re-use in other publications. The right to re-use the final Contribution or parts thereof for any publication authored or edited by the Contributor (excluding journal articles) where such re-used material constitutes less than half of the total material in such publication. In such case, any modifications should be accurately noted. [This applies to each article, not the three articles in total].

Kind regards

Heike Weller

Rights Manager

Rights & Licenses

Wiley-VCH Verlag GmbH & Co. KGaA

Boschstraße 12

69469 Weinheim

Germany

[www.wiley-vch.de](http://www.wiley-vch.de)

T + (49) 6201 606-585

F + (49) 6201 606-332

[rightsDE@wiley.com](mailto:rightsDE@wiley.com)

## 4.2 Additional Data

### 4.2.1 Different approaches to generate anti-MHC class I micropatterns

For the generation of anti-MHC class I micropatterns, I tested all anti-MHC class I antibodies that are commonly used for standard methods such as co-immunoprecipitation, flow cytometry, immunofluorescence, or Western blots in the Springer laboratory. It is commonly known that a given monoclonal antibody is not necessarily suitable for all applications. Similarly, the antibody isoform can influence the functionality of the protein. Most antibodies are produced in our lab by the purification from hybridoma supernatant (see section 2.1). I used such supernatants and purified antibodies from them via protein A affinity chromatography. I then stained the purified antibodies with NHS dyes and tested them (see section 2.1).

Since MHC class I proteins are a trimeric complex, different strategies exist to target the protein with antibodies. One can target the individual subunits, i.e., the heavy chain, or the light chain beta-2 microglobulin ( $\beta_2m$ ), or one can use the peptide to capture the empty MHC class I proteins (see section 1.4.2 for MHC class I structure). I have tested all three possibilities as described in the following.

#### 4.2.1.1 Anti-MHC class I heavy chain

Most of the antibodies that are available in our lab target an epitope that is located in the heavy chain of the MHC class I protein (see table 1.5 for antibody epitopes). They usually recognize conformation-dependent epitopes that consist of several amino acids in the tertiary structure of the protein, i.e., they usually recognize the folded protein. Since folding of the MHC class I heavy chain strongly depends on the association of  $\beta_2m$ , many antibodies recognize the fully conformed complexes that involve residues of  $\beta_2m$ . This can include the empty dimer (i.e., the complex of the MHC class I heavy chain and  $\beta_2m$ ) or the peptide-bound trimer (the complex of heavy chain,  $\beta_2m$ , and peptide) (see section 1.4.2 for reference). Some antibodies, in contrast, exclusively bind to the free heavy chains. Due to the lab's expertise with murine MHC class I allotypes, I mostly worked with the two murine allotypes H-2K<sup>b</sup> (K<sup>b</sup>) and H-2D<sup>b</sup> (D<sup>b</sup>). The table in section 1.5 lists all antibodies that were tested in this thesis project, specifying their epitopes and references. Figure 4.2.1.1 shows micropatterns of the available antibodies that were purified and labeled. To my surprise, all antibodies, except B22.249 and 25.D1.16, remained functional when printed onto glass surfaces and are in principle suitable for

anti-MHC class I micropatterns. For the antibody 20-8-4S, I used unlabeled antibody, seeded cells, and stained afterwards with a labeled goat-anti-mouse antibody to visualize the antibody micropatterns.



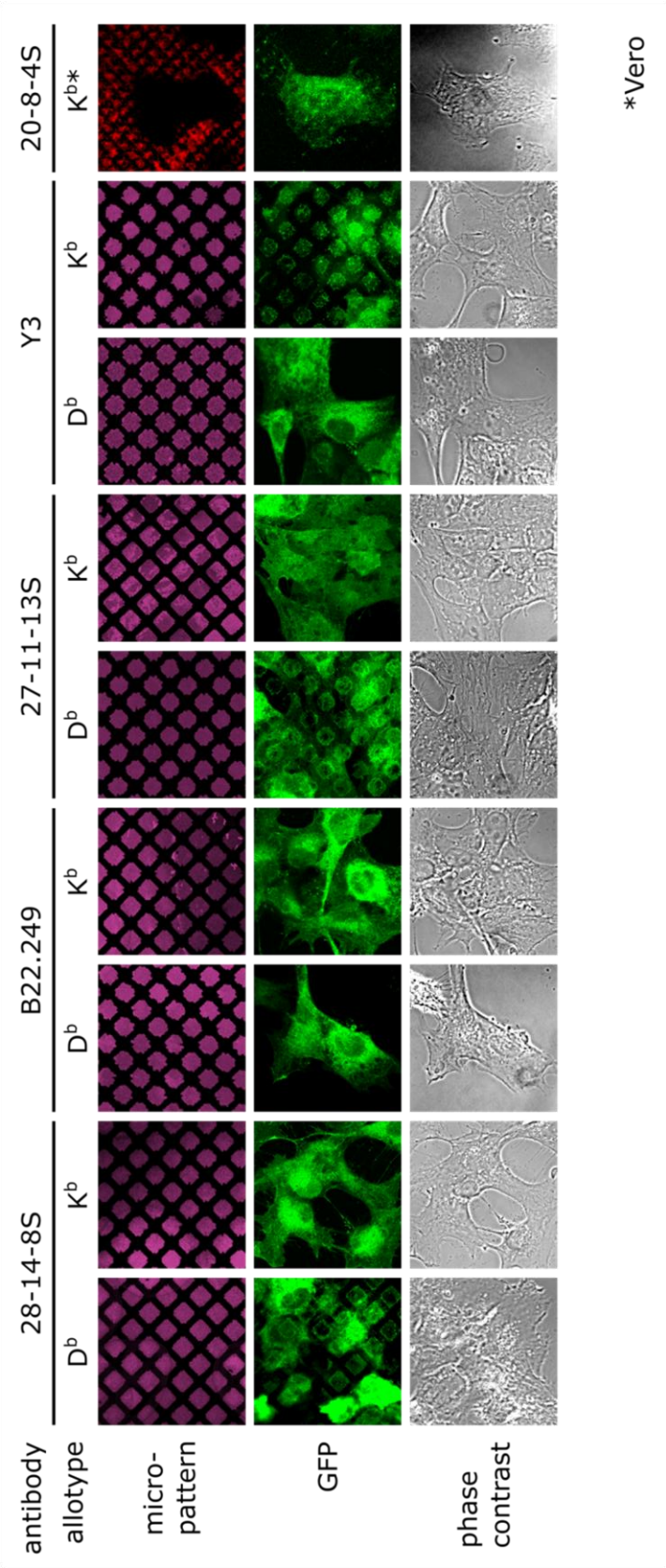


**Figure 4.2.1.1: Anti-MHC class I antibody micropattern screen.** Different anti-MHC class I antibodies were tested for their functionality in antibody micropatterns. Labeled (AF647) antibodies were printed according to the standard protocol on untreated glass coverslides (magenta/red). STF1/K<sup>b</sup>-GFP and STF1/D<sup>b</sup>-GFP (or Vero cells transfected with K<sup>b</sup>-GFP; see asterisk) were seeded to test for capture efficiency and allotype specificity (green). Bar, 25 μm.

### 4.2.1.2 Anti- $\beta_2m$

Instead of targeting the heavy chain of MHC class I directly, one can also target the light chain  $\beta_2m$ , which is associated with the heavy chain, with an anti- $\beta_2m$  antibody (BBM.1). I have performed several trials with anti- $\beta_2m$  antibody micropatterns, but I was not able to capture  $K^b$ -GFP efficiently with this antibody (data not shown). I assume that the used BBM.1 antibody is also less stable, similar to our observations with 25.D1.16, and perhaps denatures on the glass surface. I am confident that functional anti- $\beta_2m$  antibody micropatterns can be generated in the future. I would first test other anti- $\beta_2m$  antibodies that are commercially available and then move on to surface coating that might help to stabilize the antibody on the glass surface.

### 4.2.1.3 Peptide micropatterns

After we established the antibody micropatterns, we were wondering whether we could use the same technique to fabricate peptide micropatterns. Since we use TAP-deficient STF1 cells, they cannot efficiently load their MHC class I with peptide. Thus, the  $K^b$ -GFP molecules at the cell surface are mostly empty or loaded with suboptimal peptides, and they should bind to high-affinity peptides. We assumed that, if we attach such peptides to the glass surface, the empty  $K^b$ -GFP molecules will bind to the immobilized peptides and thus become captured on the pattern elements. Figure 4.2.1.3 shows a first trial experiment, where I printed the unlabeled high affinity peptide SL8 conjugated to biotin (bio-SIINFEKL in the single letter amino acid code) according to the standard antibody printing protocol on untreated, streptavidin- or APTES-coated coverslides. We know that the bio-SIINFEKL peptide, which has a 6-aminohexanoic acid linker between the biotin and the lysine side chain, can be bound by H-2K<sup>b</sup> and by streptavidin at the same time (Praveen et al., 2009), and we reasoned that the immobilized streptavidin would hold the peptide a small distance from the surface such that the  $K^b$ -GFP molecules would be able to bind to it.



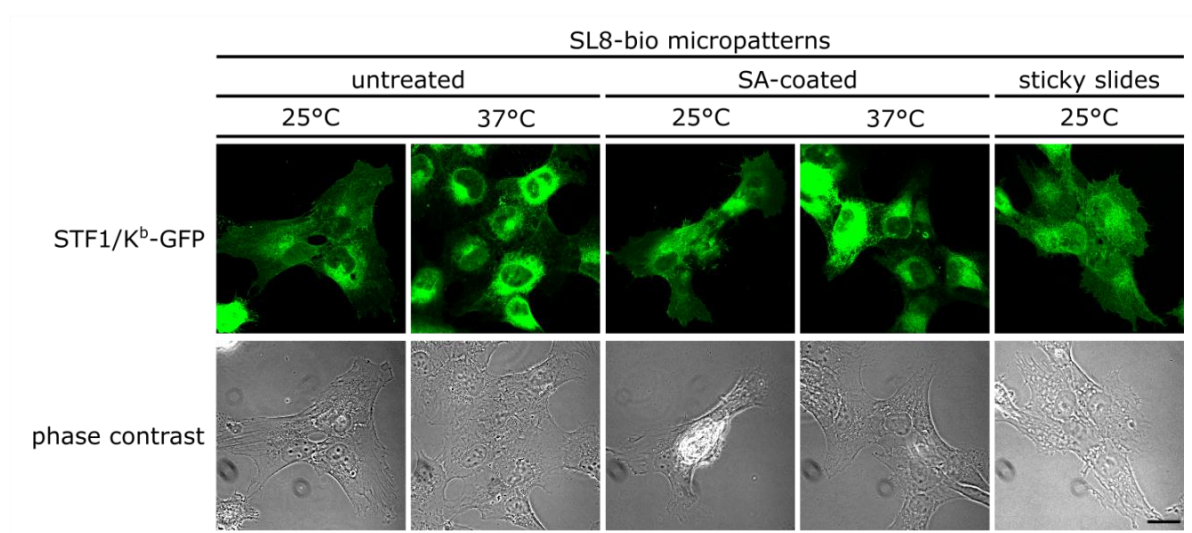


**Figure 4.2.1.3: Testing SL8-peptide micropatterns.** Biotinylated SL8 (SL8-bio) was printed on differently coated glass surfaces according to the standard protocol. STF1/K<sup>b</sup>-GFP were seeded onto the SL8-micropatterns and incubated at different temperature to test for their ability to capture K<sup>b</sup>-GFP. Bar, 25 μm.

Since the SL8 was unlabeled, I was not able to confirm that the peptide was transferred to the glass coverslide. Nonetheless, STF1/K<sup>b</sup>-GFP cells were seeded, incubated at different temperatures, and fixed. Still, none of the samples showed any capture of K<sup>b</sup>-GFP.

There are various possible explanations why this trial experiment did not work. One is that the printing of the peptide did not work. The SL8 peptide consists of 50% hydrophobic amino acids, thus it is possible that the ink, here the SL8 peptide, is repelled by the PDMS, thus the stamp is not efficiently inked, and subsequently no SL8 print will be generated on the glass surface. If we assume that we generated SL8 micropatterns nonetheless, it is reasonable to imagine that the K<sup>b</sup>-molecules cannot bind to it, since class I needs to wrap around the entire peptide. Printing the peptide directly on the glass surface might not be sufficient to allow for this interaction due to steric hindrance. Even our idea to orient the peptide by the biotin-streptavidin interaction and to provide some distance to the glass surface, to allow class I to bind the peptide properly, did not help. Perhaps, the binding conditions close to the glass surface necessitate a longer linker than in solution.

### 4.2.2 The special case of the 25.D1.16 antibody

The antibody 25.D1.16 binds specifically SL8-loaded  $K^b$  and is considered a T cell receptor-like antibody. The crystal structure of 25.D1.16 and the  $K^b$ -SL8 complex shows that 25.D1.16 – unlike other antibodies – reads out the structure of the bound peptide by the canonical diagonal binding mode utilized by most TCRs (Mareeva et al., 2008). This led to the idea to use 25.D1.16 antibody micropatterns to develop an inducible capture assay. In this setup, STF1/ $K^b$ -GFP cells will be seeded on 25.D1.16 antibody micropatterns that were generated according to our standard method. Since STF1 cells lack the TAP transporter, the  $K^b$  molecules cannot be efficiently loaded with peptide, and the  $K^b$  molecules that arrive at the cell surface are mostly empty or suboptimally loaded. Especially, they contain no SL8 peptide since the SIINFEKL peptide sequence does not naturally occur in human cells. Therefore, the printed 25.D1.16 antibodies will not bind to these  $K^b$  molecules. When the SL8 peptide is then added to the cell culture medium, it will bind to the empty  $K^b$  molecules at the cell surface, which thus gain the epitope for the 25.D1.16 antibody. With this assay we would be able to specifically induce the capture of class I into patterns upon addition of peptide, e.g., after the cells have adhered. This is in contrast to the current situation, where we cannot control the capture and accumulate  $K^b$  molecules immediately upon seeding. Also, we might use this system to follow the capture of  $K^b$  molecules over a defined time period, for example to quantify the arrival of  $K^b$  molecules at the cell surface under specific conditions. In our trial experiments, we printed the 25.D1.16 antibody according to our standard procedure on untreated glass, seeded HA- $K^b$ -GFP expressing cells on the patterns, and added SL8 peptide to the cell culture medium (see figure 4.2.2, columns 5 and 6). Although this approach was successful for the other antibodies, we were surprised to find that the 25.D1.16 antibody can be printed but completely loses its functionality on the glass surface. We tried to improve the stability of the antibody by pre-treating the surfaces with PLL (see figure 4.2.2, columns 3 and 4), but could not restore the functionality. Throughout the project, I repeated the experiment with the 25.D1.16 antibody several times, but until now, I have not been able to capture  $K^b$ -GFP with this antibody. In several of these experiments, binding of the same batch of 25.D1.16 to the same cells was verified by flow cytometry (data not shown). It is possible that this antibody is rather sensitive and needs more flexibility to bind to its target epitope, similar to an induced fit interaction, or that it is especially sensitive to denaturation on the glass surface. Since certain antibody isoforms are prone to aggregation, and 25.D1.16 is the only antibody of the IgG1 isoform among all antibodies used, whereas all others belong to the IgG2 isoform, it is also possible that the isoform plays a role for the antibody stability.

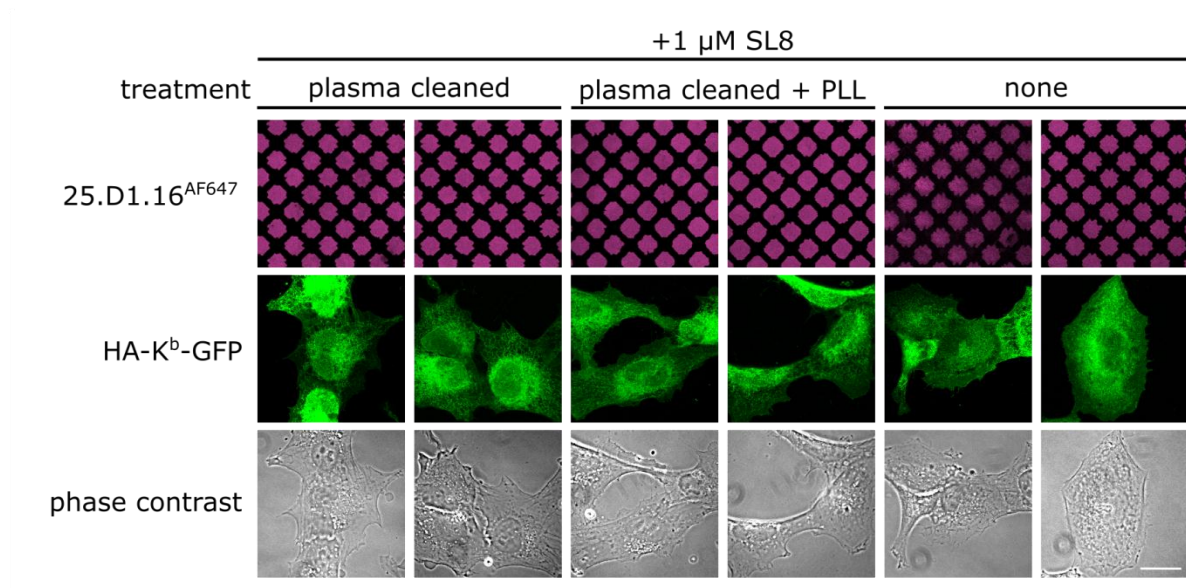


**Figure 4.2.2: Testing different pre-coated surfaces for their ability to stabilize 25.D1.16 antibody micropatterns.** Labeled 25.D1.16 (25.D1.16<sup>AF647</sup>) was printed on different plasma treated and/ or PLL-coated glass coverslides (magenta). Then, STF1/HA-K<sup>b</sup>-GFP cells were seeded on the 25.D1.16 antibody micropatterns, and 1 μM SL8 was added to the cell culture medium. Cells were incubated overnight at 25°C. Bar, 25 μm.

### 4.2.3 Peptide binding to captured D<sup>b</sup> on 27.11.13S prints

Similar to the binding of SL8 to captured K<sup>b</sup>-GFP (see section 4.1.4.4), I repeated this experiment with D<sup>b</sup> and the respective peptide. For this, I seeded the STF1/D<sup>b</sup>-GFP cells on 27.11.13S antibody micropatterns and added the D<sup>b</sup>-specific peptide FL9 (FAPGNYPAL in the single letter amino acid code) to the cell culture medium. To test if the fluorescent dye has any influence on this assay, such as unspecific binding to the glass coverslides, I also tried FL9 conjugated to TAMRA as well as to Dy633. Figure 4.2.3 shows that both peptides bound specifically to the captured D<sup>b</sup>-GFP in this experiment, indicating that both fluorescent dyes can be used for this assay.

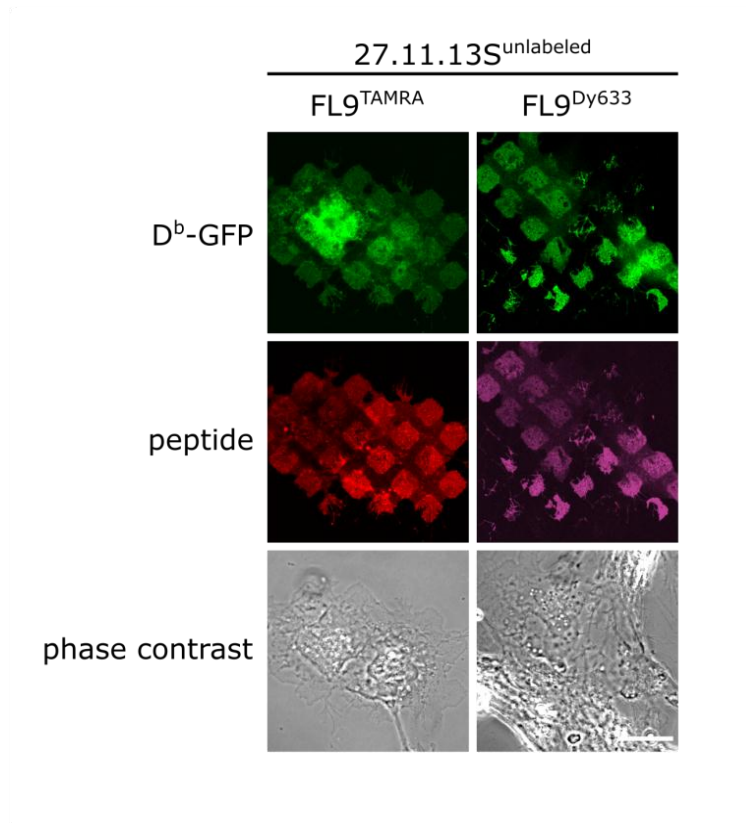


**Figure 4.2.3: Peptide binding to captured D<sup>b</sup>-GFP.** The D<sup>b</sup>-specific antibody 27.11.13S (unlabeled) was printed according to the standard protocol. STF1/D<sup>b</sup>-GFP were seeded onto the antibody micropattern and incubated overnight at 25°C to accumulate D<sup>b</sup>-GFP surface levels (green). The next day, the D<sup>b</sup>-specific peptide FL9 with two different fluorescent labels (FL9<sup>TAMRA</sup> and FL9<sup>Dy633</sup>) was added to the cells (final concentration=2 μM) and incubated for 20 min at 37°C (TAMRA, red; Dy633, magenta). Bar: 25 μm.

#### 4.2.4 Cells sense antibody micropatterns: ‘feet’ formation

In our first attempts of antibody micropattern fabrication and seeding of cells onto different pattern sizes, we saw the phenomenon that cells react to the pattern element sizes. If the pattern elements are big enough for the cells to sit on, they will either choose the pattern elements for attachment or will avoid them completely and occupy only the interspaces (see also 1.3.5.3).

Throughout the project, I observed that the cells were crawling across the surface. In these cases they usually left traces behind, where pieces of the cell membrane remained on the antibody pattern elements. While the great majority of cells generally spread evenly across the antibody pattern elements, there were cases where the cells formed protrusions, like little ‘feet’, that were binding to

single pattern elements. Sometimes, these little protrusions only became visible after fixation, e.g. when the cells were shrinking during the fixation process. These ‘feet’ occurred randomly and also on various treated surfaces. The micrographs in figure 4.2.4 show two examples of such observed feet (white arrows).

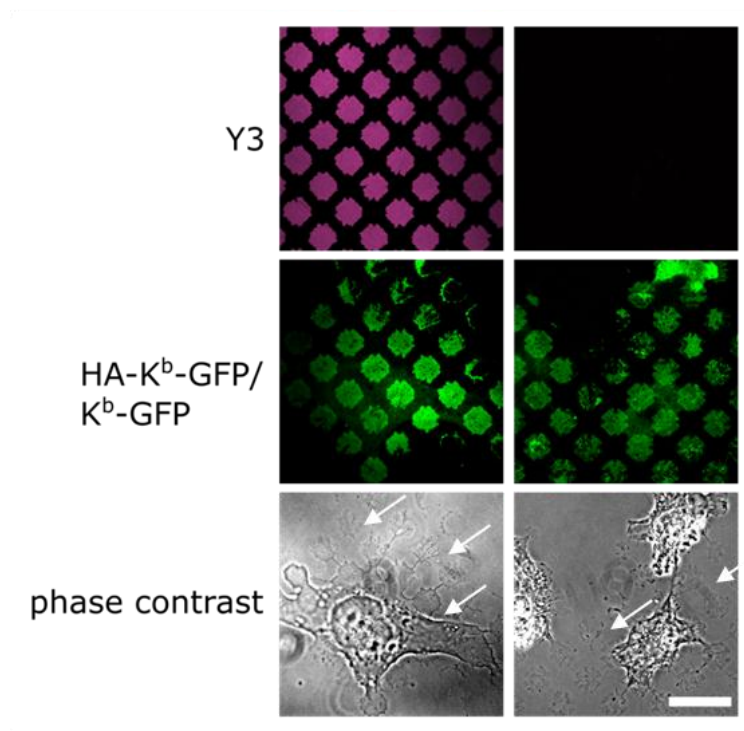


**Figure 4.2.4: Cells stick to the antibody pattern elements.** STF1/HA-K<sup>b</sup>-GFP or STF1/K<sup>b</sup>-GFP cells were seeded on Y3 antibody micropatterns (labeled Y3<sup>AF647</sup>, magenta; unlabeled, black) and incubated according to the standard protocol. Cells were then fixed and imaged. White arrows indicate the protrusions of the cell. Bar, 25  $\mu$ m.

### 4.2.5 Dipeptide exchange trials

Our assay demonstrated that we can pattern functional  $K^b$  at the cell surface that can bind peptides specifically (see section 4.1). For the development of a peptide binding assay that can be used with living cells, we wanted to test whether we can also exchange high affinity peptides with the dipeptide technology on the captured  $K^b$ -GFP (see Saini et al., 2015 for reference). In this published paper, peptide exchange was also successfully tested on living cells (see figures 5 A and B in (Saini et al., 2015)). For first proof-of-concept experiments, we repeated the described experiments on the patterns, where FL9 was exchanged with SL8, and we also tried to exchange SL8 with  $SL8^{TAMRA}$ . For our experiments, we seeded STF1/ $K^b$ -GFP cells on Y3 antibody micropatterns and incubated them overnight at 25 °C to accumulate  $K^b$ -GFP at the cell surface. The next day, we added 2  $\mu$ M of the test peptides (leaving peptides) to the cell culture medium for 15 min at 37 °C to load all captured  $K^b$ -GFP with these peptides. After peptide loading, the cells were washed twice with medium to remove any excess peptide. For the peptide exchange reaction, 1  $\mu$ M fluorescently labeled index peptide ( $SL8^{TAMRA}$ ) was added alone or together with 10 mM glycyl-cyclohexylalanine (GCha) to the cell culture medium at 37 °C for 30 min. Finally, the cells were washed and fixed with PFA and fluorescence images were acquired.

In Figure 4.2.5 A, both peptide exchange reactions are shown. The fluorescence signal of the index peptide ( $SL8^{TAMRA}$ ) can be used to judge how much peptide was exchanged during the exchange reactions. In our control sample, we loaded the captured  $K^b$ -GFP directly with the index peptide  $SL8^{TAMRA}$  to show that the captured  $K^b$ -GFP molecules are functional and bind peptide (column 1). In the negative control experiments, we blocked with the respective test peptides and added the index peptide. Surprisingly and against previous observations, the blocking was not complete in these experiments (column 2 and 4), since the fluorescently labeled peptide was always binding to the captured  $K^b$ -GFP. In the exchange reactions, in presence of GCha, the fluorescent signal was slightly increased as expected (column 3 and 5).



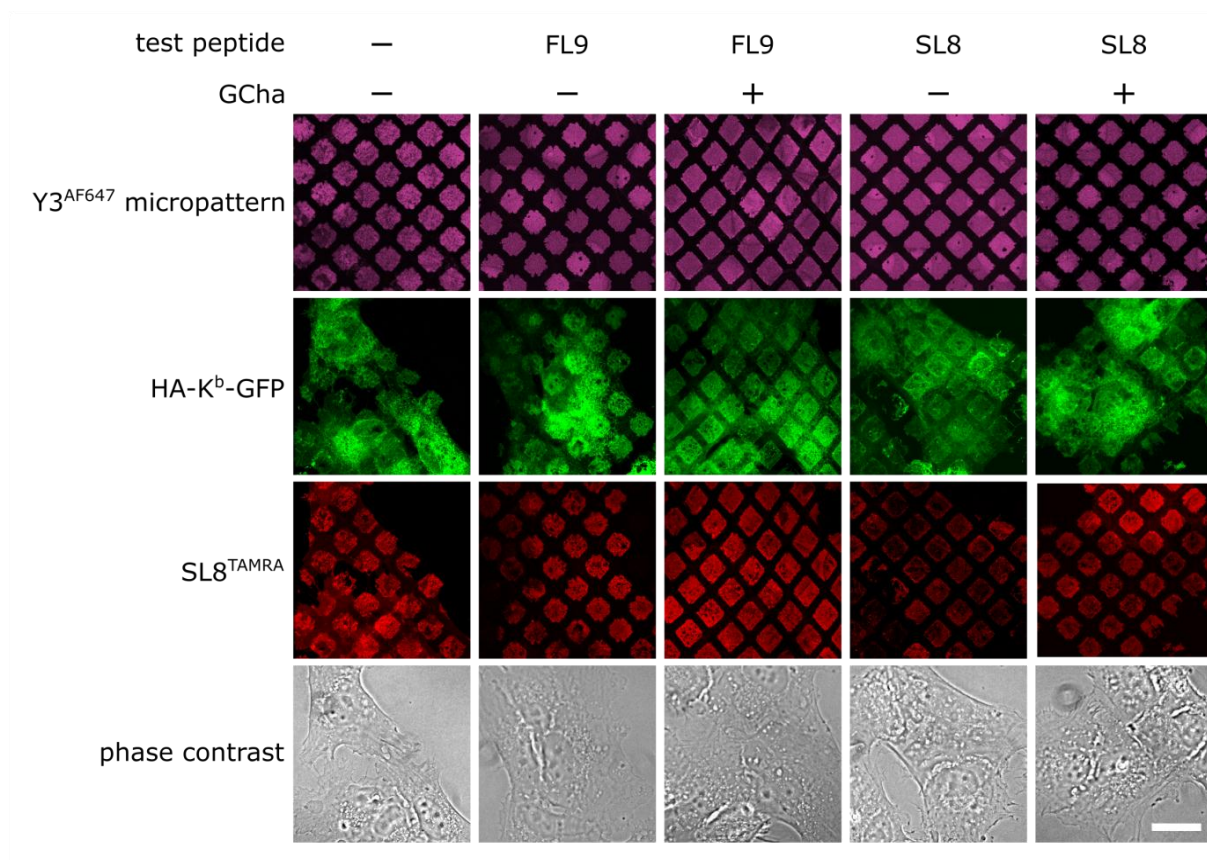


**Figure 4.2.5 A: Dipeptide exchange trials with Y3 antibody micropatterns.** STF1/HA-K<sup>b</sup>-GFP cells were seeded on Y3<sup>AF647</sup> antibody micropatterns, incubated at 37°C to adhere and were then shifted to 25°C overnight. The next day, unlabeled SL8 or FL9 peptide (test peptide) was added for blocking and cells were incubated at 25°C for 15 min. For the exchange reaction, SL8<sup>TAMRA</sup> was added alone or with GCha and incubated at 37°C for 1 hour at 37°C. Cells were washed and fixed. Bar, 25  $\mu$ m.

The results of the exchange experiment are difficult to interpret. The insufficient blocking is surprising, since it worked well in previous experiments (see figure 4.1.4.4). Since it was expected that the blocking will inhibit the binding of the fluorescent index peptide, the effect of GChA addition is rather weak. It is possible that the incubation times were too long, and that newly synthesized K<sup>b</sup>-GFP arrived at the plasma membrane during the exchange reactions. In this scenario, the new K<sup>b</sup>-GFP molecules would be directly loaded with the index peptide. From my experience however, the amount of new K<sup>b</sup>-GFP molecules at the cell surface is rather low. To exclude that the fluorescent signal is caused by the new arrival of K<sup>b</sup>-GFP at the cell surface, the experiment should be repeated in the presence of Brefeldin A (BFA) to block surface delivery of newly synthesized K<sup>b</sup>-GFP.

It is also possible that the capture via the Y3 antibody micropatterns has an effect on peptide exchange. It is possible that the Y3 antibody stabilizes the peptide-bound form in such a way that peptide dissociation is impaired. To test this hypothesis, I repeated the experiment with HA antibody micropatterns (figure 4.2.5 B). Since the test peptides are added immediately after the 25 °C overnight incubation, dissociation of  $\beta_2m$  will be inhibited, and the captured K<sup>b</sup>-GFP should remain stable during the exchange reaction. In this experiment, the control as well as the blocking was successful except for some unspecific background staining (columns 1 and 2). In the exchange sample, the test peptide was almost completely exchanged for SL8<sup>TAMRA</sup> (column 3).



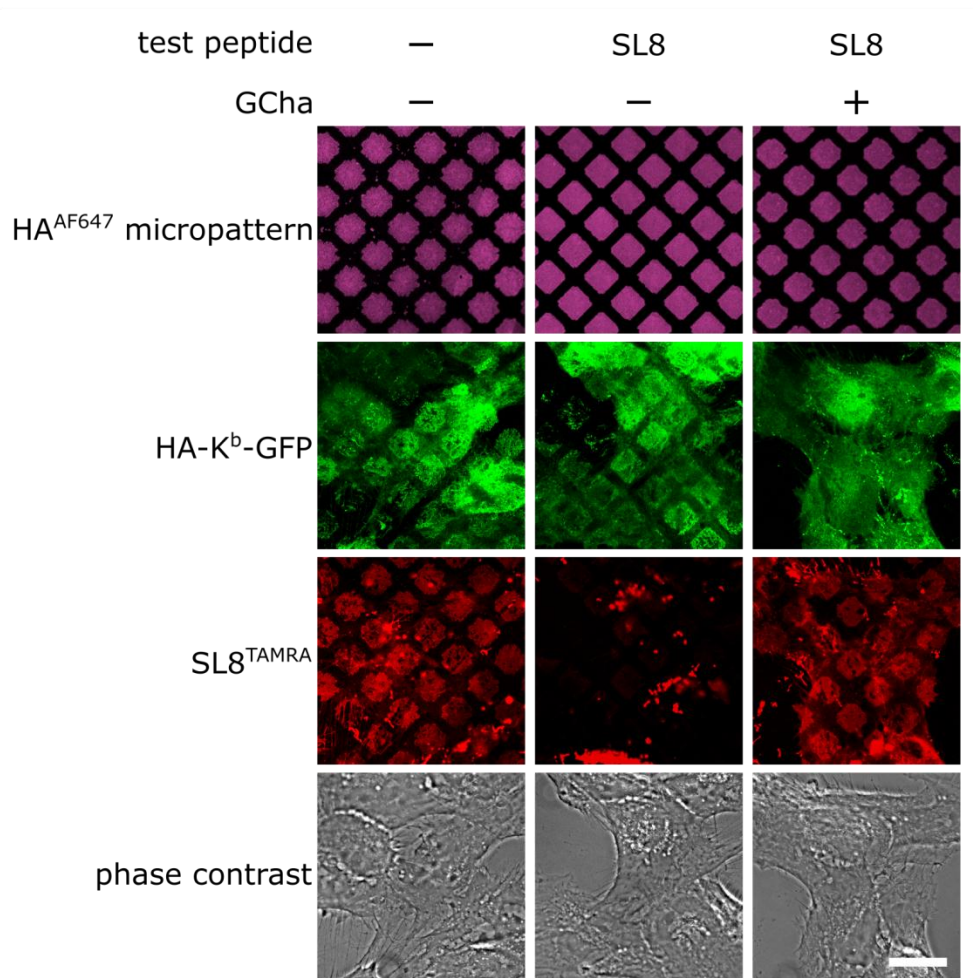


**Figure 4.2.5 B: Dipeptide exchange trials with anti-HA antibody micropatterns.** STF1/HA-K<sup>b</sup>-GFP cells were seeded on HA<sup>AF647</sup> antibody micropatterns (magenta), incubated at 37°C to adhere and were then shifted to 25°C overnight. The next day, unlabeled SL8 peptide (test peptide) was added for blocking and cells were incubated at 25°C for 15 min. For the exchange reaction, SL8<sup>TAMRA</sup> was added alone or with GCha and incubated at 37°C for 1 hour at 37°C (red). Cells were washed and fixed. Bar, 25 µm

### 4.2.6 Release from pattern with HA peptide

While working on the optimization of the antibody micropatterns, we were wondering whether we could release the captured K<sup>b</sup>-GFP from the patterns. Such a system would enable us to synchronize the internalization of the MHC class I proteins from the cell surface, which would be useful for the study of endocytosis, especially since we are able to generate and capture specific conformations of MHC class I molecules (see section 5.1). The controlled release of the captured K<sup>b</sup>-GFP molecules at a specific time point from the antibody micropatterns would be an ideal setup, since it allows for the observation of a distinct cohort of proteins and would avoid the background problems that we observe so far. Previous studies have shown that the full-length HA peptide (nonameric peptide; YPYDYPDYA in the single letter amino acid code) can be used as a competitor to release the HA tagged fusion proteins from the HA antibody, e.g. in affinity chromatography. We therefore wished to investigate whether we could integrate the HA peptide into our system to release the captured proteins from the antibody micropatterns. For this, we chose a stepwise approach, and first verified that we can use the full-length HA peptide to release the HA antibody from HA-stained STF1/HA-K<sup>b</sup>-GFP cells in solution, and then moved on to experiments on the antibody micropatterns as described in the following.

We also used di- and tripeptides of the full-length nonameric HA peptide and tested whether also shorter peptides can be used for the release, adapting the concept of peptide exchange on MHC class I molecules with dipeptides (Saini et al., 2015). Table 4.2.64.2.6 lists all tried di- and tripeptides that were used in the experiments.

**Table 4.2.6: Di- and tripeptides tested for HA-release.** Peptide sequences are in the single letter amino acid code.

Peptide	Sequence	Stock concentration (in ddH <sub>2</sub> O)
full-length peptide		
HA full-length peptide	YPYDYPDYA	1 mM
di- and tripeptides		
HA-1	DYA	300 mM
HA-2	Ac-DYA	300 mM
HA-3	DY-NH <sub>2</sub>	300 mM
HA-4	DEPDY	does not dissolve in ddH <sub>2</sub> O

#### 4.2.6.1 Flow cytometry

In a first control experiment, I tested the full-length HA peptide and the di- and tripeptides listed in table 4.2.6 on cells that were kept in solution according to typical staining protocols for flow cytometry in our laboratory. In these experiments, I used STF1/HA-K<sup>b</sup>-GFP cells and labelled them with the same HA hybridoma that I used for the generation of antibody micropatterns. According to the standard staining protocol for flow cytometry experiments, I incubated the cells for 30 min on ice with the HA hybridoma. After labeling, the cells were washed and incubated with different concentrations of the full-length HA peptide ( $c = 10$  to  $20 \mu\text{M}$ ) and/or a mix of the di- and tripeptides ( $c = 10 \text{ mM}$ ) for 30 min at  $37^\circ\text{C}$  to initialize the release of the HA antibody. The cells were washed again to remove the eluted HA antibody and stained with a secondary APC conjugated goat-anti-mouse antibody (dilution 1:100) for 25 min on ice and washed with PBS. The fluorescence signal was finally read out in flow cytometry.

Interestingly, the HA signal was decreased only by addition of the full-length peptide (see figure 4.2.6.1 B), whereas the mix of the di- and tripeptides was not able to remove any of the pre-bound HA antibody (see figure 4.2.6.1 A). Importantly, re-binding of the HA antibody was also possible, indicating that the HA peptide only interferes with the antibody binding sites and not with HA-K<sup>b</sup>-GFP itself and the reduction of HA epitopes was not due to endocytosis of the labeled HA-K<sup>b</sup>-GFP (see figure 4.2.6.1 B).

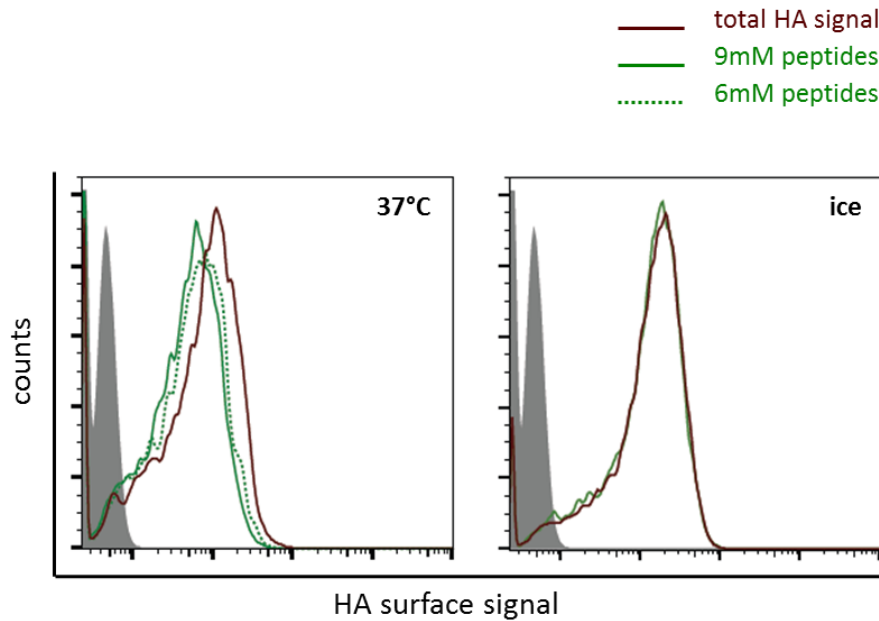


**Figure 4.2.6.1 A: Release of anti-HA antibody from the cell surface in flow cytometry.** STF1/HA-K<sup>b</sup>-GFP cells were incubated with anti-HA antibody according to the standard protocol. Cells were then incubated with a mixture of di- and tripeptides (green lines) at different temperatures (37°C or on ice) to induce the release of the anti-HA antibody, or cells were left untreated (solid brown line). Cells were then stained with a fluorescent secondary antibody to detect the remaining anti-HA antibody on the cell surface.

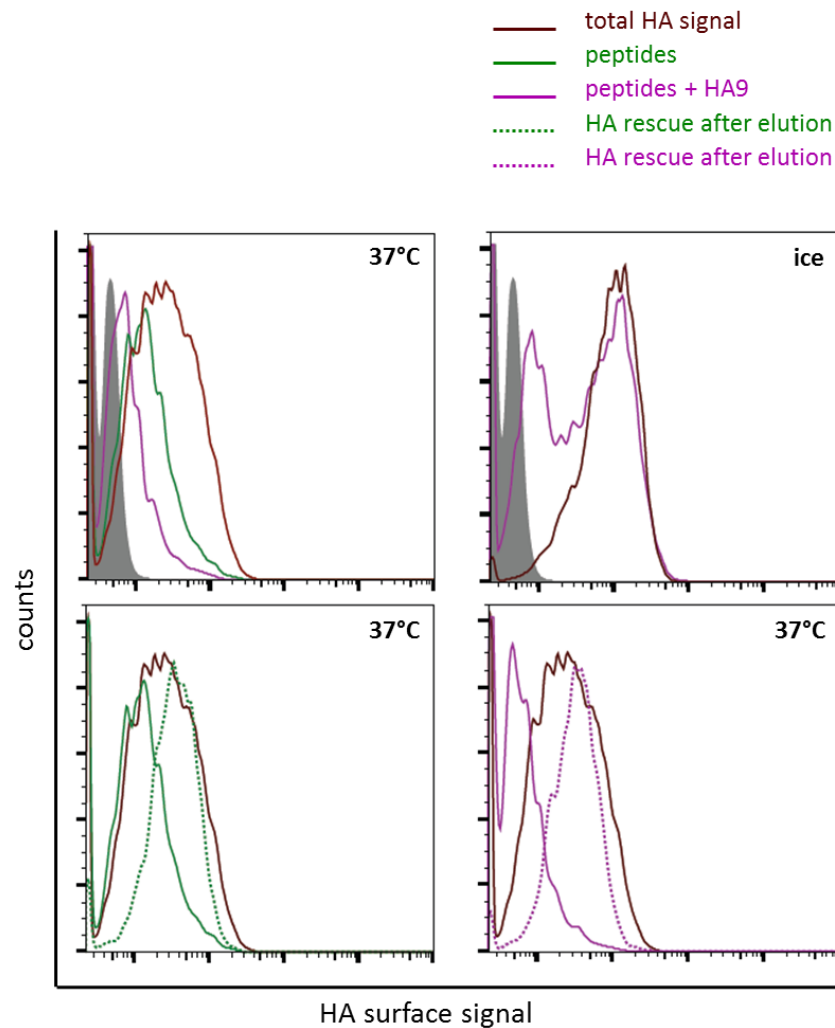


**Figure 4.2.6.1 B: Release and rebinding of anti-HA antibody with HA full length peptide.** STF1/HA-K<sup>0</sup>-GFP cells were incubated with anti-HA antibody according to the standard protocol to stain for total HA surface levels (solid brown line). Cells were then incubated with the tri-peptide mix alone (solid green line) or with additional full length HA-peptide (solid magenta line) to induce the release of HA antibody. After the release of the HA antibody, the cells were re-incubated with the HA-antibody to show reversibility of the antibody-staining (dashed lines).

### 4.2.6.2 Release from patterns with full-length HA peptide

After the successful release of the pre-bound HA antibody by the full-length HA peptide in the flow cytometry experiment (see figures 4.2.6.1 B), I wanted to apply the established protocol to antibody micropatterns. I thus seeded STF1/HA-K<sup>b</sup>-GFP cells on anti-HA antibody micropatterns according to the standard protocol to capture HA-K<sup>b</sup>-GFP. According to the flow cytometry experiment, I then added the HA full-length peptide with or without a mix of the di- and tripeptides to the cell culture medium to initialize the release of the HA tagged protein from the anti-HA antibody micropatterns similar to the flow cytometry experiment. Cells were incubated up to several hours with the HA peptides at 37 °C, but the HA-K<sup>b</sup>-GFP remained captured throughout the experiment (see figure 4.2.6.2). Importantly, the current readout by fluorescence microscopy only allows for the detection of the GFP signal, but it cannot discriminate between individual HA-K<sup>b</sup>-GFP molecules. This means that it is possible that there is exchange between individual HA-K<sup>b</sup>-GFP molecules on the pattern element, but the overall GFP pattern remains the same. I think that it is likely that some captured HA-K<sup>b</sup>-GFP molecules are indeed released but immediately re-captured on the antibody micropatterns, since the released HA antibodies cannot be washed away in the micropattern setup (in contrast to the above flow cytometry experiment). In such a scenario, the high abundance of HA binding sites on the pattern elements is just too high to be out-competed by the HA peptide to initiate the bulk release of all HA K<sup>b</sup>-GFP molecules from one pattern element that would result in the expected disappearance of the GFP signal.

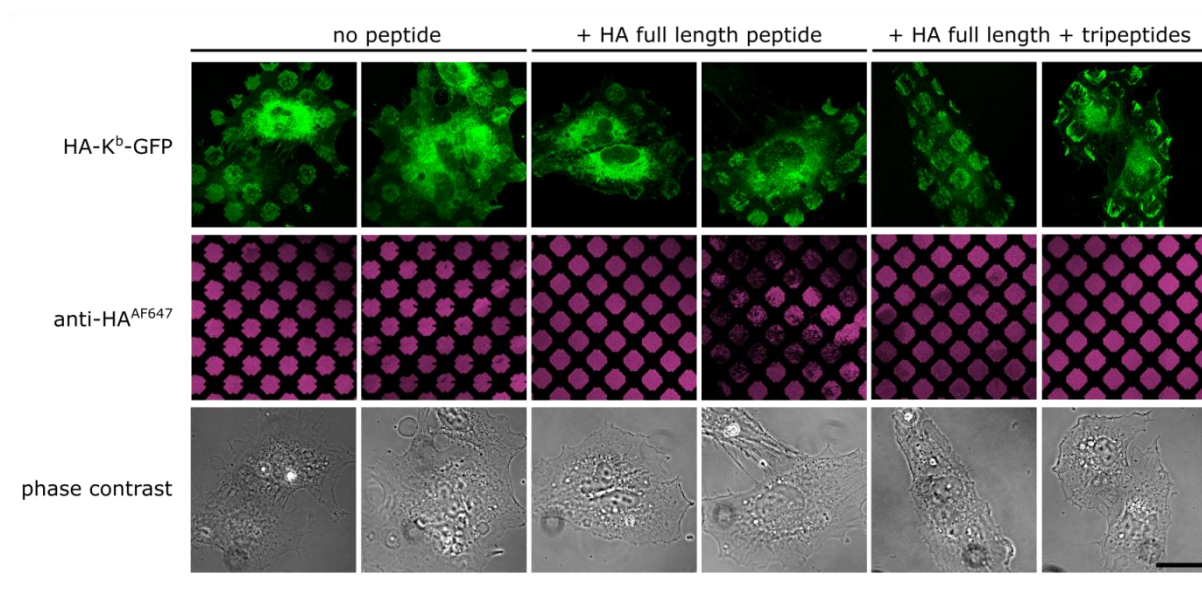


**Figure 4.2.6.2: Release of captured proteins from anti-HA micropatterns with HA full-length peptide.** STF1/HA-K<sup>b</sup>-GFP cells were seeded on anti-HA micropatterns according to the standard protocol. Then, the HA full-length peptide was added alone or together with the di- and tripeptides to the cell culture medium and incubated for several hours at 37°C to induce the release of the captured HA-K<sup>b</sup>-GFP proteins. Cells were then imaged in the heating chamber (live cell imaging). Bar, 25  $\mu$ m.

#### 4.2.6.3 Blocking HA patterns with HA full-length peptide

To test whether the full-length HA peptide is at all able to bind to the anti-HA antibody micropatterns, I tried blocking experiments. For this, I used the standard protocol to generate anti-HA antibody micropatterns, but immediately added the HA peptide to the cell culture medium to block the binding sites of the printed HA antibodies and thus inhibit the capture of the HA-K<sup>b</sup>-GFP molecules when seeding the STF1/HA-K<sup>b</sup>-GFP cells. I then proceeded according to the standard protocol. Surprisingly, the capture of HA-K<sup>b</sup>-GFP molecules was not impaired by the addition of the HA full-length peptide (see figure 4.2.6.3).

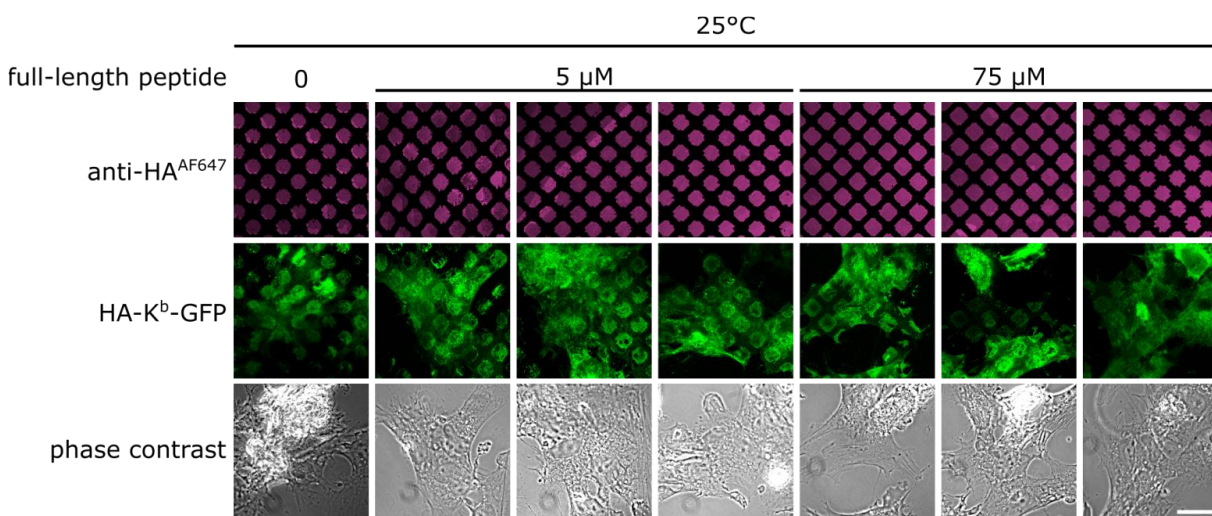


**Figure 4.2.6.3: Blocking protein capture with HA full-length peptide.** STF1/HA-K<sup>b</sup>-GFP cells were seeded on anti-HA micropatterns and incubated overnight at 25°C. The HA full-length peptide was added at two different concentrations immediately upon cell seeding to block the antigen binding sites of the anti-HA antibody micropatterns. The amounts of captured HA-K<sup>b</sup>-GFP were compared between the control (no addition of peptide, left column) and the blocked antibody micropatterns. Bar, 25 μm



### 4.2.7 Bifunctional patterns

Our observations that proteins passively adsorb to the pattern interspaces when we incubate a protein pattern with a second protein solution (see section 2.6.4) led us to the idea to generate patterns with two different immobilized antibodies. Such a bifunctional pattern would allow for the capture of two distinct protein conformations at the same time. For a proof-of-concept experiment, we tried to generate patterns with HA and Y3 antibodies. During incubation at 25 °C, we would capture the MHC class I trimer with both antibodies. When we shift cells to 37 °C,  $\beta_2m$  can only dissociate from the class I proteins that were captured by the HA antibodies, whereas the molecules captured by the Y3 antibody are stabilized in their trimeric form. Binding of fluorescent peptide would then provide a readout for the differential capture on both antibodies. For the generation of such antibody micropatterns, we printed either HA or Y3 antibodies ( $c = 0.3 \mu\text{g}/\mu\text{L}$ ). These prints were then further incubated for 2.5 min at RT with a solution of the other antibody ( $c = 0.3 \mu\text{g}/\mu\text{L}$ ), assuming that these antibodies will then passively attach to the interspaces of the print, thus forming a grid pattern. Then, cells were seeded onto the bifunctional micropatterns and incubated at different temperatures and stained with fluorescently labeled SL8 peptide ( $\text{SL8}^{\text{TAMRA}}$ ) to identify the conformation of the captured  $\text{K}^b$ -GFP molecules.

#### 4.2.7.1 Anti-HA and Y3 mixed antibody patterns

In Figure 4.2.7.1, we printed labeled HA ( $\text{HA}^{\text{AF647}}$ ) and incubated the prints subsequently with unlabeled Y3 antibody, thus generating antibody micropatterns in which the interspaces are occupied with the Y3 antibody (figure 4.2.7.1 A). In a second experiment, we fabricated the opposite antibody micropatterns by printing unlabeled Y3 ( $\text{Y3}^{\text{unlabeled}}$ ) and filling the interspaces with  $\text{HA}^{\text{AF647}}$ , thus generating HA grids pattern (magenta) in which the dark squares are occupied with the Y3 antibody (figure 4.2.7.1 B).

We then seeded STF1/ $\text{K}^b$ -GFP cells on these micropatterns and incubated them either at 26°C or 37°C overnight according to the standard protocol. We found that the capture was generally heterogeneous, and patterning was rather weak, except for column 2 (figure 4.2.7.1 B), where the HA- $\text{K}^b$ -GFP molecules were mostly found on the Y3 antibody elements (GFP signal). Generally, the amount of captured HA- $\text{K}^b$ -GFP was higher in the 26°C samples as expected according to the enhanced  $\text{K}^b$  surface levels at lower temperatures (columns 1 and 2 in figures 4.2.7.1 A and B).

Next, I wished to investigate which conformations of HA- $\text{K}^b$ -GFP were captured on the different pattern elements and whether the mixed patterns allow for the capture of two different conformations on a

single cell. After overnight incubation on the mixed pattern at the indicated temperatures, I added SL8<sup>TAMRA</sup> to the cell culture medium to test for peptide-receptive HA-K<sup>b</sup>-GFP. I expected to find peptide receptive HA-K<sup>b</sup>-GFP at 26°C independently of the capture antibody, since  $\beta_2m$  dissociation is inhibited at this temperature. In contrast to this prediction, peptide binding (red) occurred primarily on the Y3 pattern elements (figure 4.2.7.1 A column 1, and figure 4.2.7.1 B columns 1 and 2). Some cells even showed enhanced peptide binding on the HA pattern elements as seen in figure 4.2.7.1 A, column 2. Similarly, at 37°C no clear preference for peptide binding was observed (figures 4.2.7.1 A and B, columns 3 and 4). In contrast to previous experiments, I also observed peptide receptive HA-K<sup>b</sup>-GFP captured on the HA<sup>AF647</sup> pattern elements after 37°C incubation (figure 4.2.7.1 A, column 3).

In conclusion, we were able to generate bifunctional anti-HA/Y3 antibody micropatterns. But the cells showed individual preferences for distinct pattern elements and thus peptide binding, probably due to local antibody concentrations. I recommend optimizing the procedures for this experiment.

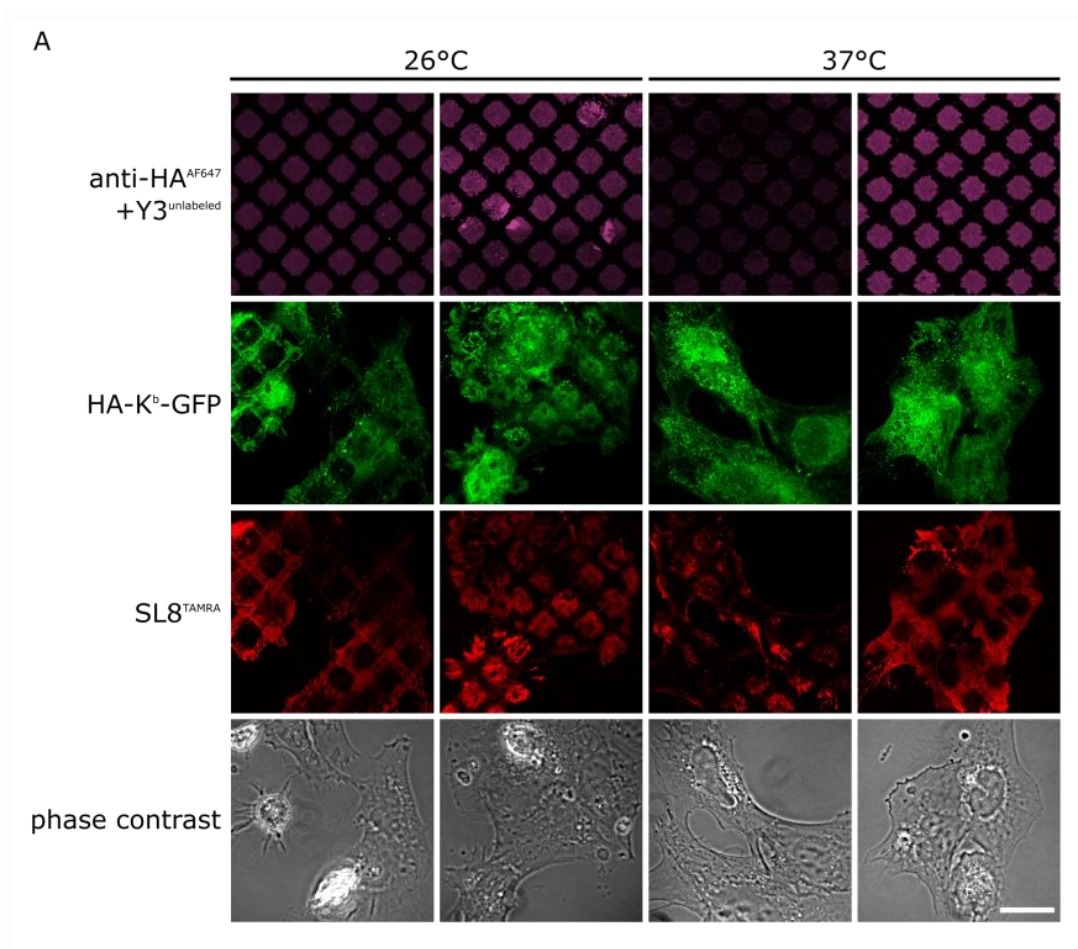


**Figure 4.2.7.1: Anti-HA and Y3 mixed antibody micropatterns.** The interspaces of standard antibody micropatterns were incubated with a second antibody to fabricate two-dimensional antibody micropatterns. **(A)** The anti-HA<sup>AF647</sup> (magenta) print was incubated with unlabeled Y3 (Y3<sup>unlabeled</sup>) to form the invisible Y3 grid pattern. The next day, cells were incubated with SL8<sup>TAMRA</sup> to stain peptide receptive HA-K<sup>b</sup>-GFP (red). Duplicates represent individual observations. Bar, 25  $\mu$ m

Figure continues on next page

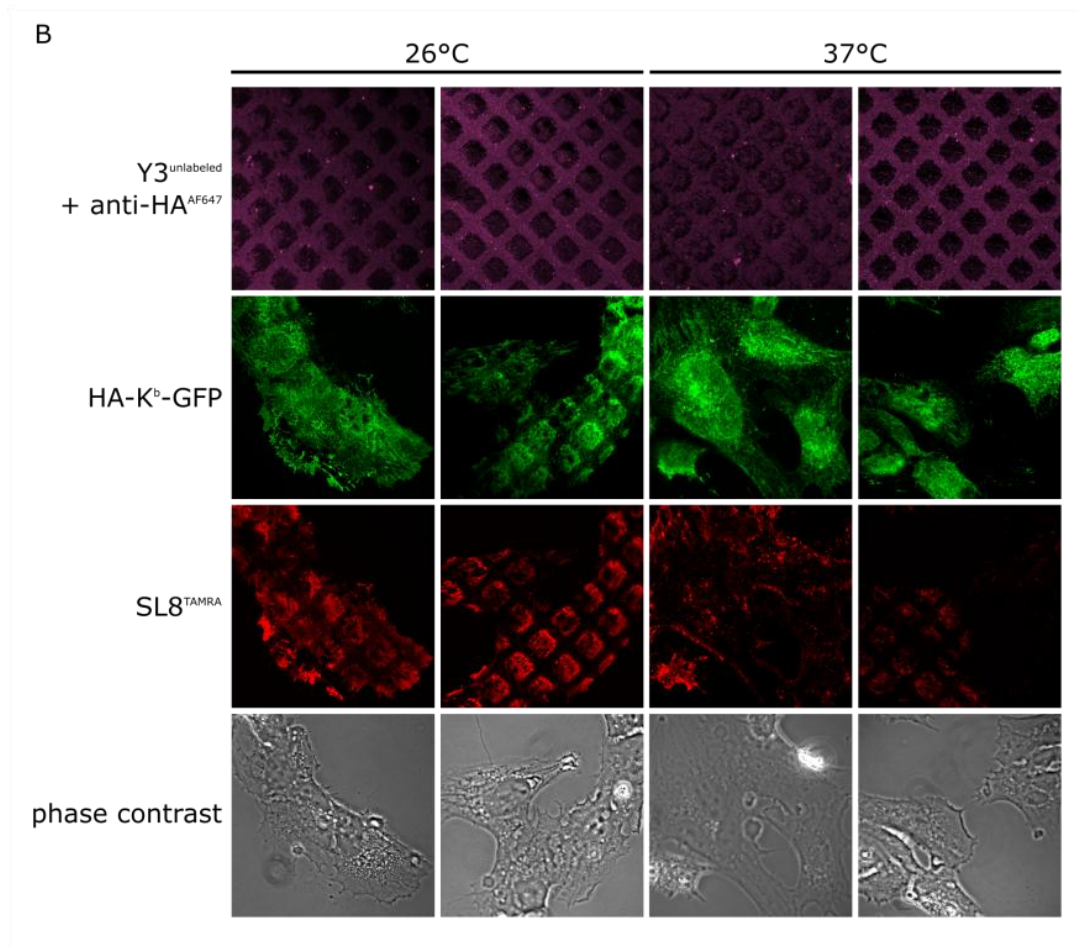


**Figure 4.2.7.1 (continued): Anti-HA and Y3 mixed antibody micropatterns. (B)** The Y3<sup>unlabeled</sup> print was incubated with HA<sup>AF647</sup>. STF1/HA-K<sup>b</sup>-GFP cells were seeded on the mixed antibody micropatterns and incubated overnight at 26°C or 37°C as indicated. The next day, cells were incubated with SL8<sup>TAMRA</sup> to stain peptide receptive HA-K<sup>b</sup>-GFP (red). Duplicates represent individual observations. Bar, 25 µm

## **5 Anti-MHC class I antibody micropatterns as a tool to study conformation-specific *in cis* interactions**

### **5.1 A novel two-hybrid antibody micropattern assay reveals conformation-specific cell surface clustering of MHC I proteins**

#### **5.1.1 About chapter 5.1**

Chapter 5.1 is a manuscript that contains some original data. The experiments in this manuscript were designed by me and performed by myself or by the indicated co-authors. The manuscript was written by Sebastian Springer and me.

The manuscript was under revision at Elife (<https://elifesciences.org/>) at the time of writing (20.02.2018) and a revised version was accepted on 24.07.2018 (DOI: 10.7554/eLife.34150).

Dirscherl, C., Ramnarayan, V., Hein, Z., Jacob-Dolan, C., and Springer, S.: **A novel two-hybrid antibody micropattern assay reveals conformation-specific cell surface clustering of MHC I proteins.**

The figure numbers were changed to match the format of this thesis.

#### **5.1.2 Abstract**

In this work, we demonstrate a novel two-hybrid assay based on antibody micropatterns to study cell surface clustering of major histocompatibility complex (MHC) class I proteins. Anti-tag and conformation-specific antibodies are used to individually capture specific forms of MHC class I and allow for a location- and conformation-specific analysis by fluorescence microscopy. The assay is used to study the formation of MHC class I clusters at the cell surface under controlled conditions and to define the involved protein conformations. Our results show that homotypic *in cis* interactions occur exclusively between specific MHC class I forms, and we identify the dissociation of the light chain (beta-2 microglobulin) from the MHC class I protein complex as the crucial step of cluster formation. The functional role of these MHC class I clusters at the cell surface needs further investigation. We propose future technical developments of our two-hybrid assay for further analysis of MHC class I clusters and, universally, for the study of protein-protein interactions.

### 5.1.3 Introduction

Protein-protein interactions are difficult to investigate, especially when they involve membrane proteins under physiological conditions, specific protein conformations or subpopulations, low affinities, or defined locations in the cell. Such challenges are not usually met by the yeast two-hybrid screens and co-immunoprecipitation approaches that are commonly used; instead, they require technically demanding methods such as fluorescence resonance energy transfer (FRET)<sup>18</sup> or fluorescence correlation spectroscopy, which only work in some cases.

Recently, antibody-based capture assays on solid supports have been described that can be used in bait-prey experiments in live cells (Löchte et al., 2014; Schwarzenbacher et al., 2008; Weghuber et al., 2010). We have now expanded this concept to characterize location- and conformation-specific protein-protein interactions in a novel two-hybrid assay read out by fluorescence microscopy. We use microprinted antibody patterns to spatially arrange specific conformations of our bait proteins in the plasma membrane of live cells (Dirscherl and Springer, 2017) and to investigate their interaction with green fluorescent protein (GFP)-tagged prey proteins. The assay is universally applicable for the investigation of protein-protein interactions.

In this paper, we use our two-hybrid assay to solve the long-standing question which forms of major histocompatibility complex (MHC) class I proteins associate laterally (*in cis*) on the plasma membrane. Class I proteins consist of a polymorphic transmembrane heavy chain (HC), the non-covalently bound light chain called beta-2 microglobulin ( $\beta_2m$ ), and a peptide of eight to ten amino acids. Assembly of HC,  $\beta_2m$ , and peptide takes place in the endoplasmic reticulum (ER), followed by transport to the cell surface, where class I proteins present the bound peptides to T cell receptors of cytotoxic T cells; they also bind inhibitory receptors on Natural Killer cells. Class I antigen presentation is central to the cellular immune response against viruses, intracellular parasites, and tumors in jawed vertebrates.

At the cell surface, class I molecules exist in three different forms: the HC/ $\beta_2m$ /peptide trimers, the ‘peptide-empty’ HC/ $\beta_2m$  dimers derived from them by dissociation of the peptide, and the ‘free’ heavy chains derived from the dimers by dissociation of  $\beta_2m$ . While the lateral association of class I proteins has been observed before (Capps et al., 1993; Arosa et al., 2007), other researchers have not detected

---

<sup>18</sup> Abbreviations:  **$\beta_2m$** , beta-2 microglobulin; **class I**, MHC class I protein(s); **ER**, endoplasmic reticulum; **fHC**, free heavy chain; **FRET**, fluorescence resonance energy transfer; **GFP**, green fluorescent protein; **HA**, (influenza) hemagglutinin; **HC**, heavy chain; **K<sup>b</sup>**, the murine class I protein H-2K<sup>b</sup>; **MHC**, major histocompatibility complex; **PDMS**, poly(dimethylsiloxane); **TAP**, transporter associated with antigen processing; **TAMRA**, carboxytetramethylrhodamine.

them (Szöllösi et al., 1989; Damjanovich et al., 1983; Liegler et al., 1991); and while optical methods have not provided conclusive evidence which forms are interacting, biochemical approaches have not clarified where in the cell the binding occurs (Capps et al., 1993; Matko et al., 1994). Moreover, the HC/ $\beta_2m$  dimers and free heavy chains are short-lived, which complicates their analysis (Montealegre et al., 2015). For the study of the proposed functions (endocytosis, synapse architecture, inflammatory response, receptor modulation) of the class I clusters, knowledge of location and conformation is essential (Dixon-Salazar et al., 2014; Chen et al., 2017; Burian et al., 2016; Nizsalóczy et al., 2014; Mocsár et al., 2016).

Our work now resolves these controversies and shows conclusively that class I free heavy chains, but not HC/ $\beta_2m$ /peptide trimers or HC/ $\beta_2m$  dimers, cluster at the plasma membrane, demonstrating the power of our antibody micropattern two-hybrid assay.

## 5.1.4 Results

### 5.1.4.1 $K^b$ and $D^b$ are specifically captured by antibody micropatterns

Membrane proteins on the surface of living cells can be captured into geometric shapes by antibodies that are printed onto the substrate in micrometer-sized patterns (figure 5.1.4.1 A; (Dirscherl et al., 2017)). We reasoned that any protein that naturally interacts with a patterned protein would also be captured into the patterns, and that this might be used for a protein-protein interaction assay (Schwarzenbacher et al., 2008). We further reasoned that if we printed antibodies that recognize only certain forms of class I (such as Y3, which requires  $\beta_2m$  bound to the  $K^b$  heavy chain), the interaction assay might be made specific for certain forms of class I.

We first tested whether the two common  $\beta_2m$ -dependent monoclonal antibodies Y3 (which binds to  $K^b$ HC/ $\beta_2m$  dimers and  $K^b$ HC/ $\beta_2m$ /peptide trimers of  $K^b$  (Hämmerling et al., 1982)) and 27.11.13S (which binds to  $D^b$ HC/ $\beta_2m$  dimers and  $D^b$ HC/ $\beta_2m$ /peptide trimers (Ozato and Sachs, 1981)) were still specific for their target allotypes when used in the pattern capture assay. We inked poly(dimethylsiloxane) (PDMS) stamps with solutions of Y3 and 27.11.13S and printed them onto the surface of untreated glass coverslips. We then seeded human STF1 fibroblasts expressing C-terminal green fluorescent protein (GFP) fusions of either  $K^b$  or  $D^b$  onto these coverslips and observed patterning of  $K^b$ -GFP and  $D^b$ -GFP by confocal laser scanning microscopy (figure 5.1.4.1 B). As anticipated,  $K^b$ -GFP only patterned with Y3, and  $D^b$  only with 27.11.13S. We concluded that the printed  $\beta_2m$ -dependent antibodies still specifically recognize their target allotypes.

In addition, we wished to be able to capture class I independent of its  $\beta_2m$  or peptide association. Thus, we next tested whether class I proteins can also be patterned via an N-terminal (extracellular) influenza hemagglutinin (HA) epitope tag (figure 5.1.4.1 C, bottom). We printed patterns of the monoclonal anti-HA antibody 12CA5 and seeded STF1 cells expressing either a HA-K<sup>b</sup>-GFP fusion construct or K<sup>b</sup>-GFP, which lacked the HA epitope. As expected, we observed patterning only with HA-K<sup>b</sup>-GFP but not with K<sup>b</sup>-GFP (figure 5.1.4.1 D). The HA tag did not interfere with the patterning of HA-K<sup>b</sup>-GFP on Y3 antibody micropatterns (figure 5.1.4.1 D). We conclude that the anti-HA antibody can be used to specifically pattern HA tagged class I proteins.



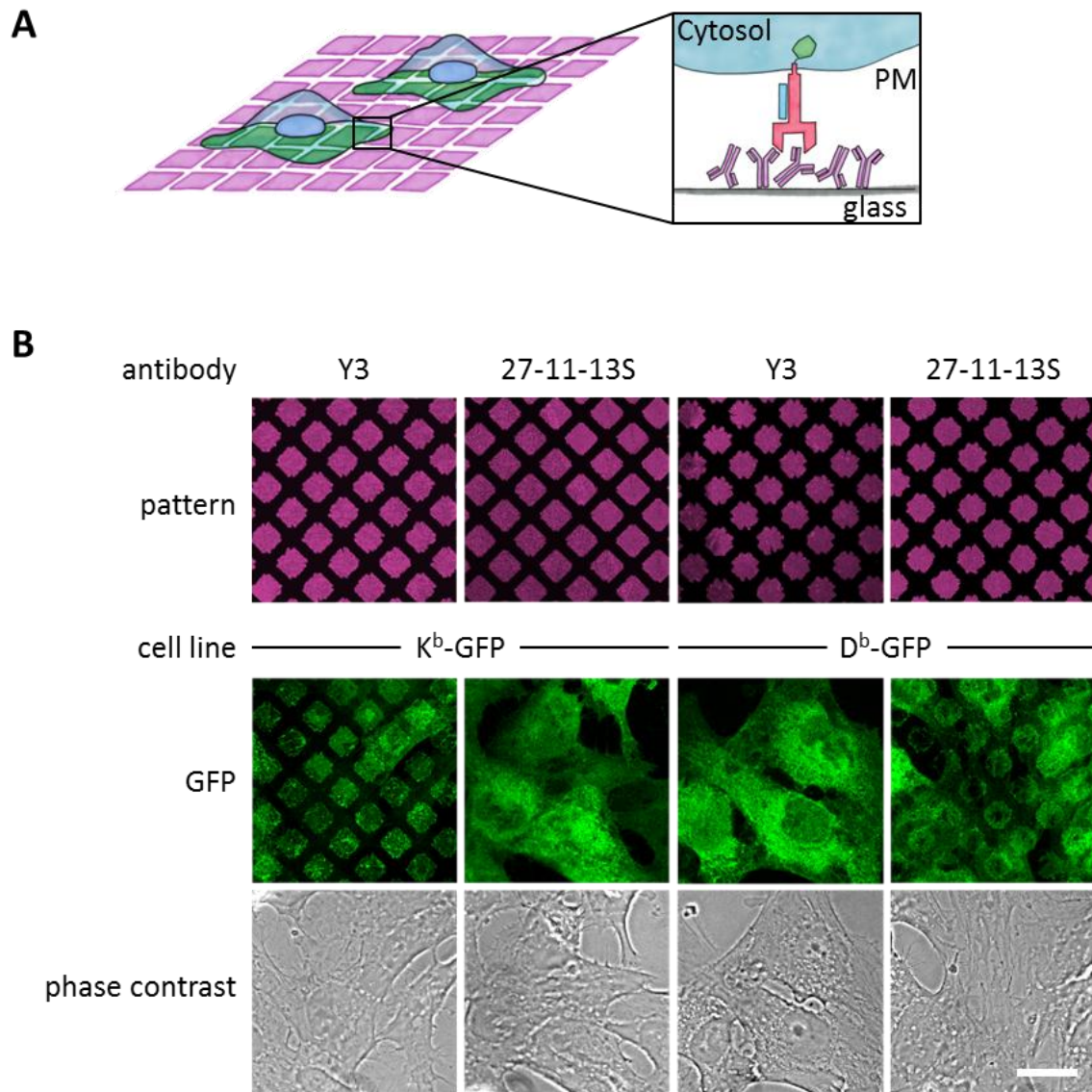


**Figure 5.1.4.1: Specific capture of cell surface K<sup>b</sup> on antibody micropatterns. (A)** schematic presentation of the capture assay. Cells transduced with K<sup>b</sup> (red) fused to GFP (green) are incubated on the Y3 antibody micropatterns (anti K<sup>b</sup>; magenta). Upon specific antibody-antigen interaction, K<sup>b</sup>-GFP is captured on its extracellular epitope by the Y3 antibody pattern elements (see enlargement). **(B)** Printed antibodies are target-specific. Control experiments demonstrate that K<sup>b</sup>-GFP is only captured by the anti-K<sup>b</sup> antibody Y3 and not by an antibody specific for D<sup>b</sup> (27.11.13S).

Figure continues on next page.

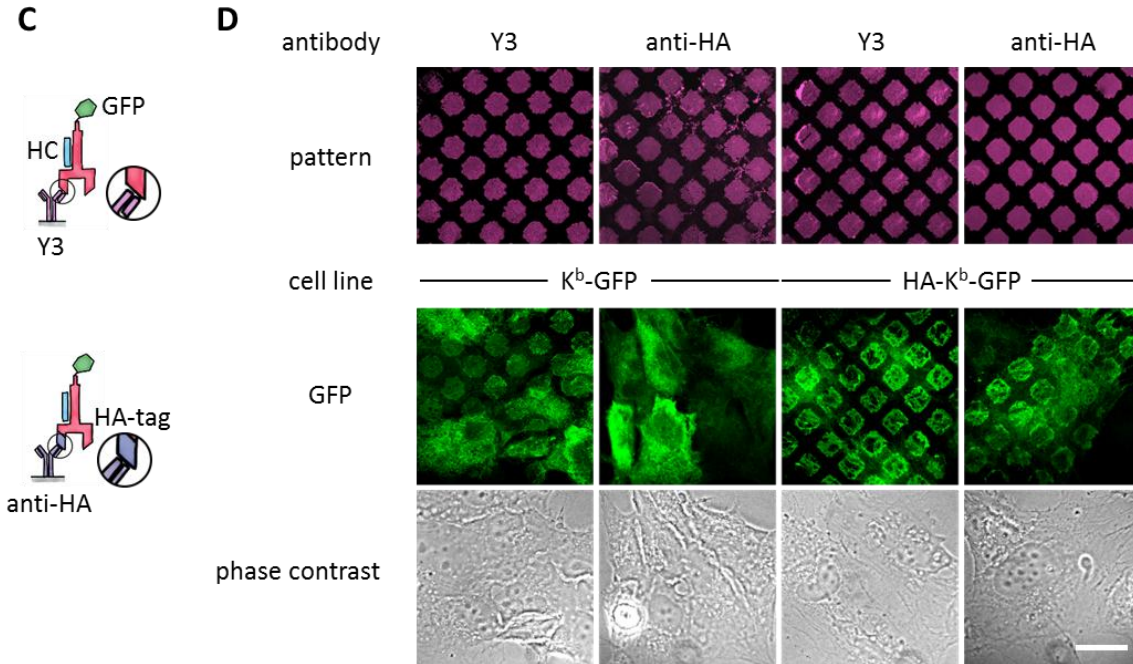


**Figure 5.1.4.1 (continued): Specific capture of cell surface K<sup>b</sup> on antibody micropatterns.** (C) Schematic displaying the different antibody epitopes on the K<sup>b</sup> molecule. The Y3 epitope reacts specifically with residues of the α2 helix of K<sup>b</sup>-GFP whereas the anti-HA antibody recognizes the additional HA-tag that was N-terminally fused to K<sup>b</sup>-GFP. (D) Surface K<sup>b</sup>-GFP can be directly captured by the anti-K<sup>b</sup> antibody Y3 or by the anti-HA antibody against the N-terminally tagged HA-K<sup>b</sup>-GFP. Cells were transduced with K<sup>b</sup>-GFP or HA-K<sup>b</sup>-GFP and tested for specificity on Y3 or anti-HA antibody micropatterns. Y3 successfully captures both constructs whereas HA only recognizes the introduced HA-tag. Scale bar: 25 μm.

#### 5.1.4.2 Stabilizing effect of conformation-specific antibodies allows for differential patterning of K<sup>b</sup> dimers and free heavy chains

We next sought to establish conditions in which K<sup>b</sup>HC/β<sub>2</sub>m dimers, without peptide, are preferentially captured in the antibody patterns. In STF1 cells, this can be achieved because they lack TAP (the transporter associated with antigen processing) and thus cannot load class I with high-affinity peptides in the ER. When such TAP-deficient cells are kept at 25 °C, the level of K<sup>b</sup>HC/β<sub>2</sub>m dimers at the cell surface is especially high (Ljunggren et al., 1990; Montealegre et al., 2015). These peptide-receptive K<sup>b</sup>HC/β<sub>2</sub>m dimers can be detected by subsequent binding of fluorescently labeled peptide (Saini et al., 2013c).

We therefore printed Y3 on glass coverslips, seeded STF1 cells expressing HA-K<sup>b</sup>-GFP onto the patterns, and then incubated at 25 °C overnight. Next morning, we added the K<sup>b</sup>-specific peptide SIINFEKL labeled with the TAMRA fluorophore (SL8<sup>TAMRA</sup>). We observed a striking patterned staining of the fluorescent

peptide, demonstrating that peptide-receptive  $K^b/\beta_2m$  dimers had been captured in the patterns (figure 5.1.4.2 A, column 2). To show that binding of the peptide was specific, we pre-incubated the cells with unlabeled SIINFEKL peptide, which blocked  $SL8^{TAMRA}$  binding (figure 5.1.4.2 A, column 3). Thus, we were able to capture  $K^bHC/\beta_2m$  dimers into patterns and subsequently bind peptide to them.

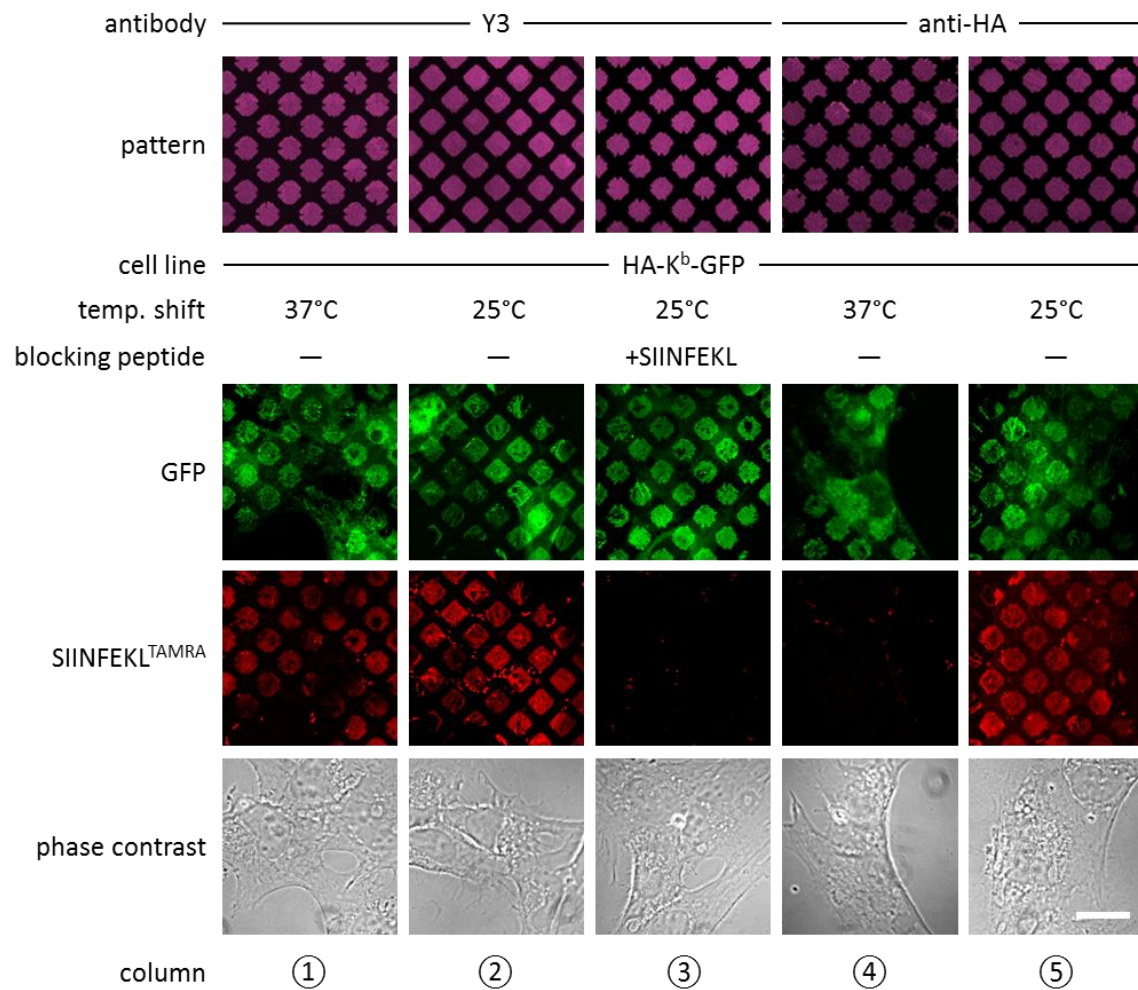
We then repeated the same experiment on patterns of anti-HA antibody, with the same result (figure 5.1.4.2 A, column 5). Thus, both Y3 and anti-HA antibodies captured peptide-receptive  $K^bHC/\beta_2m$  dimers on the surface of the STF1 cells.

We next wished to induce the dissociation of  $\beta_2m$  from the captured  $K^bHC/\beta_2m$  dimers in order to obtain patterned free heavy chains. At 37 °C, dissociation of  $\beta_2m$  from  $K^bHC/\beta_2m$  dimers occurs rapidly, whereas at 25 °C, the rate of dissociation of  $\beta_2m$  is significantly reduced (Montealegre et al., 2015; Day et al., 1995). Thus, we repeated the above experiments on anti-HA and Y3 patterns, but before adding the  $SL8^{TAMRA}$  peptide, we shifted the cells to 37 °C for two to three hours. As expected, after incubation at 37 °C, HA- $K^b$ -GFP patterns showed no binding of  $SL8^{TAMRA}$  (figure 5.1.4.2 A, column 4), which shows that the HA-captured class I proteins lost their peptide-binding capacity, probably due to the dissociation of  $\beta_2m$ . Very interestingly, HA- $K^b$ -GFP patterned with Y3 retained its ability to bind peptide at 37 °C (figure 5.1.4.2 A, column 1). This suggests that the  $\beta_2m$ -specific Y3 antibody stabilizes the  $K^bHC/\beta_2m$  dimer complex to which it is bound by preventing the dissociation of  $\beta_2m$ , similar to the action of peptide (Townsend and Bodmer 1989).

To test the hypothesis that the lack of peptide binding of the  $K^b$  proteins that were captured by HA and incubated at 37 °C was due to the loss of  $\beta_2m$ , we repeated the same experiment, but instead of adding fluorescent peptide, we fixed the cells and immuno-stained with the anti- $\beta_2m$  antibody BBM.1 directly labeled with Atto 542 (BBM.1<sup>Atto542</sup>) (figure 5.1.4.2 B). As predicted by the hypothesis, the Y3 micropatterns stained positive for  $\beta_2m$  at both temperatures (columns 1, 2), whereas anti-HA micropatterns stained for  $\beta_2m$  only at 25 °C (columns 3 and 5). When we added SIINFEKL to the cells on anti-HA micropatterns before shifting them to 37 °C, we observed that BBM.1<sup>Atto542</sup> staining was restored in these samples (column 4). We conclude that patterned  $K^b$  free heavy chains can be generated by inducing the dissociation of  $\beta_2m$  from  $K^bHC/\beta_2m$  dimers captured on anti-HA patterns.

Taken together, we are able to selectively hold three different forms of  $K^b$  on the surface of STF1 cells: free heavy chains (at 37 °C on HA patterns),  $K^bHC/\beta_2m$  dimers (at 25 °C on anti-HA patterns, or at 25 or 37 °C on Y3 patterns), and  $K^bHC/\beta_2m$ /peptide trimers (by addition of peptide on anti-HA and Y3 patterns).

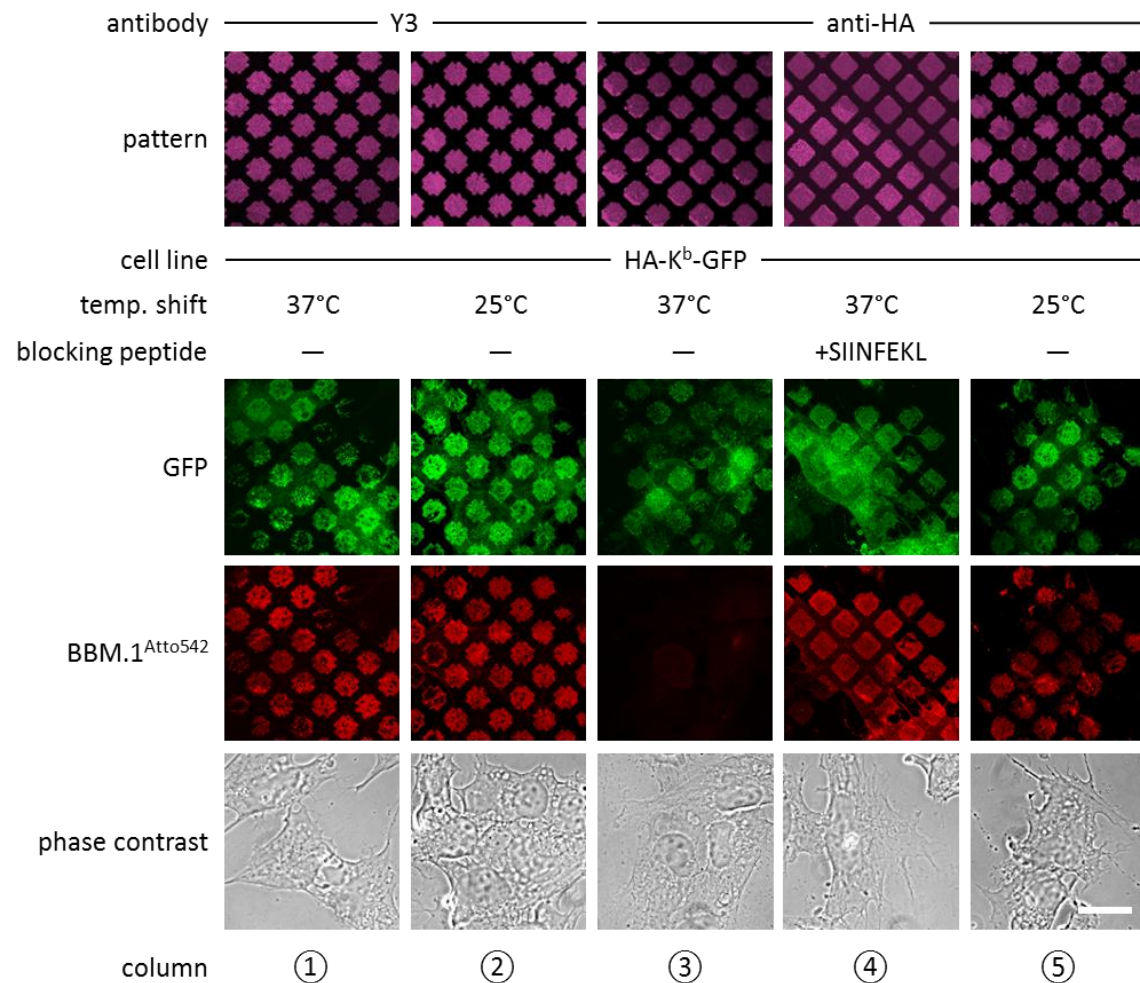
**A**



**Figure 5.1.4.2: Antibody micropatterns determine stability of the captured K<sup>b</sup> population. (A)** Cells expressing HA-K<sup>b</sup>-GFP were captured on Y3 or anti-HA antibody micropatterns and incubated at 25 °C or 37 °C to induce the dissociation of  $\beta_2m$ . For the identification of the nature of the captured K<sup>b</sup>-GFP population (green channel) specific fluorescent peptide SIINFEKL (SL8<sup>TAMRA</sup>; red channel) was added to the samples. Based on their ability to bind peptide, one can distinguish between the peptide-receptive K<sup>b</sup>HC/ $\beta_2m$  dimer and the K<sup>b</sup> free heavy chains, which are incapable to bind peptide. Scale bar, 25  $\mu$ m.

Figure continues on next page.



**B**

**Figure 5.1.4.2 (continued): Antibody micropatterns determine stability of the captured K<sup>b</sup> population. (B)** For further characterization of the captured HA-K<sup>b</sup>-GFP on Y3 or anti-HA antibody micropatterns, immunostaining experiments were performed. Immunostaining of captured HA-K<sup>b</sup>-GFP molecules with the anti- $\beta_2$ m antibody (BBM.1<sup>Atto542</sup>) reveals dissociation of  $\beta_2$ m from anti-HA antibody micropatterns at 37 °C (column 3). Addition of the specific ligand peptide SIINFEKL (SL8) during 37 °C incubation rescues  $\beta_2$ m dissociation (column 4). Scale bar, 25  $\mu$ m.

### 5.1.4.3 Antibody micropatterns reveal conformation-dependent *in cis* interactions of K<sup>b</sup> free heavy chains

Since we were able to distinguish the three different forms of K<sup>b</sup> held in the patterns, we next investigated whether any of these forms associate *in cis* on the plasma membrane. For this, we designed a two-hybrid assay (figure 5.1.4.3 A): One K<sup>b</sup> construct had an N-terminal HA tag but no GFP (HA-K<sup>b</sup>), the other carried a C-terminal GFP but no HA tag (K<sup>b</sup>-GFP). We reasoned that HA-K<sup>b</sup> would be captured by the anti-HA antibodies, but the GFP pattern would only become detectable by microscopy if HA-K<sup>b</sup> and K<sup>b</sup>-GFP interacted together, since K<sup>b</sup>-GFP alone is not captured by anti-HA micropatterns (figure 5.1.4.1 D). To perform the experiment, we co-transduced STF1 cells with HA-K<sup>b</sup> and K<sup>b</sup>-GFP, seeded the cells on anti-HA micropatterns, and incubated them overnight at 25 °C to accumulate K<sup>b</sup>HC/β<sub>2</sub>m dimers of both K<sup>b</sup> constructs at the cell surface. The next day, we either left them at 25 °C or shifted them to 37 °C and followed the patterning of the GFP fluorescence.

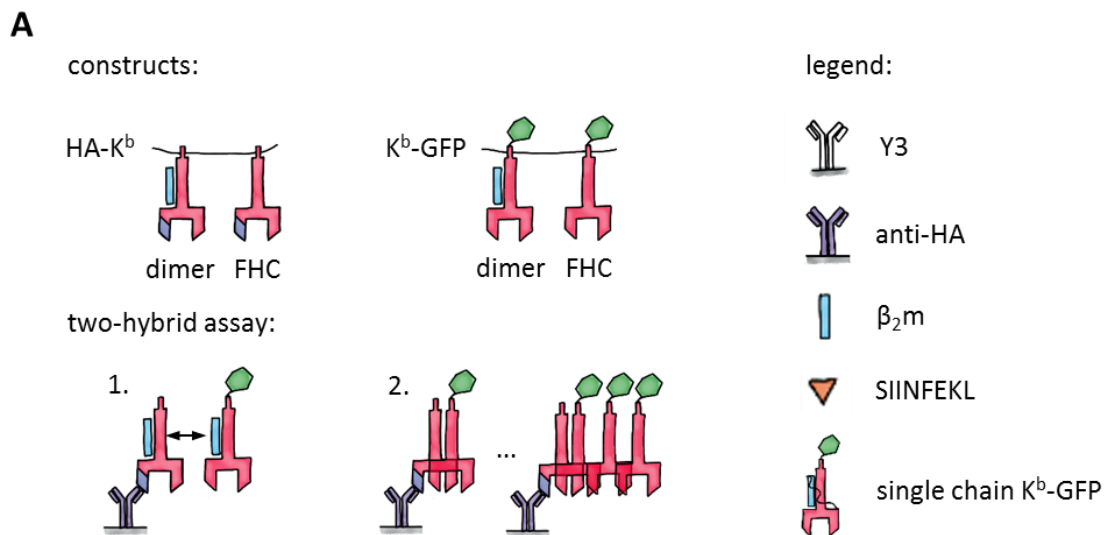


**Figure 5.1.4.3: Antibody micropatterns reveal conformation-dependent *in cis* interactions of captured K<sup>b</sup>-GFP.**(A) For the two-hybrid assay, cells were co-transduced with two K<sup>b</sup>-constructs: K<sup>b</sup> with an N terminal HA tag (HA-K<sup>b</sup>) and K<sup>b</sup>-GFP (GFP fused to the cytoplasmic tail)

Figure continues on next page.

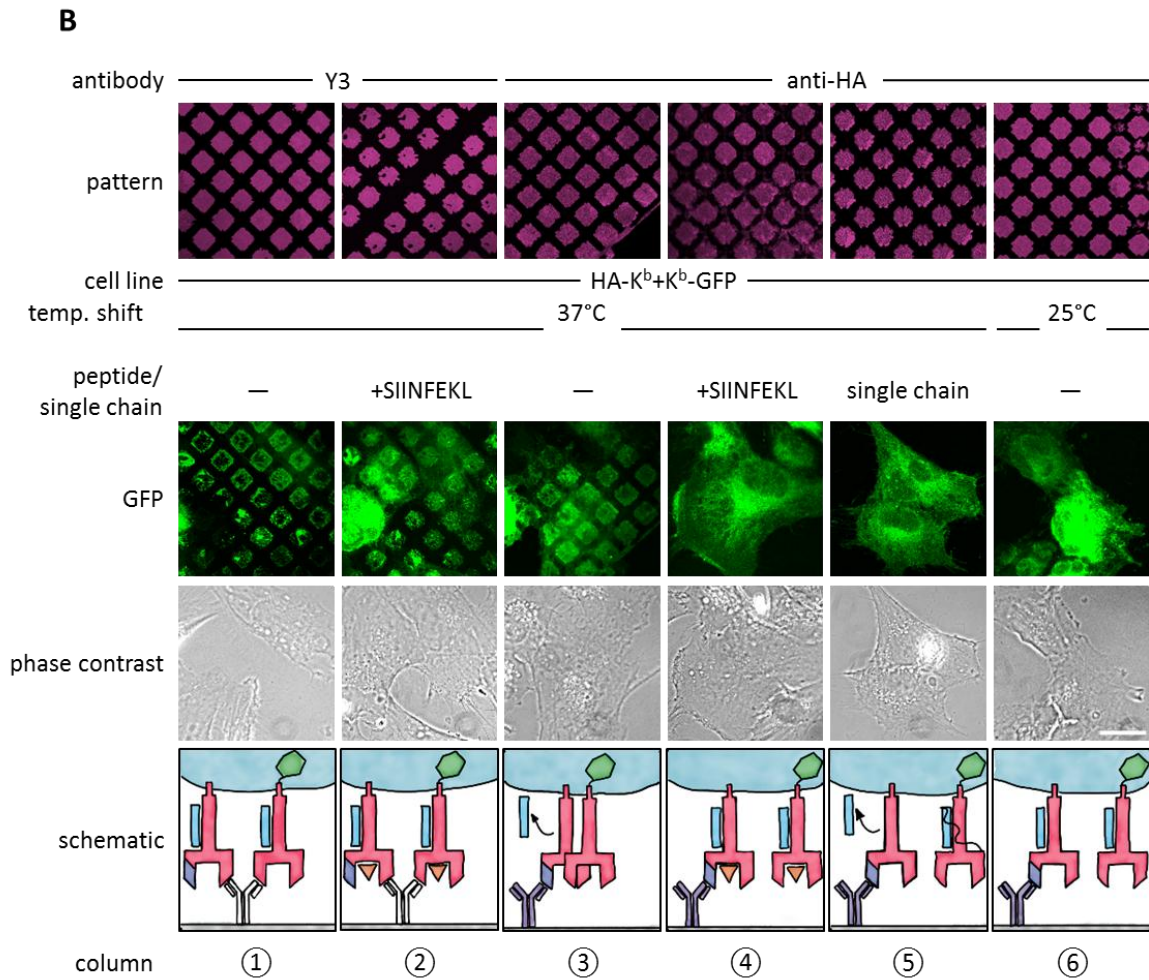


**Figure 5.1.4.3 (continued): Antibody micropatterns reveal conformation-dependent *in cis* interactions of captured K<sup>b</sup>-GFP. (B)** Cells were incubated on anti-HA or Y3 antibody-micropatterns at different temperatures. Recruitment of K<sup>b</sup>-GFP (green channel) to the anti-HA antibody micropatterns occurs specifically at 37 °C and can be inhibited by addition of the SIINFEKL (SL8) peptide (column 3 and 4). The single chain mutant, scK<sup>b</sup>-GFP, where  $\beta_2m$  is covalently linked to the K<sup>b</sup> heavy chain is also not recruited to the antibody micropatterns (column 5). From top to bottom: Antibody micropatterns, K<sup>b</sup>-GFP, phase contrast, and schematic representation. Scale bar: 25  $\mu$ m.

We observed strong co-patterning of both forms after 37 °C incubation, suggesting that free heavy chains can interact *in cis* in the membrane (figure 5.1.4.3 B, column 3). When we inhibited dissociation of  $\beta_2m$  by addition of SIINFEKL peptide (column 4) or incubation at 25 °C (column 6), co-patterning was abolished. (As a control, on Y3 patterns, in contrast, where both HA-K<sup>b</sup> and K<sup>b</sup>-GFP are directly bound by the antibody, strong patterning of K<sup>b</sup>-GFP was visible even in the presence of SIINFEKL (columns 1 and 2)). These data show that K<sup>b</sup> does not associate *in cis* as long as  $\beta_2m$  is bound.

To further test this conclusion, we co-transfected STF1 cells with HA-K<sup>b</sup> and sCK<sup>b</sup>-GFP, a single-chain construct in which the K<sup>b</sup> heavy chain and  $\beta_2m$  are linked by a peptide linker such that  $\beta_2m$  cannot dissociate (Montealegre et al., 2015). As in the previous control experiment, no co-patterning was observed (column 5). These controls also demonstrated that the clustering of the free heavy chains was not simply induced by the GFP domain of the K<sup>b</sup>-GFP fusion proteins.

To demonstrate that the non-fluorescent HA-K<sup>b</sup> molecules were indeed present in the patterns together with the K<sup>b</sup>-GFP, we repeated the experiment in figure 5.1.4.3 B (column 3) with the construct E3-HA-K<sup>b</sup>, in which an additional tag of a 21 amino acids (the E3 tag; see Materials and Methods) is attached to the N terminus of HA-K<sup>b</sup>. This tag specifically binds to the fluorescently labeled synthetic peptide, K4<sup>Atto633</sup>. After co-patterning of K<sup>b</sup>-GFP was observed, we additionally stained with K4<sup>Atto633</sup> and found close colocalization with K<sup>b</sup>-GFP in the patterns (figure 5.1.8.3). We conclude that the free heavy chain of E3-HA-K<sup>b</sup> is indeed captured on the patterns and then recruits the free heavy chain of K<sup>b</sup>-GFP by an *in cis* interaction.

Taken together, our data demonstrate that K<sup>b</sup> free heavy chains, but not K<sup>b</sup>HC/ $\beta_2m$  dimers or K<sup>b</sup>HC/ $\beta_2m$ /peptide trimers, associate, or cluster, *in cis* in the plasma membrane of live cells.



#### 5.1.4.4 *In cis* interactions of K<sup>b</sup> confirmed by co-immunoprecipitation

We next tested this finding in a co-immunoprecipitation experiment, without the use of micropatterns. We used the same STF1 cells co-transfected with HA-K<sup>b</sup> and K<sup>b</sup>-GFP and incubated them at 25 °C overnight to accumulate both K<sup>b</sup> constructs at the cell surface. The cells were then shifted to 37 °C for 15 minutes (the half-life of K<sup>b</sup>HC/β<sub>2</sub>m dimers at the cell surface (Montealegre et al. 2015)) to dissociate β<sub>2</sub>m and induce cluster formation. Then, the cells were trypsinized and lysed, and HA-K<sup>b</sup> was immunoprecipitated with the anti-HA antibody. We found efficient co-precipitation of K<sup>b</sup>-GFP with HA-K<sup>b</sup>, which was abolished if SIINFEKL peptide was added to the cells during the 37 °C incubation (figure 5.1.4.4, 5.1.8.1). Thus, just like in the micropattern assay, the peptide clearly inhibited the interaction, suggesting that only free heavy chains were co-precipitating.

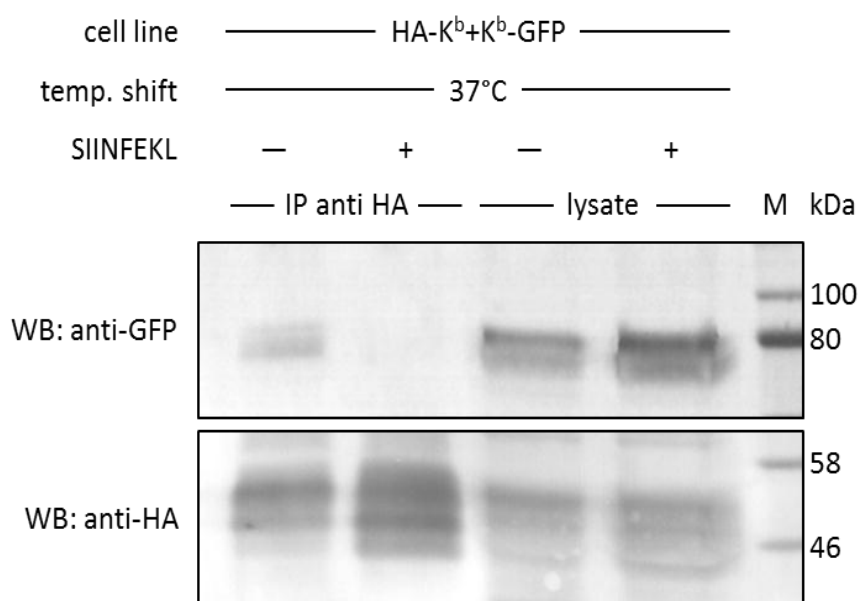


**Figure 5.1.4.4: *In cis* interactions of K<sup>b</sup>-GFP and HA-K<sup>b</sup> are peptide dependent and generally occur in cells at 37°C.** For co-immunoprecipitation, the same co-transduced cells from the previous experiment were used (STF1/ HA-K<sup>b</sup> and K<sup>b</sup>-GFP). Cells were incubated at 25°C overnight to enrich K<sup>b</sup> cell surface levels and then shifted to 37°C to induce the dissociation of β<sub>2</sub>m from the K<sup>b</sup> heavy chain. The SIINFEKL (SL8) peptide was added as control to inhibit β<sub>2</sub>m dissociation (lanes 2 and 4). Cells were then lysed and successfully immunoprecipitated with an anti-HA antibody (bottom row). Immunoisolates and lysate control samples were analysed by Western blotting by sequential staining with an anti-GFP antibody (top row) and an anti-HA antibody (bottom row). The K<sup>b</sup>-GFP construct was specifically co-immunoprecipitated in the absence of peptide, similar to the result on antibody micropatterns (lane 1).

### 5.1.5 Discussion

Here, we have developed antibody micropatterns into a novel two hybrid assay for the detailed investigation of conformation-specific interactions of our model protein. The versatility of our assay using HA and GFP fusions allows for a broad range of applications, especially in the study of specific protein interactions that require investigation in the native environment of live cells.

The example of MHC class I demonstrates the challenges of functional analysis of protein interactions and the limitations of conventional methods, which lack important information such as spatial resolution or the distinction of different protein conformations. Previous experiments using FRET revealed cluster formation of antibody-labeled class I proteins at the cells surface, but the involvement of free heavy chains was only indirectly shown (Matko et al., 1994). Other studies involved co-immunoprecipitation experiments that revealed the existence of free heavy chain dimers of different murine class I allotypes by pull-down with conformation-specific antibodies. However, it was not excluded that the detected interactions were enhanced, or indeed caused, by detergents after cell lysis. Additional pulse chase experiments suggested the formation of the detected free heavy chain dimers at the cell surface but could only confirm that it occurs after the proteins have traversed the medial Golgi (Capps et al., 1993).

Our own co-immunoprecipitation experiments have confirmed these observations for the murine K<sup>b</sup> allotype, but they also lack spatial resolution (figure 5.1.4.4). Differential co-immunoprecipitation of surface biotinylated class I proteins finally confirms the presence of clusters at the cell surface (figure 5.1.8.1 ) but cannot entirely exclude the involvement of intracellular class I proteins.

With our novel two-hybrid assay, we were finally able to definitively solve these questions and also to clarify the hypothesized involvement of  $\beta_2m$ . It allowed us to establish a system in which we are able to generate defined conformations of class I proteins and induce the controlled formation of clusters. The results clearly demonstrate that cluster formation is strictly dependent on the generation of free heavy chains and suggest that these free heavy chains originate from the captured empty K<sup>b</sup>HC/  $\beta_2m$  dimers at the cell surface upon dissociation of  $\beta_2m$  by incubation at 37 °C (figure 5.1.4.3 B). Moreover, we were able to show that clusters are indeed generated at the cell surface. Of course, it is possible that in addition, free heavy chains are generated elsewhere in the cell by  $\beta_2m$  dissociation, for example in endosomes, and that they might cluster in these locations also.

For MHC class I clusters at the cell surface, various functional roles have been proposed. Clusters might be a means of accelerated disposal for free heavy chains, preventing re binding of  $\beta_2m$  and peptide and

perhaps leading to enhanced internalization and degradation in lysosomes (Montealegre et al., 2015). This hypothesis is supported by our finding that clustered class I molecules do not bind peptide well (figure 5.1.8.2) and therefore probably do not interact with TCRs. They might still be ligands for NK cell receptors or similar proteins, perhaps signaling stress or activation states (Garcia-Beltran et al., 2016; Burian et al., 2016). We cannot entirely exclude that the clusters contain some  $K^b$ HC/ $\beta_2m$  dimers that are peptide receptive, as has been suggested for human class I clusters (Bodnár et al., 2003), but free heavy chains are clearly essential for clustering, since single-chain  $K^b$ HC/ $\beta_2m$  dimers form no clusters (figure 5.1.4.3 A). Another possibility is that free heavy chain clusters might influence the surface levels of other proteins with which class I is known to interact, such as APLP or insulin receptor, thereby mediating non-immunological functions of class I (Tuli et al., 2008; Shatz, 2009; Dixon-Salazar et al., 2014). Our assay is a promising tool to extend the interaction studies for class I by the proposed interaction partners.

We have shown here the formation of homotypic clusters of the murine class I allotype  $K^b$ . Interestingly, previous work suggests that the tendency of cluster formation varies among class I allotypes (Capps et al., 1993). Thus, it was hypothesized that those class I allotypes that do not form clusters are not internalized (by the proposed accelerated disposal mechanism) and will bind exogenous peptides to provoke autoimmune reactions (Capps et al., 1993). In addition, covalent clusters of HLA-B27 were implicated in inflammatory autoimmune diseases such as spondyloarthropathies (Chen et al., 2017). Due to its universal versatility, our assay allows for the development of a screen to test different allotypes for their tendency to form clusters. This may be extended to human class I proteins, whose empty dimers may be enriched at the cell surface by incubation with low-affinity dipeptide ligands (Saini et al., 2015), and even to the empty forms of HLA-F that were recently discovered to bind NK cell receptors (Garcia-Beltran et al., 2016; Burian et al., 2016). Consequently, by its application to the human system, this screening tool can be developed to investigate the correlation between cell surface cluster formation and human autoimmune disease. Generation of anti HA antibody micropatterns by microcontact printing on conventional glass coverslips makes this assay especially suitable for such high throughput approaches.

In addition to its demonstrated application in the detection of protein interactions, the assay can be further developed towards detailed analysis of the clusters. One possibility is the integration of conventional immunostaining for the identification of other proteins involved in cluster formation. For class I, e.g. the accumulation of adaptor proteins involved in endocytic processes (e.g. Rab proteins) in

the clustered areas will contribute to understand the nature of class I endocytosis and the functional role of class I clusters.

Another possible technical development is to combine the assay with FRAP measurements to test the dynamics of the interactions (i.e. dissociation and re-association). Such a combined two hybrid-FRAP assay is potentially superior to conventional FRET experiments, since the enrichment of proteins in the pattern elements increases the abundance of the interaction partners and would allow for the detection of very weak interactions.

## **5.1.6 Materials and Methods**

### **5.1.6.1 Photolithography**

Silicon master molds were prepared by semiconductor photolithography as described previously. See (Dirscherl et al., 2017) for details.

### **5.1.6.2 PDMS stamps and antibody patterns**

PDMS stamps were generated from basic elastomer and curing agent (Sylgard 184 Silicone Elastomer Kit) from Dow Corning (Midland, USA) mixed in a 10:1 ratio. The prepared stamps were inked with the indicated antibody solutions and then placed on round microscopy glass coverslips (#1, 22 mm). See (Dirscherl et al., 2017) for details.

### **5.1.6.3 Patterning cell surface proteins**

Coverslips were placed into sterile 6-well plates. Cells were immediately seeded as indicated at a concentration of  $\approx 50.000$  cells per well and incubated on the antibody patterns. Usually, cells were incubated for 4-6 hours at 37 °C for adhesion and then shifted to 25 °C overnight to accumulate  $K^b$  molecules at the cell surface for a better signal-to-noise ratio of patterned  $K^b$  molecules. For clustering experiments, samples were then kept at 25° C or shifted back to 37 °C for 3-4 hours to induce dissociation of  $\beta_2m$ .

### **5.1.6.4 Antibodies**

Mouse monoclonal hybridoma supernatants Y3 (against the complex of  $K^b$  free heavy chain with  $\beta_2m$  (Hämmerling et al., 1982), 27.11.13S (against the complex of  $D^b$  free heavy chain with  $\beta_2m$  (Ozato and

Sachs, 1981)), hemagglutinin (HA) 12CA5 (Niman et al., 1983), and BBM.1 (Brodsky et al., 1979) were described previously. Antibodies for immunoprecipitation were rabbit anti-GFP (Abcam ab290), rabbit antisera against H-2K<sup>b</sup> and H-2D<sup>b</sup> (Charles River Laboratories, Kisslegg, Germany), and goat anti-rabbit IgG-AP conjugate (1706518, Biorad, Munich, Germany). Secondary antibody against the HA antibody was donkey anti-mouse IgG Alexa Fluor 568 (a10037, Thermo Fisher Scientific, Darmstadt, Germany).

#### 5.1.6.5 Dyes

Purified antibodies were either labeled with the Alexa Fluor™-647 NHS ester (Y3, B22.249 and 12CA5) or with the Atto 542 NHS ester (BBM.1) according to the manufacturers' protocols. Alexa Fluor™-647 NHS was obtained from Thermo Fisher Scientific (Darmstadt, Germany) and the Atto 542 NHS from ATTO-TEC (Siegen, Germany).

#### 5.1.6.6 Peptides

Peptide were synthesized by GeneCust (Ellange, Luxemburg) and emc microcollections (Tübingen, Germany) and purified by HPLC (90% purity). The K<sup>b</sup> specific peptide SL8 (SIINFEKL in the single-letter amino acid code) was labeled with the fluorescent dye 5'-Carboxytetramethylrhodamine (TAMRA) on the lysine side chain (avoiding interference with peptide binding to K<sup>b</sup>) to give SIINFEKL-TAMRA. Labeled and unlabeled peptides were added to the cells at a final concentration of 2 μM for 15-30 min at 37 °C to detect peptide binding. Cells were then washed with phosphate buffered saline (PBS, 10 mM phosphate pH 7.5, 150 mM NaCl), fixed, and observed by confocal laser scanning microscopy (cLSM).

#### 5.1.6.7 Cell lines and gene expression

For experiments, TAP-deficient human fibroblasts STF1 (kindly provided by Henri de la Salle, Etablissement de Transfusion Sanguine de Strasbourg, Strasbourg, France) were chosen, so that their endogenous human class I proteins would not interfere with the antibody micropatterns. They were stably transduced with K<sup>b</sup>-GFP, D<sup>b</sup>-GFP, and E3-HA-K<sup>b</sup>-GFP. Lentiviruses were produced and used for gene delivery as described previously (Hein et al., 2014). For clustering experiments, co-transduced STF1 cells were used. The cells were first selected with puromycin for E3-HA-K<sup>b</sup> (the additional E3 tag (EIAALEK)<sub>3</sub> is a 21 amino-acid long extracellular tag that was initially introduced for co-staining experiments). Cells were then transduced with the indicated K<sup>b</sup>-GFP constructs and again selected with puromycin to obtain STF1/E3-HA-K<sup>b</sup>+K<sup>b</sup>-GFP or STF1/E3-HA-K<sup>b</sup>+hβ<sub>2</sub>m-GFP (single chain K<sup>b</sup>, single chain construct in which the light chain β<sub>2</sub>m is fused by a linker to the K<sup>b</sup> heavy chain).

#### 5.1.6.8 Staining with the K4 peptide

The K4 peptide was synthesized by emc microcollections (Tübingen, Germany). The E3-tag specific peptide K4 (a 28 amino-acid long peptide abbreviated as (KIAALKE)<sub>4</sub> in the single-letter amino acid code) was labeled with an Atto 633 fluorophore at the N terminus. For co-staining experiments, cells were fixed with 3% paraformaldehyde (PFA), washed, and permeabilized with 0.1% Triton X-100. The K4<sup>Atto633</sup> peptide was added to the cells at a final concentration of 25 nM in PBS and incubated for 5 min at RT to stain the transduced E3-HA-K<sup>b</sup> construct.

#### 5.1.6.9 Immunofluorescence stainings

For antibody co-staining experiments, cells were fixed with 3% PFA, washed and permeabilized with 0.1% Triton X-100 and stained with the respective antibodies.

#### 5.1.6.10 Microscopy

A confocal laser scanning microscope (LSM 510 Meta, Carl Zeiss Jena GmbH, Germany) equipped with argon and helium-neon lasers at 488, 543 and 633 nm. Images were recorded with a 63x Plan Apochromat oil objective (numerical aperture 1.4) at a resolution of 1596 x 1596 pixels. Data acquisition was performed with the LSM 510 META software, release 3.2 (Carl Zeiss Jena GmbH). During image acquisition, patterns and cells were imaged in the same focal plane at a pinhole of  $\approx 1$  Airy unit. Image analysis and processing were performed using ImageJ (National Institutes of Health, Bethesda, USA). Image processing comprises cropping, rotation and adjustment of brightness and contrast levels.

#### 5.1.6.11 Co-immunoprecipitation

For co-immunoprecipitation with the anti-HA antibody, co-transduced (E3-HA-K<sup>b</sup>+K<sup>b</sup>-GFP) and selected STF1 cells were incubated at 25 °C overnight. Next day, cells were incubated in presence or absence of 10  $\mu$ M SL8 for 10 min at 25 °C, then shifted to 37 °C for 15 min, trypsinised and harvested. Cell pellets were lysed in native lysis buffer (50 mM Tris-Cl (pH7.4), 150 mM NaCl, 5 mM EDTA, and 1% Triton X-100) for 1 hour at 4 °C. After lysis, the supernatant was immunoprecipitated with the HA antibody for 30 min at 4 °C. Beads were washed and resuspended in LSB buffer and boiled at 95 °C for 10 min. The immunisolates were separated by SDS-PAGE and immunoblotted sequentially by an anti-GFP antibody and anti-HA antibody.

For co-immunoprecipitation of the cell surface K<sup>b</sup> molecules with the biotinylated K4 peptide (K4<sup>biotin</sup>), co-transduced (E3-HA-K<sup>b</sup>+Kb-GFP) and selected STF1 cells were incubated at 25 °C overnight. Next day, cells were incubated in presence or absence of 10 µM SL8 for 10 min at 25 °C. E3-tagged K<sup>b</sup>-molecules were labeled with K4<sup>biotin</sup> for 5 min at room temperature using 200 nM biotinylated K4 peptide. Following biotinylation, cells were placed at 37 °C for 15 min to allow cluster formation. Cells were collected into native lysis buffer (50 mM Tris-Cl (pH 7.4), 150 mM NaCl, 5 mM EDTA, and 1 % Triton X-100) by scraping and lysed for 45 min at 4 °C. Biotinylated E3-HA-K<sup>b</sup> (with K4<sup>biotin</sup>) was immunoprecipitated from post-nuclear supernatants using neutravidin-agarose beads (Thermo Fisher Scientific, Darmstadt Germany). Beads were washed in lysis buffer and wash buffer (50 mM Tris-Cl (pH 7.4), 150 mM NaCl, 5 mM EDTA, and 0.1 % Triton X-100) and supplemented with endoglycosidase F1 for 2h at 37 °C, or left untreated. Isolated proteins were retrieved from beads by boiling and separated by SDS-PAGE. K<sup>b</sup>-GFP was detected by anti-GFP antiserum and E3-HA-K<sup>b</sup> was detected by 12CA5 (anti-HA) following western blotting.

### 5.1.7 Acknowledgements

The authors thank Susanne Illenberger und Susanne Fritzsche for suggestions on the manuscript; Ursula Wellbrock for the cultivation of hybridoma cell lines and excellent technical assistance; and Catherine Jacob-Dolan for the purification of antibodies from hybridoma supernatants and antibody labeling and for the preparation of PDMS stamps and antibody micropattern prints. The work was supported by the Bundesministerium für Bildung und Forschung in the framework of the Biotechnology 2020+ initiative (Grant 031A153A to S.Sp.).

## 5.1.8 Supporting Information

### 5.1.8.1 Figure S1

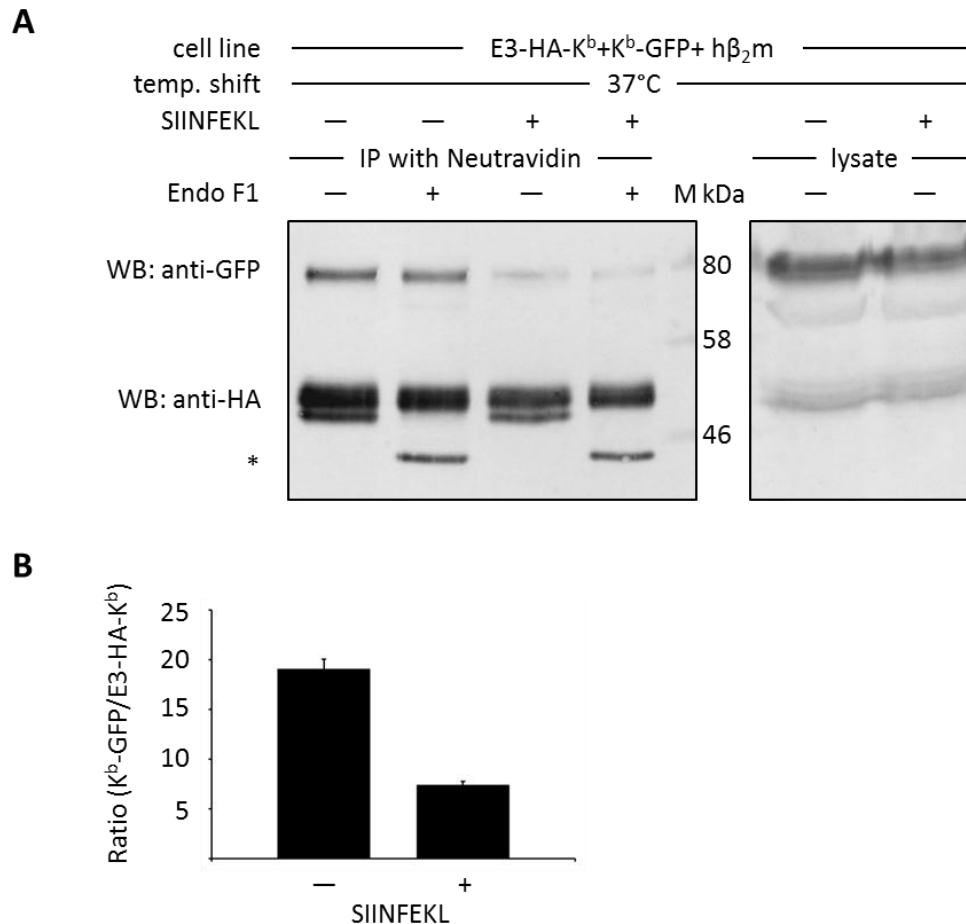


**Figure 5.1.8.1: Co-immunoprecipitation of cell surface K<sup>b</sup> molecules with K4-peptide.**

For co-immunoprecipitation of cell surface proteins, stable STF1 cells co-transfected with E3-HA-K<sup>b</sup> and K<sup>b</sup>-GFP were used. Cells were incubated at 25 °C overnight to enrich K<sup>b</sup> cell surface levels and incubated in presence or absence of SIINFEKL (SL8) as indicated. For cell surface labeling, the biotinylated K4-peptide (K4-biotin; binds to the extracellular E3 tag of E3-HA-K<sup>b</sup>) was added and cells were shifted to 37 °C to induce β<sub>2</sub>m dissociation as described previously. Cells were lysed and co-immunoprecipitated with neutravidin-agarose binding to the biotinylated E3-HA-K<sup>b</sup> cell surface population. The immunisolates were then treated with EndoF1 as indicated to distinguish the cell surface population (EndoF1 resistant, top bands) from the intracellular population of isolated K<sup>b</sup> molecules (EndoF1 sensitive K<sup>b</sup> molecules, see asterisk). **(A)** Sequential Western blot analysis with an anti-GFP antibody (top row) and anti-HA antibody (bottom row) demonstrates that only free heavy chains co-precipitate (lane 1) with E3-HA-K<sup>b</sup>. **(B)** Quantification of (A): The ratio of co-precipitated K<sup>b</sup>-GFP to total protein amounts was quantified.



## 5.1.8.2 Figure S2

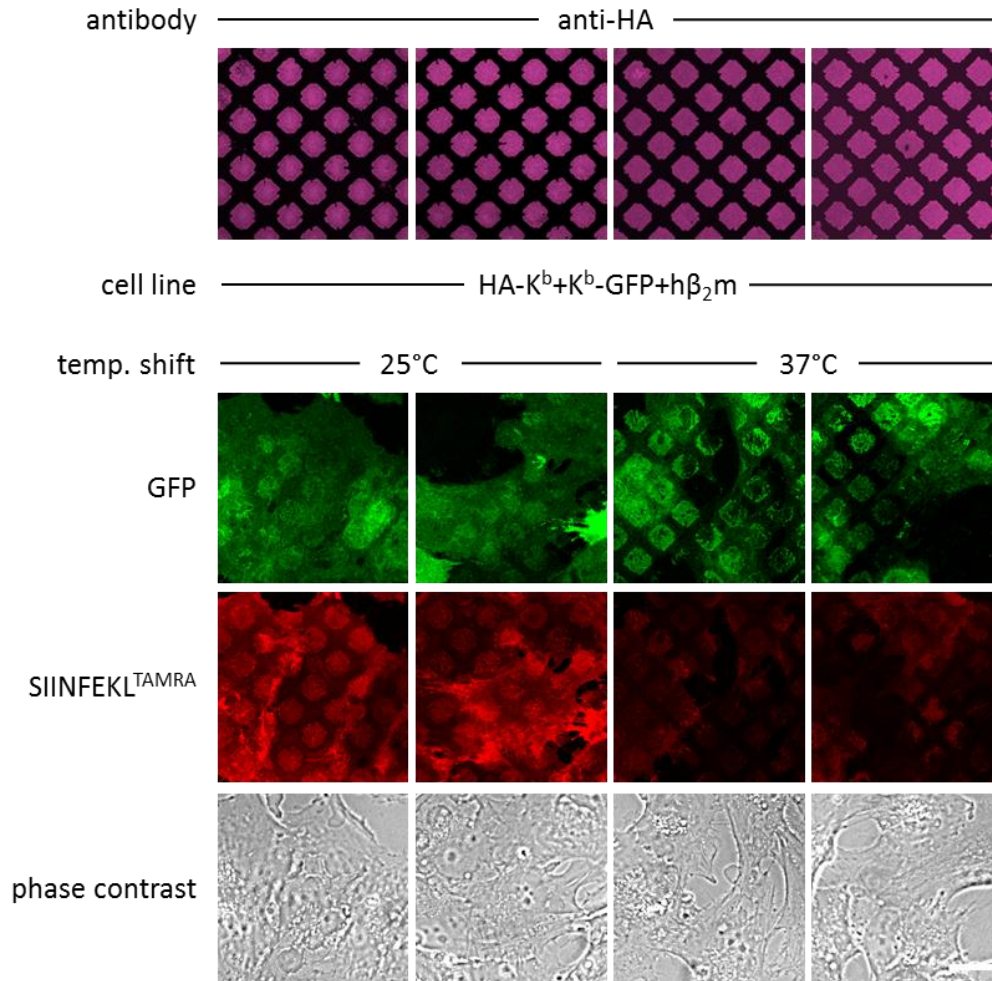


**Figure 5.1.8.2: Binding SIINFEKL<sup>TAMRA</sup> to K<sup>b</sup>-clusters.** Co-transduced cells with E3-HA-K<sup>b</sup> and K<sup>b</sup>-GFP were incubated overnight on anti-HA micropatterns and either left at 25 °C or shifted to 37 °C to induce cluster formation as described previously. Cells were then incubated with SIINFEKL-TAMRA (SL8<sup>TAMRA</sup>) peptide. Peptide binding was reduced in K<sup>b</sup> clusters at 37°C (columns 3 and 4), indicating that only free heavy chains interact *in cis*. Duplicates are shown. Scale bar: 25 μm

### 5.1.8.3 Figure S3

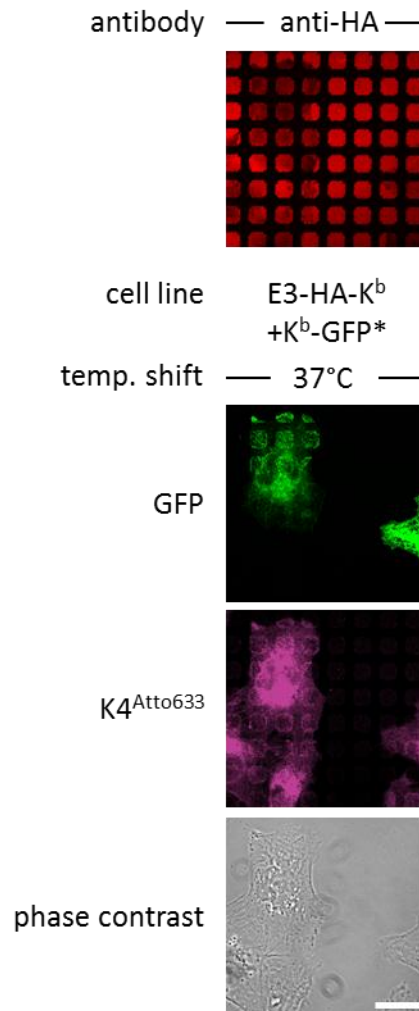


**Figure 5.1.8.3: Staining E3-HA-Kb with K4-peptide.** The stable cell line STF1/ E3-HA-K<sup>b</sup> was electroporated with K<sup>b</sup>-GFP and incubated overnight on anti-HA micropatterns and either left at 25 °C or shifted to 37 °C to induce cluster formation as described previously. Cells were then stained with the K4-Atto633 peptide, binding specifically to the E3-tag of the E3-HA-K<sup>b</sup> construct, which was captured by its HA-tag on the anti-HA micropatterns. Scale bar: 25 µm.

## 5.2 Additional Data

### 5.2.1 Co-expression and immunostaining of marker proteins to characterize captured K<sup>b</sup>-GFP

In order to characterize the captured protein population, I used conventional immunofluorescence staining approaches to identify the conformation of the captured K<sup>b</sup> protein population and also to identify candidate proteins that might be involved in – for example – MHC class I endocytosis. We assume that any protein interacting with MHC class I would naturally co-cluster with the captured K<sup>b</sup>-GFP and could thus be identified by immunostaining or the co-expression of known candidate proteins.

For co-expression experiments, we transiently transfected STF1/h $\beta_2$ m-2A-K<sup>b</sup> cells (without GFP) with the GFP-fusions of candidate interaction proteins and seeded them on anti-HA antibody micropatterns to test whether they would accumulate on the antibody pattern elements (see Montealegre et al., 2015 for reference of 2A sequence). In these experiments we followed the standard protocol for the capture assay. All tested candidate proteins are proposed to be involved in the endocytosis of MHC class I. We hypothesized that especially those proteins that are helping in the internalization of MHC class I might accumulate if their target proteins cannot be internalized due to their mechanical capture at the cell surface. Unfortunately, we were not able to identify any co-localization on the pattern elements; this was mostly due to failure of the transfection (see table 5.2.1)

Alternatively, I tried to immunostain endogenous proteins. In these approaches, I used antibody micropatterns, seeded STF1/K<sup>b</sup>-GFP cells on the patterns, incubated them at specific temperatures, and fixed them. For the stainings, I permeabilized the cells with 0.1% Triton X-100 (from AppliChem, Item No: A4975,0100) for 5 min at RT, washed them twice with PBS, and stained them with the indicated antibodies. Permeabilization is necessary in such staining experiments, because the staining antibodies do not have access underneath the cells if the cells are not permeabilized. Contrarily, the staining with peptides works without prior permeabilization (see figure 5.1.4.2), suggesting that only small molecules can reach underneath the cells. Due to permeabilization, intracellular proteins will also be stained in this experiment, leading to intracellular background signal, e.g. ER.

Table 5.2.1 lists all proteins that I have tested for co-localization experiments.

**Table 5.2.1: List of expression plasmids and antibodies for the identification of proposed MHC class I interaction partners.** Plasmids were used for transient co-transfections; and antibodies were used in immunostaining experiments.**Co-expression**

Protein	Plasmid	Involved in	Remarks
Arf6	Arf6-GFP	MHC class I endocytosis	Transient transfection did not work, only 1 trial
Dynamin	Dynamin-GFP	MHC class I endocytosis	Transient transfection did not work, only 1 trial
EHD-1	EHD 1-GFP	MHC class I endocytosis	No co-clustering observed, only 1 trial

**Co-stainings**

Antibody	Company	Target	concentrations/ dilutions
20-8-4S <sup>Atto542</sup>	purified from hybridoma supernatant	$\alpha 1$ domain ( $K^b/\beta_2m$ )	0.3 $\mu\text{g}/\mu\text{L}$
$\gamma 3^{\text{Atto542}}$	purified from hybridoma supernatant	$\alpha 2$ domain ( $K^b/\beta_2m$ )	0.3 $\mu\text{g}/\mu\text{L}$
W6/32 <sup>Atto542</sup>	purified from hybridoma supernatant	HLA-A/B/C	0.3 $\mu\text{g}/\mu\text{L}$
anti-Rab5	rb mAb to Rab5 from Cell Signaling C8B1	endogenous levels of total Rab5A protein. (human, mouse, rat, monkey)	1:400
anti-Rab4	rb pAb to Rab4 from Abcam ab13252	specific to Rab4 protein. No cross reactivity known. (mouse, rat, dog, human)	1:200

**Secondary antibodies**

gamAF488	polyclonal goat anti-mouse AF488 from Invitrogen Cat No A11001	mouse IgG (H+L)	1 $\mu\text{g}/\text{mL}$ (stock: 2mg/mL)
garAF488	polyclonal goat anti-rabbit AF488Invitrogen Cat No A11008	rabbit IgG (H+L)	4 $\mu\text{g}/\text{mL}$ (stock: 2mg/mL)
gamCy3	polyclonal goat anti-mouse Cy3 from Abcam ab97035	mouse IgG (H+L)	1 $\mu\text{g}/\text{mL}$ (stock: 0.5 mg/mL)

### 5.2.1.1 Staining with anti-class I antibodies

To identify which form of K<sup>b</sup> is captured on the patterns, I completed the experiments in figure 5.1.4.2 and stained the captured K<sup>b</sup>-molecules with several anti-MHC class I antibodies. In Figure 5.2.1.1 A, I seeded STF1/HA-K<sup>b</sup>-GFP cells on anti-HA antibody micropatterns, incubated them at 30 °C, and stained them with the K<sup>b</sup>-specific antibody 20-8-4S directly labeled with Atto542 (20-8-4S<sup>Atto542</sup>). The staining with the 20-8-4S antibody is rather weak and mostly in the ER. Partial co-localization can be observed in figure 5.2.1.1 A, column 1 and 2. Although we capture via the introduced HA tag, it is possible that the epitope for 20-8-4S is partially blocked by the capture antibody. However, the K<sup>b</sup> surface staining of cells seeded on glass (off pattern) is also very weak, suggesting that the 20-8-4S is generally a weak antibody in immunofluorescence stainings. This was also reported for other cell types such as 3T3 cells in our lab.

We used the same approach to test if all captured K<sup>b</sup>-GFP molecules bind in a 1:1 ratio to the antibodies in the pattern elements, or if they can also be indirectly recruited by already captured K<sup>b</sup>-GFP. The idea was to capture K<sup>b</sup>-GFP with Y3 antibody micropatterns and to stain them afterwards with Y3 to see how many free Y3 epitopes exists in the pattern elements, which will give an idea of how many K<sup>b</sup>-GFP molecules reacted directly with the antibody and how many are indirectly recruited to the pattern elements. In Figure 5.2.1.1 B, we patterned STF1/HA-K<sup>b</sup>-GFP with Y3 antibody micropatterns and stained them with Y3<sup>Atto542</sup>. Staining with Y3<sup>Atto542</sup> is homogenous throughout the cell, demonstrating that only a subpopulation of K<sup>b</sup>-GFP is captured on the antibody micropatterns as expected. Surprisingly, there is a strong signal of Y3<sup>Atto542</sup> on pattern elements outside the cells, which colocalizes with K<sup>b</sup>-GFP, suggesting that there is also indirect recruitment of K<sup>b</sup>-GFP to pattern elements. The simplest explanation for this observation is that the cell left membrane patches on the pattern elements which contain free K<sup>b</sup>-GFP molecules that were not captured by the antibody but remained fully folded due to the 26°C incubation and thus reacted with Y3<sup>Atto542</sup>.

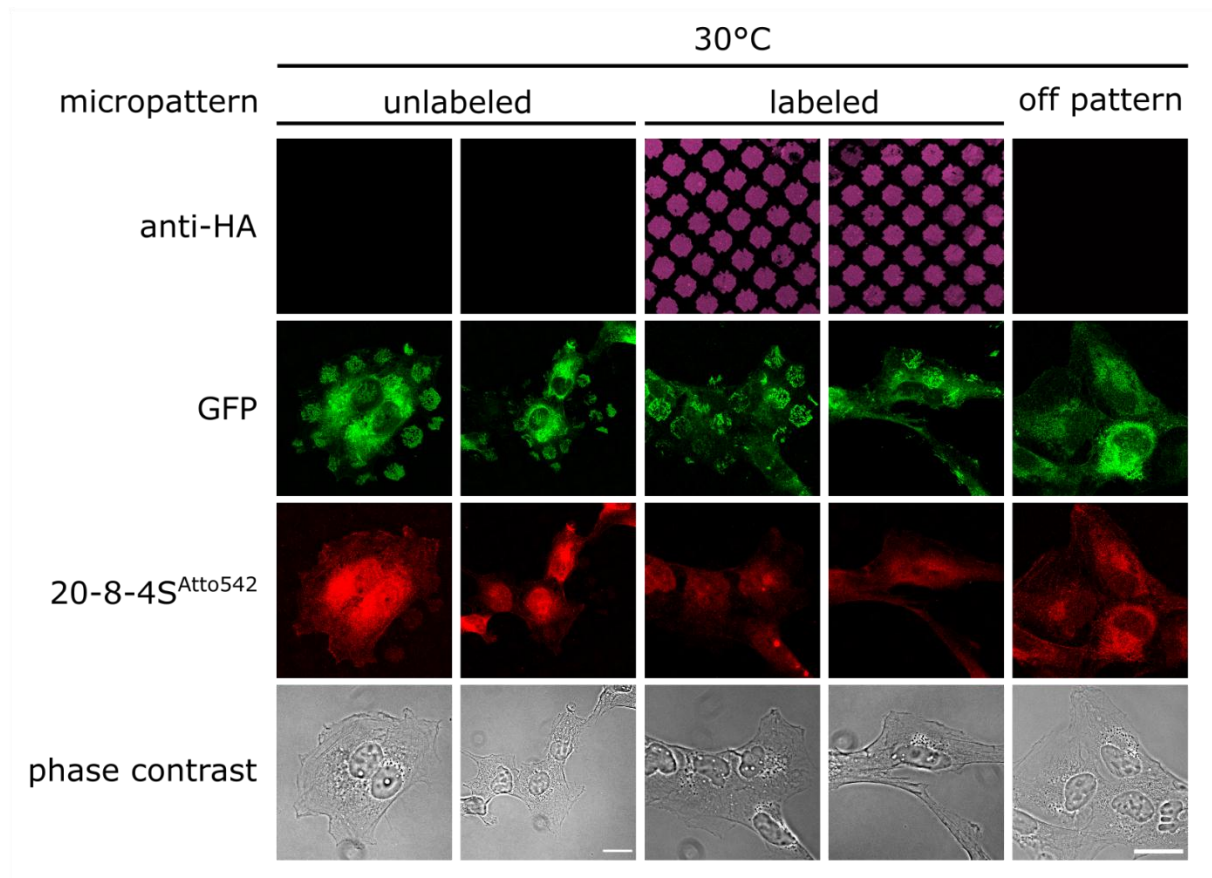


**Figure 5.2.1.1 A: Co-staining of captured HA-K<sup>b</sup>-GFP on anti-HA antibody micropatterns with 20-8-4S.** STF1/HA-K<sup>b</sup>-GFP were seeded on anti-HA antibody micropatterns (HA<sup>AF647</sup>, magenta; HA<sup>unlabeled</sup>, black) and incubated overnight at 30°C to capture sufficient amounts of HA-K<sup>b</sup>-GFP on the antibody pattern elements (green). Cells were then fixed, permeabilized and stained with labeled 20-8-4S<sup>Atto542</sup> (red). Bar, 25 µm.

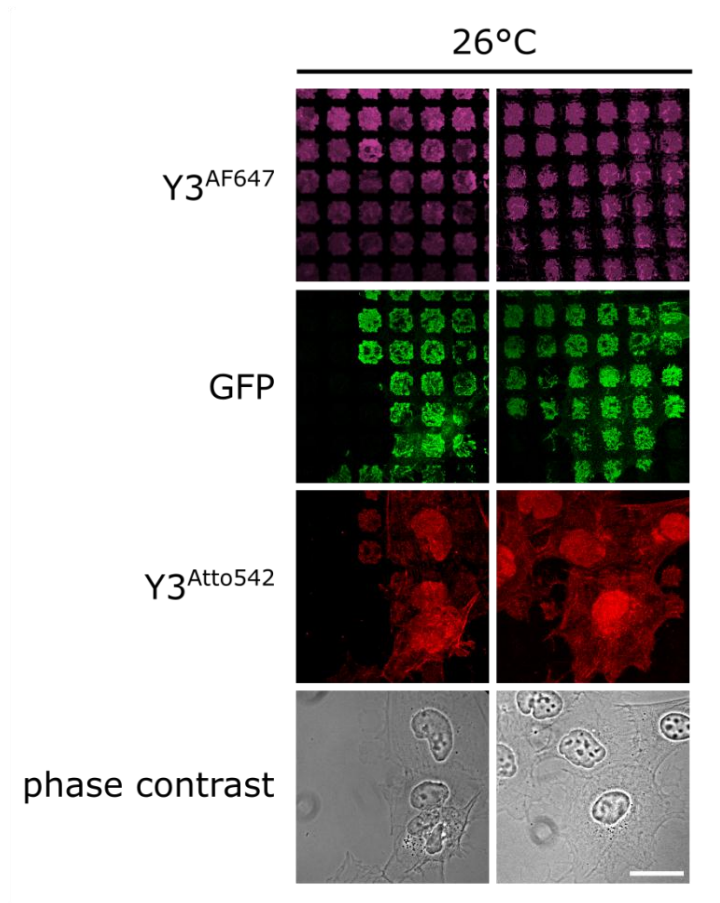


**Figure 5.2.1.1 B: Co-staining of captured HA-K<sup>b</sup>-GFP on Y3 antibody micropatterns with Y3.** STF1/HA-K<sup>b</sup>-GFP were seeded on Y3<sup>AF647</sup> antibody micropatterns (magenta) and incubated overnight at 26°C to capture sufficient amounts of HA-K<sup>b</sup>-GFP on the antibody pattern elements (green). Cells were then fixed, permeabilized and stained with labeled Y3<sup>Atto542</sup> (red). Bar, 25 µm.

We next wanted to test whether also endogenous human MHC class I molecules co-cluster with the captured K<sup>b</sup>-GFP. For this, we seeded STF1/HA-K<sup>b</sup>-GFP as previously and stained them afterwards with labeled antibody W6/32<sup>Atto542</sup> to stain the human MHC class I HLA-A, B and C. STF1 cells express endogenously the human allotypes HLA-A\*03:01 and HLA-B\*15:16 (personal communication with Zeynep Hein). In figure 5.2.1.1 C, the signal is rather weak and diffuse and we cannot detect any colocalization with the captured K<sup>b</sup>-GFP. For clear conclusions, the staining protocol for W6/32 needs to be optimized.

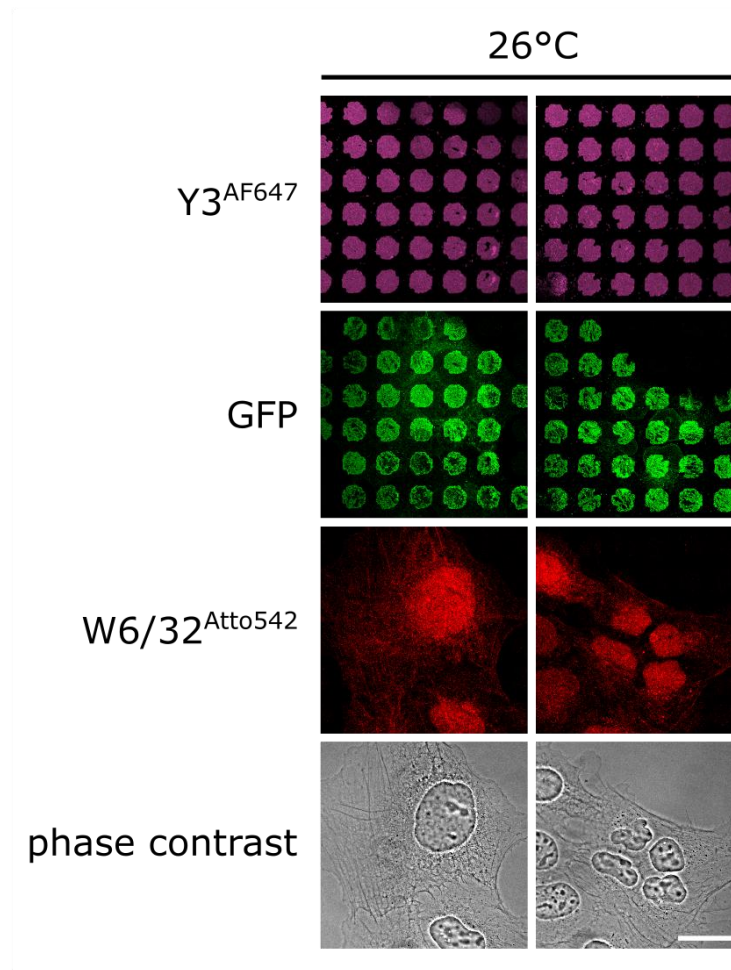


**Figure 5.2.1.1 C: Co-staining of captured HA-K<sup>b</sup>-GFP on Y3 antibody micropatterns with W6/32.** STF1/HA-K<sup>b</sup>-GFP were seeded on Y3<sup>AF647</sup> antibody micropatterns (magenta) and incubated overnight at 26°C to capture sufficient amounts of HA-K<sup>b</sup>-GFP on the antibody pattern elements (green). Cells were then fixed, permeabilized and stained with labeled W6/32<sup>Atto542</sup> (red). Bar, 25 µm.



### 5.2.1.2 Anti-Rab4 co-stainings

Since we capture proteins at the cell surface that are normally quickly internalized and degraded (Montealegre et al., 2015), we hypothesized that proteins of the endocytic machinery of the cell might accumulate at the sites of captured proteins, too. To test this, we repeated the co-staining experiments as described above but stained the samples for Rab proteins of the early endocytic pathway. The small GTPase Rab4 regulates the formation of recycling endosomes and is thus associated with early endosomes (Sönnichsen et al., 2000). In our experiments, we seeded STF1/K<sup>b</sup>-GFP cells on anti-HA<sup>AF647</sup> micropatterns and incubated at 37 °C for 48 hours to accumulate HA-K<sup>b</sup>-GFP at the cell surface (see figure 5.2.1.2). We prolonged the incubation time at 37 °C to 48 hours to enhance the amount of Rab proteins in these pattern elements. We hypothesized that Rab4 proteins will accumulate over time while trying to remove the “old” HA-K<sup>b</sup>-GFP captured in the antibody pattern elements. In figure 5.2.1.2, the staining of Rab4 is spread out throughout the cell and does not clearly colocalize with the pattern elements. I had the impression that the Rab4 staining looked a little bit like the antibody micropattern in a few cells, but the signal was generally too weak to draw a clear conclusion (see figure 5.2.1.2, white arrows). It is difficult to judge, whether the Rab 4 proteins did not interact with the captured HA-K<sup>b</sup>-GFP, or whether this is not visible with the strong cellular background. One could probably improve the experimental setup, such as increasing the amount of captured K<sup>b</sup>-GFP. Another option is to co-express a Rab4-GFP fusion protein with an unlabeled K<sup>b</sup> construct. With all drawbacks of Rab4 overexpression, this might represent a reasonable experiment to test whether there is any interaction at all between Rab4 and K<sup>b</sup> at the plasma membrane.

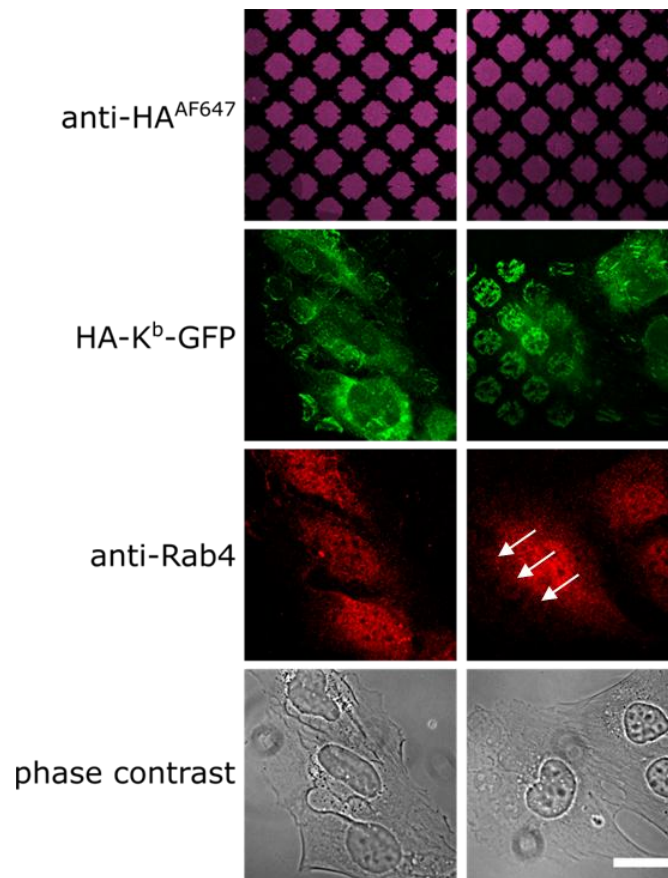


**Figure 5.2.1.2: Anti-Rab 4 co-stainings.** STF1/HA-K<sup>b</sup>-GFP were seeded on anti-HA<sup>AF647</sup> antibody micropatterns, shifted to 25°C overnight and incubated at 37°C for 48 hours. Cells were then fixed and permeabilized and stained with anti-Rab4 antibodies according to the standard protocol (red). Only very weak co-patterning of the Rab 4 signal was observed in individual cells (white arrows). Duplicates are shown. Bar, 25 µm

### 5.2.1.3 Anti-Rab 5 co-stainings

Similar to the Rab 4 stainings, we also stained our samples with an anti-Rab 5 antibody. Rab 5 also belongs to the group of small GTPases that are primarily localized to the early endosomes (Sönnichsen et al., 2000). Although the antibody staining seems to work well in our samples, we were also not able to find any colocalization between Rab 5 and K<sup>b</sup>-GFP or HA-K<sup>b</sup>-GFP, and thus the conclusions for the previous experiments with Rab 4 apply here also (see figure 5.2.1.3 A).

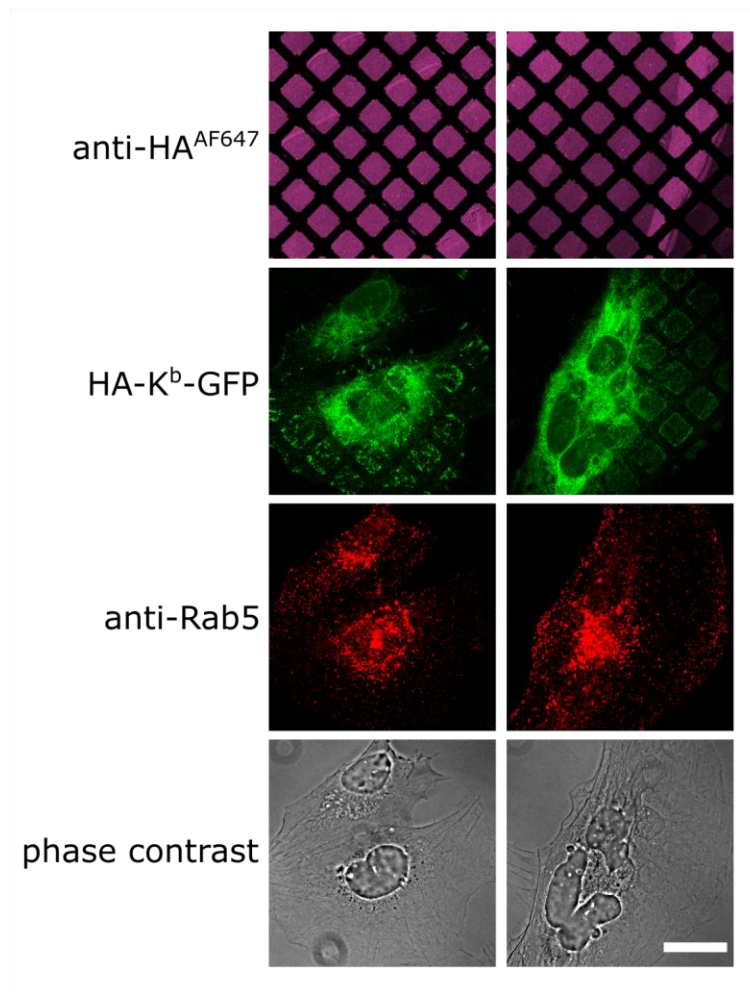


**Figure 5.2.1.3 A: Anti-Rab5 co-stainings on anti-HA antibody micropatterns.** STF1/HA-K<sup>b</sup>-GFP cells were seeded on anti-HA antibody micropatterns (magenta), shifted to 25°C overnight and incubated at 37°C for 48 hours. Cells were then fixed and permeabilized and stained with anti-Rab 5 antibodies according to the standard protocol (red). Duplicates are shown. Bar, 25 µm.

I also repeated the same Rab 5 co-staining experiment on Y3 antibody micropatterns (figure 5.2.1.3 B). In this experiment, I also compared cells that were growing on (columns 1 and 2) and off the antibody

micropatterns (columns 3 and 4). The Rab 5 staining were similar in both conditions and no co-localization with the antibody micropatterns was observed.

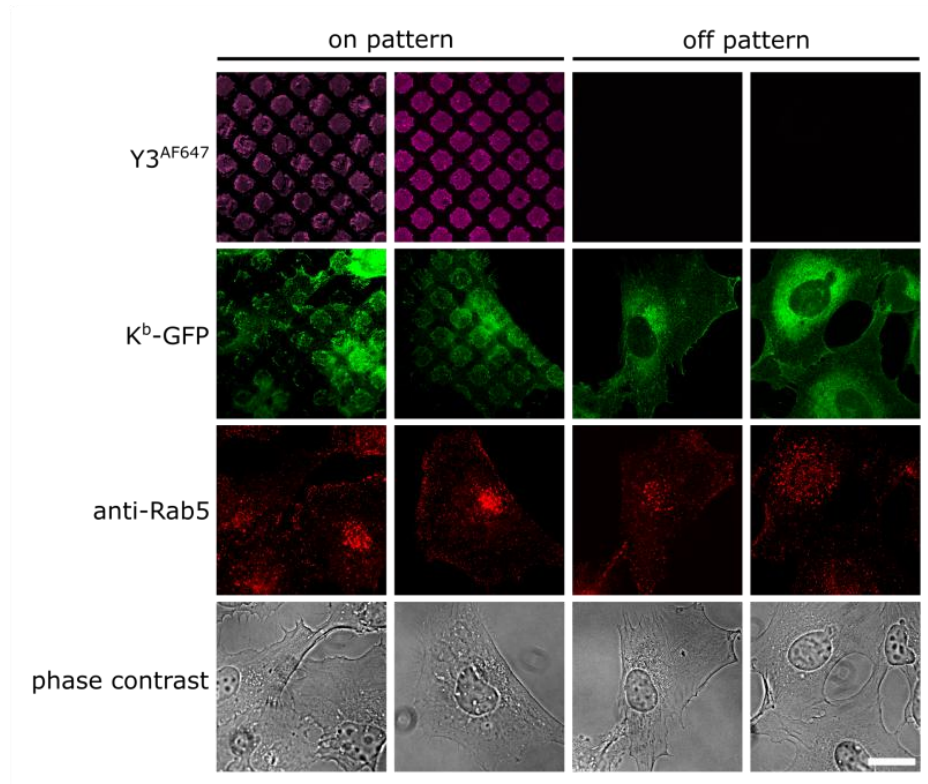


**Figure 5.2.1.3 B: Anti-Rab5 co-stainings on Y3 antibody micropatterns.** STF1/Kb-GFP cells were seeded on Y3 antibody micropatterns, shifted to 25°C overnight and incubated at 37°C for 48 hours. Cells were then fixed and permeabilized and stained with anti-Rab 5 antibodies according to the standard protocol (red). Duplicates are shown. Bar, 25  $\mu$ m

### 5.2.2 Allele specificity of MHC class I *in cis* interactions

After our findings of specific  $K^b$  *in cis* interactions in 5.1.4.3, we asked ourselves whether these interactions might represent a general mechanism of MHC class I molecules with a functional role such as a marker for endocytosis, or whether these interactions are only relevant for H-2K<sup>b</sup>. To figure out whether the *in cis* interactions are allotype-dependent, we repeated the experiments in section 5.1.4.3 and generated co-transduced STF1 cells with the following combinations of  $K^b$  and  $D^b$ : a) HA- $D^b$  +  $D^b$ -GFP, b) HA- $K^b$  +  $D^b$ -GFP, and c) HA- $D^b$  +  $K^b$ -GFP (see table 2.4 for reference). Micrographs of the experiments are shown in figure 5.2.2. The respective co-transduced cells were seeded on anti-HA micropatterns and, according to the protocol in 5.1.6, were either incubated at 25 °C or shifted to 37 °C to induce the dissociation of  $\beta_2m$  and thus the clustering of the murine MHC class I molecules. In our experiments, we observed heterotypic clustering of HA- $K^b$  +  $D^b$ -GFP at 37 °C but not at 25 °C to different extents as seen in figure 5.2.2. Compared to the  $K^b$ - $K^b$  clusters (see figure 5.1.4.3), the heterotypic interactions appear much weaker. In previous experiments, we have observed that the  $D^b$  affinity to  $\beta_2m$  is weaker than for  $K^b$  similar to the observations of others (Rock et al., 1991). Therefore, there might be in general less  $D^b$  than  $K^b$  at the cell surface (this has to our knowledge not been measured), which may cause the decreased levels of  $K^b$ - $D^b$ -pairs.

For  $D^b$ - $D^b$  homotypic interactions, we observed clustering at 37 °C, but only outside cells or in one sample where the cells were seeded very thinly (i.e., where cells did not have any contact to neighboring cells) (data not shown).

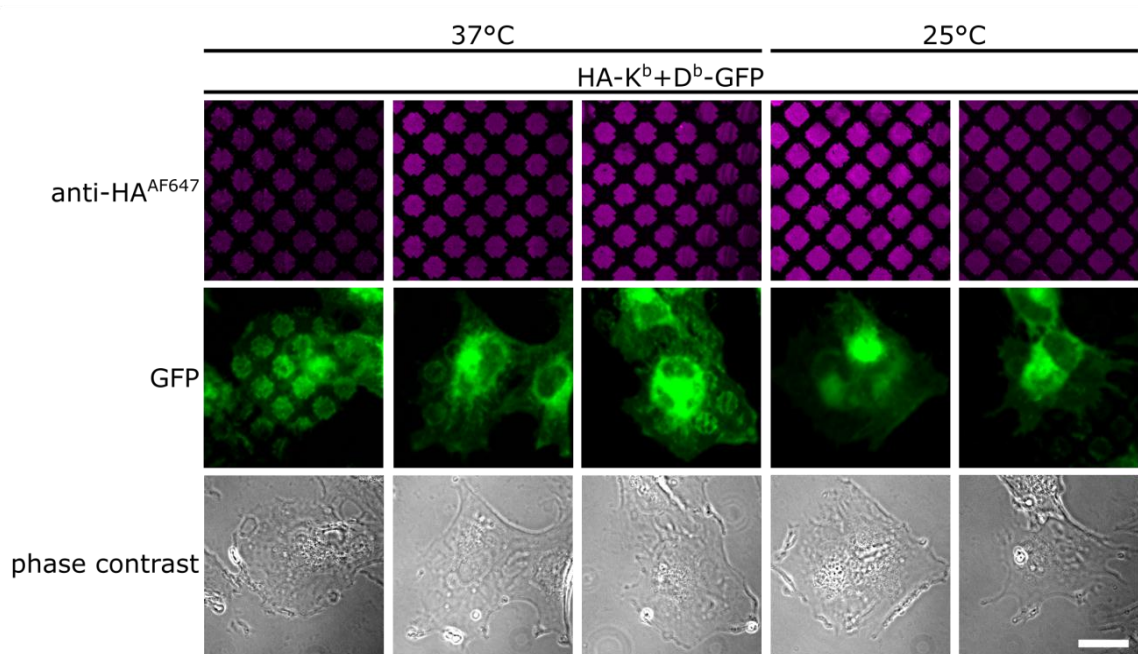


**Figure 5.2.2: Heterotypic *in cis* interactions of  $K^b$  and  $D^b$ .** STF1/HA- $K^b+D^b$ -GFP (stable cell line, selected with puromycin) were seeded on anti-HA antibody micropatterns (anti-HA<sup>AF647</sup>, magenta) and incubated overnight at 25°C to accumulate MHC class I surface levels. Cells were then shifted to 37°C or left at 25°C as control to induce clustering (green). Bar, 25  $\mu$ m. This experiment was designed by me and performed by Catherine Jacob-Dolan.

## 5.3 Further discussions

### 5.3.1 Localization of MHC class I clusters

If the clustering occurs specifically with free heavy chains, the question remains why MHC class I does not form aggregates in the ER during protein synthesis. A possible explanation is that the chaperones in the ER, especially calnexin and BiP (Cresswell et al., 1994; Margolese et al., 1993; Nössner and Parham, 1995), prevent the formation of clusters by binding to the free heavy chains and only release properly folded and peptide loaded MHC class I into the secretory pathway. With our approach, we can only detect MHC class I cluster formation at the cell surface, and thus cannot formally show that cluster do not form in other compartments of the cells.

### 5.3.2 General ideas and remarks on MHC class I clusters

#### 5.3.2.1 MHC class I expression levels

While performing the cluster experiments, I observed that the levels of MHC class I clusters varied between single cells. After doing many repeats, I am certain that the levels of clustered MHC class I correlate directly with the expression levels of the individual cells. Although I mainly worked with transduced and selected cell lines, the expression levels vary between individual cells. From my experience I conclude that the overall expression levels as well as the ratio of the two transduced constructs play an important role. In microscopy, I can usually only judge the expression level of the GFP-fusion construct and it is very clear that neither the very bright overexpressing cells, nor the very dim cells with very little GFP expression form clusters. The pattern is generally best in cells that have a moderate GFP expression. When I stained the co-transduced cells in flow cytometry for HA, I observed that the expression of the HA-fusion construct correlates with the GFP expression (data not shown). In agreement with this observation, I conclude that a moderate expression level of both fusion constructs is the best condition for clustering experiments.

In our system, MHC class I surface levels also depend on the availability of  $\beta_2m$  inside the cells. Due to the overexpression of two  $K^b$  heavy chain fusion constructs in cells that already have endogenous human MHC class I molecules with higher affinity to  $\beta_2m$  (Hein et al., 2014),  $\beta_2m$  might be the limiting factor and  $K^b$  might get stuck in the ER as free heavy chain. To overcome this limitation, we co-transduced cells with a plasmid containing a 2A ribosomal skipping sequence, where the  $K^b$  heavy chain and  $\beta_2m$  are expressed

in a 1:1 ratio from the same plasmid (Montealegre et al., 2015). In these cells, the surface levels are enhanced, and K<sup>b</sup>-K<sup>b</sup> clusters are forming much better (see figure S2 in 5.1.8 for reference).

Interestingly, we have also found that cell confluency influences cluster formation in cells. We saw enhanced clustering in sparsely seeded cells, whereas we almost never observed clustering in confluent samples. This may be because during the cell cycle, expression of some proteins required for class I surface transport and/or maturation might change, and thus amounts and/or forms of class I at the cell surfaces might be different. Importantly, these observations were not studied in great detail, but I generally advise to seed enough cells such that they have cell-cell contact but do not overgrow on the antibody micropatterns to form fully confluent cell sheets, as recommended in section 2.3.1

Since the clustering effect relies on the expression levels of the two MHC class I fusion constructs, it is difficult to analyze the assay in a quantitative fashion and can so far only be a qualitative measure. To overcome this limitation, one would have to sort the cells with defined fluorescence intensity. Another option is to optimize the assay with inducible or tunable promoters to adjust the expression levels.

### 5.3.2.2 Mechanism of cluster formation

Our observations of MHC class I cluster formation raise the questions of what these clusters look like in molecular terms, and especially how big they are. One might speculate about two extreme scenarios. In the first scenario, the clusters are homodimers that are formed in a structure-dependent fashion between two MHC class I free heavy chains. Here, one can speculate that the free heavy chains are not completely unfolded and that the partially unfolded molecules are required to form the dimers, possibly due to steric hindrance of the completely folded molecules. Alternatively, conformational changes or specific residues might be involved in the formation of the clusters such as the proposed roles of cysteines in the cytoplasmic tails as discussed in sections 1.4.7.2 and 7.1.1.

In the other extreme scenario, the clusters are large aggregates of unfolded proteins that form unspecifically and do not involve any defined protein sequences or folded protein structures. Here, one would expect that the clusters form due to the complete unfolding of the proteins, thus generating a big chunk of clustered proteins. Of course, intermediate or mixed cluster formation mechanisms between the two extremes are also possible.

The mechanisms of cluster formation and the structure of the clusters are not easy to investigate. One option is to mutagenize the class I heavy chain, for example by removal of the cysteines or by domain swap between allotypes or with other proteins, such as CD4.



## 6 Additional results and discussion on pattern fabrication

### 6.1 Patterns from the KIT

In trial experiments, we tried in collaboration with the Rapp group at the Karlsruhe Institute of Technology (KIT) to produce antibody micropatterns with their novel maskless photolithography technique (Waldbaur et al., 2012). In their approach, they use fluorescein-labeled biotin to induce photoactivated radical chemistry crosslinks in defined patterns between BSA, which is spread uniformly on a surface, and a protein of interest.

For our first trial experiment with maskless photolithography, we wanted to test whether we can generate protein micropatterns similar to those that we generally print with our PDMS stamps. To test this, we immobilized biotin on the surface and stained it with labeled streptavidin (streptavidin-Cy3). Although the micropatterns in the micrograph are blurry, we are indeed able to fabricate micropatterns with the same dimensions with this method (see figure 6.1 A).

In another experiment, we performed the same procedure but used unlabeled Y3 antibody instead of biotin. To detect the immobilized Y3 antibody, we stained it with a labeled secondary antibody (g $\alpha$ m-AF488). As seen in the micrograph in figure 6.1 B, the antibody was successfully immobilized and can be detected with a fluorescent secondary antibody. We conclude that we were able to produce antibody micropatterns with maskless photolithography, but they were not very defined and appeared blurry in the micrographs. This might be optimized during the fabrication process, when the focus is better adjusted, in order to achieve a clear and defined transfer of the pattern to the surface.

It remains to be tested whether the antibody micropatterns are functional when generated with maskless photolithography. For this, one needs to seed cells on the antibody micropatterns and check for the successful capture of MHC I proteins. We have performed one trial experiment, where we used protein A micropatterns that were also fabricated by maskless lithography and loaded them with labeled Y3<sup>AF647</sup>. We then seeded STF1/HA-K<sup>b</sup>-GFP cells on this pattern (see figure 6.1 C). Although the antibody did bind to the immobilized protein A, no protein capture was observed. This trial experiment demonstrates that the concentration of antibody needs to be further optimized, since the excess antibody was binding to the STF1/HA-K<sup>b</sup>-GFP at the cell surface. According to this observation, the proteins are not available for protein capture since they have already bound the antibody from the solution.

Once we have demonstrated that these micropatterns are functional, we can start to test other micropatterns. In principle, the technique enables the transfer of any grayscale image to the glass surface and thus also to achieve detailed protein micropatterns that even vary in their concentrations (i.e., protein densities on the surface).

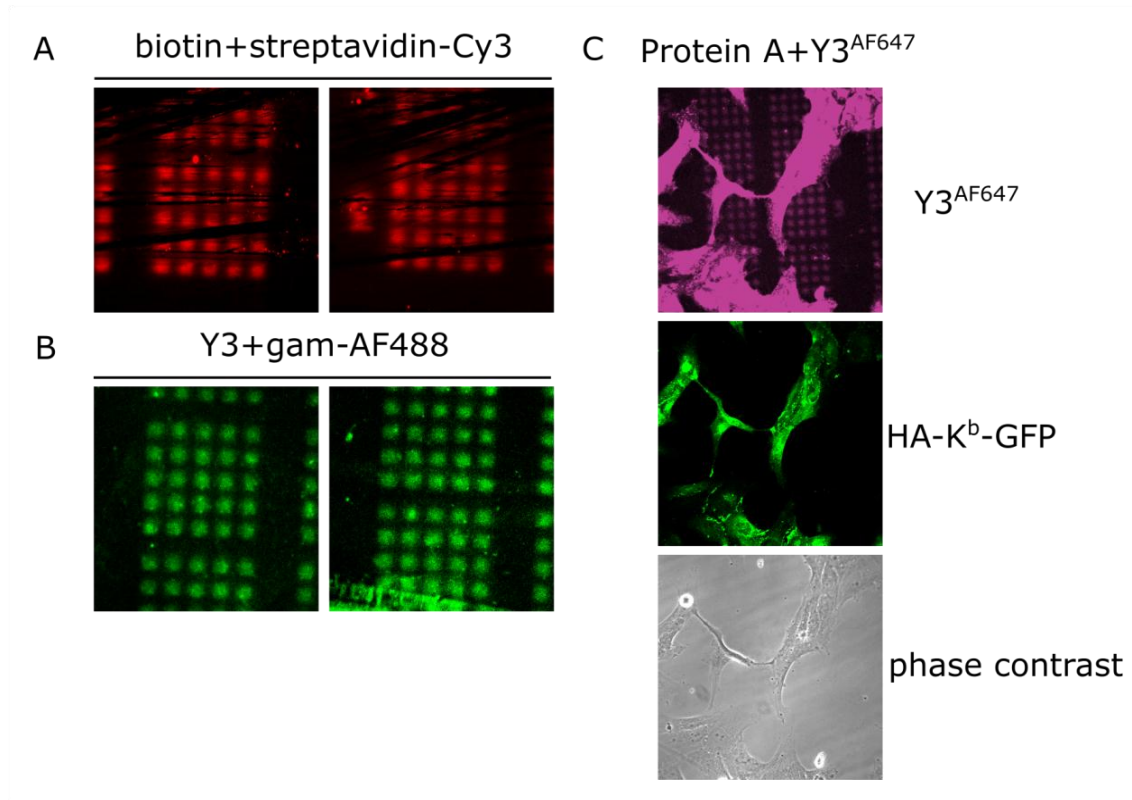


**Figure 6.1: Trial experiments with alternative protein micropatterns.** The pattern elements (squares) have a diameter of 10 $\mu$ m and 5  $\mu$ m interspaces according to the pattern that we fabricate with PDMS stamos. **(A)** Biotin-5 fluorescein was immobilized via the maskless lithography technique from KIT. The fluorescein is bleached during the fabrication process. The immobilized biotin pattern was then stained with labeled streptavidin (streptavidin-Cy3, red) and imaged with the cLSM. **(B)** unlabeled Y3 was immobilized with the same strategy and was then labeled with a fluorescent secondary antibody (gam-AF488, green). **(C)** Protein A patterns were first loaded with fluorescent Y3<sup>AF647</sup> (magenta) and then STF1/HA-K<sup>b</sup>-GFP cells were seeded onto these patterns and incubated according to the standard protocol.

## 7 Future perspectives

In this chapter, I will give brief ideas and comments on how I propose to proceed with this project based on the current findings. The first part of this chapter deals with future investigation of the clusters and speculations about their functional role.

In the second part, I propose possible future developments of the antibody micropatterns to study MHC class I dynamics.

The third part of this chapter focuses on the investigation of possible interaction partners and the development of an open screen for the discovery of interaction partners.

The last part of this chapter discusses possible technical developments of the established antibody patterns such as induced capture or the release of captured protein populations from the antibody micropatterns. The last section provides ideas about the adaptation of our assay towards a T cell screening tool.

### 7.1 Further investigations of MHC class I clusters

#### 7.1.1 Role of cysteines in the cytoplasmic tail

Previous work of Zuñiga and coworkers has also shown the presence of MHC class I dimers (referred to as clusters in the following) by co-immunoprecipitation experiments (see section 1.4.7.2). Analysis of the detected dimers revealed that they consist of MHC class I free heavy chains. In their work, the authors focus on the MHC class I allotype H-2L<sup>d</sup> (L<sup>d</sup>) and hypothesize that the unpaired cysteines in the cytoplasmic tail of L<sup>d</sup> are responsible for the formation of disulfide bonds that link the MHC class I free heavy chains together. Mutagenesis studies finally identified Cys 340 as the responsible disulfide linkage for L<sup>d</sup> dimers. (Capps et al., 1993)

Interestingly, the unpaired cysteines are conserved among the murine and human MHC class I protein family – with the exception of H-2K<sup>d</sup> – as shown in table 7.1.1; this supports the hypothesis that all MHC class I proteins share this feature as part of a common molecular mechanism to form clusters. To test whether the free cysteines play a general role in MHC class I cluster formation, I suggest performing analogous mutagenesis experiments to the described L<sup>d</sup> mutants with the allotypes used in our studies, K<sup>b</sup> and D<sup>b</sup>. For first trial experiments, simple alanine or serine substitution experiments are probably sufficient. I would try the simplest approach and mutate only one construct, e.g. K<sup>b</sup>-GFP, and transfect

stable STF1/HA-K<sup>b</sup> cells with this K<sup>b</sup>-GFP mutant and seed them onto HA antibody micropatterns according to the standard clustering protocol. According to the hypothesis, one would expect that clustering is abolished in these cells, since the disulfide bond cannot be formed between the two constructs.

**Table 7.1.1: Amino acid sequence of the cytoplasmic tails of human and murine MHC class I.** Amino acid sequence of the cytoplasmic tails in the single letter amino acid code. The glycine that in H-2K<sup>d</sup> substitutes the conserved cysteine is shown in bold. Numbers refer to the aligned sequences and do not represent the residues of the amino acid sequences of the individual proteins. From: Springer lab Wiki.

murine class I								
Residue nr.					330		345	
H-2K <sup>b</sup>	KM	RRRNT	GGKGG	DYALA	--PGS	-QTSD	LSLPD	CKVMV HDPHS LA
H-2K <sup>d</sup>	KM	RR-NT	GGKGV	NYALA	--PGS	-QTSD	LSLPD	<b>G</b> KVMV HDPHS LA
H-2K <sup>k</sup>	VMKM	RRRNT	GGKGG	DYALA	--PGS	-QTSD	LSLPD	CKVMV HDPHS LA
H-2D <sup>b</sup>	K-	RRRNT	GGKGG	DYALA	--PGS	-QSSE	MSLRD	CKA
H-2D <sup>d</sup>	K-	RRRNT	GGKGG	DYALA	--PGS	-QSSD	MSLPD	CKV
H-2D <sup>k</sup>	VM-M	MRRNT	GGKGG	DYTLT	--PGS	-QSSE	MSLPD	CKA
H-2L <sup>d</sup>	VMK-	RRRNT	GGKGG	DYALA	--PGS	-QSSE	MSLRD	CKA

human class I								
HLA-A26		RRKSS	DRKGG	SYSQA	ASSDS	AQGSD	MSLTA	CKV
HLA-A*0209	MW	RRKSS	DRKGG	SYSQA	ASDDS	AQGSD	VSLTA	CKV
HLA-B	MC	RRKSS	GGKGG	SYSQA	ACSDS	AQGSD	VSTA	
HLA-C	MC	RRKSS	GGKGG	SCSQA	ASSNS	AQGSD	ESLIA	CKA
HLA-E	IW	RKKSS	GGKGG	SYSQA	EWSDS	AQGSE	SHSL	
HLA-F	MW	RKKSS	DRNRG	SYSQA	AVTDS	AQGS	VSLTA	NKV
HLA-G	LW	RKKSS	D					

If we find that cysteines also play a role in K<sup>b</sup> and D<sup>b</sup> clusters, the hypothesis of a general mechanism is supported, and a functional role – for example in the rapid endocytosis from the cell surface – will be further investigated.

To elucidate the molecular mechanism, one has to consider our own and also Zuñiga's observations that only free heavy chains cluster and that the dissociation of  $\beta_2m$  plays an important role. Here, the presence of unpaired cysteines in the cytoplasmic tail alone is not sufficient for cluster formation. Either, the cysteines can only form a disulfide bond if also the extracellular domains of the class I molecules interact; or, the dissociation of  $\beta_2m$  initiates a conformational change or switch in the cytoplasmic tail that brings the two cysteines in close contact to form the disulfide linkage. The complex correlation of  $\beta_2m$  dissociation and disulfide linkage will be addressed once we have found indications for a general mechanism.

Our finding of heterotypic *in cis* interactions between K<sup>b</sup> and D<sup>b</sup> (see 5.2.2) represents indirect evidence for a general mechanism, since both allotypes have the conserved cysteine residues that can form a disulfide bond (see table 7.1.1).

### 7.1.2 Functional analysis of cluster formation

While I would like to figure out how the MHC class I clusters are formed, I am also curious to find out what the function of MHC class I clusters might be. For such a functional analysis, I suggest starting with a screen of diverse MHC class I allotypes to obtain an overview of the significance of the observed phenomenon.

Similar to us, Zuñiga and coworkers also found that MHC class I clusters are allotype-dependent, i.e., they found that L<sup>d</sup> and D<sup>b</sup> cluster better than other mouse MHC class I in their experiments. In our own experiments, we found that K<sup>b</sup> clusters better than D<sup>b</sup> (see 5.2.2). Zuñiga and coworkers also suggested that the observed allotype dependency of cluster formation correlates with MHC class I-associated disorders (see discussion in 5.1.5).

To find such a correlation, one has to screen murine and human MHC class I allotypes for their ability to form clusters. Antibody micropatterns are a suitable tool for such a screening approach, since they are easy and quick to fabricate. The only drawback at the moment is the read-out of single cells in the LSM. But the system is in principle adaptable to a read-out in a fluorescence scanner. With this, a broad analysis could be realized soon. In order to screen a library of different MHC class I allotypes, one has to clone the respective tagged MHC class I proteins. For each allotype one needs two constructs, one with the extracellular HA tag and a second with a GFP fusion at the cytoplasmic tail. Transient co-transfection should be sufficient for a first screen, especially if the read-out is accelerated by an automatic fluorescence scanner.

Once we have an overview of different cluster abilities, we will first correlate these data with disease-associated MHC class I molecules. This will give first indications towards a functional role of the clusters.

## 7.2 Testing the dynamics of MHC class I capture and clusters

In this section, I would like to suggest ways to figure out what happens on the molecular level. How fast are the clusters internalized? Is the endocytic machinery specifically targeting clusters or is this just a matter of size or membrane curvature?

The established system can so far only give a qualitative measurement of MHC class I capture or protein-protein interactions. As of now, we can only see that MHC class I proteins are being captured over a period of time. It is not yet possible to investigate protein dynamics or protein interaction ratios, which will give valuable information about the nature of MHC class I clusters.

The established antibody micropattern system can be easily modified for the analysis of dynamics with a modified read-out. This can be achieved with a better microscopic setup – such as super-resolution microscopy – that allows for temporal and spatial resolution of single molecules or a method called fluorescence recovery after photobleaching (FRAP; see 7.2.1). Another option to improve resolution is electron microscopy or the modification of antibody micropatterns into a single-antibody pattern (7.2.3).

All ideas and their potential applications for the detailed study of MHC class I protein dynamics are being discussed in the following.

### **7.2.1 Analysis of capture dynamics with FRAP**

We have shown that the antibody micropatterns can in principle be combined with live-cell microscopy to measure protein dynamics or peptide binding constants (see 4.1). An interesting question that arose from the detection of capture of MHC class I proteins into antibody pattern elements is whether the capture is dynamic or not. We would like to find out in particular whether the  $K^b$ -GFP fusion constructs are permanently trapped in the antibody pattern elements or if they can exchange with free  $K^b$ -GFP.

To address this question, the antibody micropatterns can be combined with live-cell microscopy and fluorescence recovery after photobleaching (FRAP). FRAP is a common technique to investigate protein dynamics that can be used in living cells. In a typical FRAP experiment, fluorescently labeled proteins are used. Then, a defined area of the sample is bleached, and the recovery of the fluorescence signal is measured; this allows the measurement of the diffusion constant of the fluorescently labeled proteins as they diffuse back into the bleached area.

In such an experiment, I would capture the  $K^b$ -GFP protein according to the standard protocol. Then I would bleach the area of a pattern element and wait for re-occurrence of the GFP signal in the bleached area. If the clusters are indeed dynamic, the GFP signal will re-occur due to the recruitment of new GFP fusion proteins into the antibody pattern elements. If the pattern elements remain dark, the clusters are static structures, without any exchange of molecules. This experiment will also demonstrate whether the captured  $K^b$ -GFP reaches the pattern elements by lateral diffusion in the plasma membrane or by the internal secretory pathway.

One drawback of this experiment is that the degree of saturation of the antibodies in the pattern elements is not known, which could lead to false positive results. This means that the re-occurring  $K^b$ -GFP molecules might also bind to antibodies in the pattern elements that were not occupied before, while the bleached  $K^b$ -GFP proteins remain bound to their antibodies but are now invisible. Thus, the re-occurrence of the GFP signal would show not dynamic capture but only the stepwise saturation of the antigen-binding sites. One could solve this problem by doing multiple rounds of bleaching to estimate when the pattern elements are saturated with  $K^b$ -GFP and then do the measurement. An alternative option is to play with the concentrations of the pattern elements to find a range in which the saturation can be achieved. I believe that these parameters can only be figured out by performing several trial experiments.

### 7.2.2 Class I interaction dynamics

Also exiting is the question whether the found clusters are static or dynamic, or if there is protein exchange into and out of the clusters. This would tell us a lot about the molecular mechanism of the clusters, and about their possible functional roles. According to our current favorite hypothesis – namely that cluster formation regulates the removal of defect MHC class I molecules – it is interesting to figure out if such clustered MHC class I proteins are moved to lysosomes to become terminally degraded, or if there is a way of return from their fate, perhaps by re-binding  $\beta_2m$  and peptide in some internal compartment (Montealegre et al., 2015). This question actually remained open for a long period of time in the field of MHC class I endocytosis.

Experiments in our lab have shown that free heavy chains are rather unstable as they do not fold and then precipitate in *in vitro* refolding experiments. This observation supports the idea that the clusters observed in cells by patterning are also some sort of terminally unfolded protein aggregates that are then destroyed. In contrast, mass spectrometry experiments of our collaborators have recently shown that free heavy chains that are generated by dissociation of  $\beta_2m$  are stable enough in solution to re-bind  $\beta_2m$  and peptide after a few minutes, albeit inefficiently (Sebastian Springer, personal communication). This suggests that the free heavy chains have some structure left and that they might undergo specific interactions. That latter hypothesis supports a scenario in which  $K^b$ -GFP binds to the captured HA- $K^b$ , dissociates, and then binds to the next captured HA- $K^b$  on the pattern element.

To test for both alternatives, one would perform the same experiment described in 7.2.1 but use the co-transfected cell lines. After the  $K^b$ -GFP is captured into the antibody pattern elements, I would again

bleach the GFP signal in individual pattern elements and measure the fluorescence recovery in the bleached area. The interpretation of the re-occurrence of the GFP signal is complicated though, since the saturation problem described above also applies here. It is possible that the K<sup>b</sup>-GFP proteins that re-appear in the bleached areas are not binding to the same captured HA-K<sup>b</sup> proteins, but that these are still occupied with the bleached K<sup>b</sup>-GFP proteins. Thus, to find out whether the binding of K<sup>b</sup>-GFP to HA-K<sup>b</sup> is reversible, one has to use other methods such as single molecule tracking.

Although the FRAP experiments cannot give valuable information about the reversibility of the protein-protein interactions, it will still determine the on rates of the protein-protein interactions. This becomes especially interesting once we can correlate the cluster formation to the dissociation of  $\beta_2m$  by a coordinated approach.

### 7.2.3 Single antibody patterns

As pointed out in the previous paragraph, I am interested to figure out whether the *in cis* interactions are reversible or if the K<sup>b</sup>-GFP is terminally trapped. This is interesting in terms of MHC class I endocytosis, but is also potentially interesting for the general investigations of protein-protein interactions in live cells beyond MHC class I proteins.

To find out specifically how many proteins are interacting in the clusters, one could develop our antibody micropatterns into a single-molecule setup. Instead of printing micropatterns with pattern elements in the micrometer range, one could make patterns with only one single antibody per spot. Several groups are currently working on approaches to generate such single protein patterns. Consequently, such a system also requires a read-out by super-resolution microscopy.

If we would generate a pattern where one antibody interacts with only one MHC class I protein, one could specifically determine how many K<sup>b</sup>-GFP proteins are recruited and characterize protein:protein interaction ratios. This system would further solve the question of the reversibility of the protein-protein interaction by following the K<sup>b</sup>-GFP signal over time. Since free heavy chains of MHC class I are not stable, alternative approaches such as surface plasmon resonance cannot be applied here (see section 1.4.9), and I am confident that antibody micropatterns will help to solve such questions.



### 7.2.4 Electron microscopy of antibody micropatterns

Electron microscopy offers an alternative approach to the above described ideas that involve mostly super-resolution microscopy techniques. To answer the question of protein:protein interaction ratios, it is possible to stain the captured antibodies with secondary antibodies that are coupled to gold nanoparticles and allow for the detection of single proteins. For characterization of the clusters, one could use a goat anti-mouse antibody to detect the printed HA antibodies and co-stain the GFP tag of the recruited K<sup>b</sup>-GFP. Although this approach is rather indirect, one could correlate how many GFP-tagged proteins are interacting with the printed HA-antibodies and obtain an estimate of the protein ratios.

## 7.3 Interaction partners of MHC class I proteins

### 7.3.1 Probing other proposed candidates for *in cis* interactions with MHC class I

The established assay (see section 5.1) can now be used to test for the interaction of other protein candidates that are proposed to interact with MHC class I. This is similar to the antibody staining experiments in paragraph 5.2.1. There are interactions mentioned in the literature, but they have not been intensively studied (see sections 1.4.6 and 1.4.7 for reference). One of these examples is the interaction of MHC class I and the insulin receptor. In the work of Dixon–Salazar, the question was also raised whether the proposed interaction between MHC class I and the insulin receptor in the brain is actually *in cis* or *in trans*. This question can be clearly answered by the use of antibody micropatterns.

### 7.3.2 Development of an open screen

Besides the screening of proposed protein interaction candidates mentioned in the previous paragraph (see section 7.3.1), it is also possible to develop the assay further into an open screen method to detect unknown protein interaction partners. In the proposed screen, the antibody micropatterns are used as described previously to accumulate MHC class I proteins on the pattern elements. Any interaction partners of MHC class I are likely to accumulate on the same pattern elements, together with the captured MHC class I. For the identification of the interaction partners, imaging MALDI (matrix-assisted laser desorption/ionization) mass spectrometry might be used (Passarelli and Ewing, 2013). By scanning over the pattern elements, one can compare and analyze the proteins on and off the pattern elements. With a colleague at the MALDI imaging core facility at Bremen University, I did one trial experiment, and we realized that the limiting factor of this methodology is the cell volume. In our test experiment, the beam cannot penetrate through the entire cell to ionize the bottom area of the cell, where the proteins have been patterned. To overcome this limitation, one has to reduce the volume by ripping the cell off the surface, for example with a nitrocellulose membrane, and then scan only the membrane and proteins at the basal membrane of the cell. This would also decrease background signals. Since all individual steps of this experiment are established, it should be possible to optimize the procedures and develop this new application. Alternatively, one might treat the pattern with a detergent to remove the cell and the membranes, and to just leave the patterned proteins and their direct interaction partners on the surface. Patterns might need to be slightly larger since the resolution of imaging MALDI is currently about 50  $\mu\text{m}$ .

## 7.4 Possible technical developments

One drawback of our established anti-MHC class I capture assay is that it does not allow for a time-coordinated capture of the MHC class I molecules. The capture of proteins occurs immediately as soon as the cells settle down on the micropatterns, and proteins will then accumulate on the antibody micropatterns throughout the incubation. Throughout the project, I generated several ideas for advanced applications of the antibody micropatterns that require technical developments that are described in the following. These include ideas for induced capture or the release of captured proteins to synchronize the internalization.

### 7.4.1 Antibody micropatterns for induced capture

While I required high amounts of captured proteins for our current applications such as peptide binding (see section 4.1) or the investigation of *in cis* interactions (see section 5.1), potential applications exist where one would wish to control the amounts of captured proteins or to synchronize the capture. This way, one could precisely target a specific protein cohort at a specific time point and presumably capture a rather homogenous protein population, which might give more control over manipulation experiments.

One example for such an inducible system is the unsuccessful trial experiment with the 25.D1.16 antibody, where I was aiming to start the capture of MHC class I trimers by the addition of peptide to peptide-deficient STF1 cells (see section 4.2.2 for reference).

Similar switchable setups might be realized with special engineered antibodies that bind their antigen only when they are switched on by an externally added molecule. Kellmann and coworkers developed antibody single-chain variable fragments (scFvs) with an allosteric regulator that changes the antigen binding affinity (Kellmann et al., 2017). In their work, they show that the introduction of calmodulin-derived linkers between the two variable domains ( $V_L$  and  $V_H$ ) of the scFv induces a conformational change that influences antigen binding by an allosteric mechanism. Upon addition of calcium and a calmodulin-binding peptide, a structural change or displacement of the  $V_L$  and  $V_H$  domains in the scFv occurs that renders the antigen binding affinity effective. These engineered antibodies are commercially available at Yumab (Germany)<sup>19</sup> and should be tested for printing for the design of switchable antibody micropatterns.

### 7.4.2 Release of captured proteins from antibody micropatterns

In addition to the induced capture of proteins, the release of captured proteins on antibody micropatterns might be of even greater interest. The study of endocytosis of MHC class I molecules in our laboratory has encountered a broad range of technical difficulties. One of them is the strong intracellular background in microscopy. The other is that MHC class I molecules are not easily to follow in the endocytic pathway, since the transitions from the different compartments are indistinct.

---

<sup>19</sup> <http://yumab.com/>

The specific labeling of a protein cohort and its controlled release from the mechanical retention at the cell surface might finally circumvent these difficulties. Also, the functional investigation of the clusters would directly benefit from such a system. I have collected several ideas of how one can realize antibody micropatterns that will allow for controlled release, and I will describe them in the following.

### 7.4.2.1 Avidin-biotin system for controlled release

The simplest approach is to generate antibody micropatterns where the antibodies are immobilized via a linker molecule from which they can be eluted. For similar requirements in protein purification systems, modified versions of avidin resins and modified forms of biotin labeling have been developed to make the avidin-biotin interaction readily reversible<sup>20</sup>. Most of these commercially available systems can be directly adapted to the antibody micropatterns and could be used to release the capture antibody with its target. An immediate idea is to immobilize biotinylated antibodies via printed avidin micropatterns. The monomeric form of avidin binds less strongly to biotin and allows for the competitive displacement of the biotinylated antibodies using excess free biotin that can be added to the cell culture medium. Thus the capture antibody will be released together with its target protein.

Another option is to use cleavable biotinylation reagents. We could use specific biotinylation reagents that contain a disulfide bond in their spacer arm to biotinylate our antibodies (such as sulfo-NHS-SS-Biotin from Thermo Fisher, Germany). Again, these antibodies will be immobilized on avidin micropatterns, and will be released by cleavage of the disulfide bond with a reducing agent. Upon cleavage, the biotin will remain bound to the avidin micropattern, while the antibody together with its captured protein will be released. After controlled release one can specifically follow this protein population.

Notable, we use IgG antibodies for our antibody micropatterns that consist of four polypeptide chains, two identical heavy chains and two identical light chains. The two heavy chains are linked to each other by disulfide bonds as well as to one light chain. This implies that we might not even need the suggested biotinylated antibodies with the cleavable disulfide bond for the release. If we can treat the cells with reducing agents like Dithiothreitol (DTT) or tris(2-carboxyethyl)phosphine (TCEP), we might just apply this to reduce our currently used antibodies. The reduction of the disulfide bonds of the IgG antibodies will lead to their separation and thus the release of the captured proteins (similar to the SDS-PAGE).

---

<sup>20</sup> See Thermo Fisher for reference: <https://www.thermofisher.com/de/de/home/life-science/protein-biology/protein-biology-learning-center/protein-biology-resource-library/pierce-protein-methods/avidin-biotin-interaction.html> (23.01.2018)

All approaches mentioned above require printing of avidin on glass surface to which the biotinylated antibody is bound. Our previous trials where we wanted to immobilize the antibodies via linker proteins such as protein A or protein G have demonstrated the difficulties with these 'indirect' immobilization approaches. I can imagine that we will encounter similar problems with avidin micropatterns. But in case our printing protocol does not work for avidin, we have access to streptavidin patterns from the Rapp group from the Karlsruhe Institute of Technology (KIT) (Waldbaur et al., 2012) that we can test as an alternative.

#### **7.4.2.2 Enzymatic cleavage of antibody micropatterns**

As mentioned above, I am afraid that the generation of avidin micropatterns and the specific binding of biotinylated antibodies to the pattern elements may require extensive optimization steps. I thus recommend finding an alternative approach that allows for the release from our currently used antibody micropatterns where the antibodies are directly bound to the glass surface. This could be achieved by enzymatic cleavage of the antibodies. Pepsin and papain are commonly used enzymes for the fragmentation of antibodies. Their specific cleavage site is located in the hinge region of the antibody and splits the antibody into its Fab and Fc fragments. Papain generates two Fab fragments and one Fc fragment, while pepsin generates one  $F(ab')_2$  fragment plus the Fc fragment.

If we assume that the antibodies are immobilized in a random orientation, there will be a population of antibodies that is bound via its Fc fragment to the glass surface. I assume that the majority of the antibodies that are able to capture proteins are actually oriented this way, since they can only bind their target protein when their antigen binding sites are located towards the cell surface. If these antibodies are cleaved with the enzymes, the Fab fragments will be released together with the target protein, while the Fc region remains bound to the glass surface and thus releases the captured proteins. It needs to be tested if the amount of proteins that can be released with this method is sufficient to be tracked.

One other possible problem with this enzymatic approach is that papain will also digest the extracellular matrix of the cells and that they will eventually detach from the surface. With longer incubation (>10 min), cells will also be lysed by the enzymes. One probably has to try how sensitive the cells are and if one can drive the reaction towards the cleavage of the antibodies by adjusting incubation times and temperatures.

Alternatively, one can engineer antibodies with a specific incorporated enzymatic cleavage site that can be specifically targeted by enzymes, which will not affect the cells themselves.

## 8 References

- Altman, J.D., P.A. Moss, P.J. Goulder, D.H. Barouch, M.G. McHeyzer-Williams, J.I. Bell, A.J. McMichael, and M.M. Davis. 1996. Phenotypic analysis of antigen-specific T lymphocytes. *Science*. 274:94–6. doi:10.1126/SCIENCE.274.5284.94.
- Arosa, F.A., S.G. Santos, and S.J. Powis. 2007. Open conformers: the hidden face of MHC-I molecules. *Trends Immunol.* 28:115–123. doi:10.1016/j.it.2007.01.002.
- Barnstable, C.J., W.F. Bodmer, G. Brown, G. Galfre, C. Milstein, A.F. Williams, and A. Ziegler. 1978. Production of monoclonal antibodies to group A erythrocytes, HLA and other human cell surface antigens-new tools for genetic analysis. *Cell*. 14:9–20.
- Barthes, J., H. Özçelik, M. Hindié, A. Ndreu-Halili, A. Hasan, and N.E. Vrana. 2014. Cell Microenvironment Engineering and Monitoring for Tissue Engineering and Regenerative Medicine: The Recent Advances. *Biomed Res. Int.* 2014:1–18. doi:10.1155/2014/921905.
- Bassani-Sternberg, M., and G. Coukos. 2016. Mass spectrometry-based antigen discovery for cancer immunotherapy. *Curr. Opin. Immunol.* 41:9–17. doi:10.1016/j.coi.2016.04.005.
- Bentzen, A.K., and S.R. Hadrup. 2017. Evolution of MHC-based technologies used for detection of antigen-responsive T cells. *Cancer Immunol. Immunother.* 66:657–666. doi:10.1007/s00262-017-1971-5.
- Bettinger, C.J., R. Langer, and J.T. Borenstein. 2009. Engineering Substrate Topography at the Micro- and Nanoscale to Control Cell Function. *Angew. Chemie Int. Ed.* 48:5406–5415. doi:10.1002/anie.200805179.
- Blackburn, J.M., and A. Shoko. 2011. Protein function microarrays for customised systems-oriented proteome analysis. *Methods Mol. Biol.* 785:305–30. doi:10.1007/978-1-61779-286-1\_21.
- Bodmer, H.C., J.M. Bastin, B.A. Askonas, and A.R. Townsend. 1989. Influenza-specific cytotoxic T-cell recognition is inhibited by peptides unrelated in both sequence and MHC restriction. *Immunology*. 66:163–9.
- Bodnár, A., Z. Bacsó, A. Jenei, T.M. Jovin, M. Edidin, S. Damjanovich, and J. Matkó. 2003. Class I HLA oligomerization at the surface of B cells is controlled by exogenous beta(2)-microglobulin: implications in activation of cytotoxic T lymphocytes. *Int. Immunol.* 15:331–9.

- Bolte, S., and F.P. Cordelières. 2006. A guided tour into subcellular colocalization analysis in light microscopy. *J. Microsc.* 224:213–232. doi:10.1111/j.1365-2818.2006.01706.x.
- Bouvier, M., and D.C. Wiley. 1994. Importance of peptide amino and carboxyl termini to the stability of MHC class I molecules. *Science*. 265:398–402.
- Bouvier, M., and D.C. Wiley. 1998. Structural characterization of a soluble and partially folded class I major histocompatibility heavy chain/beta 2m heterodimer. *Nat. Struct. Biol.* 5:377–84.
- Brodsky, F.M., W.F. Bodmer, and P. Parham. 1979. Characterization of a monoclonal anti- $\beta$ 2-microglobulin antibody and its use in the genetic and biochemical analysis of major histocompatibility antigens. *Eur. J. Immunol.* 9:536–545. doi:10.1002/eji.1830090709.
- Bromley, S.K., W.R. Burack, K.G. Johnson, K. Somersalo, T.N. Sims, C. Sumen, M.M. Davis, A.S. Shaw, P.M. Allen, and M.L. Dustin. 2001. THE IMMUNOLOGICAL SYNAPSE. *Annu. Rev. Immunol.* 19:375–396. doi:10.1146/annurev.immunol.19.1.375.
- Brooks, S.E., S.A. Bonney, C. Lee, A. Publicover, G. Khan, E.L. Smits, D. Sigurdardottir, M. Arno, D. Li, K.I. Mills, K. Pulford, A.H. Banham, V. van Tendeloo, G.J. Mufti, H.-G. Rammensee, T.J. Elliott, K.H. Orchard, and B. Guinn. 2015. Application of the pMHC Array to Characterise Tumour Antigen Specific T Cell Populations in Leukaemia Patients at Disease Diagnosis. *PLoS One*. 10:e0140483. doi:10.1371/journal.pone.0140483.
- Burian, A., K.L. Wang, K.A.K. Finton, N. Lee, A. Ishitani, R.K. Strong, and D.E. Geraghty. 2016. HLA-F and MHC-I Open Conformers Bind Natural Killer Cell Ig-Like Receptor KIR3DS1. *PLoS One*. 11:e0163297. doi:10.1371/journal.pone.0163297.
- Capps, G.G., B.E. Robinson, K.D. Lewis, and M.C. Zúñiga. 1993. In vivo dimeric association of class I MHC heavy chains. Possible relationship to class I MHC heavy chain-beta 2-microglobulin dissociation. *J. Immunol.* 151:159–69.
- Cavalcanti-Adam, E.A., A. Micoulet, J. Blümmel, J. Auernheimer, H. Kessler, and J.P. Spatz. 2006. Lateral spacing of integrin ligands influences cell spreading and focal adhesion assembly. *Eur. J. Cell Biol.* 85:219–24. doi:10.1016/j.ejcb.2005.09.011.
- Chen, B., J. Li, C. He, D. Li, W. Tong, Y. Zou, and W. Xu. 2017. Molecular medicine reports. 15. D.A. Spandidos. 1943-1951 pp.
- Cresswell, P., M.J. Androlewicz, and B. Ortman. 1994. Assembly and transport of class I MHC-peptide

- complexes. *Ciba Found. Symp.* 187:150-62–9.
- Damjanovich, S., L. Trón, J. Szöllösi, R. Zidovetzki, W.L. Vaz, F. Regateiro, D.J. Arndt-Jovin, and T.M. Jovin. 1983. Distribution and mobility of murine histocompatibility H-2Kk antigen in the cytoplasmic membrane. *Proc. Natl. Acad. Sci. U. S. A.* 80:5985–9.
- Das, D.K., Y. Feng, R.J. Mallis, X. Li, D.B. Keskin, R.E. Hussey, S.K. Brady, J.-H. Wang, G. Wagner, E.L. Reinherz, and M.J. Lang. 2015. Force-dependent transition in the T-cell receptor  $\beta$ -subunit allosterically regulates peptide discrimination and pMHC bond lifetime. *Proc. Natl. Acad. Sci. U. S. A.* 112:1517–22. doi:10.1073/pnas.1424829112.
- David J. Graber, \*,†, ‡ Thomas J. Zieziulewicz, ‡ David A. Lawrence, † and William Shain, and J.N. Turner†. 2003. Antigen Binding Specificity of Antibodies Patterned by Microcontact Printing. doi:10.1021/LA034199F.
- Day, P.M., F. Esquivel, J. Lukszo, J.R. Bennink, and J.W. Yewdell. 1995. Effect of TAP on the generation and intracellular trafficking of peptide-receptive major histocompatibility complex class I molecules. *Immunity.* 2:137–147. doi:10.1016/S1074-7613(95)80014-X.
- Deng, L., S. Cho, E.L. Malchiodi, M.C. Kerzic, J. Dam, and R.A. Mariuzza. 2008. Molecular architecture of the major histocompatibility complex class I-binding site of Ly49 natural killer cell receptors. *J. Biol. Chem.* 283:16840–9. doi:10.1074/jbc.M801526200.
- Deviren, G., K. Gupta, M.E. Paulaitis, and J.P. Schneck. 2007. Detection of antigen-specific T cells on p/MHC microarrays. *J. Mol. Recognit.* 20:32–38. doi:10.1002/jmr.805.
- Dirscherl, C., R. Palankar, M. Delcea, T.A. Kolesnikova, and S. Springer. 2017. Specific Capture of Peptide-Receptive Major Histocompatibility Complex Class I Molecules by Antibody Micropatterns Allows for a Novel Peptide-Binding Assay in Live Cells. *Small.* 13. doi:10.1002/sml.201602974.
- Dirscherl, C., and S. Springer. 2017. Protein micropatterns printed on glass - novel tools for protein-ligand binding assays in live cells. *Eng. Life Sci.* doi:10.1002/elsc.201700010.
- Dixon-Salazar, T.J., L. Fourgeaud, C.M. Tyler, J.R. Poole, J.J. Park, and L.M. Boulanger. 2014. MHC Class I Limits Hippocampal Synapse Density by Inhibiting Neuronal Insulin Receptor Signaling. *J. Neurosci.* 34.
- Doucey, M.-A., L. Scarpellino, J. Zimmer, P. Guillaume, I.F. Luescher, C. Bron, and W. Held. 2004. Cis association of Ly49A with MHC class I restricts natural killer cell inhibition. *Nat. Immunol.* 5:328–



336. doi:10.1038/ni1043.
- Falconnet, D., G. Csucs, H. Michelle Grandin, and M. Textor. 2006. Surface engineering approaches to micropattern surfaces for cell-based assays. *Biomaterials*. 27:3044–3063. doi:10.1016/j.biomaterials.2005.12.024.
- Freeman, S.A., J. Goyette, W. Furuya, E.C. Woods, C.R. Bertozzi, W. Bergmeier, B. Hinz, P.A. van der Merwe, R. Das, and S. Grinstein. 2016. Integrins Form an Expanding Diffusional Barrier that Coordinates Phagocytosis. *Cell*. 164:128–40. doi:10.1016/j.cell.2015.11.048.
- Gandor, S., S. Reisewitz, M. Venkatachalapathy, G. Arrabito, M. Reibner, H. Schröder, K. Ruf, C.M. Niemeyer, P.I.H. Bastiaens, and L. Dehmelt. 2013. A protein-interaction array inside a living cell. *Angew. Chem. Int. Ed. Engl.* 52:4790–4. doi:10.1002/anie.201209127.
- Gao, G.F., A.K. Sewell, B.K. Jakobsen, M. Sami, J.I. Bell, E. Gostick, D.A. Price, D.K. Cole, N.J. Pumphrey, and J.M. Boulter. 2007. MHC Class Restriction Human TCR-Binding Affinity is Governed by Human TCR-Binding Affinity Is Governed by MHC Class Restriction. *J Immunol Ref.* 178:5727–5734. doi:10.4049/jimmunol.178.9.5727.
- Garcia, K.C., M. Degano, R.L. Stanfield, A. Brunmark, M.R. Jackson, P.A. Peterson, L. Teyton, and I.A. Wilson. 1996. An alphabeta T cell receptor structure at 2.5 Å and its orientation in the TCR-MHC complex. *Science*. 274:209–19.
- Hämmerling, G.J., E. Rüşch, N. Tada, S. Kimura, and U. Hämmerling. 1982. Localization of allodeterminants on H-2Kb antigens determined with monoclonal antibodies and H-2 mutant mice. *Proc. Natl. Acad. Sci. U. S. A.* 79:4737–41.
- Hanenberg, H., K. Hashino, H. Konishi, R.A. Hock, I. Kato, and D.A. Williams. 1997. Optimization of fibronectin-assisted retroviral gene transfer into human CD34+ hematopoietic cells. *Hum. Gene Ther.* 8:2193–206. doi:10.1089/hum.1997.8.18-2193.
- Harris, M.R., Y.Y. Yu, C.S. Kindle, T.H. Hansen, and J.C. Solheim. 1998. Calreticulin and calnexin interact with different protein and glycan determinants during the assembly of MHC class I. *J. Immunol.* 160:5404–9.
- Van Hateren, A., E. James, A. Bailey, A. Phillips, N. Dalchau, and T. Elliott. 2010. The cell biology of major histocompatibility complex class I assembly: towards a molecular understanding. *Tissue Antigens*. 76:259–275. doi:10.1111/j.1399-0039.2010.01550.x.

- Hein, Z., and S. Springer. 2018. Distinct mechanisms survey the structural integrity of HLA-B\*27:05 intracellularly and at the surface. *PLoS One*.
- Hein, Z., H. Uchtenhagen, E.T. Abualrous, S.K. Saini, L. Janßen, A. Van Hateren, C. Wiek, H. Hanenberg, F. Momburg, A. Achour, T. Elliott, S. Springer, and D. Boulanger. 2014. Peptide-independent stabilization of MHC class I molecules breaches cellular quality control. *J. Cell Sci.* 127:2885–97. doi:10.1242/jcs.145334.
- Held, W., and R.A. Mariuzza. 2008. Cis interactions of immunoreceptors with MHC and non-MHC ligands. *Nat. Rev. Immunol.* 8:269–78. doi:10.1038/nri2278.
- Held, W., and R.A. Mariuzza. 2011. Cis–trans interactions of cell surface receptors: biological roles and structural basis. *Cell. Mol. Life Sci.* 68:3469–3478. doi:10.1007/s00018-011-0798-z.
- Huppa, J.B., and M.M. Davis. 2003. T-cell-antigen recognition and the immunological synapse. *Nat. Rev. Immunol.* 3:973–983. doi:10.1038/nri1245.
- Iversen, L., N. Cherouati, T. Berthing, D. Stamou, and K.L. Martinez. 2008. Templated protein assembly on micro-contact-printed surface patterns. Use of the SNAP-tag protein functionality. *Langmuir.* 24:6375–81. doi:10.1021/la7037075.
- Kane, R.S., S. Takayama, E. Ostuni, D.E. Ingber, and G.M. Whitesides. 1999. Patterning proteins and cells using soft lithography. *Biomaterials.* 20:2363–76.
- Kaufmann, T., and B.J. Ravoo. 2010. Stamps, inks and substrates: polymers in microcontact printing. doi:10.1039/b9py00281b.
- Kellmann, S.-J., S. Dübel, and H. Thie. 2017. A strategy to identify linker-based modules for the allosteric regulation of antibody-antigen binding affinities of different scFvs. *MAbs.* 9:404–418. doi:10.1080/19420862.2016.1277302.
- Kern, W. 1990. The Evolution of Silicon Wafer Cleaning Technology. *J. Electrochem. Soc.* 137:1887. doi:10.1149/1.2086825.
- Kerppola, T.K. 2008. Bimolecular fluorescence complementation (BiFC) analysis as a probe of protein interactions in living cells. *Annu. Rev. Biophys.* 37:465–87. doi:10.1146/annurev.biophys.37.032807.125842.
- Khademhosseini, A., R. Langer, J. Borenstein, and J.P. Vacanti. 2006. Microscale technologies for tissue engineering and biology. *Proc. Natl. Acad. Sci. U. S. A.* 103:2480–2487.

- Kim, S.T., K. Takeuchi, Z.-Y.J. Sun, M. Touma, C.E. Castro, A. Fahmy, M.J. Lang, G. Wagner, and E.L. Reinherz. 2009. The alphabeta T cell receptor is an anisotropic mechanosensor. *J. Biol. Chem.* 284:31028–37. doi:10.1074/jbc.M109.052712.
- Korf, U. 2011. Protein microarrays : methods and protocols. Humana Press. 398 pp.
- Kumar, R., S. Weigel, R. Meyer, C.M. Niemeyer, H. Fuchs, M. Hirtz, C.M. Niemeyer, C.M. Niemeyer, H. Fuchs, S. Koeber, and T. Mappes. 2016. Multi-color polymer pen lithography for oligonucleotide arrays. *Chem. Commun.* 52:12310–12313. doi:10.1039/C6CC07087F.
- Kwong, G.A., C.G. Radu, K. Hwang, C.J. Shu, C. Ma, R.C. Koya, B. Comin-Anduix, S.R. Hadrup, R.C. Bailey, O.N. Witte, T.N. Schumacher, A. Ribas, and J.R. Heath. 2009. Modular Nucleic Acid Assembled p/MHC Microarrays for Multiplexed Sorting of Antigen-Specific T Cells. *J. Am. Chem. Soc.* 131:9695–9703. doi:10.1021/ja9006707.
- de la Salle, H., J. Zimmer, D. Fricker, C. Angenieux, J.-P. Cazenave, M. Okubo, H. Maeda, A. Plebani, M.-M. Tongio, A. Dormoy, and D. Hanau. 1999. HLA class I deficiencies due to mutations in subunit 1 of the peptide transporter TAP1. *J. Clin. Invest.* 103:R9–R13. doi:10.1172/JCI5687.
- LaGraff, J.R., and Q. Chu-LaGraff. 2006. Scanning force microscopy and fluorescence microscopy of microcontact printed antibodies and antibody fragments. *Langmuir.* 22:4685–93. doi:10.1021/la0522303.
- Lanzerstorfer, P., D. Borgmann, G. Schütz, S.M. Winkler, O. Höglinger, and J. Weghuber. 2014. Quantification and kinetic analysis of Grb2-EGFR interaction on micro-patterned surfaces for the characterization of EGFR-modulating substances. *PLoS One.* 9:e92151. doi:10.1371/journal.pone.0092151.
- Lee, J.E., J.H. Seo, C.S. Kim, Y. Kwon, J.H. Ha, S.S. Choi, and H.J. Cha. 2013. A comparative study on antibody immobilization strategies onto solid surface. *Korean J. Chem. Eng.* 30:1934–1938. doi:10.1007/s11814-013-0117-5.
- Leisner, C., N. Loeth, K. Lamberth, S. Justesen, C. Sylvester-Hvid, E.G. Schmidt, M. Claesson, S. Buus, and A. Stryhn. 2008. One-pot, mix-and-read peptide-MHC tetramers. *PLoS One.* 3:e1678. doi:10.1371/journal.pone.0001678.
- Liegler, T., J. Szollosi, W. Hyun, and R.S. Goodenow. 1991. Proximity measurements between H-2 antigens and the insulin receptor by fluorescence energy transfer: evidence that a close association does not influence insulin binding. *Proc. Natl. Acad. Sci. U. S. A.* 88:6755–9.

- Liston, E.M. 1989. Plasma Treatment for Improved Bonding: A Review. *J. Adhes.* 30:199–218. doi:10.1080/00218468908048206.
- Liu, A.P., D. Loerke, S.L. Schmid, and G. Danuser. 2009. Global and Local Regulation of Clathrin-Coated Pit Dynamics Detected on Patterned Substrates. *Biophys. J.* 97:1038–1047. doi:10.1016/j.bpj.2009.06.003.
- Ljunggren, H.-G., N.J. Stam, C. Öhlén, J.J. Neefjes, P. Höglund, M.-T. Heemels, J. Bastin, T.N.M. Schumacher, A. Townsend, K. Kärre, and H.L. Ploegh. 1990. Empty MHC class I molecules come out in the cold. *Nature.* 346:476–480. doi:10.1038/346476a0.
- Löchte, S., S. Waichman, O. Beutel, C. You, and J. Piehler. 2014. Live cell micropatterning reveals the dynamics of signaling complexes at the plasma membrane. *J. Cell Biol.* 207:407–18. doi:10.1083/jcb.201406032.
- Los, G. V, and K. Wood. 2007. The HaloTag: a novel technology for cell imaging and protein analysis. *Methods Mol. Biol.* 356:195–208.
- Madden, D.R. 1995. The Three-Dimensional Structure of Peptide-MHC Complexes. *Annu. Rev. Immunol.* 13:587–622.
- Makaraviciute, A., and A. Ramanaviciene. 2013. Site-directed antibody immobilization techniques for immunosensors. *Biosens. Bioelectron.* 50:460–471. doi:10.1016/j.bios.2013.06.060.
- Mareeva, T., E. Martinez-Hackert, and Y. Sykulev. 2008. How a T cell receptor-like antibody recognizes major histocompatibility complex-bound peptide. *J. Biol. Chem.* 283:29053–9. doi:10.1074/jbc.M804996200.
- Margolese, L., G.L. Waneck, C.K. Suzuki, E. Degen, R.A. Flavell, and D.B. Williams. 1993. Identification of the region on the class I histocompatibility molecule that interacts with the molecular chaperone, p88 (calnexin, IP90). *J. Biol. Chem.* 268:17959–66.
- Masuda, A., A. Nakamura, T. Maeda, Y. Sakamoto, and T. Takai. 2007. Cis binding between inhibitory receptors and MHC class I can regulate mast cell activation. *J. Exp. Med.* 204:907–920. doi:10.1084/jem.20060631.
- Matic, J., J. Deeg, A. Scheffold, I. Goldstein, and J.P. Spatz. 2013. Fine tuning and efficient T cell activation with stimulatory aCD3 nanoarrays. *Nano Lett.* 13:5090–7. doi:10.1021/nl4022623.
- Matko, J., Y. Bushkin, T. Wei, and M. Edidin. 1994. Clustering of class I HLA molecules on the surfaces of

- activated and transformed human cells. *J. Immunol.* 152.
- Matsui, K., J.J. Boniface, P.A. Reay, H. Schild, B. Fazekas de St Groth, and M.M. Davis. 1991. Low affinity interaction of peptide-MHC complexes with T cell receptors. *Science*. 254:1788–91.
- McCloskey, M.A., and M.M. Poo. 1986. Rates of membrane-associated reactions: reduction of dimensionality revisited. *J. Cell Biol.* 102:88–96. doi:10.1083/JCB.102.1.88.
- Messing, R.A. 1975. Adsorption of proteins on glass surfaces and pertinent parameters for the immobilization of enzymes in the pores of inorganic carriers. *J. Non. Cryst. Solids*. 19:277–283. doi:10.1016/0022-3093(75)90093-9.
- Mocsár, G., J. Volkó, D. Rönnlund, J. Widengren, P. Nagy, J. Szöllősi, K. Tóth, C.K. Goldman, S. Damjanovich, T.A. Waldmann, A. Bodnár, and G. Vámosi. 2016. MHC I Expression Regulates Co-clustering and Mobility of Interleukin-2 and -15 Receptors in T Cells. *Biophys. J.* 111:100–112. doi:10.1016/j.bpj.2016.05.044.
- Montealegre, S., V. Venugopalan, S. Fritzsche, C. Kulicke, Z. Hein, and S. Springer. 2015. Dissociation of  $\beta$ 2-microglobulin determines the surface quality control of major histocompatibility complex class I molecules. *FASEB J.* 29:2780–8. doi:10.1096/fj.14-268094.
- Moore, C.D., O.Z. Ajala, and H. Zhu. 2016. Applications in high-content functional protein microarrays. *Curr. Opin. Chem. Biol.* 30:21–7. doi:10.1016/j.cbpa.2015.10.013.
- Mossman, K.D., G. Campi, J.T. Groves, and M.L. Dustin. 2005. Altered TCR signaling from geometrically repatterned immunological synapses. *Science*. 310:1191–3. doi:10.1126/science.1119238.
- Nguyen, A.T., S.R. Sathe, and E.K.F. Yim. 2016. From nano to micro: topographical scale and its impact on cell adhesion, morphology and contact guidance. *J. Phys. Condens. Matter*. 28:183001. doi:10.1088/0953-8984/28/18/183001.
- Nguyen, H., J. Park, S. Kang, and M. Kim. 2015. Surface Plasmon Resonance: A Versatile Technique for Biosensor Applications. *Sensors*. 15:10481–10510. doi:10.3390/s150510481.
- Nicolau, D. V, K. Burrage, R.G. Parton, and J.F. Hancock. 2006. Identifying optimal lipid raft characteristics required to promote nanoscale protein-protein interactions on the plasma membrane. *Mol. Cell. Biol.* 26:313–23. doi:10.1128/MCB.26.1.313-323.2006.
- Nikkhah, M., F. Edalat, S. Manoucheri, and A. Khademhosseini. 2012. Engineering microscale topographies to control the cell–substrate interface. *Biomaterials*. 33:5230–5246.

- doi:10.1016/j.biomaterials.2012.03.079.
- Niman, H.L., R.A. Houghten, L.E. Walker, R.A. Reisfeld, I.A. Wilson, J.M. Hogle, and R.A. Lerner. 1983. Generation of protein-reactive antibodies by short peptides is an event of high frequency: implications for the structural basis of immune recognition. *Proc. Natl. Acad. Sci. U. S. A.* 80:4949–53.
- Nizsalóczki, E., I. Csomós, P. Nagy, Z. Fazekas, C.K. Goldman, T.A. Waldmann, S. Damjanovich, G. Vámosi, L. Mátyus, and A. Bodnár. 2014. Distinct Spatial Relationship of the Interleukin-9 Receptor with Interleukin-2 Receptor and Major Histocompatibility Complex Glycoproteins in Human T Lymphoma Cells. *ChemPhysChem*. 15:3969–3978. doi:10.1002/cphc.201402501.
- Nössner, E., and P. Parham. 1995. Species-specific differences in chaperone interaction of human and mouse major histocompatibility complex class I molecules. *J. Exp. Med.* 181:327–37.
- Ozato, K., and D.H. Sachs. 1981. Monoclonal antibodies to mouse MHC antigens. III. Hybridoma antibodies reacting to antigens of the H-2b haplotype reveal genetic control of isotype expression. *J. Immunol.* 126.
- Passarelli, M.K., and A.G. Ewing. 2013. Single-cell imaging mass spectrometry. *Curr. Opin. Chem. Biol.* 17:854–9. doi:10.1016/j.cbpa.2013.07.017.
- Perosa, F., G. Luccarelli, M. Prete, E. Favoino, S. Ferrone, and F. Dammacco. 2003. Beta 2-microglobulin-free HLA class I heavy chain epitope mimicry by monoclonal antibody HC-10-specific peptide. *J. Immunol.* 171:1918–26.
- Porgador, A., J.W. Yewdell, Y. Deng, J.R. Bennink, and R.N. Germain. 1997. Localization, quantitation, and in situ detection of specific peptide-MHC class I complexes using a monoclonal antibody. *Immunity*. 6:715–26.
- Praveen, P.V.K., R. Yaneva, H. Kalbacher, and S. Springer. 2009. Tapasin edits peptides on MHC class I molecules by accelerating peptide exchange. *Eur. J. Immunol.* 40:214–224. doi:10.1002/eji.200939342.
- Pröschel, M., R. Detsch, A.R. Boccaccini, and U. Sonnewald. 2015. Pröschel, M., Detsch, R., Boccaccini, A. R., & Sonnewald, U. (2015). Engineering of Metabolic Pathways by Artificial Enzyme Channels. *Frontiers in Bioengineering and Biotechnology*, 3, 168. <https://doi.org/10.3389/fbioe.2015.00168> Engineering of Metabolic P. *Front. Bioeng. Biotechnol.* 3:168. doi:10.3389/fbioe.2015.00168.

- Rock, K.L., C. Gramm, and B. Benacerraf. 1991. Low temperature and peptides favor the formation of class I heterodimers on RMA-S cells at the cell surface. *Proc. Natl. Acad. Sci. U. S. A.* 88:4200–4.
- Rodenko, B., M. Toebes, S.R. Hadrup, W.J.E. van Esch, A.M. Molenaar, T.N.M. Schumacher, and H. Ovaa. 2006. Generation of peptide–MHC class I complexes through UV-mediated ligand exchange. *Nat. Protoc.* 1:1120–1132. doi:10.1038/nprot.2006.121.
- Saini, S.K. 2014. Dipeptide mediated modulation of peptide binding to MHC class I molecules By Sunil Kumar Saini Doctor of Philosophy in Biochemistry School of Engineering and Science. Jacobs University Bremen.
- Saini, S.K., E.T. Abualrous, A.-S. Tigan, K. Covella, U. Wellbrock, and S. Springer. 2013a. Not all empty MHC class I molecules are molten globules: Tryptophan fluorescence reveals a two-step mechanism of thermal denaturation. *Mol. Immunol.* 54:386–396. doi:10.1016/j.molimm.2013.01.004.
- Saini, S.K., K. Ostermeir, V.R. Ramnarayan, H. Schuster, M. Zacharias, and S. Springer. 2013b. Dipeptides promote folding and peptide binding of MHC class I molecules. *Proc. Natl. Acad. Sci. U. S. A.* 110:15383–8. doi:10.1073/pnas.1308672110.
- Saini, S.K., K. Ostermeir, V.R. Ramnarayan, H. Schuster, M. Zacharias, and S. Springer. 2013c. Dipeptides promote folding and peptide binding of MHC class I molecules. *Proc. Natl. Acad. Sci.* 110:15383–15388. doi:10.1073/pnas.1308672110.
- Saini, S.K., H. Schuster, V.R. Ramnarayan, H.-G. Rammensee, S. Stevanović, and S. Springer. 2015. Dipeptides catalyze rapid peptide exchange on MHC class I molecules. *Proc. Natl. Acad. Sci. U. S. A.* 112:202–7. doi:10.1073/pnas.1418690112.
- Satav, T., J. Huskens, and P. Jonkheijm. 2015. Effects of Variations in Ligand Density on Cell Signaling. *Small.* 11:5184–5199. doi:10.1002/sml.201500747.
- Schwarzenbacher, M., M. Kaltenbrunner, M. Brameshuber, C. Hesch, W. Paster, J. Weghuber, B. Heise, A. Sonnleitner, H. Stockinger, and G.J. Schütz. 2008. Micropatterning for quantitative analysis of protein-protein interactions in living cells. *Nat. Methods.* 5:1053–1060. doi:10.1038/nmeth.1268.
- Seu, K.J., A.P. Pandey, F. Haque, E.A. Proctor, A.E. Ribbe, and J.S. Hovis. 2007. Effect of surface treatment on diffusion and domain formation in supported lipid bilayers. *Biophys. J.* 92:2445–50. doi:10.1529/biophysj.106.099721.
- Shatz, C.J. 2009. MHC class I: an unexpected role in neuronal plasticity. *Neuron.* 64:40–5.

- doi:10.1016/j.neuron.2009.09.044.
- Singer, S.J., and G.L. Nicolson. 1972. The fluid mosaic model of the structure of cell membranes. *Science*. 175:720–31. doi:10.1126/SCIENCE.175.4023.720.
- Soen, Y., D.S. Chen, D.L. Kraft, M.M. Davis, and P.O. Brown. 2003. Detection and Characterization of Cellular Immune Responses Using Peptide–MHC Microarrays. *PLoS Biol.* 1:e65. doi:10.1371/journal.pbio.0000065.
- Solheim, J.C., N.A. Johnson, B.M. Carreno, W.-R. Lie, and T.H. Hansen. 1995.  $\beta$ 2-microglobulin with an endoplasmic reticulum retention signal increases the surface expression of folded class I major histocompatibility complex molecules. *Eur. J. Immunol.* 25:3011–3016. doi:10.1002/eji.1830251104.
- Sönnichsen, B., S. De Renzis, E. Nielsen, J. Rietdorf, and M. Zerial. 2000. Distinct membrane domains on endosomes in the recycling pathway visualized by multicolor imaging of Rab4, Rab5, and Rab11. *J. Cell Biol.* 149:901–14.
- Springer, S. 2015. Transport and quality control of MHC class I molecules in the early secretory pathway. *Curr. Opin. Immunol.* 34:83–90. doi:10.1016/j.coi.2015.02.009.
- St John, P.M., R. Davis, N. Cady, J. Czajka, C.A. Batt, and H.G. Craighead. 1998. Diffraction-based cell detection using a microcontact printed antibody grating. *Anal. Chem.* 70:1108–11.
- Stam, N.J., H. Spits, and H.L. Ploegh. 1986. Monoclonal antibodies raised against denatured HLA-B locus heavy chains permit biochemical characterization of certain HLA-C locus products. *J. Immunol.* 137.
- Stearns, N.A., S. Zhou, M. Petri, S.R. Binder, D.S. Pisetsky, and S. Muller. 2016. The Use of Poly-L-Lysine as a Capture Agent to Enhance the Detection of Antinuclear Antibodies by ELISA. *PLoS One*. 11:e0161818. doi:10.1371/journal.pone.0161818.
- Stone, J.D., W.E. Demkowicz, and L.J. Stern. 2005. HLA-restricted epitope identification and detection of functional T cell responses by using MHC-peptide and costimulatory microarrays. *Proc. Natl. Acad. Sci.* 102:3744–3749. doi:10.1073/pnas.0407019102.
- Sun, P.D., J.C. Boyington, S.A. Motyka, P. Schuck, and A.G. Brooks. 2000. Crystal structure of an NK cell immunoglobulin-like receptor in complex with its class I MHC ligand. *Nature*. 405:537–543. doi:10.1038/35014520.
- Sunzenauer, S., V. Zojer, M. Brameshuber, A. Tröls, J. Weghuber, H. Stockinger, and G.J. Schütz. 2013.



- Determination of binding curves via protein micropatterning in vitro and in living cells. *Cytom. Part A*. 83:847–854. doi:10.1002/cyto.a.22225.
- Szöllösi, J., S. Damjanovich, M. Balázs, P. Nagy, L. Trón, M.J. Fulwyler, and F.M. Brodsky. 1989. Physical association between MHC class I and class II molecules detected on the cell surface by flow cytometric energy transfer. *J. Immunol.* 143:208–13.
- Szymczak, A.L., C.J. Workman, Y. Wang, K.M. Vignali, S. Dilioglou, E.F. Vanin, and D.A.A. Vignali. 2004. Correction of multi-gene deficiency in vivo using a single “self-cleaving” 2A peptide–based retroviral vector. *Nat. Biotechnol.* 22:589–594. doi:10.1038/nbt957.
- Thery, M. 2010. Micropatterning as a tool to decipher cell morphogenesis and functions. *J. Cell Sci.* 123:4201–4213. doi:10.1242/jcs.075150.
- Tomlinson, D.R., and N.J. Gardiner. 2008. Glucose neurotoxicity. *Nat. Rev. Neurosci.* 9:36–45. doi:10.1038/nrn2294.
- Townsend, A., and H. Bodmer. 1989. Antigen Recognition by Class I-Restricted T Lymphocytes. *Annu. Rev. Immunol.* 7:601–624. doi:10.1146/annurev.iy.07.040189.003125.
- Townsend, A., C. Ohlén, L. Foster, J. Bastin, H.G. Ljunggren, and K. Kärre. 1989. A mutant cell in which association of class I heavy and light chains is induced by viral peptides. *Cold Spring Harb. Symp. Quant. Biol.* 54 Pt 1:299–308.
- Townsend, A.R., F.M. Gotch, and J. Davey. 1985. Cytotoxic T cells recognize fragments of the influenza nucleoprotein. *Cell.* 42:457–67. doi:10.1016/0092-8674(85)90103-5.
- Tsai, W.C., C.J. Chen, J.H. Yen, T.T. Ou, J.J. Tsai, C.S. Liu, and H.W. Liu. 2002. Free HLA class I heavy chain-carrying monocytes--a potential role in the pathogenesis of spondyloarthropathies. *J. Rheumatol.* 29:966–72.
- de Valence, S., J.-C. Tille, C. Chaabane, R. Gurny, M.-L. Bochaton-Piallat, B.H. Walpoth, and M. Möller. 2013. Plasma treatment for improving cell biocompatibility of a biodegradable polymer scaffold for vascular graft applications. *Eur. J. Pharm. Biopharm.* 85:78–86. doi:10.1016/J.EJPB.2013.06.012.
- Valeur, B., and M.N. Berberan-Santos. 2013. Molecular Fluorescence : principles and applications. Wiley-VCH. 569 pp.
- Waldbaur, A., B. Waterkotte, K. Schmitz, and B.E. Rapp. 2012. Maskless Projection Lithography for the Fast and Flexible Generation of Grayscale Protein Patterns. *Small.* 8:1570–1578.

- doi:10.1002/sml.201102163.
- Wedeking, T., S. Löchte, C.P. Richter, M. Bhagawati, J. Piehler, and C. You. 2015. Single Cell GFP-Trap Reveals Stoichiometry and Dynamics of Cytosolic Protein Complexes. *Nano Lett.* 15:3610–5. doi:10.1021/acs.nanolett.5b01153.
- Weghuber, J., M. Brameshuber, S. Sunzenauer, M. Lehner, C. Paar, T. Haselgrübler, M. Schwarzenbacher, M. Kaltenbrunner, C. Hesch, W. Paster, B. Heise, A. Sonnleitner, H. Stockinger, and G.J. Schütz. 2010. Detection of Protein–Protein Interactions in the Live Cell Plasma Membrane by Quantifying Prey Redistribution upon Bait Micropatterning. *In Methods in enzymology.* 133–151.
- Weinrich, D., P. Jonkheijm, C.M. Niemeyer, and H. Waldmann. 2009. Applications of Protein Biochips in Biomedical and Biotechnological Research. *Angew. Chemie Int. Ed.* 48:7744–7751. doi:10.1002/anie.200901480.
- Wilbur, J.L., A. Kumar, E. Kim, and G.M. Whitesides. 1994. Microfabrication by microcontact printing of self-assembled monolayers. *Adv. Mater.* 6:600–604. doi:10.1002/adma.19940060719.
- Willcox, B.E., L.M. Thomas, and P.J. Bjorkman. 2003. Crystal structure of HLA-A2 bound to LIR-1, a host and viral major histocompatibility complex receptor. *Nat. Immunol.* 4:913–919. doi:10.1038/ni961.
- Wilson, D.S., and S. Nock. 2003. Recent developments in protein microarray technology. *Angew. Chem. Int. Ed. Engl.* 42:494–500. doi:10.1002/anie.200390150.
- Wu, M., D. Holowka, H.G. Craighead, and B. Baird. 2004. Visualization of plasma membrane compartmentalization with patterned lipid bilayers. *Proc. Natl. Acad. Sci. U. S. A.* 101:13798–803. doi:10.1073/pnas.0403835101.
- Xia, Y., and G.M. Whitesides. 1998. SOFT LITHOGRAPHY. *Annu. Rev. Mater. Sci.* 28:153–184. doi:10.1146/annurev.matsci.28.1.153.
- Xu, X., N.J. Wittenberg, L.R. Jordan, S. Kumar, J.O. Watzlawik, A.E. Warrington, S.-H. Oh, and M. Rodriguez. 2013. A patterned recombinant human IgM guides neurite outgrowth of CNS neurons. *Sci. Rep.* 3:2267. doi:10.1038/srep02267.
- Yewdell, J.W. 2006. Confronting Complexity: Real-World Immunodominance in Antiviral CD8+ T Cell Responses. *Immunity.* 25:533–543. doi:10.1016/j.immuni.2006.09.005.
- You, C., and J. Piehler. 2016. Functional protein micropatterning for drug design and discovery. *Expert Opin. Drug Discov.* 11:105–19. doi:10.1517/17460441.2016.1109625.

- 
- Yu, C., H. Wu, Y. Kaizuka, R.D. Vale, and J.T. Groves. 2010. Altered actin centripetal retrograde flow in physically restricted immunological synapses. *PLoS One*. 5:e11878. doi:10.1371/journal.pone.0011878.
- Yue, C., M. Oelke, M.E. Paulaitis, and J.P. Schneck. 2010. Novel Cellular Microarray Assay for Profiling T-Cell Peptide Antigen Specificities. *J. Proteome Res.* 9:5629–5637. doi:10.1021/pr100447b.
- Zacharias, M., and S. Springer. 2004. Conformational flexibility of the MHC class I alpha1-alpha2 domain in peptide bound and free states: a molecular dynamics simulation study. *Biophys. J.* 87:2203–14. doi:10.1529/biophysj.104.044743.